



US 20120021414A1

(19) **United States**

(12) **Patent Application Publication**  
Shen-Orr et al.

(10) **Pub. No.: US 2012/0021414 A1**  
(43) **Pub. Date: Jan. 26, 2012**

(54) **DIAGNOSTIC MARKERS OF IMMUNOSENESCENCE AND METHODS OF USE THEREOF**

**Related U.S. Application Data**

(60) Provisional application No. 61/358,884, filed on Jun. 25, 2010.

(75) Inventors: **Shai S. Shen-Orr**, Menlo Park, CA (US); **Atul J. Butte**, Menlo Park, CA (US); **Mark M. Davis**, Atherton, CA (US); **David Furman**, San Francisco, CA (US); **Brian A. Kidd**, Palo Alto, CA (US)

**Publication Classification**

(51) **Int. Cl.**  
*C12Q 1/68* (2006.01)  
*G01N 33/53* (2006.01)  
(52) **U.S. Cl.** ..... **435/6.11; 436/501; 435/7.1**  
(57) **ABSTRACT**

(73) Assignees: **Howard Hughes Medical Institute**, Chevy Chase, MD (US); **The Board of Trustees of the Leland Stanford Junior University**, Palo Alto, CA (US)

Embodiments of the present invention provide diagnostic markers of immunosenescence and methods of identifying individuals with impaired immune function based on a combination of such markers obtained from various analyses, primarily from blood, testing immune function including the analysis of immune cell subset frequencies, gene expression, cytokine and chemokine levels, and signaling responses to stimulation with cytokines ('cytokine response'). Particular combinations of markers can predict with high accuracy whether an individual will respond to active vaccination and become protected against recurring diseases.

(21) Appl. No.: **13/168,974**

(22) Filed: **Jun. 25, 2011**

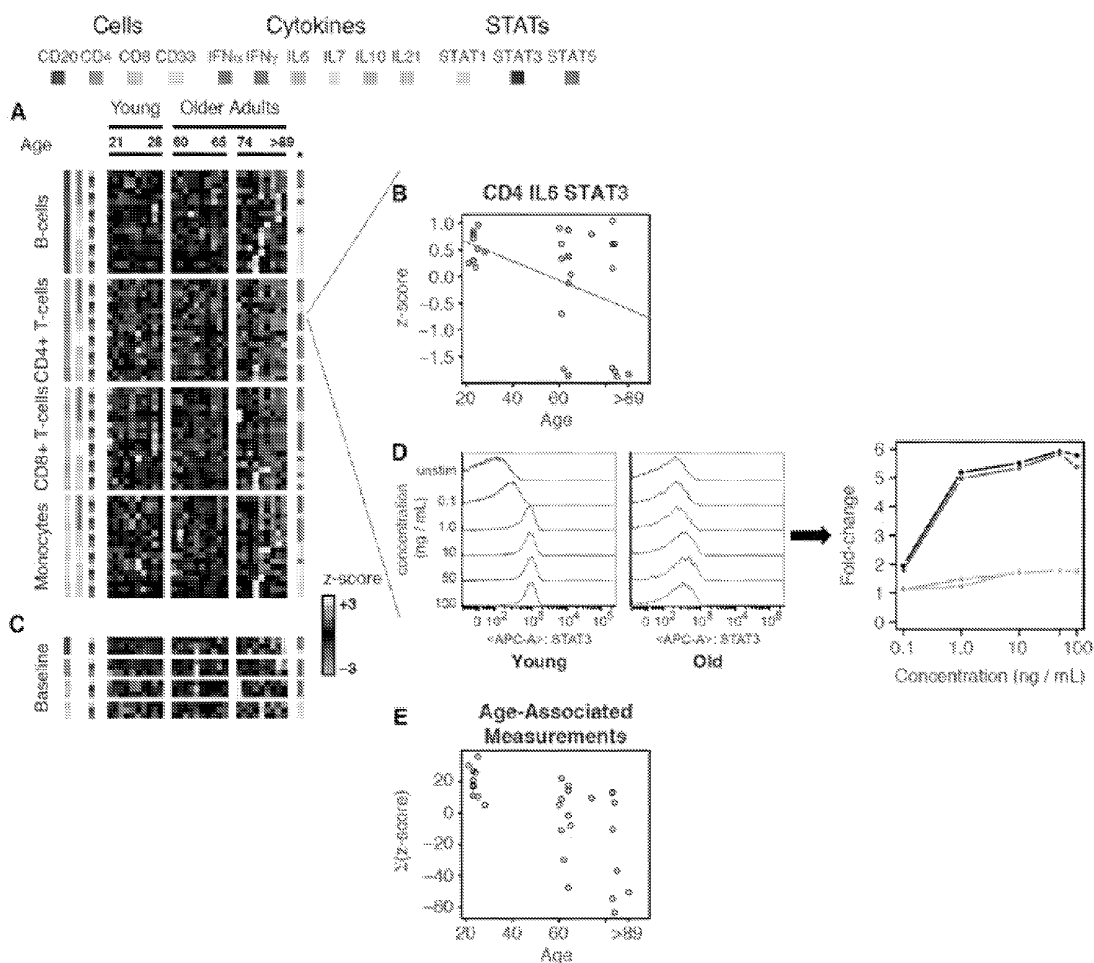


Figure 1

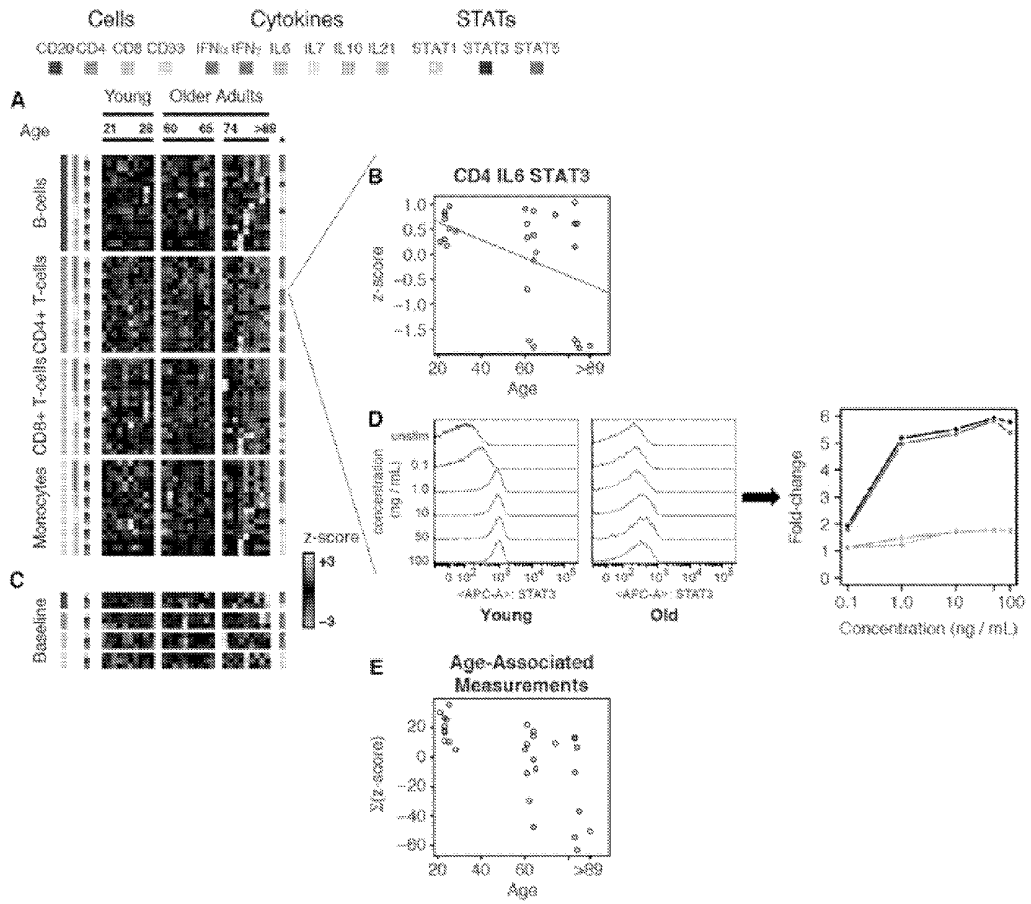


Figure 2A

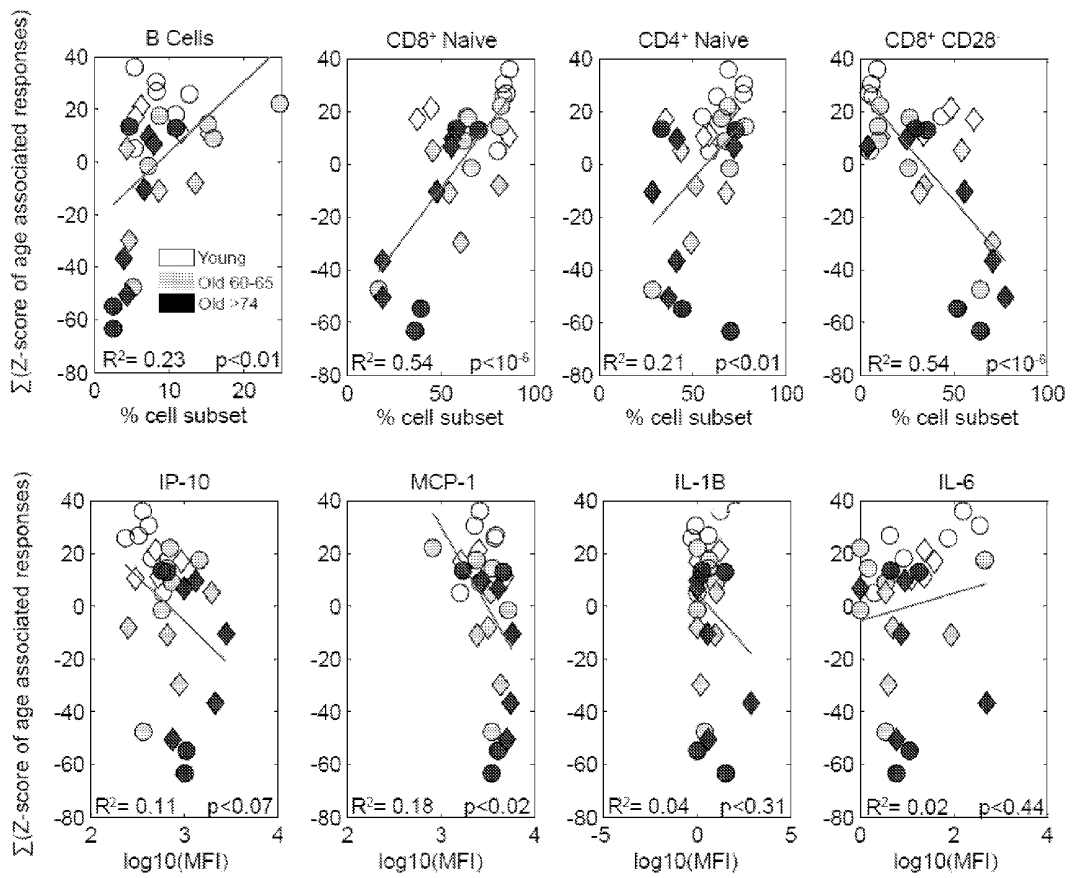


Figure 2B

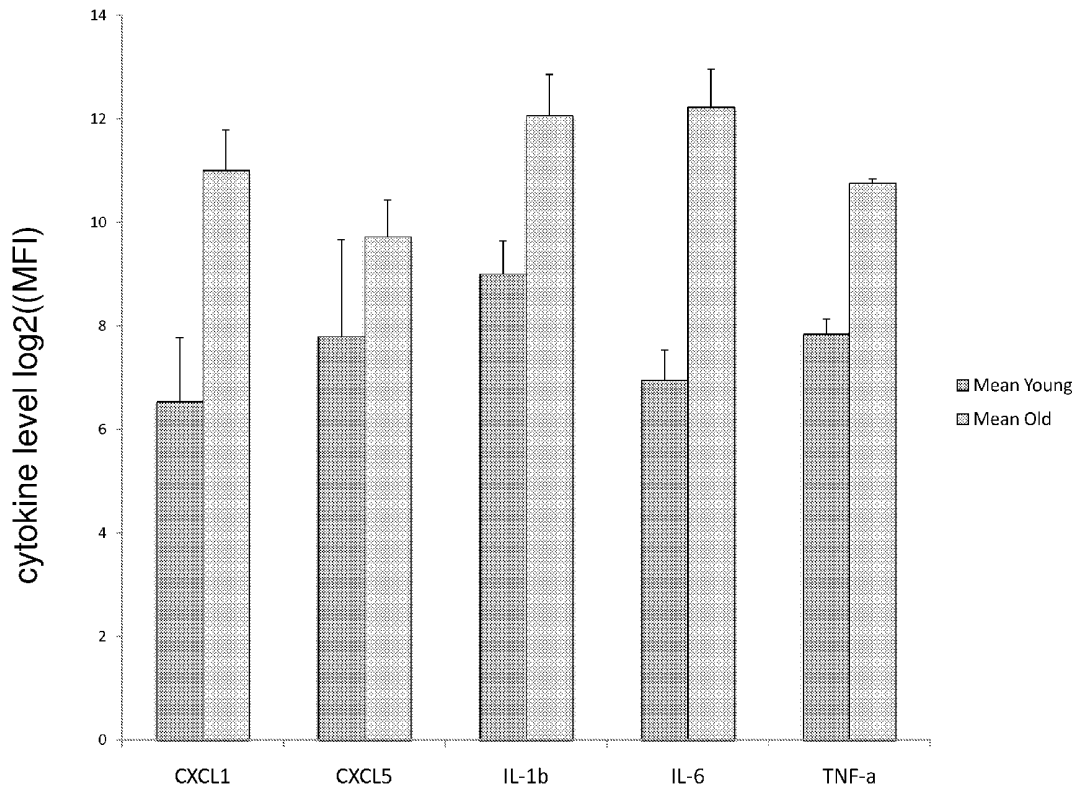


Figure 2C

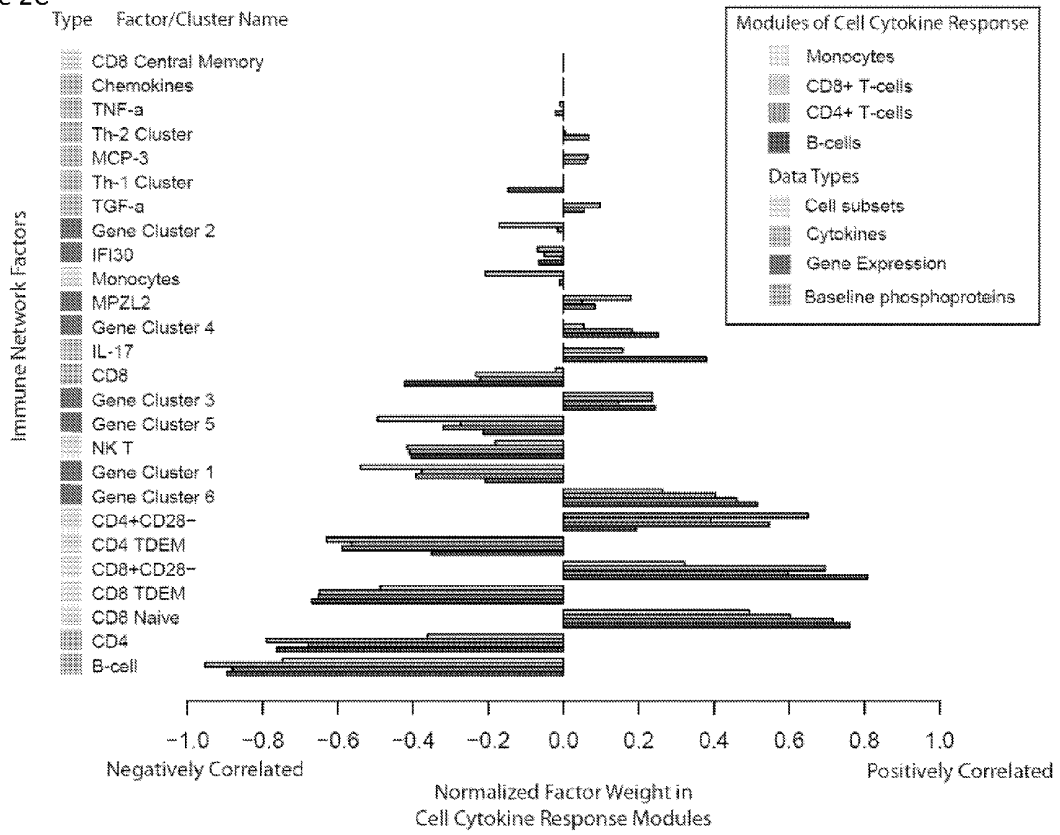


Figure 3A

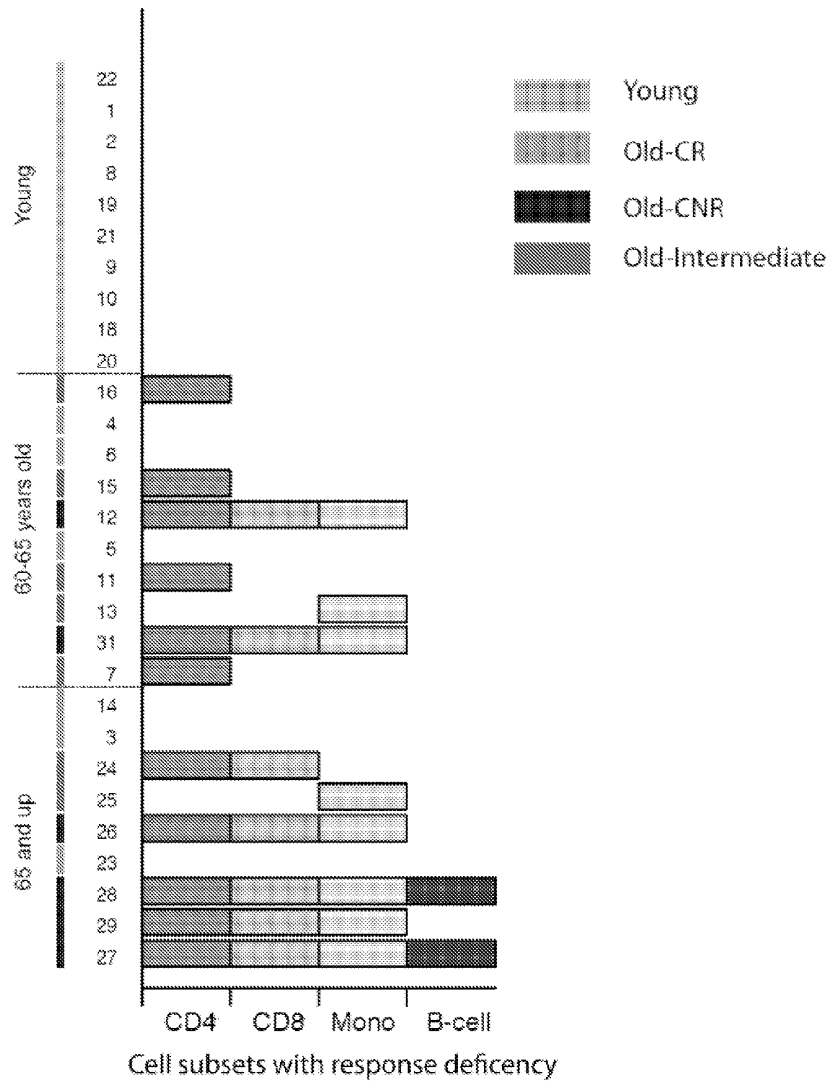


Figure 3B

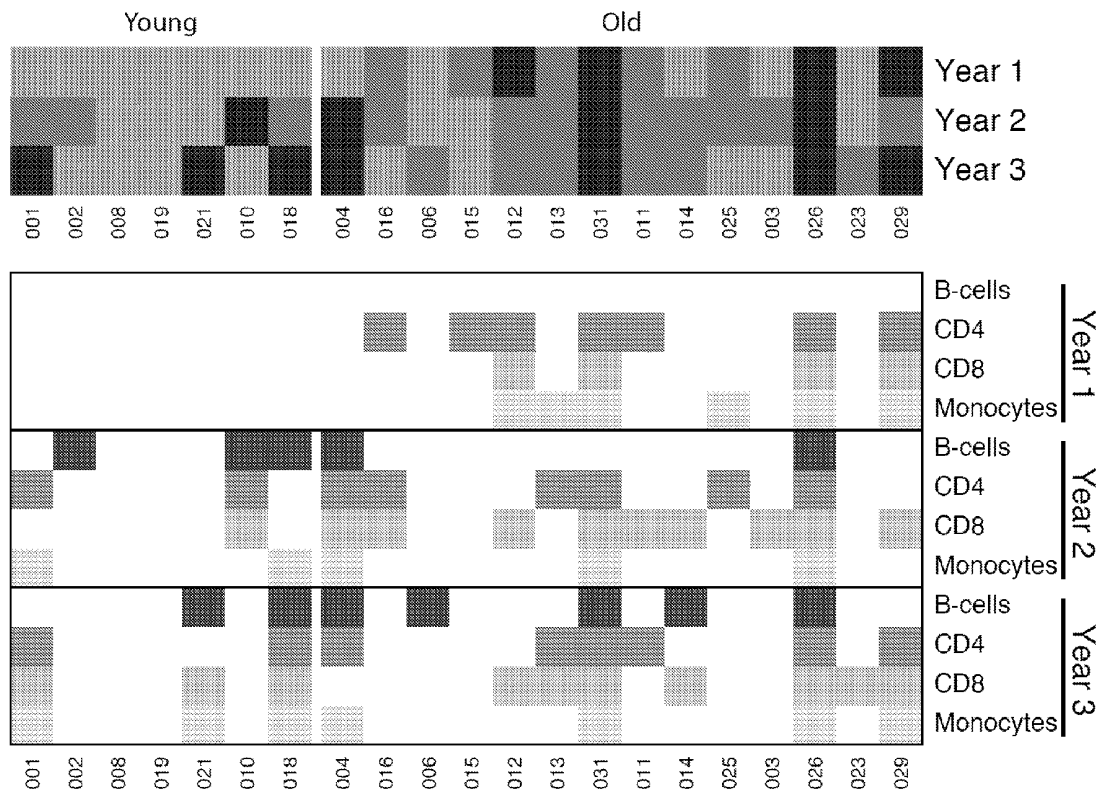


Figure 4A

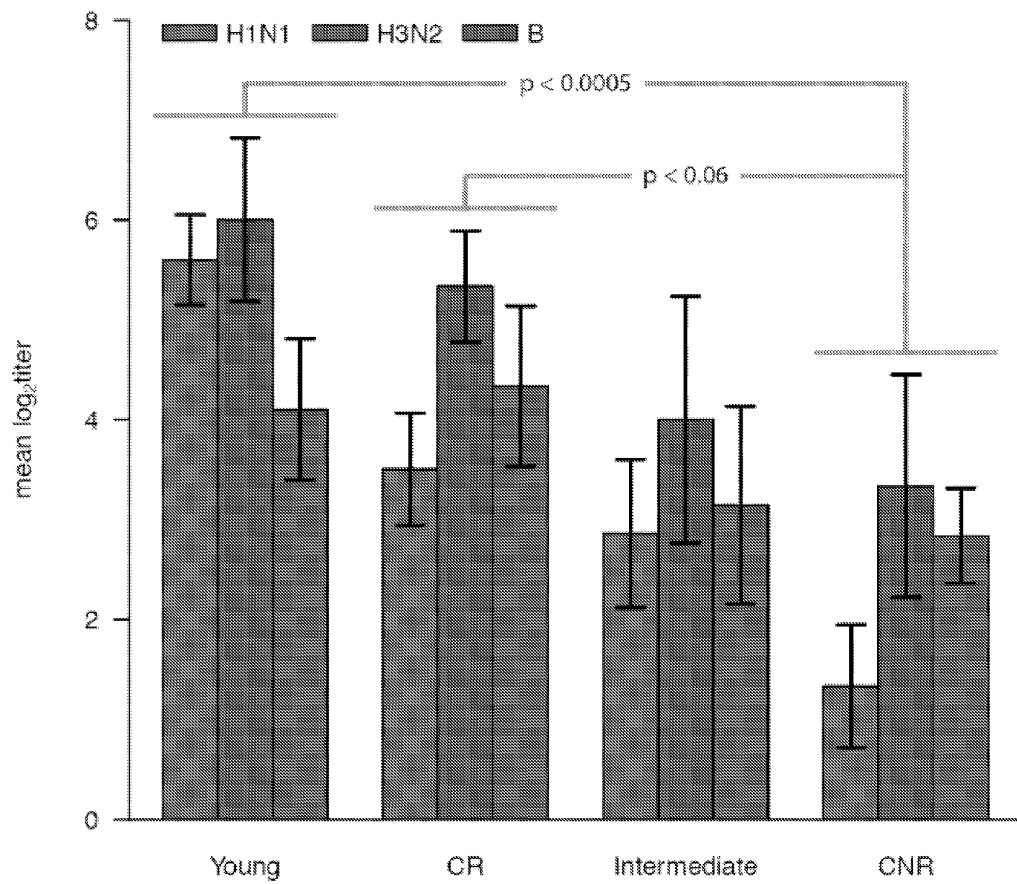


Figure 4B

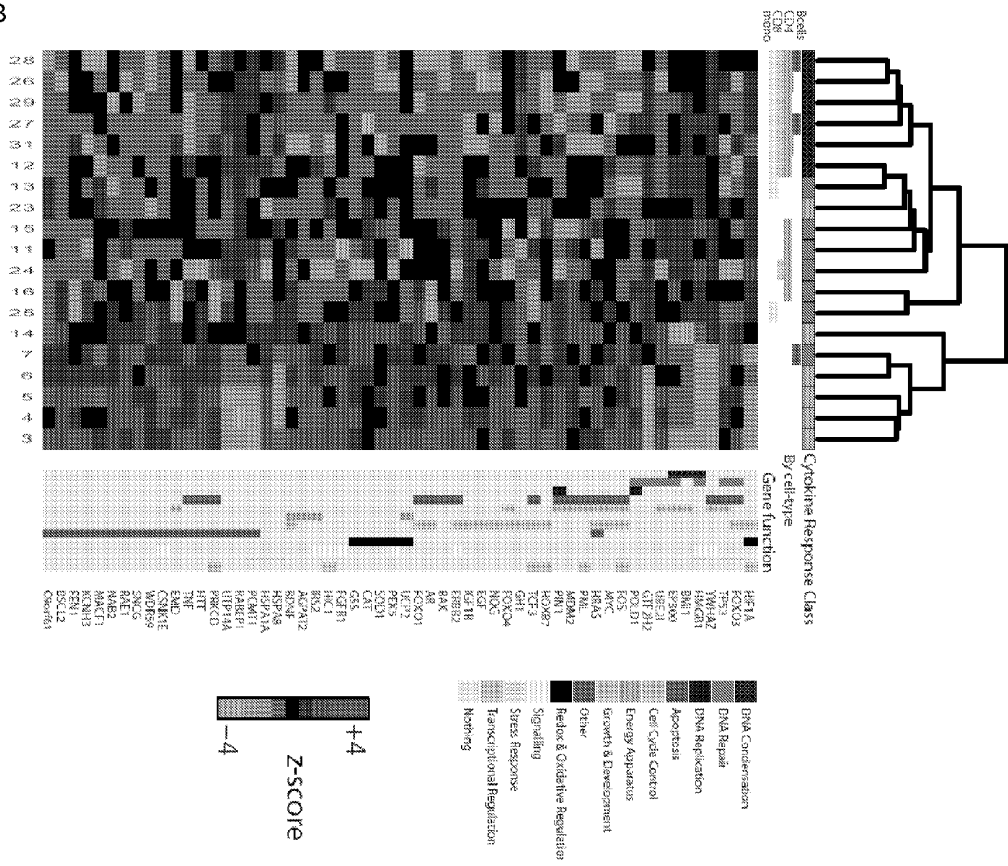


Figure 5A

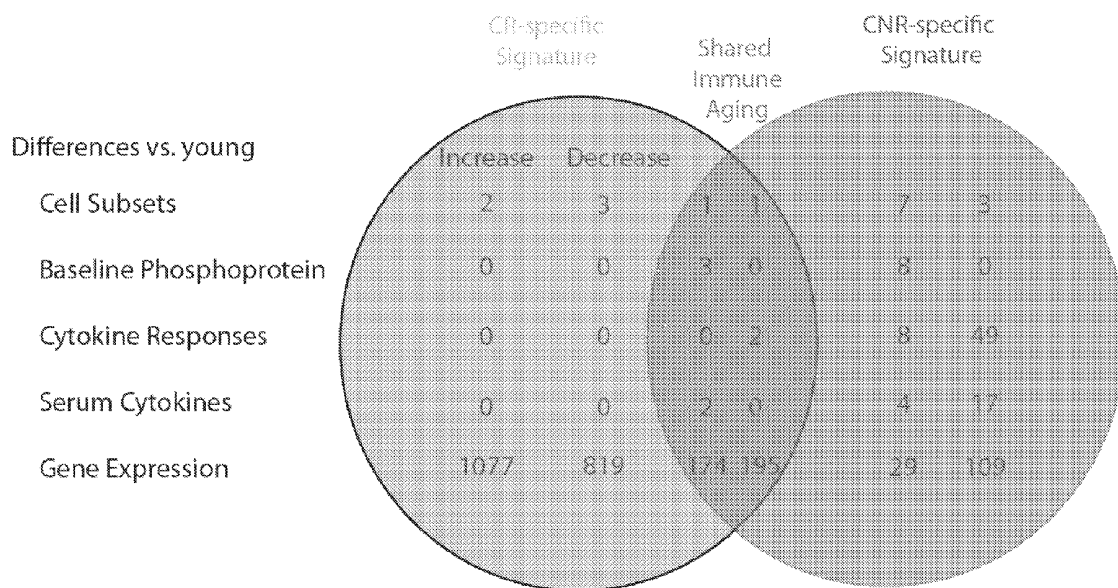


Figure 5B

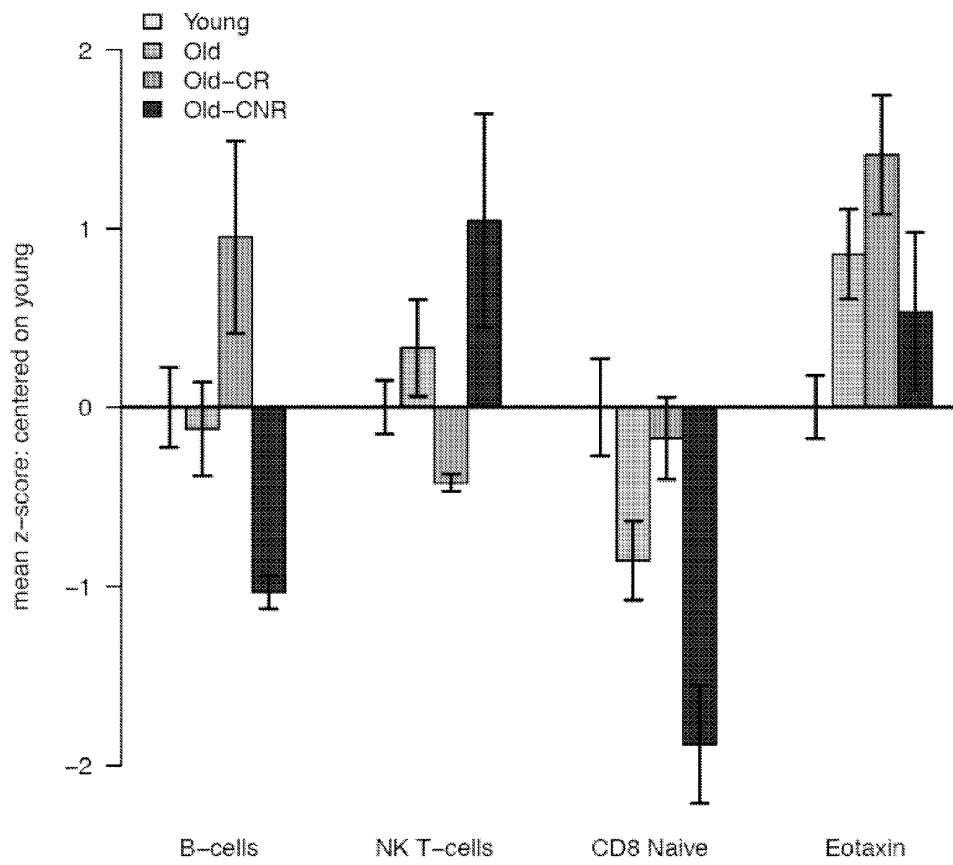


Figure 6A

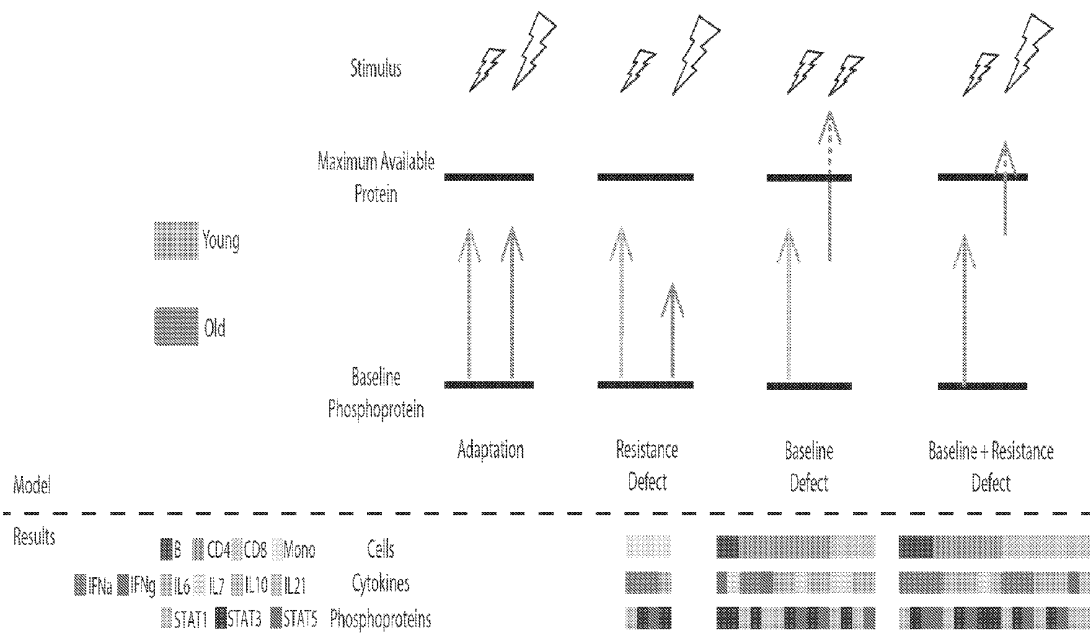


Figure 6B

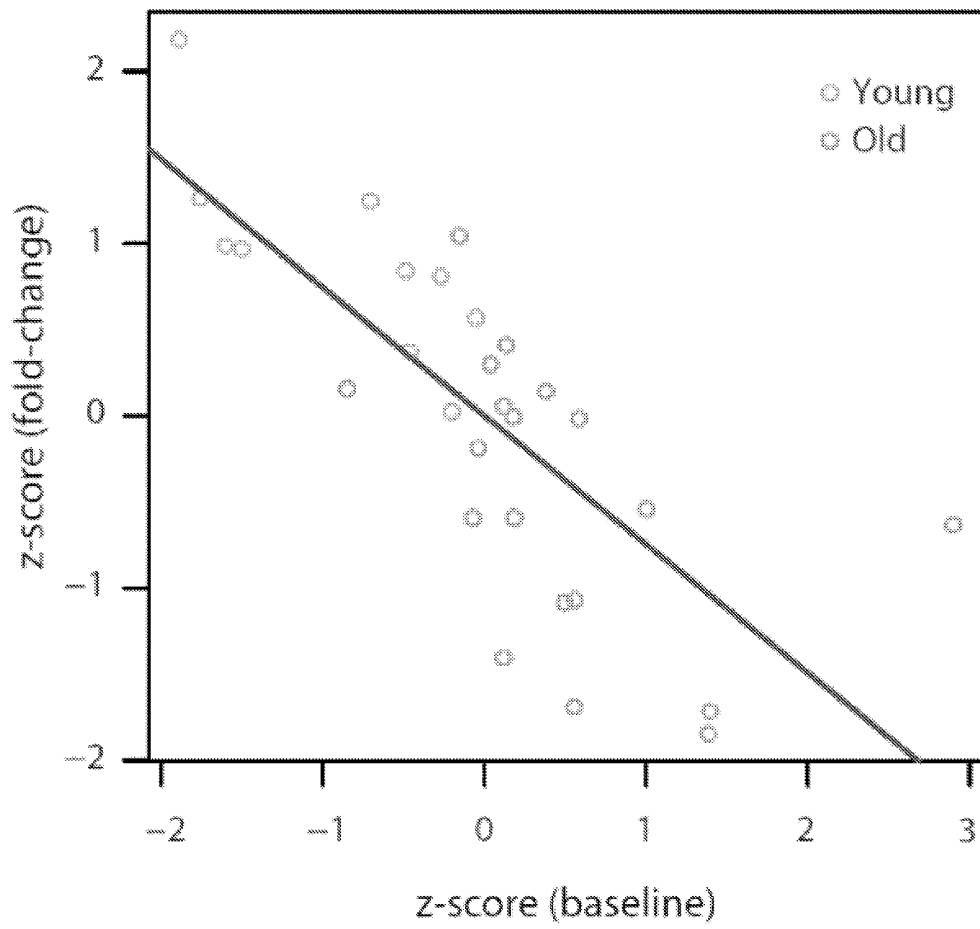


Figure 6C

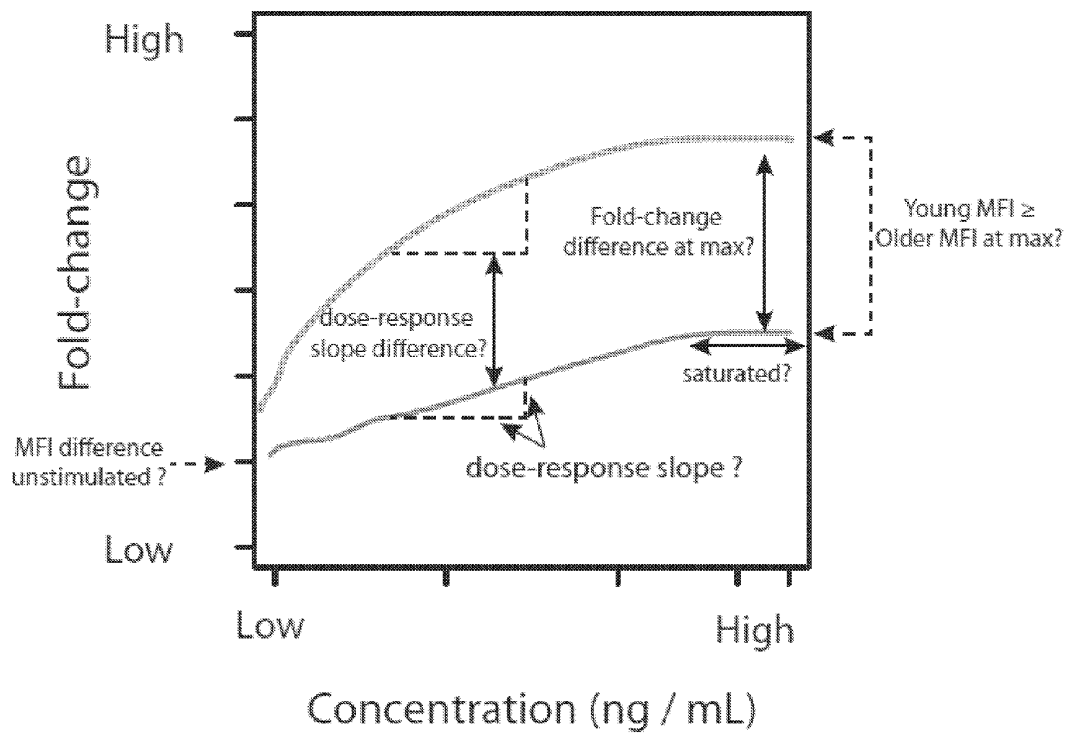


Figure S1

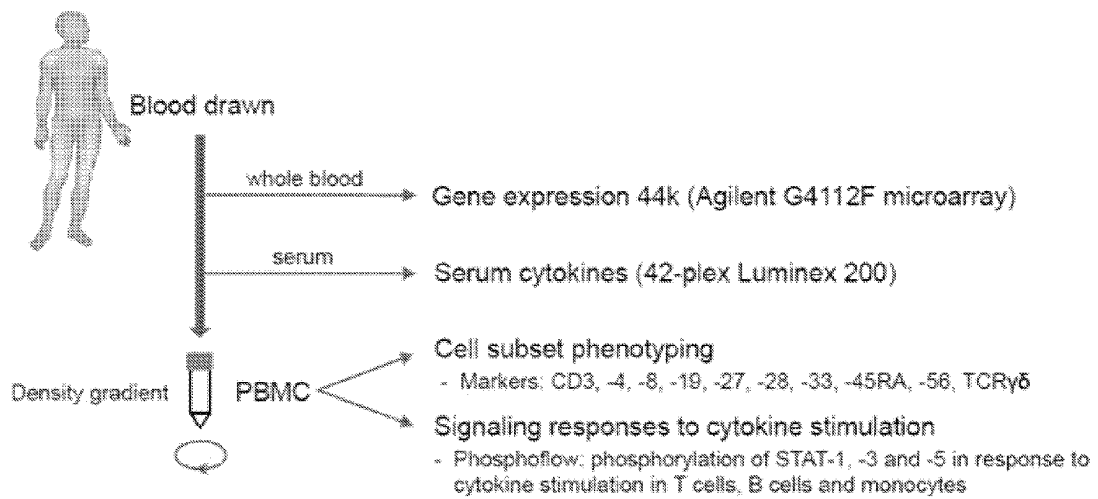


Fig. S2

Fig. S2, Part A

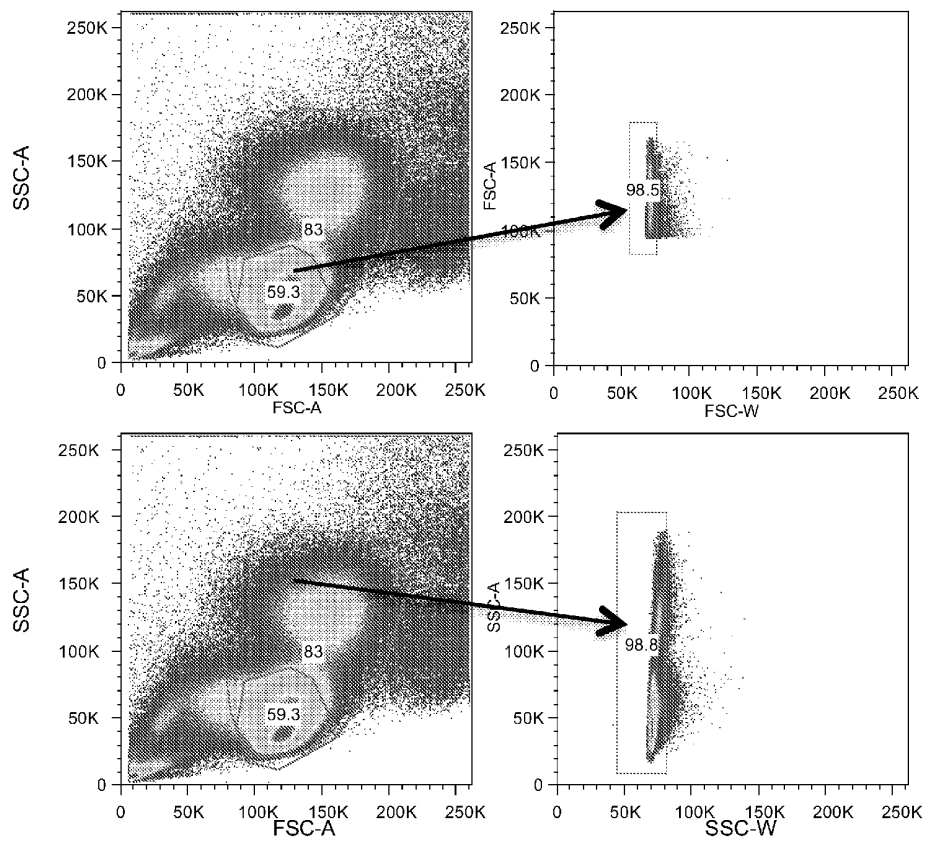


Fig S2 - Continued

Fig. S2, Part B

Barcode key

	Unstim	IFN-a	IFN-g	IL-6	IL-7	IL-10	IL-21	IL-2
Pacific Orange	-	Low	High	-	Low	-	Low	High
Alexa Fluor 750	-	-	-	Low	Low	High	High	Low

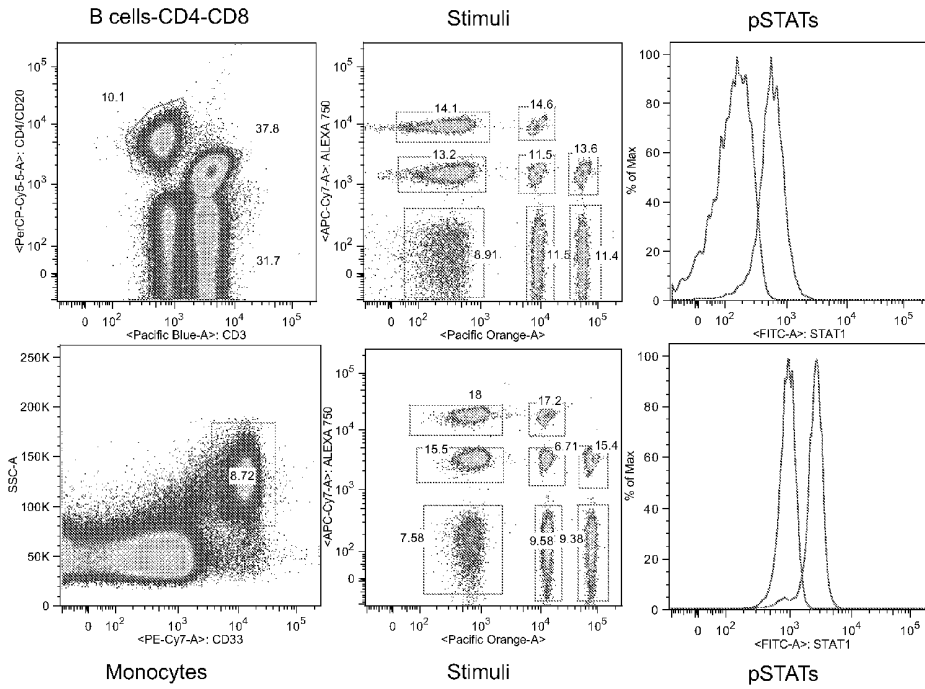


Figure S3

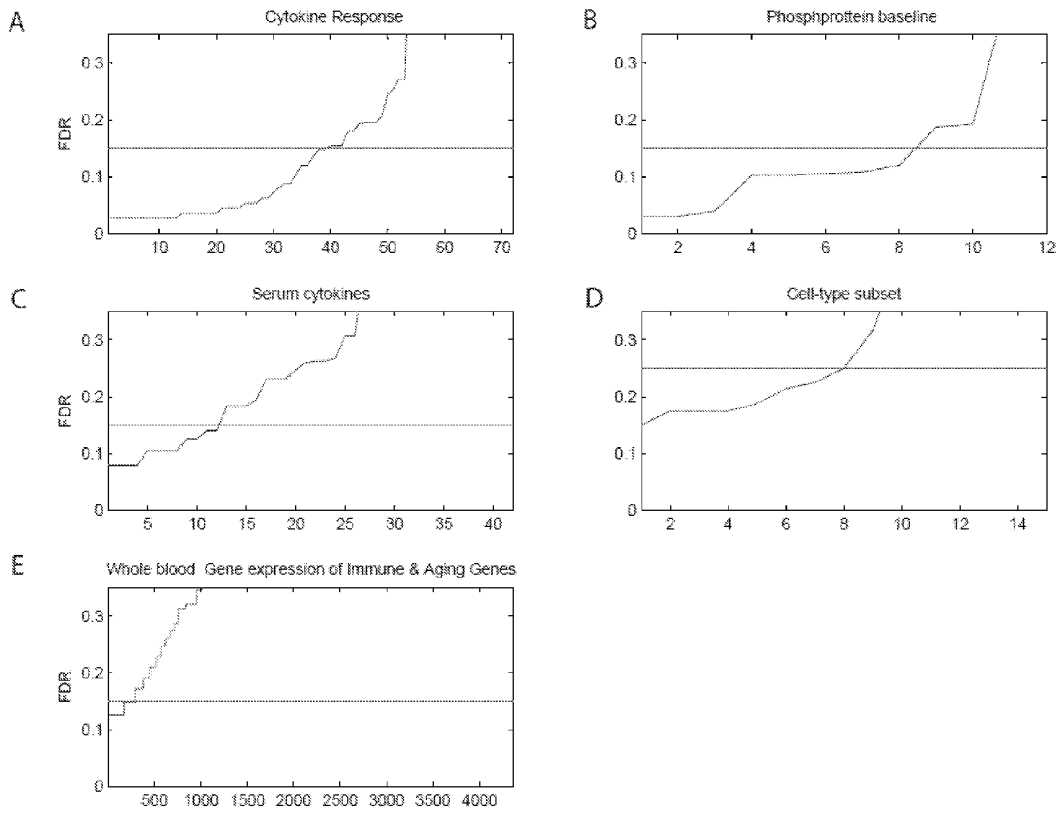
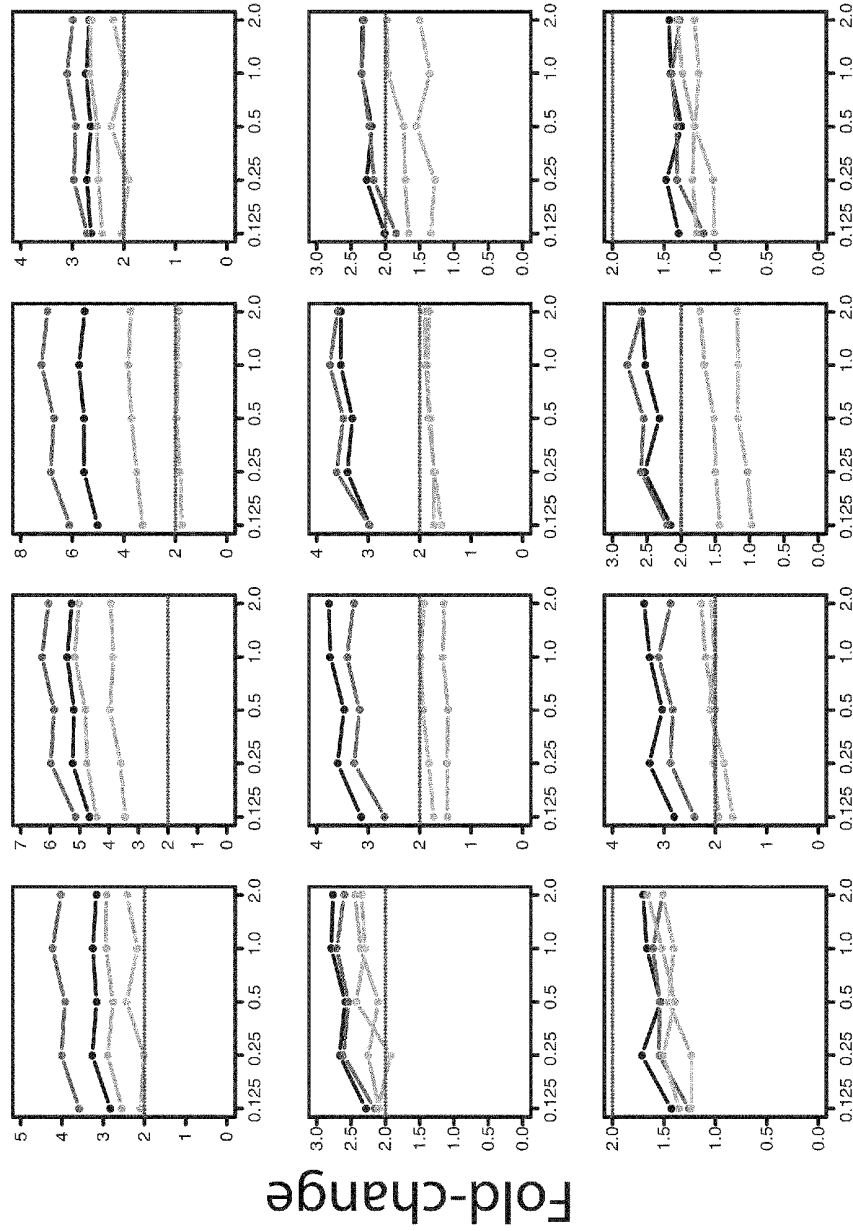


Figure S4  
Top-left  
panel

Bcell CD4 CD8 Mono

IFN $\alpha$



Concentration ( x10<sup>4</sup> U/mL)

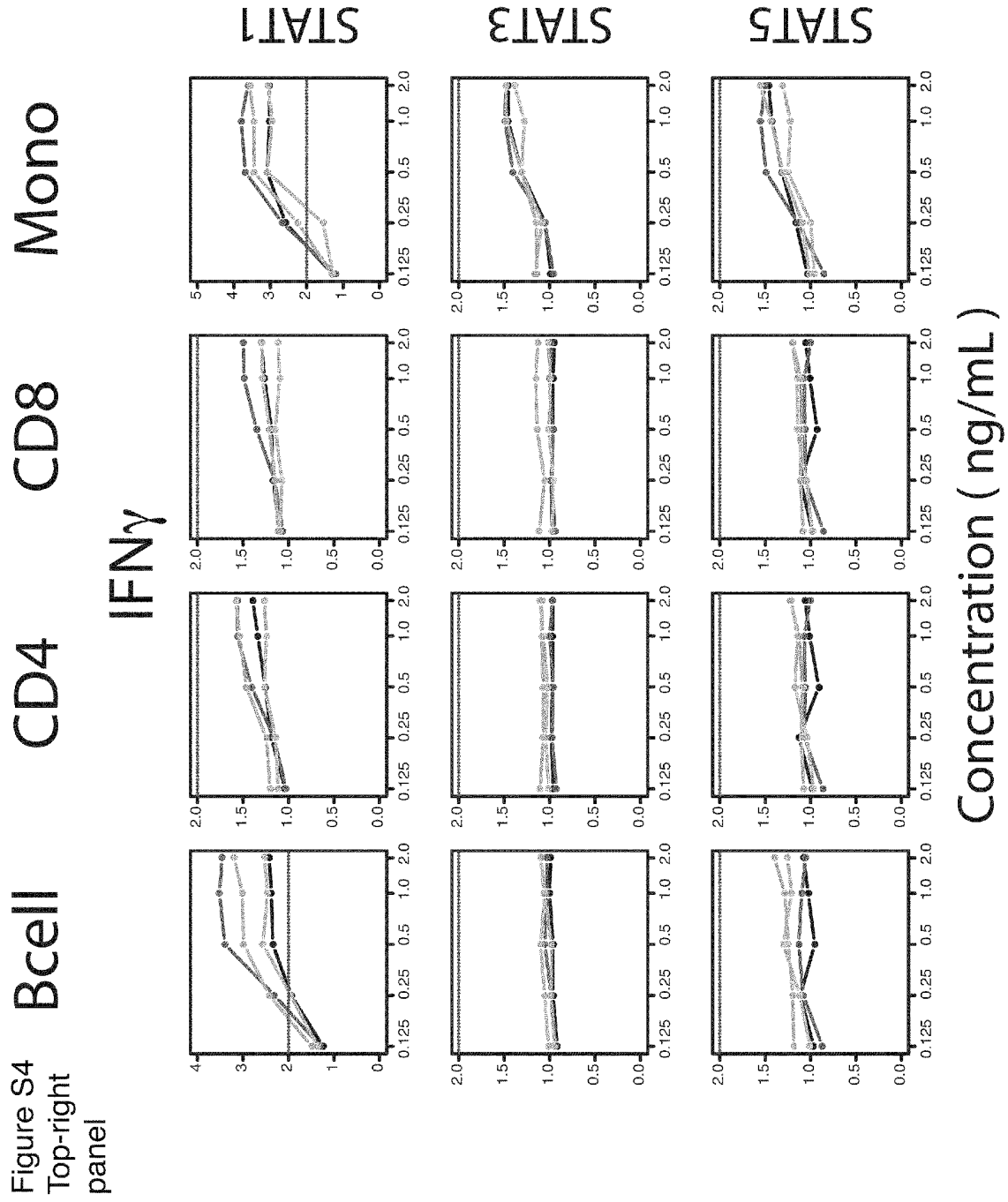


Figure S4  
Mid-left  
panel

IL-6

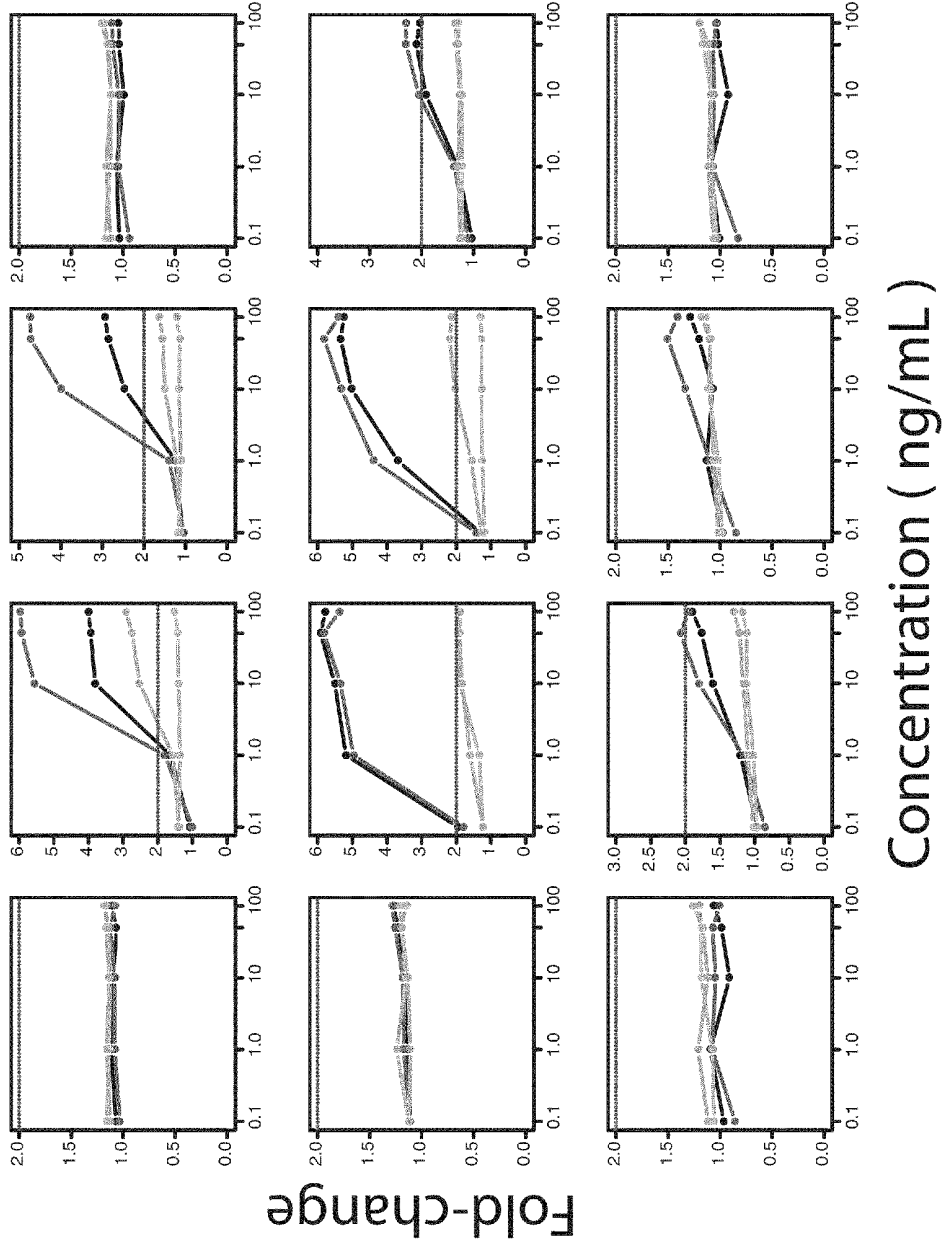


Figure S4  
Mid-right  
panel

IL-7

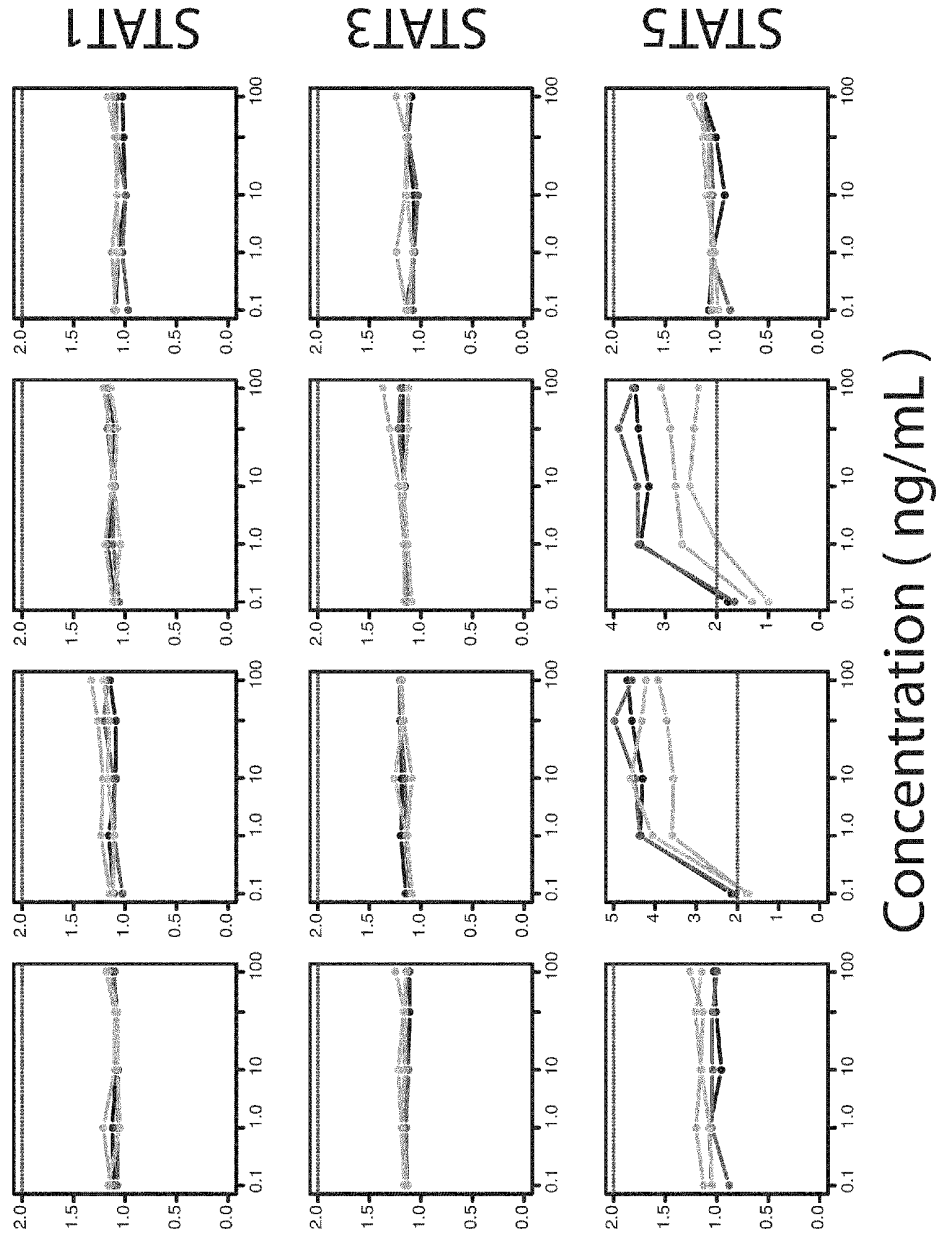


Figure S4  
Bottom-left  
panel

### IL-10

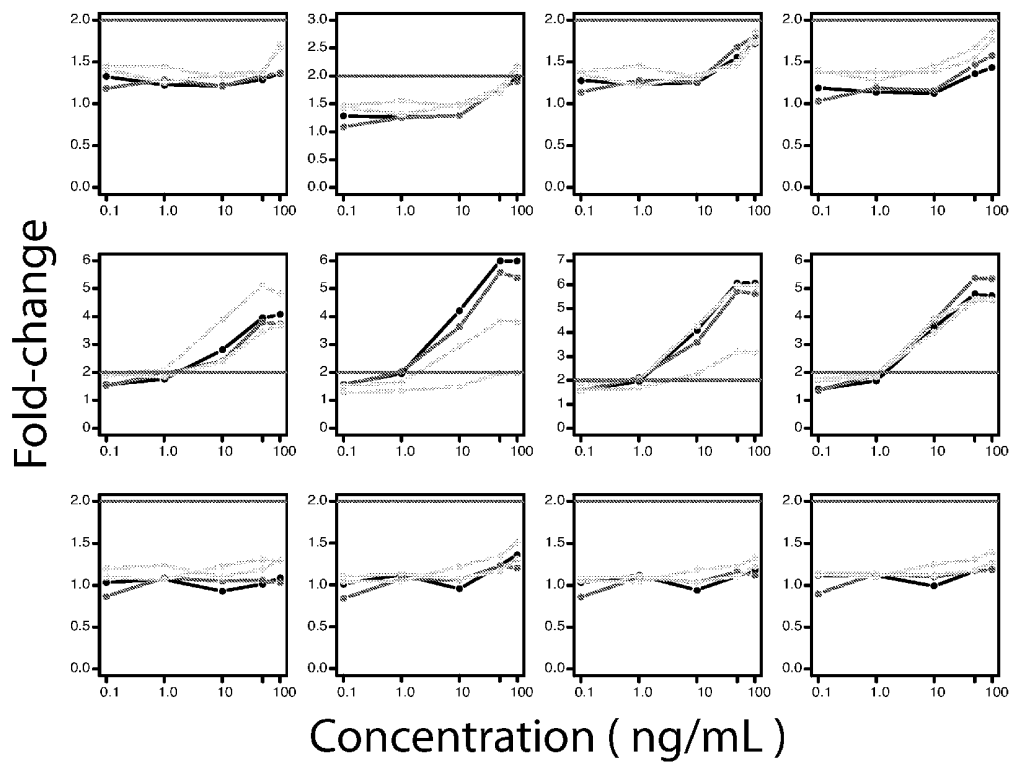


Figure S4  
Bottom-right  
panel

### IL-21

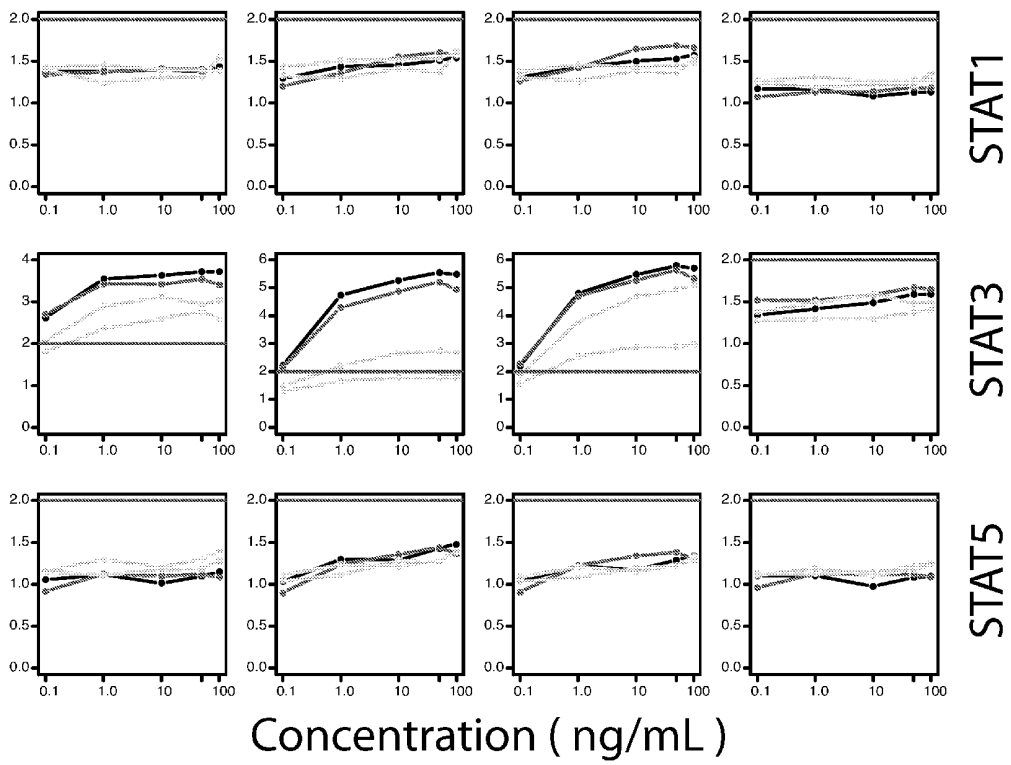


Figure S5

Difference in responses at highest doses / standard deviation of responses at all doses

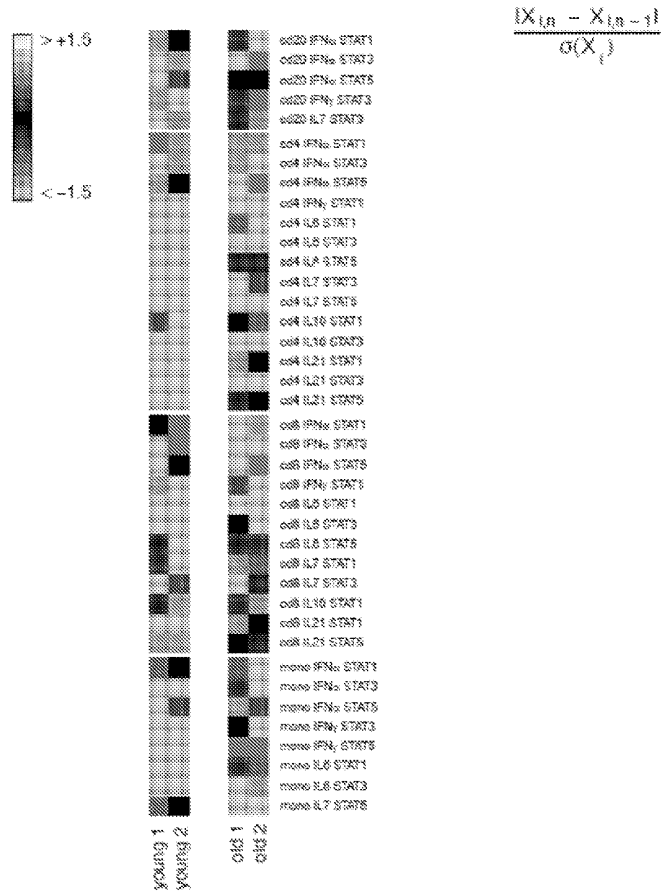


Figure S6

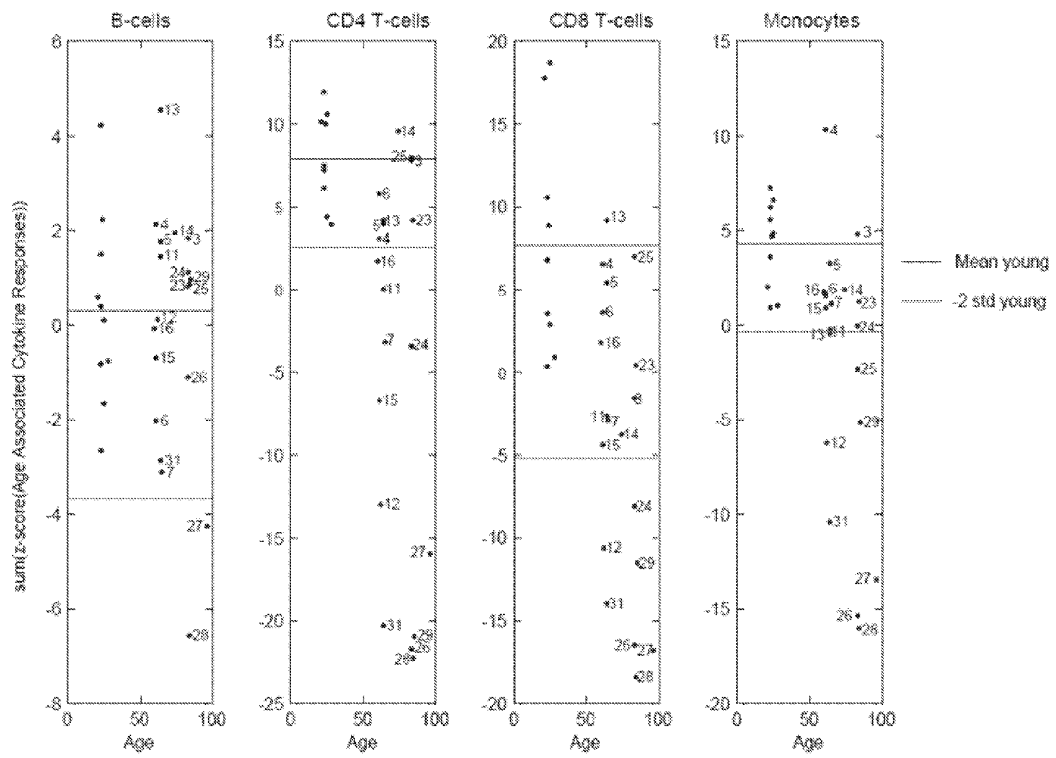


Figure S7

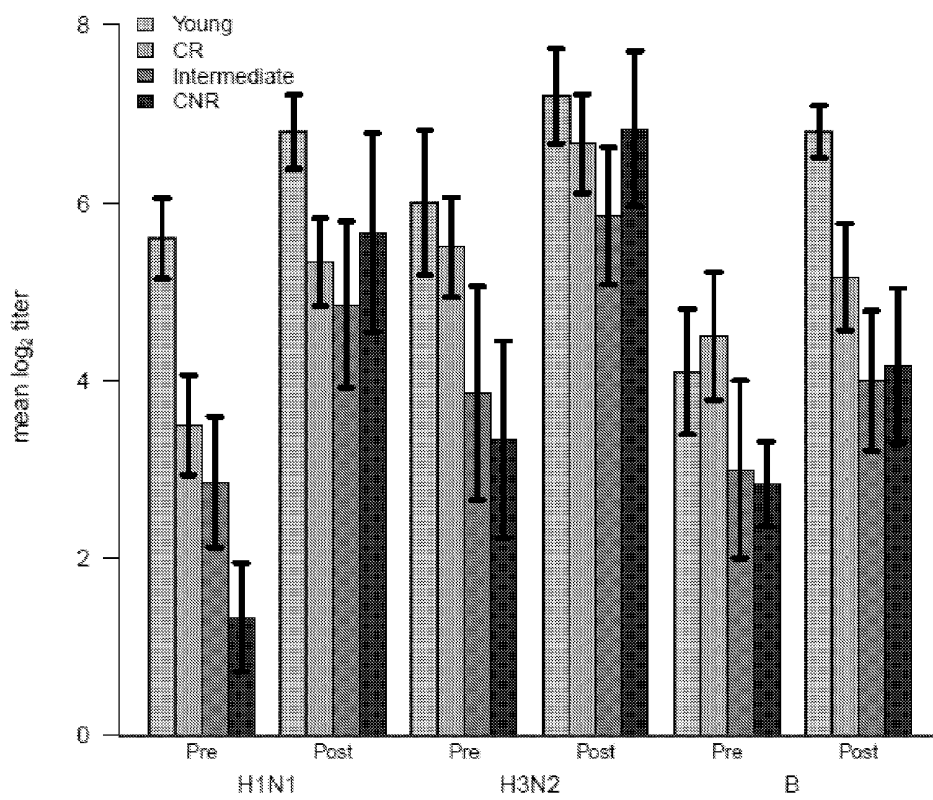


Figure S8

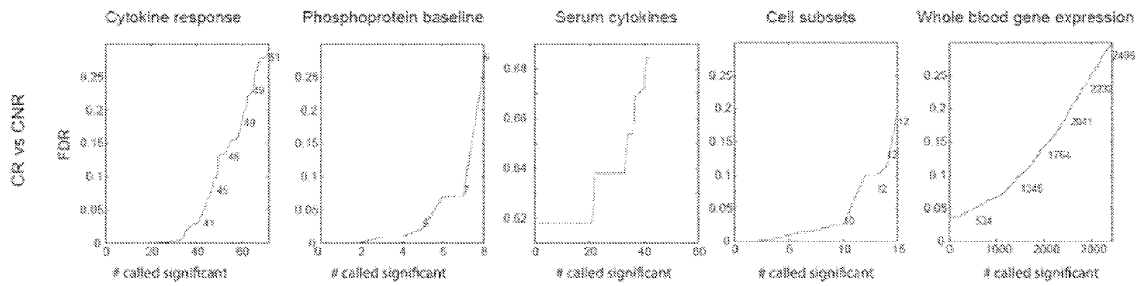


Figure S9

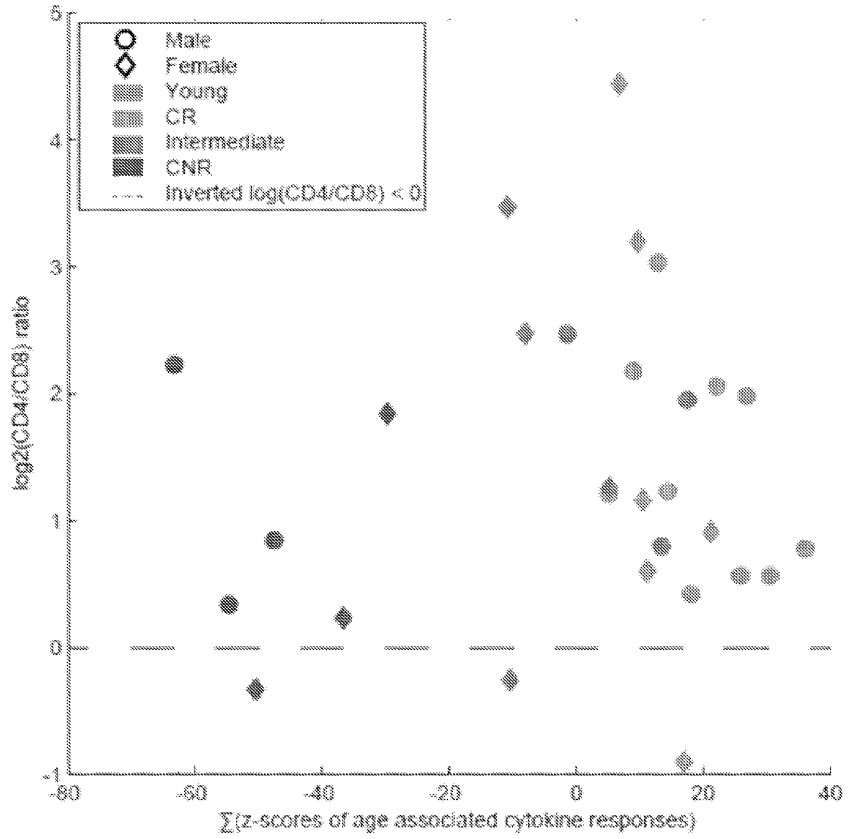


Figure S10

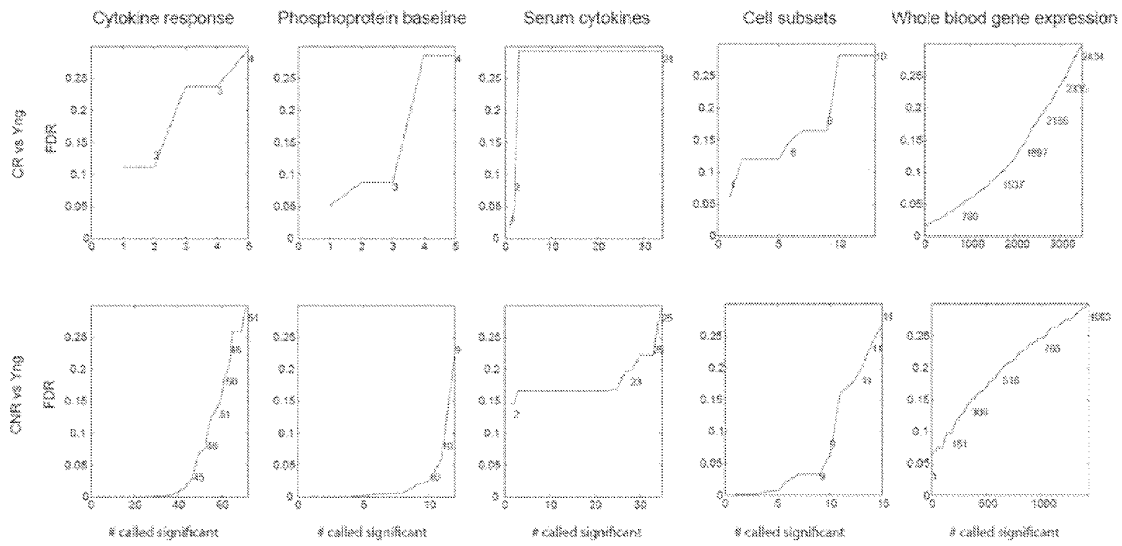


Fig S11:

Increase versus young

Decrease versus young

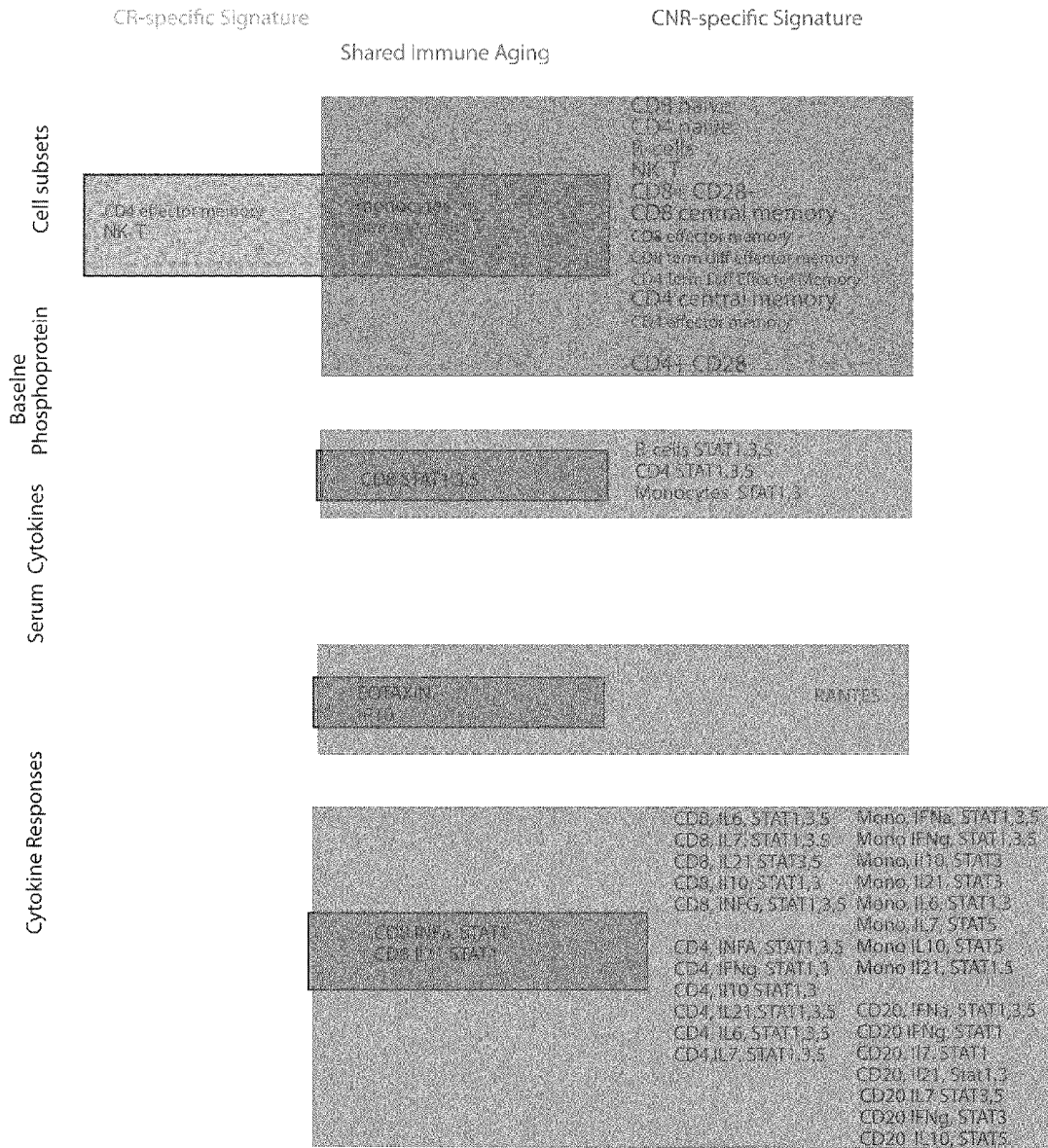


Figure S12  
Top-left  
panel

Bcell CD4 CD8 Mono

IFN $\alpha$

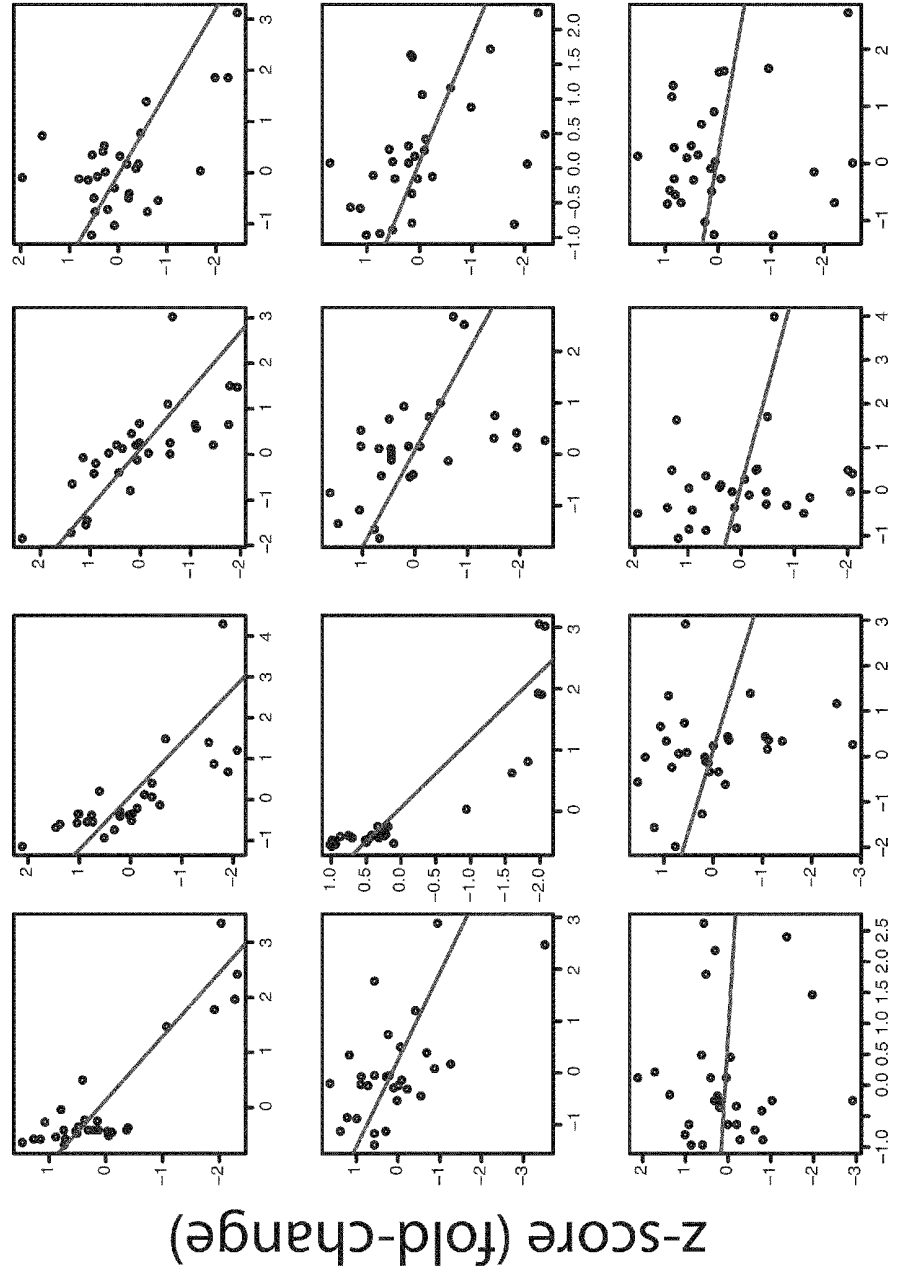
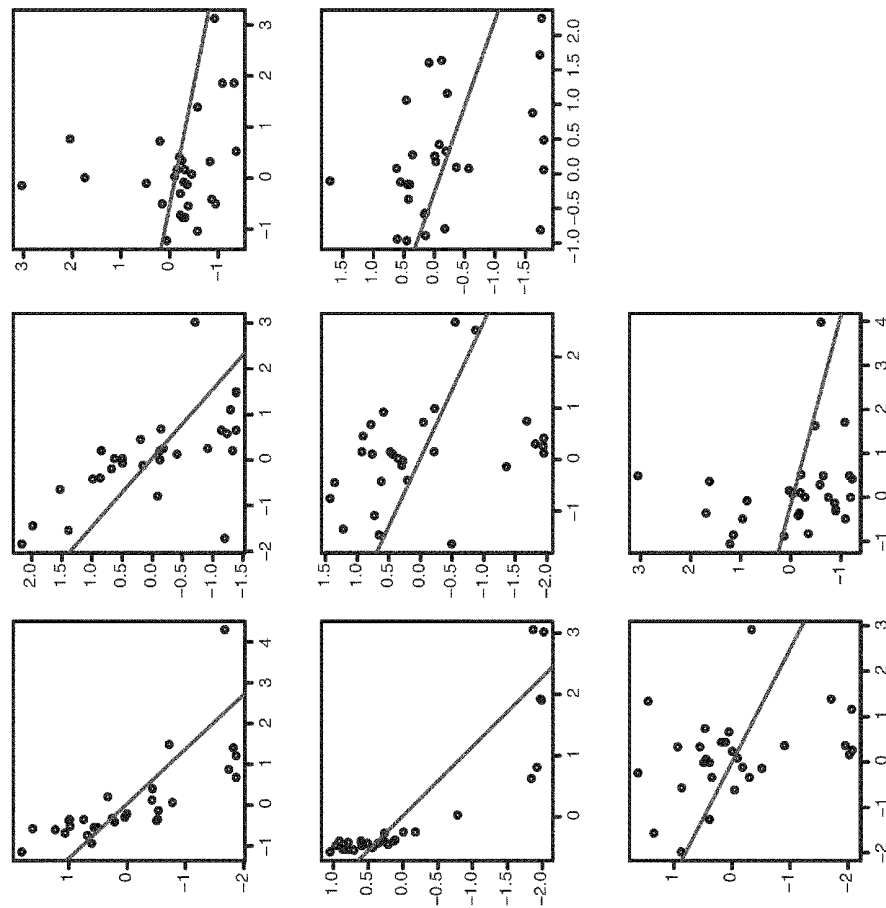


Figure S12  
Mid-left  
panel

IL-6



z-score (fold-change)

Figure S12  
Mid-right  
panel

IL-7

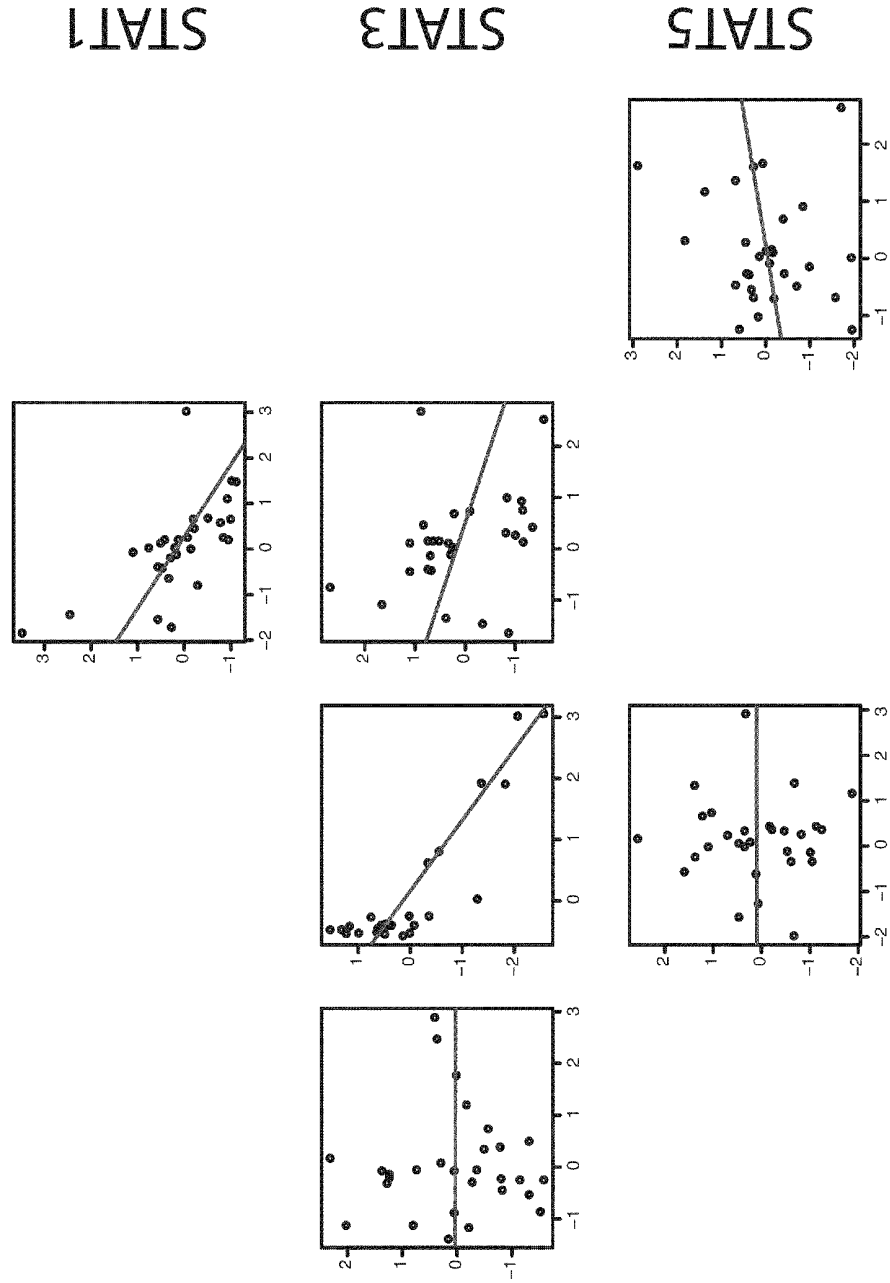
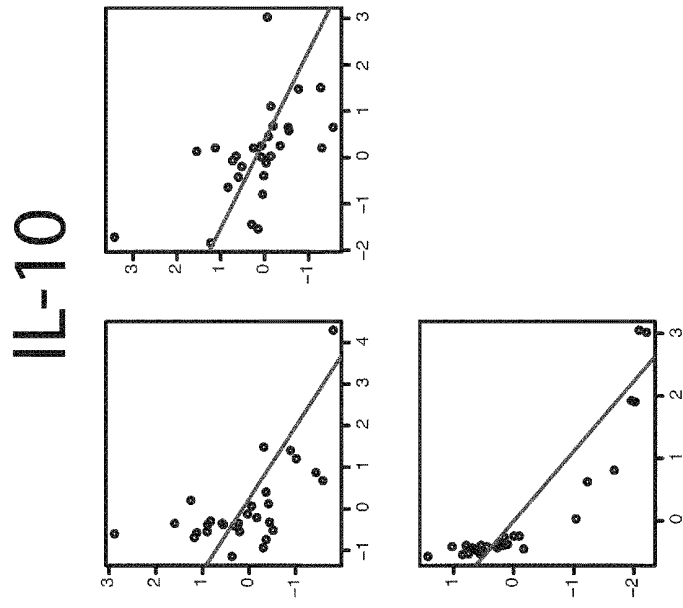


Figure S12  
Bottom-left  
panel



z-score (fold-change)

z-score (baseline)

Figure S12  
Bottom-right  
panel

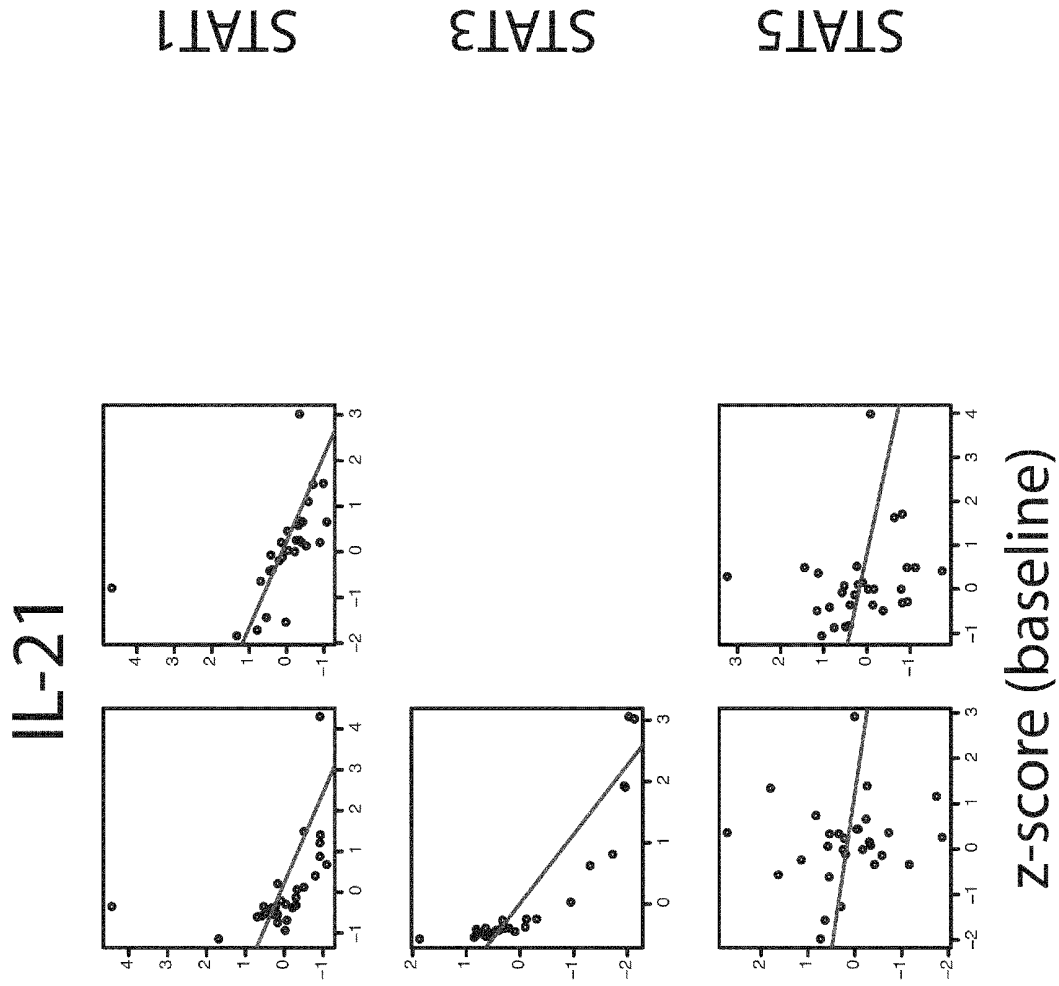
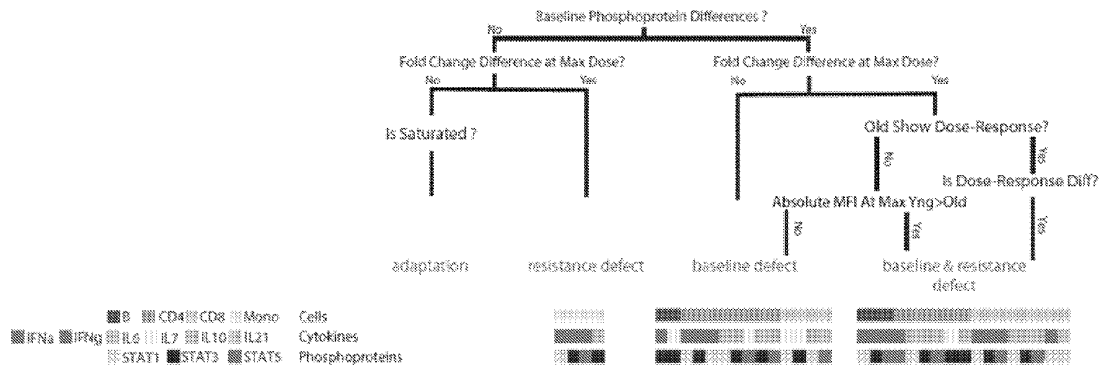


Figure S13



<ul style="list-style-type: none"> <li>CD4 CD8 Mono Cells</li> <li>IFN<math>\alpha</math> IFN<math>\gamma</math> IL6 IL7 IL10 IL21 Cytokines</li> <li>STAT1 STAT3 STAT5 Phosphoproteins</li> </ul>	<ul style="list-style-type: none"> <li>CD4 CD8 Mono Cells</li> <li>IFN<math>\alpha</math> IFN<math>\gamma</math> IL6 IL7 IL10 IL21 Cytokines</li> <li>STAT1 STAT3 STAT5 Phosphoproteins</li> </ul>	<ul style="list-style-type: none"> <li>CD4 CD8 Mono Cells</li> <li>IFN<math>\alpha</math> IFN<math>\gamma</math> IL6 IL7 IL10 IL21 Cytokines</li> <li>STAT1 STAT3 STAT5 Phosphoproteins</li> </ul>
--	--	--

**DIAGNOSTIC MARKERS OF  
IMMUNOSENESCENCE AND METHODS OF  
USE THEREOF**

RELATED APPLICATION

**[0001]** This application claims priority and other benefits from U.S. Provisional Patent Application Ser. No. 61/358,884, filed Jun. 25, 2010, entitled "Methods of identifying individuals with impaired immune function". Its entire content is specifically incorporated herein by reference.

STATEMENT OF GOVERNMENT SUPPORT

**[0002]** This invention was made with government support under U19 AI057229 awarded by the National Institutes of Health. The government has certain rights in the invention.

BACKGROUND

**[0003]** Deterioration of immune function is a prominent hallmark of aging and is only partially explainable by a loss of naïve and central memory CD4 T cells due to thymic involution. Defects in both the innate and adaptive immune system of the elderly have been described and include changes in immune cell-subsets abundance and relative frequencies, altered hematopoiesis, impairments in antigen presentation, decreased B cell as well as T cell proliferation, a reduced TCR repertoire and defect in antibody production (Weiskopf et al., 2009). Ultimately these alterations result in a sharp decline in the response to new and persisting antigens (immunosenescence). Thus it is not surprising that infectious diseases are one of the major causes of mortality in those over the age of 65 and that protective vaccination of the elderly is more difficult to establish than in younger individuals (Goodwin, 2006).

**[0004]** Active immunization and activation of T cell-mediated as well as humoral immune response can be achieved through the administration of immunogenic material or vaccines. Vaccination seeks to prevent, ameliorate or even treat against the harmful effects of pathogens and carcinogens, and regular vaccination has become an integral part of preventive medicine.

**[0005]** Due to the complexity of the immune system, studies of immunosenescence often only investigate one or a few variables of an individual's immune system. This has made it difficult to draw general conclusions about the phenomena being described or how they might relate to each other. Individuals who suffer from an impaired immune function generally face the risk of increased morbidity and mortality. This is particularly relevant for older individuals who show a reduced response to vaccination or have persistent cytomegalovirus infection (Strindhall et al., 2007). The immune system of those individuals can be phenotypically characterized as having an inverted CD4+ to CD8+ T-cell ratio (below one), and a high frequency of CD8+CD28- T-cells (Wikby et al., 2008). There is also evidence that other major causes of mortality in older individuals, such as cardiovascular diseases, cancer and Alzheimer's disease, might involve defects in normal immune function (Hansson, 2005; de Visser et al., 2006; Rojo et al., 2008). This raises the possibility that a functional immune response is a key factor in the maintenance of good health and longevity.

**[0006]** One of the most challenging topics facing the maintenance of good health and longevity is the identification of immunocompromised individuals who might appear healthy,

but who have an underlying, undetected impairment of immune function and, so, face the risk of increased morbidity and mortality. The present invention addresses this issue.

SUMMARY

**[0007]** Embodiments of the present invention provide diagnostic markers of immunosenescence and methods of identifying individuals with impaired immune function based on a combination of such markers obtained from various analyses, primarily from blood, testing immune function including the analysis of immune cell subset frequencies, gene expression, cytokine and chemokine levels, and signaling responses to stimulation with cytokines ('cytokine response'). Particular combinations of markers can predict with high accuracy whether an individual will respond to active vaccination and become protected against recurring diseases.

**[0008]** The above summary is not intended to include all features and aspects of the present invention nor does it imply that the invention must include all features and aspects discussed in this summary.

INCORPORATION BY REFERENCE

**[0009]** All publications mentioned in this specification are herein incorporated by reference to the same extent as if each individual publication or patent application was specifically and individually indicated to be incorporated by reference.

DRAWINGS

**[0010]** The accompanying drawings illustrate embodiments of the invention and, together with the description, serve to explain the invention. These drawings are offered by way of illustration and not by way of limitation; it is emphasized that the various features of the drawings may not be to-scale.

**[0011]** FIG. 1: Phosphorylation of STATs in response to cytokine stimulation drops with age. (A) Heat map of 72 cytokine stimulation assays measured across 29 individuals of different ages. Each assay measures the fold-change phospho-STAT-1, -3 or -5 in one of four immune cell subsets (B-cell, CD4 T-helper cells, CD8 cytotoxic T cells and monocytes) stimulated by one of six cytokines (IFN- $\alpha$ , IFN- $\gamma$ , IL6, IL7, IL10 and IL21) and measured by flow cytometry. Each assay appears in a single row and is color coded (left of heatmap) by the condition (cell subset, cytokine, pSTAT combination) (see legend on top). Coloring of the heat map cells reflects the normalized fold-change z-scores, that is, the number of standard deviations from the population mean of the assay. Age-associated differences at a ( $q \leq 0.15$ ) are marked on right (red decrease with age, purple, increase; grey, no significant difference). (B) Example scatter plot illustrating the reduced fold-change response of some older individual in CD4+ T cells stimulated by IL6 and assayed for STAT-3 phosphorylation. (C) Baseline phosphoSTAT levels increase with age. Shown are normalized z-scores. (D) Reduced cellular response in old individuals is independent of stimulus concentration. The entire 72-condition cytokine response assay was repeated at five different doses per stimuli for two young and two older individuals, whose average fold-change response to cytokine stimulation was respectively high or low. Shown is an example histogram (left) and line plot visualization (right) of the fold-change cytokine response as a function of cytokine stimuli concentration for each of the two young (black) and two old (cyan) individuals.

A fold change of 1 signifies no change from baseline. The young individuals show a significantly higher fold-change response than that observed in old individuals, at all concentrations (See Fig. S4 for all other assays). (E) A general reduction in cytokine responses is observed with age with some individuals showing systemic impairments in multiple assays. The y-axis plots the sum of z-scores all 39 age-associated responses.

**[0012]** FIG. 2: Systemic impairments in cytokine responses with age co-occur in a single individual with dysfunctional immune cell subsets and increased inflammation. (A) Age associated cytokine response deficiencies correlate with known cell subset immunosenescence markers such as the drop CD4<sup>+</sup> and CD8<sup>+</sup> naïve cell frequency, and known serum chemokine changes with age, but as measured in serum, not with cytokines such as IL-6 and IL-1 that are proinflammatory and known to rise with age. (B) Biological validation of increased pro-inflammatory cytokine environment at baseline in sorted monocytes of two cytokine stimulation non-responsive older individuals (cyan) compared to two young individuals (orange). (C) Sparse canonical correlation analysis identifies a module of network nodes whose weighted linear combination is maximally correlated with the cytokine response deficiency of a given cell type. The normalized weights of each cell's maximally correlated module are shown in a bar plot format (grayscale), sorted by the weights of the module maximally correlated with B-cell cytokine response.

**[0013]** FIG. 3: Cytokine responses define distinct age-related subgroups that are longitudinally stable. (A) Individuals are stratified as CR (green), CNR (blue) or an intermediate phenotype (purple) by scoring the number of cell-types for that individual in which significant impairment was observed compared with the mean of the young. (B) A longitudinal study of cytokine non-response (cytokine deficiency) in 21 returning individuals. Cytokine response state is stable or worsen with time ( $p < 0.02$ ). Shown are cytokine response class (top) or cell state (bottom) for baseline (year 1) and two subsequent years.

**[0014]** FIG. 4: Cytokine responder and non-responder older individuals have distinctly different immune system profiles. (A) The young and the CR group show more robust pre-vaccination antibody titer levels, compared with the CNR when considered simultaneously across all strains. At the population level, an antibody titer of 1:30-1:40 (above 5 on log<sub>2</sub> scale) represents probability of 50% protection against Influenza infection. Standard errors are shown. (B) Heatmap showing the association between immune system state and longevity. The z-score normalized expression of the top 60 longevity-associated genes from GenAge that are differentially expressed between CR and CNR (out of 159). Shown are all older individuals. Colored boxes on top reflect their cytokine response classification and the specific cells in which their response was reduced. Two distinct clusters of CR and CNR are observed with additional individuals clustering in CR. Genes are clustered by pathway membership (matrix on right).

**[0015]** FIG. 5: Stratification of older individuals by cytokine response yields increased resolution to age dependent changes. (A) Venn diagram summarizing the number of identified markers for each of the CR and CNR-specific signatures, as well as those changes that occur, independent of cytokine responses, with age. (B) Differing proportions of CR and CNR older individuals in aging studies may explain many

of the controversies in the immunosenescence literature. Examples highlight changes in age which either exclusive for both CR and CNR or common to both. Distinct: changes in the frequency of Eotaxin, NKT cells and B cells that are masked by the heterogeneity of older individuals. Common: The reduction in CD8<sup>+</sup> naïve cells is common to all older individuals, though much more dramatic in CNR. Standard errors are shown.

**[0016]** FIG. 6: Reduced responses to cytokine stimulation are primarily due to increased basal levels of phosphorylated STAT proteins and to alterations in response potential of IL6 and IFN $\alpha$  pathways. (A) Top: Four model classes which may yield the observed unresponsive cells phenotype: (1) successful adaptation to increased background abundance of cytokines, (2) a resistance defect in the signaling machinery of cells from older individuals, (3) an increase in baseline pSTAT levels, which may yield a reduced fold-change response to stimulation by exhausting finite quantities of protein to phosphorylate (4) a combination of both baseline and resistance defect factors. Bottom: Each age-associated cytokine responses deficiencies is classified into one of the four models using a decision tree. No adaptation is observed. Only the monocyte stimulations could be classified solely as a resistance defect. The rest all showed a significant elevation in the older individuals' baseline pSTAT levels, with IL6 and IFN $\alpha$  also showing defects in resistance pathways. (B) Inverse relationship between normalized baseline phosphoprotein abundance of pSTAT1 in CD8 cells (X-axis) and normalized fold-change response to stimulation by IFN $\alpha$  (Y-axis). Older individuals show a higher baseline level of pSTAT1 with a decreased response. (C) A cartoon model illustrating the queries used to discriminate between the different models of immune cells unresponsiveness.

**[0017]** Figure S1: Study schematic design—'One stop shop' multi-level biological analysis of blood from subjects of different age groups & gender

**[0018]** Figure S2: Immune cell subset gating scheme.

**[0019]** Figure S3: Number of measurements called significantly associated with age as a function of false discovery rate. Gene expression studies focused primarily on the immune and aging associated 2863 genes on the array which are measured by 4364 probes.

**[0020]** Figure S4: Reduced cellular response in the elderly is not concentration dependent. Shown are all dose-response curves for the 72 assays performed between young (grey) and old (cyan).

**[0021]** Figure S5: The majority of age-associated cytokine responses reach saturation in both young and older subjects at the highest concentration level. The standard deviation of the two last points in the dose response curve was calculated and visualized in a heatmap format. Very few of the assays are still changing significantly. Shown are all assays in which a fold-change response  $\geq 2$  is observed in at least one concentration in one or more subjects.

**[0022]** Figure S6: Cytokine stimulation responses by cell-type used to define CR and CNR. Sum of z-score normalized age-associated cytokine stimulation responses by cell-type. Dashed black line is the average of the young subjects. Dashed red line is 2 standard deviations from the young average. The IDs of older subject subjects are listed for each cell-type.

**[0023]** Figure S7: HAI titers grouped by cytokine responses. Titer levels pre and post vaccine grouped by response category and strain in vaccine. Seroprotection is

clinically defined as a value of  $\sim 5$  on this scale and seroconversion as a four-fold of higher change.

**[0024]** Figure S8: Number of measurements called significantly different between CR and CNR as a function of false discovery rate.

**[0025]** Figure S9: The “Immune Risk Profile” of inverted CD4/CD8 ( $<1$ ) ratio is not age specific and is highly variable. Though correlated, an inverted CD4/CD8 ratio is not specific or required for systemic impairments in cytokine responses. Shown is the ratio of CD4 to CD8 frequency as a function of the sum of all age-associated cytokine response assays. Young, CR, CNR and Intermediates are colored by their cytokine response class in year 1 in orange, green, purple or blue respectively.

**[0026]** Figure S10: Number of measurements called significantly different between CR and the young and CNR and the young as a function of false discovery rate.

**[0027]** Figure S11: Detailed classification of age-associated changes by cytokine response. Venn diagram illustrating the identified markers for each of the CR and CNR specific signatures, as well as those changes that occur, independent of cytokine responses, with age. For gene expression and statistics, see Table S7-S9.

**[0028]** Figure S12: An Inverse relationship between normalized baseline phosphoprotein abundance and fold-change. Shown are only those 39 assays for which an age-associated difference was detected in the data. Normalized Fold-change response on the Y axis, normalized baseline on the X.

**[0029]** Figure S13: Classification of cytokine response deficiency by cause. A decision tree over the cytokine response fixed dose and dose-response assays can discriminate between the different models of immune cells unresponsiveness. Shown are the decision tree classification for all age-associated cytokine responses as identified from the entire study population. No adaptation is observed. Only the monocyte stimulations could be classified solely as a resistance defect. The rest all showed a significant elevation in the older subjects’ baseline pSTAT levels, with IL6 and IFN $\alpha$  also showing defects in resistance pathways.

**[0030]** Table S1: Study design demographics

**[0031]** Table S2: Significant age-associated measurement from regression analysis of all subjects.

**[0032]** Table S3: GEO Datasets used in meta-analysis of aging gene expression data. Table lists all GSM data ids used for comparisons.

**[0033]** Table S4: Genes found to be significantly associated with age in the meta-analysis.

**[0034]** Table S5: Network cluster membership.

**[0035]** Table S6: Cytokine response modules feature weights

**[0036]** Table S7: Significant differences between CR and CNR.

**[0037]** Table S8: Medication category listing for CR and CNR.

**[0038]** Table S9: Age-associated differences common to both CR and CNR,

**[0039]** Table S10: CR-specific measurements.

**[0040]** Table S11: CNR-specific measurements.

**[0041]** Table S12: Dose-response classification results.

#### DEFINITIONS

**[0042]** The practice of the present invention may employ conventional techniques of chemistry, molecular biology,

recombinant DNA, microbiology, cell biology, immunology and biochemistry, which are within the capabilities of a person of ordinary skill in the art. Such techniques are fully explained in the literature. For definitions, terms of art and standard methods known in the art, see, for example, Sambrook and Russell ‘Molecular Cloning: A Laboratory Manual’, Cold Spring Harbor Laboratory Press (2001); ‘Current Protocols in Molecular Biology’, John Wiley & Sons (2007); William Paul ‘Fundamental Immunology’, Lippincott Williams & Wilkins (1999); M. J. Gait ‘Oligonucleotide Synthesis: A Practical Approach’, Oxford University Press (1984); R. Ian Freshney ‘Culture of Animal Cells: A Manual of Basic Technique’, Wiley-Liss (2000); ‘Current Protocols in Microbiology’, John Wiley & Sons (2007); ‘Current Protocols in Cell Biology’, John Wiley & Sons (2007); Wilson & Walker ‘Principles and Techniques of Practical Biochemistry’, Cambridge University Press (2000); Roe, Crabtree, & Kahn ‘DNA Isolation and Sequencing: Essential Techniques’, John Wiley & Sons (1996); D. Lilley & Dahlberg ‘Methods of Enzymology: DNA Structure Part A: Synthesis and Physical Analysis of DNA Methods in Enzymology’, Academic Press (1992); Harlow & Lane ‘Using Antibodies: A Laboratory Manual: Portable Protocol No. 1’, Cold Spring Harbor Laboratory Press (1999); Harlow & Lane ‘Antibodies: A Laboratory Manual’, Cold Spring Harbor Laboratory Press (1988); Roskams & Rodgers ‘Lab Ref: A Handbook of Recipes, Reagents, and Other Reference Tools for Use at the Bench’, Cold Spring Harbor Laboratory Press (2002); Alon U (2007). An introduction to systems biology: design principles of biological circuits (Boca Raton, Fla.: Chapman & Hall/CRC). Each of these general texts is herein incorporated by reference.

**[0043]** Unless defined otherwise, all technical and scientific terms used herein have the same meaning as commonly understood by a person of ordinary skill in the art to which this invention belongs. The following definitions are intended to also include their various grammatical forms, where applicable.

**[0044]** The term “impaired immune function”, as used herein, refers to any reduction in immune function in an individual, as compared to a fully healthy individual. Individuals with an impaired immune function are readily identifiable by substantially increased abundance of CD8+ CD28- cells or more broadly by reduced cytokine responses, increased baseline phosphoprotein levels and other co-occurring measures.

**[0045]** The term “older individual”, “elderly individual” or “elderly”, as used herein, defines a human being who is about 60 years of age or older.

**[0046]** The term “young individual”, as used herein, defines a human being between 18 and 30 years of age.

**[0047]** The term “activation”, as used herein, refers to a physiological condition upon exposure to a substance, allergen, drug, protein, chemical, or other stimulus, or upon removal of a substance, allergen, drug, protein, chemical or other stimulus.

**[0048]** The terms “active immunization”, “immunization”, and “vaccination”, as used herein, refer to the acquisition of immunologic memory and long-term protection against recurring diseases through antibody production in response to administration of an immunogenic antigen.

**[0049]** The term “cytometry”, as used herein, refers to a process in which physical and/or chemical characteristics of single cells, or by extension, of other biological or nonbio-

logical particles in roughly the same size or stage, are measured. In “flow cytometry”, the measurements are made as the cells or particles pass through the measuring apparatus (flow cytometer) in a fluid stream. A cell sorter, or flow sorter, is a flow cytometer that uses electrical and/or mechanical means to divert and collect cells (or other small particles) with measured characteristics that fall within a user-selected range of values.

**[0050]** Immune system profiling and data output. In order to identify impairment of immune function in an individual, an immune system profile is established from measurements of immune cell subset frequencies, gene expression, cytokine and chemokine levels, and signaling responses to stimulation with cytokines. Following data analysis, the identified immune system profile is transformed into information for graphical display or output to a computer-readable medium, computer or computer network.

#### DETAILED DESCRIPTION

**[0051]** Embodiments of the present invention provide diagnostic markers of immunosenescence and methods of identifying individuals with impaired immune function based on a combination of such markers obtained from various analyses, primarily from blood, testing immune function including the analysis of immune cell subset frequencies, gene expression, cytokine and chemokine levels, and signaling responses to stimulation with cytokines (‘cytokine response’). Particular combinations of markers can predict with high accuracy whether an individual will respond to active vaccination and become protected against recurring diseases.

#### Cells of the Immune System

**[0052]** White blood cells or leukocytes are cells of the immune system that defend the human body against infectious disease and foreign materials and are often characterized as granulocytes or agranulocytes, depending on the presence or absence of granules. There are various types of leukocytes, which are all produced in the bone marrow and derived from (multipotent) hematopoietic stem cells. Leukocytes are found throughout the body, including the blood and lymphatic system. Granulocytes encompass neutrophils, basophils, and eosinophils, while agranulocytes include lymphocytes, monocytes and macrophages.

**[0053]** B lymphocytes (“B cells”) and T (thymus) lymphocytes (“T cells”) constitute the two major classes of lymphocytes and play crucial roles in the immune response; hereby provide B cells a ‘humoral’ immune response through secreted antibodies, while T cells provide a cell-mediated immune response through the activation of various cells of the immune systems such as macrophages, natural killer cells, cytotoxic T cells, cytokines etc.

**[0054]** B cells are precursors of antibody-secreting cells and, upon activation, differentiate either into antibody-secreting cells for a primary response via secreted antibodies upon a first exposure to an antigen or into memory B cells which provide a strong antibody response upon a second exposure to that same antigen.

**[0055]** T cells can function as (i) effector cells in cell-mediated responses, as (ii) helper cells in both humoral and cell-mediated immune responses or as (iii) regulatory cells. Typical functions of effector T cells are, for example, the lysis of pathogen-infected cells or the lysis of neoplastic cells, while typical functions of helper T cells are aiding in the

production of specific antibodies by B cells; (immune) regulatory T cells, in contrast, are able to suppress immune responses.

#### The Innate Immune System and Immune Response

**[0056]** Pathogens such as viruses cause an inflammatory reaction in the body through chemokine-mediated recruitment of leukocytes to the site of infection. Neutrophils are attracted first, followed by monocytes, macrophages, natural killer cells, cytokines as well as other innate immune cells. Those innate immune cells then provide critical signals for dendritic cells that help to initiate a T cell-mediated, antigen-dependent or adaptive immune.

**[0057]** Cytokines are peptides, proteins and glycoproteins that are secreted by cells of the immune system and, as signaling molecules, carry signals between cells. Based on their function, cytokines can be classified as lymphokines, interleukins and chemokines. They are often categorized into a) the IL-2 subfamily, b) the interferon (IFN) subfamily and c) the IL-10 subfamily.

#### T Cell-Mediated, Antigen-Dependent or Adaptive Immune Response

**[0058]** Secondary lymphoid tissues are the focal point of an adaptive immune response, because there naïve T cells are presented with and activated through physical contact with mature dendritic cells that present specific foreign antigen peptide/MHC complexes.

**[0059]** The transition from innate to adaptive phases of the immune response involves antigen uptake by antigen-presenting cells, particularly by dendritic cells. Dendritic cells support clonal expansion and differentiation of activated, antigen-specific T cells by providing proliferative information through foreign antigen peptide/MHC complexes and possibly through costimulatory ligands such as CD80 and CD86, which are ligands for CD28, an important cell-surface receptor on T cells that helps to initiate mitogenic signaling in naïve T cells.

**[0060]** After naïve helper T cells (CD4 T cells) have become activated and begin to divide and differentiate according to signals from dendritic cells and other co-stimulatory ligands, at least three subsets of effector CD4 T cells ( $T_{H1}$ ,  $T_{H2}$  and  $T_{H17}$ ) emerge with specialized homing properties and functions in the adaptive immune response.

#### Immunosenescence

**[0061]** Defects in both the innate and adaptive immune system have been described and include changes in immune cell subsets abundance and relative frequencies, altered hematopoiesis, impairments in antigen presentation, decreased B cell as well as T cell proliferation, a reduced TCR repertoire and defects in antibody production (Weiskopf et al., 2009). Ultimately these alterations result in a sharp decline in the response to new and persisting antigens and are referred to in the aggregate as immunosenescence. Thus it is not surprising that infectious diseases are one of the major causes of mortality in those over the age of 65 and that protective vaccination of the elderly is more difficult to establish than in younger individuals (Goodwin et al., 2006).

#### Signal Transducers and Activator of Transcription (STAT) Proteins

**[0062]** The STAT proteins regulate many aspects of cell growth, survival and differentiation. The transcription factors

of this family are activated by the Janus Kinase JAK and dysregulation of this pathway is frequently observed in primary tumors and leads to increased angiogenesis, enhanced survival of tumors and immunosuppression.

**[0063]** There are seven STAT proteins, namely STAT1, STAT2, STAT3, STAT4, STAT5A, STAT5B and STAT6. STAT proteins were originally described as latent cytoplasmic transcription factors that require phosphorylation for nuclear retention. The unphosphorylated STAT protein shuttles between cytosol and the nucleus waiting for its activation signal. Once the activated transcription factors reaches the nucleus it binds to a consensus DNA-recognition motif called gamma activated sites (GAS) in the promotor region of cytokine inducible genes and activates transcription of these genes.

#### UTILITY OF THE INVENTION

**[0064]** While it is well known that the immune response in older individuals decreases with increasing age, no clear causal link has been established. Due to the complexity of the immune system, only a small fraction of the immune system is conventionally investigated which has made it difficult to draw general conclusions about the phenomena observed to date.

**[0065]** Embodiments of the present invention provide methods to identify individuals, particularly older individuals, who look on the outside healthy, but might already be at an increased risk for infection due to an impairment of their immune system, by comprehensively evaluating, primarily from blood specimen, a multitude of biomarkers obtained from various analyses testing immune function including the analysis of immune cell subset frequencies, gene expression, cytokine and chemokine levels, and signaling responses to stimulation with cytokines ('cytokine response'). This provides a full picture readout with wide diagnostic applications to individuals of any age who might be at risk of developing an impaired immune function or already experiencing signs of an impaired immune function. Diagnostic application of these biomarkers to individuals of any age and health status followed by an appropriate treatment, if necessary, may reduce the risk of infection as well as morbidity and increase lifespan.

**[0066]** Embodiments of the present invention provide diagnostic markers of immunosenescence and methods of identifying individuals with impaired immune function based on a combination of such markers obtained from various analyses, primarily from blood, testing immune function including the analysis of immune cell subset frequencies, gene expression, cytokine and chemokine levels, and signaling responses to stimulation with cytokines ('cytokine response'). Particular combinations of markers can predict with high accuracy whether an individual will respond to active vaccination and become protected against recurring diseases

**[0067]** Following active vaccination, older individuals often don't develop a fully functioning adaptive immune response, as would be evidenced by a strong antibody production against an introduced immunogen, and, thus, do not obtain the benefits of long-lasting protection against recurring diseases. It is an advantage of the present invention that particular combinations of markers can predict with a very high accuracy whether an individual will respond appropriately to active vaccination and become protected against recurring diseases.

**[0068]** As illustrated in particular embodiments of the present invention, cell cytokine responses are reduced with age and independent from the stimuli dose (see FIGS. 2 and 3), and correlate with increased cytokine baseline levels (see FIG. 4). Poor cytokine response correlates with other immunosenescence phenotypes (see FIG. 5). Stratification of older adults by cytokine response yields increased resolution to age dependent changes.

**[0069]** As will be apparent to those of skill in the art upon reading this disclosure, each of the individual embodiments described and illustrated herein has discrete components and features which may be readily separated from or combined with the features of any of the other several embodiments without departing from the scope or spirit of the present invention. Any recited method can be carried out in the order of events recited or in any other order which is logically possible. In the following, experimental procedures and examples will be described to illustrate parts of the invention.

#### EXPERIMENTAL PROCEDURES

**[0070]** The following methods and materials were used in the examples that are described further below.

**[0071]** Sample Collection. Peripheral blood samples were obtained from 29 male and female volunteers aged 18-96 (see Table S8 for demographics) at the Stanford Clinical Trials Research Unit as part of an influenza vaccine study. All volunteers were considered to be currently healthy after an evaluation of their medical history and assessment of their vital signs. Females of childbearing potential were tested for pregnancy by a urine sample. Volunteers had no active systemic or serious concurrent illness, no history of immunodeficiency, nor any known or suspected impairment of immunologic function, including clinically significant liver disease, diabetes mellitus treated with insulin, moderate to severe renal disease, blood pressure >150/95 at screening, chronic hepatitis B or C, recent or current use of immunosuppressive medication. In addition, none of the volunteers were recipients or donors of blood or blood products within the past 6 months and 6 weeks respectively nor showed any signs of febrile illness on day of enrollment and baseline blood draw. Informed consent was obtained from all of the subjects enrolled in this study, and the study protocol was approved by the Stanford University Administrative Panels on Human Subjects in Medical Research (IRBs). In total, 120 ml whole blood (~40 mL/visit) whole blood was drawn per subject and processed by standard procedures to PBMC and serum, if needed (see below). All analyses described here were performed from samples drawn on the same visit (visit 1) with the exception of cell-subset phenotyping, which were analyzed from blood drawn 21 days after initial visit following verification that cell-subset frequencies do not alter significantly in that time frame.

**[0072]** Whole Blood Gene Expression. Total RNA was extracted from the PAXgene RNA blood (PreAnalytiX GmbH, VWR part # 77776-026, USA) using the QIAcube automation RNA extraction procedure according to the manufacturer's protocol (Qiagen Inc., Valencia, Calif., USA). Amount of total RNA, and A260/A280 and A260/A230 nm ratios were assessed using the NanoDrop 1000 (Thermo Fisher Scientific Inc., Wilmington, Del.). RNA integrity was assessed using the Agilent 2100 Bioanalyzer (Agilent Technologies, Santa Clara, Calif.). In each sample the RNA integrity number (RIN) were measured. A two-color gene expression system was used to determine the expressed

mRNAs in the given samples. For each sample, 500 ng of total RNA were labeled with Cyanine 3-CTP and 500 ng of Universal Human Reference RNA (Stratagene, Cat Nr: 740000) were labeled with Cyanine 5-CTP. The combined labeled samples were hybridized onto the Agilent whole human genome microarrays (G4112F, Agilent Technologies, Santa Clara, USA). After hybridization, the mRNA slides were scanned on an Agilent DNA microarray scanner (Agilent Technologies, Santa Clara, USA). Agilent Feature Extraction Software (Version 10.5.1.1) was used to extract the microarray images data. After checking the quality of each subject array, the Feature Extraction files were imported into R Bioconductor and analyzed using the Agi4x44PreProcess package for probe filtering, quantile normalization and replicate probe summarization. We required that probes be detected, above background and the negative controls on the array, unsaturated, and not be detected as a population outlier, or non-uniform outlier with a lower limit of detection of 75. For all subsequent analyses, we included 29,849 array elements whose expression fulfills these criteria. The original microarray data files were entered into the Stanford Microarray Database (<http://genome-www5.stanford.edu/>), and they can be accessed by choosing "public login" and then selecting experimenter "HIMC" and experiments "Gergana".

**[0073]** Serum cytokine levels. Serum samples were obtained by centrifugation of clotted blood and stored at  $-80^{\circ}\text{C}$ . before cytokine levels determination. 42-plex kits were purchased from Millipore and used according to manufacturer's recommendations with modifications as described below. Briefly, samples were mixed with antibody linked polystyrene beads on 96-well filter plates and incubated at room temperature for 2 hours followed by overnight incubation at  $4^{\circ}\text{C}$ . Plates were then vacuum filtered and washed twice prior to 2-hour incubation with biotinylated detection antibody. Samples were filtered as above, washed twice and resuspended in streptavidin-PE. After incubation for 40 minutes at room temperature, two additional vacuum washes were performed, and the samples resuspended in Reading Buffer. Each sample was measured in duplicate. Plates were read using a Luminex LabMap200 instrument with a lower bound of 100 beads per sample per cytokine. The Luminex LabMap200 outputs the fluorescence intensity of each bead measured for a given cytokine in a sample. For each well, we considered the median fluorescence intensity (MFI) of all beads measured for that cytokine in a well as its abundance and averaged the MFI of the two replicates to obtain the abundance of a cytokine in a sample.

**[0074]** HAI assays. Participants were immunized with one dose of the trivalent inactivated seasonal influenza vaccine (TIV) post baseline blood draw, as described above. Blood samples were collected on day 0 before vaccination, as well as day 7 and day 28 post vaccination. Sera were prepared with the day 0 and day 28 blood samples. The HAI assay was performed using a standard technique (Prevention, 1998); serially diluted 25- $\mu\text{l}$  aliquots of serum samples in PBS were mixed with 25- $\mu\text{l}$  aliquots of virus, corresponding to four HA units, in V-bottom 96-well plates (Nunc, Rochester, N.Y., USA) and incubated for 30 minutes at room temperature. At the end of the incubation, 50  $\mu\text{l}$  of 0.5% chicken (for influenza A/H1N1 and B viruses) or turkey (for influenza A/H3N2 virus) red blood cells was added and incubated for a minimum of 45 minutes before reading for HAI activity. The HAI titer of a given sample was defined as the reciprocal of the last

serum dilution with no HA activity. A titer of 2 was assigned to all samples in which the first dilution (1:4) was negative.

**[0075]** PBMC phenotyping. Whole blood samples were subjected to density gradient centrifugation and PBMC were collected for phenotyping and phosphoflow assay (see below). Cells were frozen in DMSO with 10% FBS at  $-80^{\circ}\text{C}$ . overnight prior to transferring to liquid nitrogen. For cell subset analysis, cells were thawed, washed twice with warm culture media and stained with the following antibody cocktail: CD3 AmCyan, CD4 Pacific Blue, CD8 APCH7, CD28 APC, CD27 PE, CD45RA PE-Cy5, CD19 Alexa Fluor700, CD56 PE, CD33 PE-Cy7, TCR $\gamma\delta$  APC, all reagents from BD Biosciences. Incubation with antibodies was performed for 30 min at  $4^{\circ}\text{C}$ . Cells were washed and resuspended in FACS buffer. Data were collected using DIVA software in an LRSII instrument (BD Biosciences). Data analysis was performed using FlowJo 8.8.6 by gating on live cells, then using double gating for singlet discrimination, followed by cell subset specific gating. The median fluorescent intensity was used in the calculation of percentage of positive cells for a given cell subset.

**[0076]** Phosphorylation of STAT Proteins in Response to Cytokine Stimulation.

**[0077]** Thawed PBMC were rested for 1 hour in warm RPMI media with 10% FBS (culture media) before stimulation. Cells were distributed in 96-deep well blocks and stimulated for 15 min at  $37^{\circ}\text{C}$ . with IFN- $\gamma$ , IL6, IL7, IL10, IL21 at 50 ng/ml or with  $10^4$  U/ml IFN- $\alpha$ . After stimulation, cells were fixed with 1.5% PFA at room temperature for 10 min and washed with an excess of plain PBS. Cells were then spun down at 2000 rpm for 5 min at  $4^{\circ}\text{C}$ . and permeabilized with 100% cold methanol for 20 min on ice. Stimuli conditions were barcoded using a 3x3 matrix with Pacific Orange and Alexa Fluor 750 (Invitrogen Corp) at 0.03 and 0.04  $\mu\text{g}/\text{ml}$  for low staining and 0.2 and 0.3  $\mu\text{g}/\text{ml}$  for high staining, respectively (Krutzik and Nolan, 2006). Incubation with barcoding dyes was performed at  $4^{\circ}\text{C}$ . for 30 minutes. After several washes with FACS buffer (PBS 2% FBS, 0.1% Na Azide) stimulated and barcoded cells were pooled into single tubes and stained for 30 min at  $4^{\circ}\text{C}$ . with an antibody cocktail containing anti pSTAT1 Alexa Fluor 488, pSTAT3 Alexa Fluor 647, pSTAT5 PE, CD3 Pacific Blue, CD4 PerCP-Cy5.5, CD20 PerCP-Cy5.5 and CD33 PE-Cy7 (all from BD Phosflow). After washing, cells were resuspended in FACS buffer and acquisition was performed on an LRSII instrument (BD Biosciences). Data were collected using DIVA software in an LRSII instrument (BD Biosciences). Data analysis was performed using FlowJo 8.8.6. by gating on live cells, then using double gating for singlet discrimination, followed by cell subset specific gating (see Fig. S2 for gating strategy). A drawback of this technology that limits the cell subset resolution is the availability of commercial antibodies that bind to epitopes resistant to methanol fixation. Therefore, we used antibodies to CD3 and CD4 to identify CD4 (CD3 $^{+}$ CD4 $^{+}$ ) and non-CD4 T cells (CD3 $^{+}$ CD4 $^{-}$ ); CD20 for B cells and CD33 to identify monocytes. One caveat of this strategy is the contribution of  $\gamma\delta$ - and NK-T cells to the CD8 signal, because all three subsets are CD3 $^{+}$ CD4 $^{-}$ . Gamma-delta and NKT cells constitute only a minority of lymphocytes while the frequency of CD8 T cells is often more than 30% of PBMC. We thus refer to the non-CD4 fraction as CD8 $^{+}$  T cells. Phosphorylation of STAT1, 3, and 5 proteins in B cells, CD4/CD8 T cells or monocytes was analyzed by debarcoding on stimulus-specific gating (see Fig. S2). Fold change between stimulated

and unstimulated conditions was calculated using the 90th percentile of the pSTAT1, 3, or 5 positive cells. Using the median fluorescent intensity instead of the 90th percentile did not alter the observation of significant age dependent decline in phosphoprotein levels in response to cytokine stimulation.

**[0078]** We analyzed 29 samples at a single cytokine stimuli concentration, performed over the course of 3 days by 2 different subjects. Baseline phosphoprotein abundance in a given cell was measured in 6 replicates, averaged and day normalized by dividing the average measurement on a given day. Fold-change difference due to stimulation was computed as the ratio of the cell, cytokine stimulation, phosphoprotein measure to the raw, un-normalized, cell-phosphoprotein matching baseline that was measured on the same plate. Fold-change values were normalized by the average fold-change difference of a given cell-cytokine stimulation-phosphoprotein measure on a given day. We tested each assay for day dependent differences. No significant differences between days were detected post-day normalization and cytokine responders and non-responders were present in all three days.

**[0079]** For the dose-response assay, we measured three pairs of old and young subjects that we paired on a single 96-deep well plate and stimulated for 15 min at 37° C. The protocol was identical to the one described above, with the exception of the cytokine stimulation doses: for IFN- $\gamma$ , IL6, IL7, IL10, and IL21 we stimulated cells with 0.1, 1, 10, 50 and 100 ng/ml of cytokine whereas for IFN- $\alpha$  we stimulated with 0.12, 0.25, 0.5 1 and  $2 \times 10^4$  U/ml. Baseline phosphorylated STAT levels were measured for each subject per plate in 5 replicates. Sample normalization was performed in the same manner as is described above for all 29 samples. To determine if a fold-change difference exists for a given cell, cytokine, phosphoprotein assay between old and young we used a t-test at the highest dose stimuli concentration and corrected for multiple hypotheses testing (Storey and Tibshirani, 2003). Of the three pairs of old-young samples we tested, one pair was missing a single, but different, measurement for each stimulus. Though the results were fully consistent with those observed in the two other old-young pairs (i.e. the young subject showed increased fold-change for all doses for a large number of assays), we did not include results from this pair in any of the analysis discussed here.

**[0080]** Cytokine levels in cultured monocytes and T cells. PBMC from two young and two older subjects were thawed and washed once with warm RPMI media supplemented with 10% FBS. After 1 hour incubation at 37° C., cells were chilled on ice and washed with cold PBS with 0.5% BSA and 2 mM EDTA. Prior to enrichment cells were incubated for 10 min with FeR blocking reagent (Miltenyi). Monocytes, CD4<sup>+</sup> and CD8<sup>+</sup> T cells were negatively selected by magnetic sorting using the Monocyte Isolation Kit 11, CD4 T cell isolation Kit 11 and CD8 T cell Isolation kit (Miltenyi), respectively. More than 85% purity was achieved as evidenced by further staining with cognate antibodies and flow cytometry analysis (not shown). Enriched cell populations were resuspended in serum-free media (AIM V, Invitrogen), plated at  $0.5 \times 10^6$ /ml and stimulated with IL-6 or IFN- $\alpha$  at 50 ng/ml and  $10^4$  U/ml, respectively or left alone. Incubation with cytokines was conducted at 37° C. for 18 hours. Supernatants were analyzed for cytokine expression using the Luminex LabMap200 platform.

**[0081]** Regression analysis for age-associated traits. We used a linear regression model to identify measurements that showed a statistically significant change in expression with

age. Our linear regression model accounted for both age and gender differences. Mathematically, our model takes the form:

$$Y_{ij} = \beta_0^j + \beta_1^{Age} * Age_i + \beta_2^{Gender} * Gender_i + e_{ij}$$

**[0082]** Where  $Y_{ij}$  is the in subject  $i$  of measurement of  $j$  where  $j$  is either a gene expression, cell-subset phenotype, cytokine abundance or baseline phosphoflow measurement. In the case of gene expression and phosphoflow cases  $Y$  is in log 2 space. We applied the model to each data measurement. To compute p-values of the beta coefficient of age and gender, we permuted the data measurement with respect to age and gender, 200 times, and then recomputed the regression. For each permutation we tested were the absolute value of the permuted derived betas was greater or equal in size to the absolute value of the true beta coefficients. P-values for each beta were then calculated as the ratio of the number of times the betas from the permuted regressions exceeded the betas the true data regression over the total number of trials. To reduce the effects of outliers on our results, for both the serum cytokine and cytokine response were single subjects (29 and 25 respectively), were outliers, we used a robust regression model with a bi-square weight model. To correct for multiple hypothesis testing, we considered the regression p-values for all measurements of a single data type simultaneously and calculated a q-value (Storey and Tibshirani, 2003) for each. We applied a q-value threshold of 0.15 (unless stated otherwise) and report the p-value of the regression, the age coefficient and q-value. In the case of gene expression we first filtered the data in an independent manner (see below).

**[0083]** Gene subset selection. For gene expression, to restrict the number of multiple hypotheses corrections we were required to make, we considered a selected gene subset of immune and aging related genes for analysis, based on independent prior evidence from unrelated experiments (Table S2).

**[0084]** For immune genes we used ImmPort—the Immunology Database and Analysis Portal (2009) which contains manually curated immune related gene list (Mar. 3<sup>rd</sup>, 2009 version). All entries that did not map to a single ENSEMBL gene ID (mostly those mapping to a specific allele or exon) were discarded. The resultant list includes 3272 genes of which we mapped to the array using Entrez gene IDs. In total 2644 genes had one or more probes on the array for a total of 4708 probes.

**[0085]** We annotated genes as being related to aging and longevity by two different methods. First, we considered any gene that was annotated as aging related in the GenAge database (*Build 15*, 17 Mar. 2010) (de Magalhaes et al., 2009) as such. GenAge is a manually curated database of genes related to aging. This includes the few genes directly related to aging in humans and the best candidate genes obtained from model organisms. This yielded 243 longevity/aging genes. In addition, we performed a meta-analysis of aging related gene expression datasets to find a robust set of aging related genes. To do so, we identified 58 gene expression datasets (GDS) or gene expression series (GSE), comprising a total of 2152 microarray chips, in NCBI's Gene Expression Omnibus (GEO) (Barrett et al., 2007) which sampled gene expression in 'normal' aging across five species: human, rat, mouse, worm, and fly. As an subject dataset or series may combine samples drawn from different experimental conditions, tissue types or populations (such as different mouse strains or genders), these were further divided into a total of 114 compari-

sons between young and old samples. To create a profile of genes differentially expressed between young and old, we performed two types of meta-analysis. We looked at genes measured in at least ten comparisons, and used the modified t-test (Tusher et al., 2001) and Fisher's exact test, to identify genes significantly differentially expressed between young and old. We also computed a meta effect estimate, a meta fold-change, using a linear model, weighted by the inverse of the variance in expression (Choi et al., 2003). Performing this procedure yielded an additional 261 aging related genes (239 could be mapped on array with an EntrezID).

**[0086]** Network construction and spCCA. We identified a set of immune system modules from peripheral blood which best correlated with cell-subset specific cytokine responses in five steps: sample outlier filtering, supervised functional classification, within data type correlation and spCCA to identify co-regulated clusters.

**[0087]** First, for each of the 5 different data types (gene expression, cell subset, serum cytokines, cytokine stimulation response and baseline phosphoprotein levels), we filtered outlier samples that may have strong effects on correlation analysis by computing for each datatype, the overall sample correlation. Samples whose distance from all other samples was markedly different were removed from this analysis. This procedure identified two outlier samples, one sample (29) from the serum cytokine dataset and one sample (25) for cytokine response assays. Next, for specific data-types we classified nodes by function and/or co-expression. In particular cytokine responses were classified by type (baseline, response or baseline and response), cytokines by functionality. For phosphoprotein baseline measurements we clustered the data from the different STAT molecules within a cell together. Cell subsets were maintained as unique nodes at the cellular level. To cluster by co-expression we used the R library WGCNA (Langfelder and Horvath, 2008) which dynamically dissect clusters of strong correlations by exponentiation of the correlation matrix by a positive value determined empirically for each dataset by a fit of cluster connectivity to a scale free topology. We set the minimal cluster size for all datasets to 1, with the exception of gene expression for which minimal cluster size was set to 10. The outcome of applying this procedure for each dataset was to group highly correlated measurements in each data type together. This procedure yielded: (1) four cytokine response nodes, one for each cell subset, (2) three phosphoprotein nodes containing all age-associated baseline differences by cell type, (3) six nodes representing cell-subset frequencies, (4) five serum cytokine nodes, and (5) six gene expression nodes and two singletons containing all 279 age-associated genes (see Table S5 for which measurements were captured in each node).

**[0088]** For the purpose of identifying those measurements that are correlated with the cytokine response phenotype, we split the above described immune measurements into two matrices, the first consisting solely of subjects' cell-type average cytokine response and the second of all other factors/clusters and then applied spCCA (Witten et al., 2009). To set the penalty tuning parameters we performed sparse canonical correlation analysis on the real data set compared the magnitude of the first maximally correlated association to that observed in 1000 permutations of the data over a range of penalty parameters equally set for each data type. We observed similarly high z-scores (above 3) across the entire range of tested parameters. Penalties of 0.5 and 0.7 were chosen for the two matrices respectively as they showed a

good z-score, strong correlations between measurements ( $r=0.89$ ,  $r_{permuted}=0.59$ ,  $p\text{-value} < 0.001$ ) and a reasonable number of non-zero weights for interpretation. Importantly, though a cytokine response may consist of a weighted average of each of the four cell types, setting the penalty to 0.5 yielded a single non-zero weight for cytokine response, corresponding to a single cell-type, for each recursive iteration of the algorithm. A more permissive penalty (0.7) yielded multiple non-zero cytokine response but for only a minor gain in increased correlation. Thus, the linear combination of immune measurement we report is based on a 0.5 penalty and to a first approximation is orthogonal and maximally correlated with a single cell-type in which the cytokine response deficiency is observed. To enable comparison of the four weighted modules, weights were normalized by the maximum weight within a given linear combination and multiplied by the correlation of that maximal correlation observed between that module and the single unit weight of the cytokine response. We note that despite normalization of all the data, the magnitude of baseline phosphoprotein and cell-type frequency association with cytokine responses may be inflated by their measurement on the same technological platform.

**[0089]** Classification and Comparison of Cytokine Response Profiles. We introduced two modifications to the cytokine response classification protocol for the longitudinal analysis the years subsequent to year 1: First, as the range of the data in the assay was reduced in the subsequent years (likely due to antibody batch effects), we used a standard deviation threshold of one (instead of two) from the responses of the young group returning that year, to determine a subject's cellular response state. Second, if a response of a young subject was in itself an outlier, the mean and standard deviation of the young group was recomputed leaving that result out, effectively maintaining the scoring system as relative to good health. This latter procedure was not required in the first year, as the cell-specific distribution of young subjects was very tight there were no outliers.

**[0090]** To evaluate how stable the cytokine response phenotype was over the course of the three years, we created a model for the likelihood of remaining in the same classification or moving toward the non-responder category and compared this to the null model where the classification for any given year is random (i.e. equal probability of being classified into one of the three categories each year).

**[0091]** In the direct comparison of CR to CNR, as the number of samples did not permit direct consideration of gender and age in the comparison, we estimated their effect by single variable comparisons of gender and old-age differences in the data.

**[0092]** Tests of significance for determining immune response deficiency type. We used the dose-response data to distinguish between baseline and response causes for the lower fold-change levels we observed in the older subjects. To do so we devised a decision tree consisting of 6 consecutive tests, the application of which on a given cell, cytokine stimulation, phosphoprotein assay should implicate the mechanism inhibiting the full fold-change response:

**[0093]** (1) Use a one-tailed t-test to test whether the baseline phosphoprotein levels in the older subjects are significantly higher than that of the young (uses the complete dataset).

**[0094]** (2) Use a one-tailed t-test to test whether a significant fold-change difference is observed between the two older subjects and the two younger at the highest dose level.

**[0095]** (3) Use an f-test on computed ratio of fold-change between the lowest and highest stimulation doses to test if dose-response curve of the older subjects show a significant incline.

**[0096]** (4) Use an f-test to test if the dose-response of the younger subjects (ratio of fold-change between the lowest and highest stimulation doses) is significantly greater than that of the elderly.

**[0097]** (5) Use a two-tailed t-test to ask if the MFI at the highest stimulation dose is equal between the elderly and young subjects.

Tests (1) and (2) are used to identify if baseline phosphoprotein level differences, fold-change or both exist. Test (3) is used to identify if a given assay is in saturation for all doses, whereas (4) identifies if saturation is only observed in the older subject group or alternatively if no saturation exists, whether the younger subjects are more sensitive in their response for an increased dose. In the case test (4) indicates saturation of response in the older subjects, test (5) asks whether both the older subjects and the young reached saturation and if so, was it at the same ceiling (total available protein for phosphorylation).

#### Examples

**[0098]** The following examples are put forth so as to provide those of ordinary skill in the art with a complete disclosure and description of how to make and use the present invention; they are not intended to limit the scope of what the inventors regard as their invention. Unless indicated otherwise, part are parts by weight, molecular weight is average molecular weight, temperature is in degrees Centigrade, and pressure is at or near atmospheric.

#### Example 1

##### Age-Dependent Differences are Detectable from the Cellular to the Molecular Level

**[0099]** Age-dependent differences were detectable from the cellular to the molecular level. To identify age-associated differences, multiple regression analysis was performed on all samples according to age and gender. For multiple hypotheses correction, a false discovery rate was chosen that maximized the number of true positives while still being amenable for follow-up analyses. The false discovery rate is denoted as q-value and was set to  $q \leq 0.15$  unless otherwise noted; see Figure S3 and Experimental Procedures.

**[0100]** In white blood cells a decrease in CD8<sup>+</sup> naïve cells was detected with age, but no other age-associated changes in cell subset frequency. A high variance in frequency was noted between individuals that was particularly prominent in the elderly group (>73 years old) and that affected the regression analysis. However, at a  $q \leq 0.25$ , 8 of the 15 cell subsets surveyed showed age-associated changes in frequency (see Table S2). These included an increase in the frequency of monocytes, and an increase in CD8<sup>+</sup> and CD4<sup>+</sup> cells lacking CD28 expression, which is a critical molecule for robust T cell activation in both CD8<sup>+</sup> and CD4<sup>+</sup> T cells. In addition, increases in the frequency of NKT cells were noted and in both CD8<sup>+</sup> and CD4<sup>+</sup> "memory" T cells, i.e., the cells that respond to previously encountered antigens.

**[0101]** Table S2 summarizes twelve serum proteins whose serum levels were changed as a function of age. These included the chemokines IP-10 and Eotaxin, both of which increased sharply with age as previously reported (Shurin et al., 2007), as did IL-12, which is known to regulate IP-10 production. The only pro-inflammatory cytokine that was found to increase with age was TNF- $\alpha$ . Both Th1 (IFN- $\gamma$  and IFN- $\alpha 2$ ) and Th2 (IL-4, 5, 7) related cytokines decreased with age, as did the macrophage activation cytokines MRC-3 and TGF- $\alpha$ . With respect to the ability of white blood cells of these individuals to functionally respond to signaling cues from cytokines, of the 12 baseline and 72 response assays that were conducted (4 cell subsets, stimulated by 6 cytokines and measuring phosphorylation level of STAT-1, -3, and -5), an age-associated difference in 8 baseline and 39 response measurements was detected, 33 of which showed a 2-fold or greater response to stimulation in at least one person (see FIG. 1A-C, Figure S3A-B).

**[0102]** The gene expression analysis in these studies was limited to those genes which had previously been independently associated with either immunological or longevity phenotypes. Based on curated databases of immunology (2009) and aging (de Magalhaes et al., 2009) 2713 immune-related genes and 239 aging-related genes were measured on human genome microarrays (Agilent 4x44 whole human genome microarrays). A cross-species meta-analysis of 114 aging-related gene expression experiments identified an additional 40 genes (see Table S3 and S4). In total, these comprised 2863 genes that corresponded to 4364 unique probes on the array. Testing this set of probes for age-associated differences yielded 294 probes ( $q \leq 0.15$ , Figure S3E), which corresponded to 279 unique immune and aging-related genes that were found up- or down-regulated with age (see Table S2).

#### Example 2

##### The Cytokine Responses of Older Adults are Systemically Reduced, Independent of Concentration

**[0103]** Cytokine response assays that assess the phosphorylation state of intracellular signaling proteins have been shown to be predictive of disease outcome in several cases (22; 27). On average older individuals exhibited lower phosphorylation states in response to stimulation than the young (FIGS. 1A and 1B). To address the possibility that low responses to cytokines might be due to low sensitivity of cells from older individuals, dose-response experiments were carried out and increasing concentrations of all 6 cytokines were assayed in all 4 cell subsets in 2 young and 2 old poor cytokine responders. Differences between old and young were consistently observed in the majority of assays (FIG. 1D, Figure S4), even at the highest, saturating doses (Figure S5). 30 age-associated differences were identified at the highest cytokine concentrations; of those, 20 showed a 2-fold or higher change and a significant reduction in the responses of older individuals versus the younger cohort (FIG. 1D, Figure S4). Thus, in comparison to young individuals, older individuals were not able to mount an equally strong response to cytokine stimulation, even at saturating levels. Furthermore, individuals who were deficient in one cytokine response were, for the most part, deficient in others as well. This correlation was also true across cell-types. For example, those individuals who were deficient in their CD4<sup>+</sup> T cell responses also tended to be deficient in their CD8<sup>+</sup> T cell responses and

in many cases in either or both monocytes and B-cells, suggesting a systemic condition (see FIG. 1E). Taken together, multiple impairments to respond to cytokine signals occurred with age, independent of the stimuli concentration.

### Example 3

#### Cytokine Response Deficiencies and Immunosenescence Markers Co-Occur in the Single Individuals

**[0104]** In further studies, a potential relationship was investigated between the cytokine response phenotype and other immune measures such as cell subsets and cytokines. This revealed a high concordance of the cytokine response deficiency with hallmarks of immunosenescence alterations in cell subsets (see FIG. 2A, top), such as the drop in CD8<sup>+</sup> and CD4<sup>+</sup> naïve cell frequencies ( $R^2=0.54$ ,  $p<10^{-6}$  and  $R^2=0.54$ ,  $p<10^{-6}$  respectively) (Fagnoni et al., 2000), the increase in occurrence of CD8<sup>+</sup>CD28<sup>-</sup> cells ( $R^2=0.54$ ,  $p<10^{-6}$ ) (Effros et al., 2005; Fagnoni et al., 1996) and the decline in B-cell frequency ( $R^2=0.23$ ,  $p<0.01$ ).

**[0105]** Cytokine responses in serum proteins showed significant association with log transformed intensity measurements of macrophage chemokine MCP-1 ( $R^2=0.23$ ,  $p<0.01$ ) and more mildly with the innate immunity chemokine IP-10 ( $R^2=0.18$ ,  $p<0.07$ ) (see FIG. 2A, bottom). However, pro-inflammatory cytokines showed no significant association with reduced cytokine responses. Aside from TNF- $\alpha$ , no increase in pro-inflammatory cytokines in serum was detected. In particular, no significant age or cytokine response association was observed for IL-6, whose increase has been associated with aging in many other studies (Franceschi et al., 2000; Shaw et al., 2010; Wikby et al., 2006), and has most recently been linked with mortality (Wassel et al., 2010). For a direct analysis of cytokine levels from sorted cells, monocytes, CD4<sup>+</sup> and CD8<sup>+</sup> T cells from PBMC of two young and two older individuals were isolated and cultured, and then the secreted cytokine levels of these cells were profiled across 50 different cytokines after 18 hours of incubation at 37° C. These assays showed a dramatically increased abundance of pro-inflammatory cytokines (IL-6, IL-1b, TNF $\alpha$ ) and chemokines (CXCL1, CXCL5) in the monocytes of the older individuals (see FIG. 2B). No other significant differences in cytokine abundance were detected either in monocytes or in the CD4<sup>+</sup> or CD8<sup>+</sup> T-cells. Taken together, these associations suggested that a subset of older individuals exhibited immune system impairments that were concomitant at multiple levels, and to which the systemic reduction in cytokine response was closely linked.

**[0106]** Sparse canonical correlation analysis (spCCA) (Witten et al., 2009), an unsupervised statistical technique, was used to identify linear combinations of weighted factors, that showed maximal correlation with cytokine response. For simplification, highly co-varying factors internal to a single type of measurement were first clustered, including the cytokine responses themselves by cell subsets. spCCA identified four distinct and significant maximally correlated sets of factors, one for each of the four cell subsets in which cytokine response deficiencies had been observed (see FIG. 2C and Table S6). These multi-factor combinations ('modules') showed considerably higher correlation with cytokine responses than the correlation that were observed with single known immunosenescence markers. The specific combination of an increase in B-cell baseline phosphoproteins, a decline in CD8<sup>+</sup> naïve cell frequency and 14 other factors

formed a module which correlated with B-cell cytokine response with an  $r=0.89$  at a significance of  $p<0.0001$ . ( $r=0.87$ ,  $0.87$ ,  $0.74$  for CD4<sup>+</sup>, CD8<sup>+</sup> and monocytes respectively). The modules correlating with a cytokine response deficiency of a given cell subset often included molecular measurements from cell subsets other than their own and at higher weights, indicating inter-cellular dependencies of these deficiencies.

### Example 4

#### Cytokine Responses Define Distinct Age-Related Subgroups that are Longitudinally Stable; Definition of Cytokine Responders Versus Cytokine Non-Responders

**[0107]** For assessing the extent of variation in the various analyses, a scoring system for cytokine deficiency was defined by first calculating for every individual the sum of age-associated cytokine responses in each cell subset, and then comparing to see if it was markedly different from that observed in the young group for that cell subset (two standard deviations from the mean of the young).

**[0108]** The scoring system was defined as a relative scoring system with respect to those generally considered healthy, and reflected the extent of both intra- and inter-cellular effects of cytokine response deficiencies on an individual's immune system.

**[0109]** Under this scoring system, none of the young individuals showed any cytokine response impairments, whereas multiple impairments were observed in older individuals. Furthermore, among older individuals we observed a high amount of variation in the cytokine response score, suggesting the possibility of distinct phenotypes. Therefore, older individuals were defined as cytokine responders (CR), if the sum of their responses in each of the cell subsets was within two standard deviations of the average response in the young individuals in at least three of the four tested cell subsets. Accordingly, older individuals were defined as cytokine non-responders (CNR), if their sum of age-associated responses was below two standard deviations of the average response in the young individuals in at least three of the four tested cell subsets (see Figure S6 and Experimental Procedures). Under these criteria, six older individuals were identified as CR and six as CNR. The remaining seven older individuals we designated as 'Intermediate', as they did not meet either of these extreme criteria, but rather showed generally milder reductions in response to cytokine stimulation than observed in CNR and in only one or two of the four tested cell subsets (see FIG. 3A).

**[0110]** To determine the stability of the cytokine response phenotype, a subset of patients ( $n=21$ ) was examined who had returned to participate in a subsequent three year-long longitudinal study. A similar scoring system was used to classify the response, with minor modifications (see Experimental Procedures). The analysis of each of the three years of the study showed conservation of the cytokine response phenotype both at the cell-type level and the class (CR, CNR or Intermediate) (see FIG. 3B,  $p=0.019$  by permutation). This was particularly notable amongst older individuals, with individuals generally maintaining either the same state or progressing towards the non-responder category.

**[0111]** Furthermore, most shifts in cytokine response state were gradual, meaning that CR did not shift to a CNR state in directly subsequent years or vice versa, but rather passed through the intermediate state. The results from the longitu-

dinal data strongly suggested that fluctuations are not random, but rather a true biological phenomenon whose phenotype in individuals is likely to remain invariant or worsen over time.

#### Example 5

##### Cytokine Responders and Cytokine Non-Responders Have Distinctly Different Immune System Profiles

**[0112]** The CR and CNR profiles form two distinct and stable extremes of an important immune phenotype. Further studies were carried out to investigate whether stratification by cytokine response and direct comparison between groups would uncover further significant differences. The participating individuals in this study were vaccinated with a seasonal, inactivated influenza vaccine containing three different strains of influenza. Their antibody titers against all three strains were tested before and approximately 3 weeks after vaccination using a standard hemagglutinin inhibition assay (HAI). It is generally accepted that, at the population level, a pre-vaccination antibody titer of 1:30 to 1:40 represents a 50% probability of protection against Influenza infection (Hobson et al., 1972; Potter and Oxford, 1979; (Coudeville et al., 2010).

**[0113]** Here, the young and the CR group showed similar pre-vaccination antibody titer levels, which were significantly more robust than those of CNR when considered simultaneously across all strains (see FIG. 4A,  $p=0.0005$  and  $p=0.06$  respectively, by Fisher's exact test performed on p-values obtained from permuted data). Response to vaccination, as measured by antibody titers post-vaccination, were similar in CR and CNR (see Figure S7), suggesting that the CNR group had remained responsive to the vaccination and would, therefore, particularly benefit from vaccination.

**[0114]** In addition, the individuals in this study were also tracked with respect to their medical history and concomitant medication. A third of CR individuals reported previous cardiovascular related surgery or hypertension versus two thirds of CNR. While there was a great variation in the medications that the individuals took, the CNR group took significantly more medications than the CR group ( $p<0.06$ ), which was likely due to the higher incidence of cardiovascular issues in the CNR group. Yet no single mechanism-of-action drug class distinguished CNR from CR (see Table S8), suggesting that the differences between the two groups were not the result of a simple drug effect, but rather a surrogate of their medical condition.

**[0115]** In further analyses, all genomic, molecular, and cellular measurements that had been obtained in the course of the described studies were investigated for specific differences between the CR and CNR groups. A uniform threshold across all measurement modalities of  $q \leq 0.1$  (see Figure S8) identified 1565 measurements that were different between CR and CNR (ANOVA, see Table S7, similar results were obtained by a permutation test). The CNR group showed a significant decrease in most (48/72) of the cytokine stimulation response assays. In agreement with our current knowledge of low phosphoprotein baseline levels being the cause for any cytokine response defects, elevated baseline phosphorylation was detected in CNR individuals for STAT1, 3 and 5 proteins in B- and CD4<sup>+</sup> T-cells, as well as for STAT1 in monocytes. 13 out of 15 measured cell-subsets had detectable differences in frequency between CR and CNR (see Table S7), including significantly lower levels of B-cells, CD8<sup>+</sup> and CD4<sup>+</sup> naïve

T-cells ( $p \leq 0.01$ ), and CD8<sup>+</sup>CD28<sup>-</sup> T-cells ( $p < 10^{-6}$ ), all known markers of immunosenescence. No serum proteins were detected as differentially expressed between the two groups.

**[0116]** The increase in CD8<sup>+</sup>CD28<sup>-</sup> T cells and the evidence of an inflammatory state was found to be consistent with the previously described "Immune Risk Profile" for immunosenescence (Wikby et al., 2006). This profile was previously estimated to be present in 16% of older individuals 60-94 years of age (Wikby et al., 2008). Furthermore, it had been reported that individuals with such a profile showed increased morbidity and mortality (Strindhall et al., 2007). An inverted CD4/CD8 cell subset ratio (below 1), is characteristic of such an immune risk profile (Strindhall et al., 2007; Wikby et al., 2008). Therefore, the relationship of the CD4/CD8 ratio to age and cytokine response was also analyzed in the present studies (see Figure S9). Only three individuals (one young, one a CNR and the other an intermediate) had a CD4/CD8 ratio below 1. Furthermore, the CD4/CD8 ratio was highly variable, not only in the present studies, but also in much larger cohorts, investigated by other groups (Lifson et al., 1985), where the CD4/CD8 ratio has been reported to generally rise as opposed to decrease with age. In the present studies, most young individuals showed much lower CD4/CD8 ratios similar to that of CNR, whereas CR showed elevated CD4/CD8 ratio levels.

**[0117]** 1493 mRNAs were detected as differentially expressed between CR and CNR (see Table S7). Further studies detected 151 longevity-associated genes that were differentially expressed between the CR and CNR individuals (Table S7). These included genes in multiple pathways associated with lifespan, such as redox (e.g. SOD1,  $p < 10^{-4}$ ), DNA surveillance (e.g. SIRT6,  $p < 0.02$ ), nutrient sensing (insulin-like growth factor 1 receptor  $p < 10^{-5}$ ), apoptosis (e.g. the forkhead transcription factor FOXO/DAF-16 family members FOXO1, FOXO3 and FOXL2  $p < 10^{-4}$ ) and cellular proliferation (e.g. cMyc, MDM2,  $p < 0.04$ ).

**[0118]** Within the context of immune cell function, these genes may either be in conflict or parallel their role in lifespan extension (match directionality). Genes of the growth hormone signaling pathway were upregulated in CR individuals, while genes of the redox response pathway were downregulated in CNR individuals, according to their expected directionality in longevity. In contrast, genes in the insulin response pathway and cellular proliferation genes were upregulated in CR over CNR, and appeared to be opposing longevity, but in tune with a functionally active immune system (Jones and Thompson, 2007), a possible necessity for long life in a non-sterile environment. The three cytokine response phenotypes (CR, intermediate or CNR), that had been identified in the older individuals, were almost entirely reflected at the gene expression level when clustering older individuals by the set of longevity associated genes, as shown in FIG. 4B. These results suggest that cytokine response stratification can identify older individuals with distinctly different immune system profiles and differing influenza protection phenotype.

#### Example 6

##### Classification of Age-Associated Differences by Cytokine Response

**[0119]** A major conundrum in the study of aging is to ascertain whether a detectable age-associated change describes a

process of deterioration or one that is protective. In the present studies, genes and immune traits were investigated that were different between either the CNR and the young or the CR and the young ( $q \leq 0.15$ , Fig. S10), but that were not different in the same direction in the reciprocal group comparison ( $q \leq 0.2$ ). A third comparison targeted age-associated differences that were shared between the CR and CNR ( $q \leq 0.2$ ). In total, this procedure classified 215, 1,901 and 378 measurements as CNR specific, CR specific or shared between the CR and the CNR (see FIG. 5A for summary statistics, Figure S11 and Tables S9-S11).

**[0120]** The majority of immunosenescence markers identified in the present studies were specific to CNR, whereas the profile of CR was closer to that of the young (see FIG. 5B). For example, the frequency of B-cells in the blood had previously been reported to decline with age (Ademokun et al., 2010), but comparing the two subgroups each directly to the young revealed that B-cell frequency decline was indeed correlated with aging, but only in the CNR group ( $p < 0.004$ ). Similarly, a NKT cell increase had been reported in aging (Shaw et al., 2010) but this was again only observed in CNR.

**[0121]** For both B-cell and NKT cell frequencies, CR showed the reciprocal phenotype (high B-cell, low NKT cell frequency) when compared to the young. For other previously identified age associated changes, such as CD8 naïve cell frequency or serum Eotaxin abundance, both groups showed consistent differences compared to the young, though the change in magnitude was not significant in CR.

**[0122]** CNR specific changes included large shifts in cell subset proportions, additional cytokine responses that were impaired and increased baseline elevations for all cells but CD8+ T-cells (see Figure S11). Only few (138) genes were detected as differentially expressed with age and specific to CNR. In contrast, for CR-specific changes, numerous genes (1896 genes) were differentially expressed with other immune phenotypic characteristics being similar to those observed in the young. In general, CR and CNR shared very few differences with respect to the young, and of them few were previously associated with aging.

**[0123]** Elevated baseline levels and decreased cytokine responses in CD8+ cells were common to both CR and CNR, though milder in CR. In addition, at higher  $q$ -value thresholds ( $q \leq 0.18$  for CNR vs. young and  $q \leq 0.3$  for CR vs. young) most measured serum cytokines significantly differed in their abundance in comparison to the young, likely reflecting increased inflammation (Franceschi et al., 2000) and large changes in cell subset composition. These results indicated that there is likely no common profile of immune aging. Instead it appeared that the immune system of CR and CNR were aging on different trajectories yielding a distinct immune system profile.

#### Example 7

Reduced Responses to Cytokine Stimulation are Primarily Due to Increased Basal Levels of Phosphorylated STAT Proteins and Alterations in Response Potential in the IL-6 and IFN- $\alpha$  Pathways

**[0124]** The present studies confirm reports that cells of older individuals, particularly of CNRs, experience in vivo an increased inflammatory environment when compared to young individuals (Franceschi et al., 2000). The reduced response to cytokine stimulation, as observed in CNRs, may either be successful adaptation to such an environment or resis-

tance to signaling cues. Considering that the changes measured in the cytokine stimulation assays are relative to a baseline pre-stimulation measurement, there are four possible models that could explain the observed unresponsive cells phenotype: (1) an increased exposure to cytokines is leading to successful adaptation and a requirement of higher cytokine concentration, (2) a reaction defect, in which the signaling machinery of cells in the older subjects is leading to a lower response in the older subjects, (3) a baseline defect, in which elevation in baseline pSTAT levels leaves no protein left to phosphorylate and thus decreased pSTAT fold-change, or (4) a combination of both the baseline and reaction pathway defects (see FIG. 6A).

**[0125]** As the observed defected cytokine response occurred systematically in different cells, cytokines, and pSTATs, each may be attributed to a separate mechanism. In the single dose assay that was performed with all 29 individuals, the concentration, baseline and response differences could not be decoupled to identify the factors contributing to the observed reduced fold-change response. Indeed, plotting each subject's cytokine response fold-change levels to the measured baseline levels of the phosphoprotein revealed an inverse correlation with the fold-change response across many of the assays (see FIG. 6B and Figure S12), showing the importance of increased baseline pSTAT levels.

**[0126]** Discriminating between the above mentioned four models could be possible by reanalyzing the dose-response assay conducted in the present studies, which included two young and two old CNR subjects, measured at each of the 72 stimulation assays and baseline for five different doses per cytokine (see Experimental Procedures). A series of tests was applied to the dose-response assay data, using information from the single dose assay whenever possible. In the successful adaptation model (Model 1), the older subjects would be expected to respond similarly to the young at a higher dose of cytokines (see FIG. 6A, top left panel). Conversely, if the relative reduction in response to cytokine stimulation compared to that of the young remained, irrespective of the dose of cytokines, then the reduced response would result from signaling resistance (Models 2-4). These four models can be distinguished for each cell subset, cytokine, and pSTAT assay combination by following a decision tree (see FIG. 6C for a sketch and Figure S13 for a full decision tree, also see Experimental Procedures).

**[0127]** The application of the decision tree (from Figure S13) showed not a single case of adaptation. Of the 30 combinations of cell, cytokine, and pSTATs in which young and older subjects show differing responses, only the monocyte stimulations could be classified solely as a reaction defect, which suggested that these cell subsets—shown to be the main source of pro-inflammatory cytokines in CNR—might not be influenced in an autocrine manner insofar as showing elevated pSTAT baseline levels. All other cytokine responses showed a significant elevation in the older subjects' baseline pSTAT levels, with 11 due solely to a baseline elevation, and 14 to a combined baseline-reaction effect (Table S12). The combined baseline and response factor differences were predominantly seen in T cells stimulated by IL-6 or CD8+ T cells stimulated by IFN- $\alpha$ , whereas elevated baseline levels of pSTATs accounted for all of the observed differences in IL-10 stimulation in CD4+, CD8+ and B-cell and to a lesser extent those involving IL-21, IL-7 and IFN- $\alpha$  response differences. Thus, the reduced cytokine responses in older individuals can predominantly be attributed to an elevation of baseline phos-

phorylation levels of STAT proteins in cells and to an altered response potential in the IL-6 and IFN- $\alpha$  pathways.

[0128] Although the foregoing invention and its embodiments have been described in some detail by way of illustration and example for purposes of clarity of understanding, it is readily apparent to those of ordinary skill in the art in light of the teachings of this invention that certain changes and modifications may be made thereto without departing from the spirit or scope of the appended claims. Accordingly, the preceding merely illustrates the principles of the invention. It will be appreciated that those skilled in the art will be able to devise various arrangements which, although not explicitly described or shown herein, embody the principles of the invention and are included within its spirit and scope.

#### REFERENCES

- [0129] ImmPort (2009)
- [0130] Ademokun A et al. (2010). The ageing B cell population: composition and function. *Biogerontology* 11, 125-137.
- [0131] Alon U (2007). An introduction to systems biology: design principles of biological circuits (Boca Raton, Fla.: Chapman & Hall/CRC).
- [0132] Barrett T et al. (2007). NCBI GEO: mining tens of millions of expression profiles—database and tools update. *Nucleic Acids Res* 35, D760-765.
- [0133] Choi J K et al. (2003). Combining multiple microarray studies and modeling interstudy variation. *Bioinformatics* 19 Suppl 1, i84-90.
- [0134] Coudeville L et al. (2010). Relationship between haemagglutination-inhibiting antibody titres and clinical protection against influenza: development and application of a bayesian random-effects model. *BMC Med Res Methodol* 10, 18.
- [0135] Davis M M (2008). A prescription for human immunology. *Immunity* 29, 835-838.
- [0136] de Magalhaes J P et al. (2009). The Human Ageing Genomic Resources: online databases and tools for biogerontologists. *Aging Cell* 8, 65-72.
- [0137] de Visser K E et al. (2006). Paradoxical roles of the immune system during cancer development. *Nat Rev Cancer* 6, 24-37.
- [0138] Effros R B et al. (2005). The role of CD8+ T-cell replicative senescence in human aging. *Immunol Rev* 205, 147-157.
- [0139] Evans E A et al. (2008). The DAF-2 insulin-like signaling pathway independently regulates aging and immunity in *C. elegans*. *Aging Cell* 7, 879-893.
- [0140] Fagnoni F F et al. (1996). Expansion of cytotoxic CD8+CD28- T cells in healthy ageing people, including centenarians. *Immunology* 88, 501-507.
- [0141] Fagnoni F F et al. (2000). Shortage of circulating naïve CD8(+) T cells provides new insights on immunodeficiency in aging. *Blood* 95, 2860-2868.
- [0142] Franceschi C et al. (2000). Inflamm-aging. An evolutionary perspective on immunosenescence. *Ann NY Acad Sci* 908, 244-254.
- [0143] Gernez Y et al. (2007). Altered phosphorylated signal transducer and activator of transcription profile of CD4+CD161+ T cells in asthma: modulation by allergic status and oral corticosteroids. *J Allergy Clin Immunol* 120, 1441-1448.
- [0144] Goodwin K et al. (2006). Antibody response to influenza vaccination in the elderly: a quantitative review. *Vaccine* 24, 1159-1169.
- [0145] Hansson G K (2005). Inflammation, atherosclerosis, and coronary artery disease. *N Engl J Med* 352, 1685-1695.
- [0146] Hobson D et al. (1972). The role of serum haemagglutination-inhibiting antibody in protection against challenge infection with influenza A2 and B viruses. *J Hyg (Lund)* 70, 767-777.
- [0147] Irish J M et al. B-cell signaling networks reveal a negative prognostic human lymphoma cell subset that emerges during tumor progression. *Proc Natl Acad Sci USA* 107, 12747-12754.
- [0148] Jones R G & Thompson C B (2007). Revving the engine: signal transduction fuels T cell activation. *Immunity* 27, 173-178.
- [0149] Kirkwood T B (2002). Evolution of ageing. *Mech Ageing Dev* 123, 737-745.
- [0150] Krutzik P O & Nolan G P (2006). Fluorescent cell barcoding in flow cytometry allows high-throughput drug screening and signaling profiling. *Nat Methods* 3, 361-368.
- [0151] Langfelder P & Horvath S (2008). WGCNA: an R package for weighted correlation network analysis. *BMC Bioinformatics* 9, 559.
- [0152] Lifson J D et al. (1985). Variables affecting T-lymphocyte subsets in a volunteer blood donor population. *Clin Immunol Immunopathol* 36, 151-160.
- [0153] Perez O D and Nolan G P (2006). Phospho-proteomic immune analysis by flow cytometry: from mechanism to translational medicine at the single-cell level. *Immunol Rev* 210, 208-228.
- [0154] Potter C W & Oxford J S. (1979). Determinants of immunity to influenza infection in man. *Br Med Bull* 35, 69-75.
- [0155] Prevention, C.f.D.C.a. (1998). The 1998-99 WHO influenza reagent kit for the identification of influenza isolates. (Atlanta, Ga., Centers for Disease Control and Prevention).
- [0156] Rodwell G E et al. (2004). A transcriptional profile of aging in the human kidney. *PLoS Biol* 2, e427.
- [0157] Rojo L E et al. (2008). Neuroinflammation: implications for the pathogenesis and molecular diagnosis of Alzheimer's disease. *Arch Med Res* 39, 1-16.
- [0158] Sarup P et al. (2011). Flies selected for longevity retain a young gene expression profile. *Age (Dordr)* 33, 69-80.
- [0159] Shaw A C et al. (2010). Aging of the innate immune system. *Curr Opin Immunol* 22, 507-513.
- [0160] Shen-Orr S S et al (2010). Cell type-specific gene expression differences in complex tissues. *Nat Methods* 7, 287-289.
- [0161] Shurin G V et al. (2007). Dynamic alteration of soluble serum biomarkers in healthy aging. *Cytokine* 39, 123-129.
- [0162] Southworth L K et al. (2009). Aging mice show a decreasing correlation of gene expression within genetic modules. *PLoS Genet* 5, e1000776.
- [0163] Storey J D & Tibshirani R. (2003). Statistical significance for genomewide studies. *Proc Natl Acad Sci USA* 100, 9440-9445.

- [0164] Strindhall J et al. (2007). No Immune Risk Profile among subjects who reach 100 years of age: findings from the Swedish NONA immune longitudinal study. *Exp Gerontol* 42, 753-761.
- [0165] Tusher V G (2001). Significance analysis of microarrays applied to the ionizing radiation response. *Proc Natl Acad Sci USA* 98, 5116-5121.
- [0166] Wassel C L et al. (2010). Association of circulating C-reactive protein and interleukin-6 with longevity into the 80s and 90s: The Rancho Bernardo Study. *J Clin Endocrinol Metab* 95, 4748-4755.
- [0167] Weiskopf D et al. (2009). The aging of the immune system. *Transpl Int* 22, 1041-1050.
- [0168] Wikby A et al. (2008). The immune risk profile is associated with age and gender: findings from three Swedish population studies of subjects 20-100 years of age. *Biogerontology* 9, 299-308.
- [0169] Wikby A et al. (2006). The immune risk phenotype is associated with IL-6 in the terminal decline stage: findings from the Swedish NONA immune longitudinal study of very late life functioning. *Mech Ageing Dev* 127, 695-704.
- [0170] Witten DM et al. (2009). A penalized matrix decomposition, with applications to sparse principal components and canonical correlation analysis. *Biostatistics* 10, 515-534.

APPENDICES

- [0171] Appendix A—Table S1
- [0172] Appendix B—Table S2
- [0173] Appendix C—Table S3
- [0174] Appendix D—Table S4
- [0175] Appendix E—Table S5
- [0176] Appendix F—Table S6
- [0177] Appendix G—Table S7
- [0178] Appendix H—Table S8
- [0179] Appendix I—Table S9
- [0180] Appendix J—Table S10
- [0181] Appendix K—Table S11
- [0182] Appendix L—Table S12

APPENDIX A

[0183]

TABLE S1

Demographics Table			
	Enrollment Category 18-30 years	Enrollment Category 60-79 years	Enrollment Category 80-100 years
Number enrolled	n = 10	n = 11	n = 8
Gender			
Female	6	6	4
Male	4	5	4
Age			
Mean (yrs)	24.42	64.21	85.44
Range (yrs)	21-28	60-74	83-96
Ethnicity			
Hispanic	3	0	0
Non-Hispanic	7	11	8
Race			
White or Caucasian	5	11	8
Asian	3	0	0
American Indian/ Alaska Native	0	0	0
Pacific Islander	0	0	0
Black/African Amer	0	0	0
More than one race	1	0	0 (More than 1: Cauc/Asian)
Other Race	1	0	0 (Other: not specified)
Declined to answer	0	0	0

Note:

Demographics table displays enrollment as per original IRB. The enrollment category 60-79 yo included 10 subject between the ages of 60-65 and one individual that was 74 yo. That individual was visualized as within the oldest age group and considered within that group for all pertinent analyses

APPENDIX B

[0184]

TABLE S2

Significant age-associated measurement from						
Cell subset - Name	Mean Yng	Mean Old	p Age	q Age	p Gender	q Gender
CD8 NAIVE	71.62	48.33	0.005	0.15	0.14	0.42
CD8 TERM	14.68	28.47	0.065	0.175	0.155	0.4
DIFF EFFECTOR MEMORY						
MONOCYTES	26.91	33.86	0.07	0.175	0.28	0.45
CD8+CD28-	22.98	43.55	0.065	0.175	0.065	0.35
CD4 TERM	0.65	3.41	0.02	0.1875	0.265	0.45
DIFF EFFECTOR MEMORY						
CD8 CENTRAL	11.78	18.48	0.095	0.2143	0.425	0.53571
MEMORY						
NK T CELLS	5.76	9.89	0.12	0.225	0.275	0.45
CD4+CD28-	1.63	4.02	0.045	0.25	0.3	0.45

TABLE S2-continued

Significant age-associated measurement from						
Serum cytokines - Name	Mean Yng	Mean Old	pAge	qAge	p Gender	q Gender
EOTAXIN	238	427.58	0.01	0.0788	0.715	0.93333
IFN-G	137.98	49.86	0.01	0.0788	0.12	0.45818
IL-7	82.02	98.27	0.01	0.0788	0.12	0.45818
MCP-3	121.81	162.92	0.01	0.0788	0.675	0.89091
IL-12-P70	28.13	19.08	0.005	0.105	0.3	0.63
IL-17	150.77	28.96	0.005	0.105	0.355	0.73044
IL-4	55.63	98.19	0.005	0.105	0.455	0.72414
TGF-a	40.08	60.01	0.005	0.105	0.14	0.42
IP10	462.3	1052.06	0.025	0.126	0.465	0.72414
TNF-A	26.09	42.98	0.025	0.126	0.02	0.35
IFNA2	51.86	91.98	0.035	0.14	0.995	1
IL-5	12.76	18.36	0.035	0.14	0.015	0.42
Cytokine responses	Yng	Old	pAge	qAge	pGender	qGender
cd20_IL7_STAT3	0.99	1.04	0	0.0277	0.15	1.54286
cd4_IFNa_STAT5	1.16	0.87	0	0.0277	0.295	1.66154
cd4_IL6_STAT5	1.26	0.71	0	0.0277	0.83	0.95294
cd4_IL21_STAT1	1.15	0.83	0	0.0277	0.515	1.00465
cd4_IL21_STAT5	1.14	0.92	0	0.0277	0.74	0.9
cd8_IFNa_STAT1	1.35	0.66	0	0.0277	0.64	0.91636
cd8_IFNa_STAT3	1.15	0.79	0	0.0277	0.435	1.09091
cd8_IFNa_STAT5	1.2	0.78	0	0.0277	0.415	1.09091
cd8_IL6_STAT1	1.57	0.58	0	0.0277	0.265	1.66154
cd8_IL6_STAT5	1.45	0.8	0	0.0277	0.42	1.09091
cd8_IL21_STAT1	1.28	0.79	0	0.0277	0.74	0.9
mono_IFNa_STAT1	1.13	0.87	0	0.0277	0.37	1.44
mono_IL7_STAT5	1.09	0.95	0	0.0277	0.48	1.09091
cd4_IL7_STAT5	1.08	1	0.005	0.036	0.72	0.9
cd8_IFNg_STAT1	1.37	0.9	0.005	0.036	0.13	1.56
cd8_IL7_STAT1	1.13	0.94	0.005	0.036	0.43	1.09091
cd8_IL10_STAT1	1.19	0.91	0.005	0.036	0.61	0.91636
cd8_IL21_STAT5	1.07	0.89	0.005	0.036	0.545	1.00465
mono_IFNa_STAT3	1.08	0.78	0.005	0.036	0.945	1
mono_IFNa_STAT5	1.04	0.81	0.005	0.036	0.7	0.91636
cd4_IFNa_STAT1	1.19	0.78	0.01	0.045	0.785	0.9
cd4_IFNa_STAT3	1.06	0.64	0.01	0.045	0.515	1.00465
cd4_IL6_STAT1	1.27	0.77	0.01	0.045	0.74	0.9
mono_IFNg_STAT3	1.07	0.89	0.01	0.045	0.8	0.9
cd20_IFNa_STAT3	1.04	0.92	0.015	0.0533	0.53	1.00465
cd8_IL6_STAT3	1.15	0.67	0.015	0.0533	0.275	1.66154
mono_IL6_STAT3	1.09	0.7	0.015	0.0533	0.97	1
cd4_IL6_STAT3	1.08	0.66	0.02	0.0621	0.595	1.00465
cd4_IL21_STAT3	1.07	0.69	0.02	0.0621	0.485	1.09091
cd8_IL7_STAT3	1.01	0.93	0.025	0.072	0.1	1.44
cd4_IL10_STAT1	1.05	0.81	0.03	0.0813	0.615	0.91636
cd20_IFNa_STAT1	1.01	0.79	0.035	0.0873	0.48	1.09091
cd4_IL10_STAT3	1.03	0.69	0.035	0.0873	0.65	0.91636
cd4_IL7_STAT3	1	0.9	0.045	0.1059	0.435	1.09091
cd20_IFNg_STAT3	0.99	1.03	0.05	0.12	0.02	1.8
mono_IL6_STAT1	1.06	1	0.05	0.12	0.555	1.00465
cd4_IFNg_STAT1	1.05	0.89	0.06	0.1362	0.325	1.44
cd20_IFNa_STAT5	1.04	0.92	0.075	0.1477	0.82	0.95294
mono_IFNg_STAT5	1.05	0.88	0.08	0.1477	0.81	0.95294
Phosphoprotein baseline	Yng	Old	pAge	qAge	pGender	qGender
cd20_Unstimulated_STAT1	0.96	1.69	0	0.03	0.94	1
cd8_Unstimulated_STAT1	0.73	1.18	0	0.03	0.24	0.45
cd4_Unstimulated_STAT1	0.87	1.55	0.005	0.04	0.17	0.432
cd20_Unstimulated_STAT3	0.98	1.03	0.055	0.1029	0.075	0.32
cd8_Unstimulated_STAT5	0.97	1.05	0.055	0.1029	0.095	0.3
cd4_Unstimulated_STAT3	0.94	2.37	0.03	0.105	0.27	0.45
cd4_Unstimulated_STAT5	0.97	1.02	0.04	0.108	0.055	0.36
cd8_Unstimulated_STAT3	0.9	1.07	0.08	0.12	0.03	0.42

TABLE S2-continued

Significant age-associated measurement from									
Gene Expression	Entrez Id	Probe Id	Yng	Old	p Age	q Age	p Gender	q Gender	is Aging
LRP10	26020	A_24_f0	7.16	7.31	0	0.1254	0.765	0.91489	0
HLA-DRB5	3127	A_23_f0	9.05	9.7	0	0.1254	0.345	0.67843	0
PSTPIP1	9051	A_23_f0	7.92	8.28	0	0.1254	0.52	0.8114	0
GRB2	2885	A_24_f0	10.69	10.81	0	0.1254	0	0.24244	1
HLA-J	3137	A_24_f0	13.73	14.28	0	0.1254	0.735	0.91489	0
PURB	5814	A_24_f0	11.3	11.41	0	0.1254	0.54	0.8114	0
CFD	1675	A_23_f0	11.32	11.56	0	0.1254	0.05	0.33742	0
LSP1	4046	A_23_f0	10.89	11.18	0	0.1254	0.13	0.40962	0
NKX2-3	159296	A_24_f0	7.13	7.42	0	0.1254	0.715	0.91489	0
MCL1	4170	A_24_f0	13.97	14.2	0	0.1254	0.655	0.8644	0
FCGR2A	2212	A_23_f0	8.04	8.16	0	0.1254	0.68	0.8644	0
HLA-B	3106	A_24_f0	13	13.46	0	0.1254	0.435	0.7506	0
IRF1	3659	A_23_f0	9.11	9.46	0	0.1254	0.15	0.43466	0
FPR1	2357	A_23_f0	9.55	10.52	0	0.1254	0.715	0.91489	0
RAB18	22931	A_23_f0	10.64	10.84	0	0.1254	0.16	0.46339	0
PTCRA	171558	A_23_f0	7.6	7.88	0	0.1254	0.1	0.37395	0
ARHGAP1	392	A_23_f0	12.76	12.9	0	0.1254	0.26	0.59509	1
SDF4	51150	A_23_f0	12.71	12.89	0	0.1254	0.86	0.96076	0
AMICA1	120425	A_24_f0	10.94	11.78	0	0.1254	0.535	0.8114	0
CD79A	973	A_23_f0	9.33	9.88	0	0.1254	0.13	0.40962	0
CD4	920	A_24_f0	10.21	10.81	0	0.1254	0.18	0.47928	0
CTNNB1	1499	A_32_f0	10.28	10.46	0	0.1254	0.525	0.8114	1
IGF2AS	51214	A_23_f0	7.78	7.93	0	0.1254	0.94	1	0
XRCC6BP1	91419	A_24_f0	7.05	6.96	0	0.1254	0.955	1	0
PAG1	55824	A_32_f0	8.54	8.38	0	0.1254	0.59	0.8114	0
CCL3L3	414062	A_24_f0	7.16	6.96	0	0.1254	0.955	1	0
DPP4	1803	A_24_f0	7.04	6.9	0	0.1254	0.32	0.67843	0
TLN2	83660	A_32_f0	7.57	7.42	0	0.1254	0.345	0.67843	0
RAC1	5879	A_23_f0	12.63	12.45	0	0.1254	0.05	0.33742	0
LOC731884	731884	A_32_f0	9.2	9.03	0	0.1254	0.575	0.8114	0
PEA15	8682	A_24_f0	9.43	9.23	0	0.1254	0.435	0.7506	0
PLG	5340	A_32_f0	7.33	7.19	0	0.1254	0.86	0.96076	0
CDH1	999	A_23_f0	11.32	11.1	0	0.1254	0.265	0.59509	0
FKBP10	60681	A_23_f0	13.53	13.4	0	0.1254	0.37	0.67843	0
RB1	5925	A_24_f0	7.64	7.49	0	0.1254	0.095	0.37395	1
TAOK2	9344	A_23_f0	8.61	8.45	0	0.1254	0.38	0.67843	0
DLL3	10683	A_23_f0	7.66	7.48	0	0.1254	0.275	0.59509	1
MCAM	4162	A_23_f0	10.61	10.45	0	0.1254	0.195	0.49367	0
PTGR1	22949	A_23_f0	11.8	11.62	0	0.1254	0.65	0.8644	0
TCTN3	26123	A_32_f0	11.84	11.62	0	0.1254	0.175	0.47521	0
CTNNA1	8727	A_23_f0	14.09	13.85	0	0.1254	0.6	0.8114	0
IGBP1	3476	A_23_f0	10.06	9.93	0	0.1254	0.67	0.8644	0
SEMA5A	9037	A_24_f0	9.34	9.17	0	0.1254	0.58	0.8114	0
CXCL12	6387	A_24_f0	6.77	6.65	0	0.1254	0.6	0.8114	0
CMTM4	146223	A_32_f0	11.34	11.22	0	0.1254	0.58	0.8114	0
APEX1	328	A_23_f0	12.82	12.64	0	0.1254	0.735	0.91489	1
SLIT2	9353	A_32_f0	7.86	7.78	0	0.1254	0.475	0.7506	0
CDH13	1012	A_32_f0	11.21	11.05	0	0.1254	0.04	0.30732	0
SLTM	79811	A_23_f0	11.67	11.5	0	0.1254	0.92	1	0
NLGN4X	57502	A_23_f0	6.8	6.65	0	0.1254	0.505	0.8114	0
IFT140	9742	A_23_f0	8.99	8.91	0	0.1254	0.565	0.8114	0
ATP5B	506	A_23_f0	14.05	13.88	0	0.1254	0.965	1	0
PSMA4	5685	A_24_f0	13.14	13.01	0	0.1254	0.15	0.43466	0
CASP4	837	A_23_f0	12.63	12.75	0	0.1254	0.485	0.7506	0
RRAGA	10670	A_23_f0	12.88	12.77	0	0.1254	0.095	0.37395	0
MYBPC3	4607	A_23_f0	7.09	7.34	0	0.1254	0.475	0.7506	0
TREML1	340205	A_23_f0	6.85	7.1	0	0.1254	0.365	0.67843	0
RARA	5914	A_23_f0	7.76	8.06	0	0.1254	0.255	0.59509	0
NRP1	8829	A_23_f0	6.93	7.05	0	0.1254	0.525	0.8114	0
SARNP	84324	A_23_f0	13.96	13.84	0	0.1254	0.225	0.59509	0
IL17D	53342	A_23_f0	8.47	8.37	0	0.1254	0.11	0.3862	0
ASB1	51665	A_32_f0	9.87	9.79	0	0.1254	0.305	0.67843	0
TYROBP	7305	A_23_f0	11.41	12.64	0	0.1254	0.67	0.8644	0
CASP9	842	A_24_f0	12.07	11.96	0	0.1254	0.425	0.7506	0
IL13RA1	3597	A_23_f0	10.58	10.49	0	0.1254	0.13	0.40962	0
HLA-B	3106	A_24_f0	14.35	14.92	0	0.1254	0.87	0.96076	0
EXOC6	54536	A_32_f0	7.2	7.09	0	0.1254	0.97	1	0
BUB3	9184	A_23_f0	12.14	12.01	0	0.1254	0.81	0.96076	1
RTN4	57142	A_23_f0	12.98	12.87	0	0.1254	0.105	0.3862	0
CADM3	57863	A_23_f0	7.24	7.49	0	0.1254	0.49	0.7506	0
HIVEP3	59269	A_24_f0	6.93	6.79	0	0.1254	0.725	0.91489	0

TABLE S2-continued

Significant age-associated measurement from									
CLDN11	5010	A_23	7.24	7.47	0	0.1254	0.265	0.59509	0
MLL3	58508	A_23	8.46	8.35	0	0.1254	0.01	0.2608	0
PPFIBP1	8496	A_23	8.84	8.73	0	0.1254	0.295	0.59509	0
CFP	5199	A_23	9.84	10.77	0	0.1254	0.915	1	0
IL16	3603	A_24	7.24	7.15	0	0.1254	0.845	0.96076	0
ACVR1B	91	A_24	8.19	8.45	0	0.1254	0.39	0.67843	0
PTGER2	5732	A_23	8.44	8.31	0	0.1254	0.745	0.91489	0
BMP2	650	A_23	8.54	8.42	0	0.1254	0.62	0.8644	0
SON	6651	A_32	11.51	11.36	0	0.1254	0.84	0.96076	0
FRK	2444	A_23	6.72	6.56	0	0.1254	0.11	0.3862	0
TOPORS	10210	A_23	9.51	9.36	0	0.1254	0.26	0.59509	0
DYRK2	8445	A_24	8.8	8.66	0	0.1254	0.25	0.59509	0
TSLP	85480	A_23	8.1	8.03	0	0.1254	0.655	0.8644	0
CTNND1	1500	A_24	7.66	7.59	0	0.1254	0.19	0.47928	0
PRKG1	5592	A_32	6.79	7.13	0	0.1254	0.1	0.37395	0
C14orf153	84334	A_24	6.77	6.66	0	0.1254	0.205	0.59509	0
CD14	929	A_24	8.14	8.67	0	0.1254	0.855	0.96076	0
PLG	5340	A_23	7.28	7.15	0	0.1254	0.845	0.96076	0
CDC42SE2	56990	A_23	8.69	8.56	0	0.1254	0.31	0.67843	0
BCAP29	55973	A_32	7.74	7.62	0	0.1254	0.91	1	0
PPARA	5465	A_23	7.39	7.29	0	0.1254	0.8	0.91489	1
THBS2	7058	A_23	13.96	13.8	0	0.1254	0.255	0.59509	0
SEMA5A	9037	A_32	8.3	8.17	0	0.1254	0.775	0.91489	0
CMTM8	152189	A_23	9.13	8.93	0	0.1254	0.635	0.8644	0
MIB1	57534	A_32	7.54	7.42	0	0.1254	0.51	0.8114	0
FXR1	8087	A_24	9.31	9.18	0	0.1254	0.975	1	0
RIMS2	9699	A_23	7.39	7.22	0	0.1254	0.755	0.91489	0
LY86	9450	A_23	9.8	10.04	0	0.1254	0.185	0.47928	0
CYCS	54205	A_24	8.22	8.1	0	0.1254	0.05	0.33742	0
COL27A1	85301	A_23	12.74	12.61	0	0.1254	0.965	1	0
CRADD	8738	A_32	10.92	10.81	0	0.1254	0.95	1	0
HLA-F	3134	A_23	12.36	12.67	0	0.1254	0.3	0.59509	0
SLAMF7	57823	A_24	8.47	8.35	0	0.1254	0.62	0.8644	0
YWHAG	7532	A_24	14.51	14.33	0	0.1254	0.125	0.40962	0
INCENP	3619	A_23	10.79	10.65	0	0.1254	0.805	0.96076	0
DSTN	11034	A_23	13.7	13.58	0	0.1254	0.84	0.96076	0
JAKMIP1	152789	A_23	9.85	9.78	0	0.1254	0.07	0.33241	0
CBLB	868	A_23	9.84	9.71	0	0.1254	0.165	0.46339	0
ERC1	23085	A_23	7.1	6.97	0	0.1254	0.975	1	0
FLJ23834	222256	A_32	7.06	6.95	0	0.1254	0.35	0.67843	0
FUT8	2530	A_23	10.7	10.59	0	0.1254	0.35	0.67843	0
FN1	2335	A_24	8.71	8.6	0	0.1254	0.635	0.8644	0
FCER1G	2207	A_23	9.27	9.76	0	0.1254	0.56	0.8114	0
NF2	4771	A_23	7.13	7	0	0.1254	0.145	0.43466	0
PDCL3	79031	A_32	11.76	11.66	0	0.1254	0.95	1	0
IRS2	8660	A_24	7.15	7.28	0	0.1254	0.19	0.47928	1
TGM2	7052	A_24	8.25	8.45	0	0.1254	0.81	0.96076	0
COL15A1	1306	A_23	9.36	9.18	0	0.1254	0.035	0.30411	0
SMAD2	4087	A_32	7.01	6.92	0	0.1254	0.86	0.96076	0
E2F2	1870	A_23	7.66	8.06	0	0.1254	0.14	0.42106	0
ABL1	25	A_24	7.51	7.42	0	0.1254	0.155	0.45429	1
GLT25D2	23127	A_24	8.45	8.57	0	0.1254	0.525	0.8114	0
PRAM1	84106	A_23	8.39	8.73	0	0.1254	0.66	0.8644	0
PBX2	5089	A_32	7.55	7.69	0	0.1254	0.885	0.96076	0
EHD1	10938	A_23	12.1	12.27	0	0.1254	0.345	0.67843	0
ITFG3	83986	A_23	11.9	12.03	0	0.1254	0.34	0.67843	0
CNTNAP2	26047	A_23	8.56	8.68	0	0.1254	0.75	0.91489	0
THBS1	7057	A_24	9.65	9.83	0	0.1254	0.705	0.91489	0
UCP3	7352	A_24	7.45	7.84	0	0.1254	0.065	0.33241	1
SSTR3	6753	A_23	7.15	7.35	0	0.1254	0.185	0.47928	1
EXOC7	23265	A_23	9.67	9.79	0	0.1254	0.58	0.8114	0
CD300LB	124599	A_23	7.02	7.29	0	0.1254	0.685	0.8644	0
LAMC2	3918	A_23	7.78	7.88	0	0.1254	0.08	0.34601	0
RUNX1	861	A_24	7.47	7.84	0	0.1254	0.215	0.59509	0
TUBB	203068	A_32	14.06	14.15	0	0.1254	0.54	0.8114	0
B3GALNT1	8706	A_23	9.33	9.47	0	0.1254	0.21	0.59509	0
MPZL2	10205	A_24	6.99	6.77	0	0.1254	0.84	0.96076	0
SBDS	51119	A_32	10.42	10.51	0	0.1254	0.865	0.96076	0
LAT2	7462	A_23	10.67	10.96	0	0.1254	0.965	1	0
MLLT6	4302	A_32	11.01	11.16	0	0.1254	0.06	0.33241	0
LALBA	3906	A_23	6.52	6.94	0	0.1254	0.275	0.59509	0
PSMB2	5690	A_24	12.84	12.93	0	0.1254	0.7	0.8644	0
XRCC6	2547	A_32	7	6.88	0	0.1254	0.185	0.47928	1
NINJ2	4815	A_23	8.93	9.09	0	0.1254	0.6	0.8114	0

TABLE S2-continued

Significant age-associated measurement from									
JAK3	3718	A_24	7.6	7.98	0	0.1254	0.09	0.36266	0
COL6A1	1291	A_32	7.38	7.55	0	0.1254	0.11	0.3862	0
LOC645166	645166	A_32	11.01	11.1	0	0.1254	0.835	0.96076	0
BCL6B	255877	A_23	6.7	6.62	0	0.1254	0.755	0.91489	0
ERCC2	2068	A_24	8.28	8.59	0	0.1254	0.09	0.36266	1
FCGR3A	2214	A_23	9.6	10.62	0	0.1254	0.785	0.91489	0
STX1A	6804	A_23	10.19	10.42	0	0.1254	0.01	0.2608	0
UMOD	7369	A_23	7.1	7.32	0	0.1254	0.025	0.28648	0
BNIP3L	665	A_23	11.6	11.74	0	0.1254	0.45	0.7506	0
NID2	22795	A_23	10.84	10.93	0	0.1254	0.57	0.8114	0
PSMB2	5690	A_23	11.96	12.16	0	0.1254	0.26	0.59509	0
KIR2DL4	3805	A_24	6.73	7.03	0	0.1254	0.32	0.67843	0
RAC2	5880	A_23	11.2	11.44	0	0.1254	0.405	0.7506	0
RBP4	5950	A_23	12.63	12.72	0	0.1254	0.49	0.7506	0
PDGFRB	5159	A_32	7.4	7.66	0	0.1254	0.105	0.3862	1
CDC42SE1	56882	A_23	9.99	10.19	0	0.1254	0.42	0.7506	0
FCN1	2219	A_23	8.04	8.74	0	0.1254	0.42	0.7506	0
IFITM2	10581	A_24	12.34	12.53	0	0.1254	0.575	0.8114	0
TNFAIP8L1	126282	A_24	7.08	6.9	0	0.1254	0.79	0.91489	0
TNFRSF11A	8792	A_23	7.39	7.19	0	0.1254	0.745	0.91489	0
APOL2	23780	A_24	11.23	11.51	0	0.1254	0.36	0.67843	0
LITAF	9516	A_23	10.27	10.38	0	0.1254	0.72	0.91489	0
TAOK2	9344	A_23	8.79	9.25	0	0.1254	0.175	0.47521	0
MINK1	50488	A_23	8.15	8.44	0	0.1254	0.07	0.33241	0
ITGB5	3693	A_23	11.96	12.05	0	0.1254	0.53	0.8114	0
CDSN	1041	A_23	7.17	7.46	0	0.1254	0.085	0.36266	0
LRP10	26020	A_23	11.57	11.66	0	0.1254	0.6	0.8114	0
XCL2	6846	A_23	6.93	6.79	0	0.1254	0.915	1	0
RHOA	387	A_24	10.45	10.59	0	0.1254	0.705	0.91489	0
HLA-DRB1	3123	A_24	9.57	10.01	0.005	0.1484	0.69	0.8644	0
FCN1	2219	A_23	11.05	12.26	0.005	0.1484	0.78	0.91489	0
7-Sep	989	A_24	9.46	9.57	0.005	0.1484	0.36	0.67843	0
MMP9	4318	A_23	8.47	8.69	0.005	0.1484	0.5	0.7506	0
MLXIPL	51085	A_24	8.89	9.37	0.005	0.1484	0.225	0.59509	0
RPSA	3921	A_32	9.35	9.43	0.005	0.1484	0.565	0.8114	0
HLA-A	3105	A_24	12.35	12.5	0.005	0.1484	0.11	0.3862	0
PHF17	79960	A_23	11.74	11.95	0.005	0.1484	0.015	0.2661	0
HLA-C	3107	A_23	14.13	14.69	0.005	0.1484	0.365	0.67843	0
CPLX2	10814	A_23	8.98	9.36	0.005	0.1484	0.05	0.33742	0
CASP8	841	A_23	8.73	8.99	0.005	0.1484	0.15	0.43466	0
BCL2	596	A_23	8.72	9.27	0.005	0.1484	0.125	0.40962	1
CACNB3	784	A_23	7.97	8.29	0.005	0.1484	0.16	0.46339	0
DGKZ	8525	A_23	9.41	9.61	0.005	0.1484	0.07	0.33241	0
PRKCD	5580	A_23	10.09	10.29	0.005	0.1484	0.745	0.91489	1
SMAD1	4086	A_23	6.96	6.85	0.005	0.1484	0.035	0.30411	0
SLFN5	162394	A_23	7.66	7.57	0.005	0.1484	0.015	0.2661	0
IGJ	3512	A_32	10.51	10.59	0.005	0.1484	0.43	0.7506	0
CCR9	10803	A_23	7.03	6.91	0.005	0.1484	0.245	0.59509	0
PPP2R1A	5518	A_32	7.43	7.32	0.005	0.1484	0.485	0.7506	0
DHRS2	10202	A_23	15.21	15.06	0.005	0.1484	0.455	0.7506	0
SGK1	6446	A_23	13.31	13.18	0.005	0.1484	0.62	0.8644	0
FNBPI1L	54874	A_24	6.87	6.76	0.005	0.1484	0.115	0.39583	0
IK	3550	A_32	12.94	12.87	0.005	0.1484	0.455	0.7506	0
PSME1	5720	A_23	9.58	9.38	0.005	0.1484	0.825	0.96076	0
GPR98	84059	A_23	9.02	8.85	0.005	0.1484	0.48	0.7506	0
C1QTNF3	114899	A_23	8.46	8.32	0.005	0.1484	0.64	0.8644	0
IL2RG	3561	A_23	7.5	7.35	0.005	0.1484	0.345	0.67843	1
SNUPN	10073	A_24	9.26	9.09	0.005	0.1484	0.31	0.67843	2
STEAP2	261729	A_23	8.13	7.93	0.005	0.1484	0.45	0.7506	0
MAP4K4	9448	A_23	9.71	9.45	0.005	0.1484	0.86	0.96076	0
IFRD1	3475	A_24	11.09	10.88	0.005	0.1484	0.82	0.96076	0
NID1	4811	A_23	8.55	8.43	0.005	0.1484	0.68	0.8644	0
LPP	4026	A_23	8.44	8.3	0.005	0.1484	0.49	0.7506	0
SMURF2	64750	A_23	8.21	8.04	0.005	0.1484	0.665	0.8644	0
CAMK2D	817	A_24	10.72	10.55	0.005	0.1484	0.86	0.96076	0
TWIST1	7291	A_23	9.22	9.12	0.005	0.1484	0.14	0.42106	0
WNK1	65125	A_24	12.08	11.89	0.005	0.1484	0.195	0.49367	0
AP2S1	1175	A_24	11.17	11.06	0.005	0.1484	0.99	1	0
SIK1	150094	A_23	10.02	9.93	0.005	0.1484	0.955	1	0
PCDHB15	56121	A_23	7.7	7.58	0.005	0.1484	0.055	0.33742	0
PUF60	22827	A_23	12.99	12.84	0.005	0.1484	0.26	0.59509	0
RFFL	117584	A_23	7.82	7.71	0.005	0.1484	0.23	0.59509	0
DDR2	4921	A_32	8.18	8.07	0.005	0.1484	0.41	0.7506	0
HLA-B	3106	A_23	13.6	13.89	0.005	0.1484	1	1	0

TABLE S2-continued

Significant age-associated measurement from									
FANCD2	2177	A_23_f0	9.92	9.82	0.005	0.1484	0.095	0.37395	0
HDAC4	9759	A_23_f0	9.91	9.82	0.005	0.1484	0.6	0.8114	0
ICAM3	3385	A_23_f0	11.88	12.15	0.005	0.1484	0.675	0.8644	0
PHB	5245	A_23_f0	11.56	11.48	0.005	0.1484	0.09	0.36266	0
MUC4	4585	A_24_f0	7.16	7.53	0.005	0.1484	0.235	0.59509	0
PURB	5814	A_23_f0	10.53	10.42	0.005	0.1484	0.175	0.47521	0
CLDN5	7122	A_23_f0	7.21	7.47	0.005	0.1484	0.295	0.59509	0
SOCS4	122809	A_24_f0	6.99	6.84	0.005	0.1484	0.015	0.2661	0
GHRHR	2692	A_24_f0	7.16	7.44	0.005	0.1484	0.11	0.3862	1
PTGR2	145482	A_23_f0	9.31	9.2	0.005	0.1484	0.785	0.91489	0
LENG8	114823	A_24_f0	11.43	11.55	0.005	0.1484	0.555	0.8114	0
HLA-DOA	3111	A_24_f0	8.42	8.84	0.005	0.1484	0.415	0.7506	0
ULBP2	80328	A_23_f0	7.8	7.69	0.005	0.1484	0.805	0.96076	0
TGFB2	7042	A_24_f0	6.9	6.8	0.005	0.1484	0.44	0.7506	0
MLLT1	4298	A_24_f0	7.57	7.73	0.005	0.1484	0.075	0.34601	0
BCAM	4059	A_23_f0	9.97	10.41	0.005	0.1484	0.165	0.46339	0
NF2	4771	A_23_f0	13.22	13.1	0.005	0.1484	0.235	0.59509	0
IFI30	10437	A_23_f0	12.68	12.85	0.005	0.1484	0.88	0.96076	0
FEN1	2237	A_24_f0	11.69	11.6	0.005	0.1484	0.5	0.7506	1
COL27A1	85301	A_24_f0	8.99	9.18	0.005	0.1484	0.055	0.33742	0
POGK	57645	A_24_f0	10.54	10.44	0.005	0.1484	0.115	0.39583	0
MYADM	91663	A_24_f0	7.97	8.16	0.005	0.1484	0.39	0.67843	0
EFNB1	1947	A_24_f0	11.62	11.51	0.005	0.1484	0.25	0.59509	0
TYMP	1890	A_23_f0	10.56	10.89	0.005	0.1484	0.995	1	0
TNFRSF19	55504	A_23_f0	6.72	6.64	0.005	0.1484	0.175	0.47521	0
ADRBK1	156	A_23_f0	6.63	6.74	0.005	0.1484	0.765	0.91489	0
EFNB2	1948	A_24_f0	9.56	9.47	0.005	0.1484	0.395	0.67843	0
MRPS30	10884	A_23_f0	10.45	10.31	0.005	0.1484	0.06	0.33241	0
FOXH1	8928	A_23_f0	7.57	7.77	0.005	0.1484	0.13	0.40962	0
LAX1	54900	A_24_f0	7.64	7.92	0.005	0.1484	0.575	0.8114	0
APOA4	337	A_24_f0	6.81	6.94	0.005	0.1484	0.13	0.40962	0
HSPE1	3336	A_23_f0	16.02	15.89	0.005	0.1484	0.64	0.8644	0
PLSCR1	5359	A_23_f0	10.23	10.13	0.005	0.1484	0.455	0.7506	0
PEAR1	375033	A_24_f0	7.29	7.49	0.005	0.1484	0.095	0.37395	0
DLC1	10395	A_23_f0	12.69	12.56	0.005	0.1484	0.76	0.91489	0
SORL1	6653	A_23_f0	11.91	12.09	0.005	0.1484	0.38	0.67843	0
CPLX1	10815	A_24_f0	7.27	7.16	0.005	0.1484	0.93	1	0
B3GALNT1	8706	A_24_f0	7.22	7.12	0.005	0.1484	0.61	0.8644	0
GYPC	2995	A_24_f0	10.99	11.28	0.005	0.1484	0.52	0.8114	0
B3GNT5	84002	A_23_f0	8.96	8.85	0.005	0.1484	0.05	0.33742	0
ICAIL	130026	A_23_f0	6.86	6.74	0.005	0.1484	0.095	0.37395	0
C2	717	A_32_f0	9.49	9.63	0.005	0.1484	0.02	0.27551	0
FCRL2	79368	A_24_f0	6.71	6.9	0.005	0.1484	0.965	1	0
CCL24	6369	A_23_f0	9.84	10.29	0.005	0.1484	0.09	0.36266	0
CDH16	1014	A_23_f0	7.15	7	0.005	0.1484	0.46	0.7506	0
C9orf61	9413	A_32_f0	6.8	6.71	0.005	0.1484	0.56	0.8114	2
SEMA3F	6405	A_23_f0	6.92	7.18	0.005	0.1484	0.94	1	0
VHL	7428	A_23_f0	15.97	16.18	0.005	0.1484	0.965	1	0
DIAPH2	1730	A_23_f0	8.32	8.25	0.005	0.1484	0.285	0.59509	0
SNX3	8724	A_23_f0	13.08	13.2	0.005	0.1484	0.14	0.42106	0
ZNF646	9726	A_24_f0	10.83	10.9	0.005	0.1484	0.31	0.67843	2
PCDHB7	56129	A_24_f0	7.8	7.88	0.005	0.1484	0.255	0.59509	0
SLC5A2	6524	A_23_f0	8.66	8.95	0.005	0.1484	0.065	0.33241	0
AZU1	566	A_23_f0	6.6	6.7	0.005	0.1484	0.135	0.42106	0
WNK1	65125	A_23_f0	10.85	10.95	0.005	0.1484	0.025	0.28648	0
PGM5	5239	A_24_f0	6.79	6.97	0.005	0.1484	0.175	0.47521	0
LTBR	4055	A_23_f0	10.13	10.25	0.005	0.1484	0.215	0.59509	0
PNN	5411	A_23_f0	13.29	13.36	0.005	0.1484	0.165	0.46339	0
HRH2	3274	A_23_f0	6.93	7.12	0.005	0.1484	0.045	0.31994	0
PLEKHF1	79156	A_24_f0	7.81	7.99	0.005	0.1484	0.005	0.25823	0
KYNU	8942	A_23_f0	12.41	12.54	0.005	0.1484	0.44	0.7506	0
PLG	5340	A_24_f0	7.44	7.61	0.005	0.1484	0.02	0.27551	0
MAP4K2	5871	A_24_f0	7.24	7.4	0.005	0.1484	0.045	0.31994	0
CXCR5	643	A_23_f0	6.65	6.76	0.005	0.1484	0.05	0.33742	0
SIGIRR	59307	A_23_f0	10.53	10.68	0.005	0.1484	0.135	0.42106	0
CEACAM19	56971	A_23_f0	8.66	9.03	0.005	0.1484	0.055	0.33742	0
HLA-E	3133	A_32_f0	13.29	13.67	0.005	0.1484	0.305	0.67843	0
GZMM	3004	A_23_f0	8.79	8.99	0.005	0.1484	0.01	0.2608	0
MAPK7	5598	A_23_f0	9.67	9.81	0.005	0.1484	0.19	0.47928	0
HLA-DPB1	3115	A_23_f0	10.52	10.72	0.005	0.1484	0.475	0.7506	0
SIGLEC5	8778	A_23_f0	7.55	7.89	0.005	0.1484	0.945	1	0
PCDH9	5101	A_24_f0	7.27	7.17	0.005	0.1484	0.555	0.8114	0
STX1A	6804	A_23_f0	10.12	10.25	0.005	0.1484	0.425	0.7506	0

TABLE S2-continued

Significant age-associated measurement from									
IGF2BP2	10644	A_23_1	7.15	6.99	0.005	0.1484	0.24	0.59509	0
HLA-DMB	3109	A_23_1	7.51	7.78	0.005	0.1484	0.925	1	0

② indicates text missing or illegible when filed

## APPENDIX C

### [0185]

TABLE S3

GEO Datasets used in meta-analysis of aging gene expression data					
GEO Data Set or Series	Title	Species	Pubmed ID	Source	Number Chips
GDS1278	Age effect on laryngeal muscle	<i>Rattus norvegicus</i>		McMullen CA, et al.	6
GDS1279	Age effect on extraocular muscles	<i>Rattus norvegicus</i>		McMullen CA, et al.	16
GDS1280	Age effect on central and peripheral nervous	<i>Rattus norvegicus</i>		McMullen CA, et al.	12
GDS1311	Age effect on lipopolysaccharide-induced neuroinflammation and				
	Muscle function and aging (HG-U95A)	<i>Homo sapiens</i>	12204100	Welle S, et al.	12
GDS1961	Male and female thymi response to aging and caloric restriction (A)	<i>Mus musculus</i>	17499630	Lustig A, et al.	40
GDS2019	Age effect on livers of long-lived Snell dwarf	<i>Mus musculus</i>		DeFord JH, et al.	14
GDS2082	Age effect on the hippocampus	<i>Mus musculus</i>	15169854	Verbitsky M, et al.	23
GDS2612	Caloric restriction effect on aged skeletal muscle	<i>Mus musculus</i>	17381838	Edwards MG, et al.	10
GDS2639	Aging and cognitive impairment: hippocampus	<i>Rattus norvegicus</i>	17376971	Rowe WB, et al.	78
GDS2654	Neurological aging models: retinas and	<i>Mus musculus</i>	15960800	Carter TA, et al.	9
GDS2681	Caloric restriction effect on aged cochlea	<i>Mus musculus</i>	16890326	Someya S, et al.	6
GDS287	Muscle function and aging - male (HG-U133A)	<i>Homo sapiens</i>	12783983	Welle S, et al.	15
GDS288	Muscle function and aging - male (HG-U133B)	<i>Homo sapiens</i>	12783983	Welle S, et al.	15
GDS2929	Aging lungs and genetic background	<i>Mus musculus</i>	17726092	Misra V, et al.	15
GDS2962	Male and female thymi response to aging and caloric restriction (B)	<i>Mus musculus</i>	18081424	Lustig A, et al.	40
GDS355	Calorie restriction and aging (Mu11K-A)	<i>Mus musculus</i>		Kayo T, et al.	10
GDS356	Calorie restriction and aging (Mu11K-B)	<i>Mus musculus</i>		Kayo T, et al.	10
GDS399	Cardiac aging	<i>Rattus norvegicus</i>	12902548	Dobson JG, et al.	11
GDS40	Cardiac development, maturation and aging	<i>Mus musculus</i>		Schinke M, et al.	15
GDS472	Muscle function and aging - female (HG-U133A)	<i>Homo sapiens</i>		Welle, et al.	15
GDS473	Muscle function and aging - female (HG-U133B)	<i>Homo sapiens</i>		Welle, et al.	15
GDS520	Hippocampal aging and cognitive impairment	<i>Rattus norvegicus</i>	12736351	Blalock EM, et al.	19
GDS583	Aging time course, normal adult	<i>Caenorhabditis elegans</i>	14730301	McCarroll SA, et al.	6
GDS707	Aging brain: frontal cortex expression profiles at various ages	<i>Homo sapiens</i>	15190254	Lu T, et al.	22
GSE11097	Coordinated Changes in Xenobiotic Metabolizing	<i>Rattus norvegicus</i>		Lee JS, et al.	21

TABLE S3-continued

GEO Datasets used in meta-analysis of aging gene expression data					
GEO Data Set or Series	Title	Species	Pubmed ID	Source	Number Chips
GSE11291	Enzyme Gene Expression in Aging Male Rats: Brown Norway and F344 Effect of age, calorie restriction and resveratrol on gene expression in mouse heart, brain, and skeletal muscle	<i>Mus musculus</i>	18523577	Barger JL, et al.	30
GSE11546	Age-related changes in the expression of schizophrenia susceptibility genes in the Aging Time course	<i>Homo sapiens</i>	18470533	Colantuoni C, et al.	33
GSE12168	Age-related behaviors have distinct transcriptional profiles in <i>Drosophila melanogaster</i>	<i>Caenorhabditis elegans</i>	18662544	Budovskaya YV, et al.	16
GSE12290	Age-related behaviors have distinct transcriptional profiles in <i>Drosophila melanogaster</i>	<i>Caenorhabditis elegans</i>	18778409	Golden TR, et al.	70
GSE12872	Ageing hematopoietic progenitor/stem cells over life span: Indy vs.	<i>Drosophila melanogaster</i>	19164521	Neretti N, et al.	25
GSE13496	Aging Liver Profiles of the Long Lived Prop-1 Mutant Mouse (Ames) and Wild Type Controls	<i>Homo sapiens</i>	18596738	Stirewelt DL, et al.	10
GSE3150	LTM in CA1 Aged versus young rats	<i>Mus musculus</i>		DeFord JH, et al.	21
GSE3531	Identification of putative learning and memory genes in the dentate gyrus of aged rats following the Morris Water Maze	<i>Rattus norvegicus</i>	16829144	Burger C, et al.	79
GSE4821	Transcriptional profile of aging human muscle	<i>Rattus norvegicus</i>		Burger C, et al.	79
GSE5086	Temporal and Spatial Transcriptional Profiles of Aging in <i>Drosophila</i>	<i>Homo sapiens</i>	16789832	Zahn JM, et al.	40
GSE6314	Transcriptional Response to Aging and Caloric Restriction in Heart and	<i>Drosophila melanogaster</i>		Yamaza H, et al.	55
GSE6718	Age Map, Cerebellum (A)	<i>Rattus norvegicus</i>	17874999	Linford NJ, et al.	25
GSE8409	Age Map, Cerebral Cortex	<i>Mus musculus</i>	17988385	Zahn JM, et al.	40
GSE8410	Age Map, Spinal Cord (A)	<i>Mus musculus</i>	17988385	Zahn JM, et al.	40
GSE8412	Age Map, Cerebellum (B)	<i>Mus musculus</i>	17988385	Zahn JM, et al.	38
GSE8414	Age Map, Cerebral Cortex	<i>Mus musculus</i>	17988385	Zahn JM, et al.	39
GSE8415	Age Map, Spinal Cord (B)	<i>Mus musculus</i>	17988385	Zahn JM, et al.	38
GSE8418	Age Map, Striatum (B)	<i>Mus musculus</i>	17988385	Zahn JM, et al.	41
GSE8419	Resistance Exercise Reverses Aging in Human Skeletal Muscle	<i>Mus musculus</i>	17988385	Zahn JM, et al.	40
GSE8479	Skeletal Muscle Transcript Profiles in Trained or Sedentary Young and Old Subjects	<i>Homo sapiens</i>	17520024	Melov S, et al.	51
GSE9103	The skeletal muscle transcript profile reflects responses to inadequate protein intake in younger	<i>Homo sapiens</i>		Asmann YW, et al.	40
GSE9419	AGEMAP_Adrenals	<i>Homo sapiens</i>	17490972	Campbell WW, et al.	66
GSE9895	AGEMAP_Bone_Marrow	<i>Mus musculus</i>	16789832	Zahn JM, et al.	80
GSE9898	AGEMAP_Eye	<i>Mus musculus</i>	18081424	Zahn JM, et al.	72
GSE9900	AGEMAP_Gonads	<i>Mus musculus</i>	18081424	Zahn JM, et al.	80
GSE9901	AGEMAP_Heart	<i>Mus musculus</i>	16789832	Zahn JM, et al.	77
GSE9902	AGEMAP_Kidney	<i>Mus musculus</i>	16789832	Zahn JM, et al.	76
GSE9904	AGEMAP_Liver	<i>Mus musculus</i>	16789832	Zahn JM, et al.	80
GSE9905	AGEMAP_Lung	<i>Mus musculus</i>	18081424	Zahn JM, et al.	64
GSE9906	AGEMAP_Skeletal_Muscle	<i>Mus musculus</i>	16789832	Zahn JM, et al.	80
GSE9907	AGEMAP_Spleen	<i>Mus musculus</i>	18081424	Zahn JM, et al.	80
GSE9908					

## APPENDIX D

[0186]

TABLE S4

Genes found to be significantly associated with age in the meta-analysis			
Entrez ID	Name	MetaEffect	pvalFisher
68031	C3	0.337698315	1.10E-54
7750	RT1-Ba	0.196164486	1.06E-41
1880	Gpnmh	0.643641429	1.01E-37
2974	Fcgr2b	0.243994532	2.05E-34
16958	Igf1	0.226477271	3.56E-32
17012	1100001E <sup>Ⓢ</sup>	0.849789673	4.49E-32
20867	Ctss	0.152554449	3.55E-31
9962	CXorf57	0.325268282	6.96E-27
86179	EG665378	1.104731656	9.48E-27
1603	RT1-Bb	0.160732706	2.23E-25
36030	C4b	0.261099138	5.33E-24
56810	Lrp1b	0.30257626	5.74E-24
5109	Adamts5	0.251108456	6.79E-24
68066	Hbb	0.164149192	7.36E-24
90902	Usp54	0.186061881	3.01E-23
14126	Il33	0.215106418	6.57E-23
7924	S100a4	0.208560953	1.86E-21
7839	Mifl	-0.2592617	8.04E-21
113759	C21orf7	0.768001812	7.61E-20
115591	LOC25924 <sup>Ⓢ</sup>	-0.15443516	1.27E-19
23032	Fam46a	0.180448732	1.38E-19
1431	Ctgf	0.183450344	5.03E-18
31070	Glra2	-0.15727832	5.78E-18
49424	CCDC69	-0.204656	1.73E-16
7986	Tyrobp	0.281565935	1.99E-16
2000	Plek	0.182525947	2.35E-16
23519	Acsf2	-0.36717971	2.72E-16
37584	Hoxb2	-0.28593823	1.51E-15
49543	ZNF415	-0.25527055	2.94E-15
122149	HMG2	0.278687741	8.90E-15
88734	MT1X	0.304942233	9.85E-15
108195	NPIP	0.210485047	2.02E-14
2086	Pros28.1	0.212491471	2.18E-14
69153	Ptpla	-0.34183304	4.75E-14
89678	LOC6850 <sup>Ⓢ</sup>	1.084414575	4.78E-14
120336	LOC49978 <sup>Ⓢ</sup>	0.216224302	5.11E-14
49694	Cxcl16	0.218628389	6.86E-14
82588	RGD15599	-0.15420995	7.29E-14
56300	CG13384	0.278803929	1.05E-13
7309	Mpzl2	0.176061389	2.81E-13
65299	Tmtc1	0.154398135	3.08E-13
74448	LOC28691 <sup>Ⓢ</sup>	-0.18157704	4.15E-13
41282	Erb2ip	0.168449838	4.66E-13
49949	COL21A1	0.199777973	8.60E-13
88747	C10orf116	0.380945602	2.17E-12
38171	Ifi30	0.262554903	2.20E-12
104063	UQCRH	-0.27138499	3.75E-12
9413	Clec4a3	0.635951202	4.74E-12
88538	170003412	-0.19778363	5.48E-12
5782	Lace1	-0.19706732	8.82E-12
2236	Clec11a	-0.18548667	1.25E-11
1209	Irf7	0.177331413	1.36E-11
17048	Ttc18	0.200712085	1.49E-11
76450	Cml3	0.36115736	2.07E-11
15446	Asb12	-0.36585936	3.52E-11
477	Fcgr3a	0.320924509	3.61E-11
20453	Cfd	0.162628176	3.63E-11
90224	1500009L1	0.225854306	9.44E-11
17057	Spata18	0.155521865	9.97E-11
115689	Plscr2	0.437399565	2.77E-10
9294	Pla1a	0.151688359	3.57E-10
18882	Paqr9	-0.19890688	3.82E-10
40707	Opn3	-0.17691302	3.90E-10
89046	RGD15641	0.185419884	4.30E-10
7945	Slfn2	0.421614816	4.39E-10
121641	His3.3A	0.219066526	4.64E-10
79796	LOC68975 <sup>Ⓢ</sup>	-0.2593191	8.52E-10

TABLE S4-continued

Genes found to be significantly associated with age in the meta-analysis			
Entrez ID	Name	MetaEffect	pvalFisher
8332	Hook2	-0.1705913	1.29E-09
108191	MT1H	0.210737894	1.72E-09
16012	Frmf3	-0.16181809	1.91E-09
35310	3-Mar	-0.15429759	2.06E-09
87124	Pedhb9	0.254572988	3.36E-09
105677	YWHAQ	0.171385197	4.10E-09
11093	Fn3krp	0.202668204	4.37E-09
11509	Ccdc28b	-0.21674847	4.68E-09
87898	ISCA1	-0.19555157	5.40E-09
45124	Gcom1	0.169362212	5.83E-09
74413	E2f3	-0.15512234	8.46E-09
48326	Glp2	0.329823574	1.10E-08
37689	PTMA	0.166331587	1.20E-08
9135	TRIM58	0.237072147	1.31E-08
23499	Synpo2l	0.24111956	1.49E-08
9574	Pcdh12	-0.22442615	1.78E-08
27392	Cpne2	0.233138906	1.79E-08
12698	Ddit4l	-0.16390882	2.06E-08
75853	Cyp4x1	0.219081962	2.92E-08
114241	RGD15594	0.469297715	3.25E-08
72226	Zfp454	0.29786873	3.38E-08
55916	S100a11	0.157104104	5.53E-08
14286	Galntf2	0.219172594	7.10E-08
294	Sox9	0.252846332	8.50E-08
104370	ZNF492	0.238974473	9.47E-08
122101	C14orf2	-0.1545888	1.10E-07
121604	DUSP13	-0.3154509	1.13E-07
62161	Vangl2	-0.18404987	1.44E-07
19108	Dhrs7c	-0.21508803	1.55E-07
45432	Slfn8	0.243086196	2.01E-07
48388	MT2A	0.299104826	3.01E-07
5353	Pdss1	-0.1508792	3.71E-07
77713	LOC36022 <sup>Ⓢ</sup>	0.150600586	3.98E-07
8835	FAM38A	0.252755946	4.57E-07
25079	TPPP2	-0.16214316	7.69E-07
86882	Fmo2	0.23321182	7.99E-07
49517	TRMT61B	-0.20121551	1.07E-06
123533	RGD13101	-0.40076548	1.11E-06
19274	4933405L1	-0.24082886	1.12E-06
86733	MGC10882	0.279660777	1.37E-06
56783	LOC31072 <sup>Ⓢ</sup>	0.267238671	1.65E-06
10073	Pnmal1	0.295057188	2.08E-06
89164	isg12(b)	0.189563208	2.15E-06
10641	CTNNBIP1	-0.25394574	2.27E-06
39074	Nmnat1	-0.15689057	2.51E-06
66117	MYH7B	0.323225125	3.03E-06
48468	H28	0.194466507	3.23E-06
74438	Ifi204	0.216986862	3.34E-06
7014	EG226654	0.267725488	3.80E-06
85555	1700019N	-0.35184516	4.34E-06
19952	Efcab7	0.15813991	4.69E-06
8024	Hcst	0.172404007	5.13E-06
7392	Kcnu1	-0.27873757	5.23E-06
23217	Plscr4	0.20548157	5.91E-06
17562	Ankle1	0.217270121	9.29E-06
68443	CLEC2B	0.204602687	9.30E-06
826	RGD13105	0.170957726	9.55E-06
9927	Fam70a	0.159236473	9.96E-06
86122	ISOC2	-0.21966312	1.04E-05
4665	Ubd	0.158771035	1.06E-05
103871	RGD13079	-0.18158672	1.43E-05
122195	1700054F2	-0.17122413	1.49E-05
45975	RGD13093	0.188776766	1.61E-05
28424	Rasef	0.185265697	1.66E-05
70768	Here6	0.164936064	1.86E-05
16320	Cthre1	-0.22905115	2.18E-05
118004	1700019C <sup>Ⓢ</sup>	0.192558616	2.52E-05
88921	C1qtnf3	-0.26565138	4.28E-05
117949	Fcn1	0.296439068	4.59E-05
121796	Krtap4-2	-0.48676484	4.66E-05
86269	Stfa2l3	0.539695764	5.11E-05

TABLE S4-continued

Genes found to be significantly associated with age in the meta-analysis			
Entrez ID	Name	MetaEffect	pvalFisher
8908	Galnac4s <sup>Ⓢ</sup>	-0.15004653	5.67E-05
22708	Itgb1bp2	-0.1846864	5.89E-05
12732	Tmem177	-0.15887907	8.44E-05
56944	Rtp4	0.160669645	8.54E-05
18680	Tmem52	0.194064654	8.72E-05
17571	Kbtbd5	0.316607601	9.22E-05
85034	OTTMUSC <sup>Ⓢ</sup>	-0.15381647	9.44E-05
9726	Gramd1c	0.157603931	9.59E-05
10813	Alpk3	0.1854543	0.00011733
84858	Cd209b	0.231577687	0.00013048
49905	1700074F <sup>Ⓢ</sup>	-0.30179196	0.00014641
76446	Tsgal3	-0.16383325	0.00014714
86705	LOC69117 <sup>Ⓢ</sup>	-0.22412126	0.0001552
114502	LOC68515 <sup>Ⓢ</sup>	0.394921169	0.00016499
18252	Fsd2	-0.16439316	0.0001684
71779	Rsph4a	0.255594277	0.00019155
34940	Arid5a	0.156559299	0.00025282
16823	CG9996	0.232308435	0.00025503
77416	Mkl	-0.16899747	0.00034472
12257	4930547C <sup>Ⓢ</sup>	1.950401446	0.00048183
41271	Arhgap15	0.159114218	0.00048941
19144	Fam171a2	-0.18584737	0.00052079
49710	TTC31	0.179167307	0.00058897
79726	Doxl1	-0.19722464	0.00061038
117975	ZNF432	0.213393951	0.00062803
110822	Klra5	0.18662964	0.00067557
89168	ZNF323	0.222940842	0.00070422
9555	Ninj2	0.154045269	0.0007144
35542	E030049C <sup>Ⓢ</sup>	-0.32681836	0.0007853
69257	ERMAP	0.172273481	0.00078899
50475	Alpk2	0.152879973	0.00085675
117700	ZNF267	0.1545496	0.00087049
18691	6430537E <sup>Ⓢ</sup>	0.153146801	0.00094589
17794	Klre1	-0.16554649	0.00098146
78018	Lrrc69	0.152806524	0.00108119
10471	MOSPD1	-0.15083294	0.00117142
108186	HMG1	0.170483349	0.00118704
28471	RGD15631	0.177024178	0.0012595
10590	1810011C <sup>Ⓢ</sup>	-0.18929868	0.00130599
10416	4933403C <sup>Ⓢ</sup>	-0.30079696	0.00132841
75166	Pmaip1	0.390056763	0.00137565

TABLE S4-continued

Genes found to be significantly associated with age in the meta-analysis			
Entrez ID	Name	MetaEffect	pvalFisher
18842	2310010M	-0.16617861	0.0014787
65996	BC046404	-0.18761865	0.00157999
65257	Ip6k3	0.183436928	0.00173745
22993	Gypc	-0.15892467	0.00190704
81055	Slc16a12	0.173590885	0.00204682
48124	Ppp1r3a	-0.16723044	0.00209565
119893	Ces6	-0.15031123	0.00212561
18692	Dpy19l3	-0.15647733	0.00214371
56428	Ppm1a	-0.15028605	0.0021799
8897	Tecpr2	0.191902469	0.00251988
88945	BC043301	-0.1536364	0.00260783
86703	Ng23	-0.19533328	0.00267018
47588	MGC116 <sup>Ⓢ</sup>	-0.1949287	0.00274781
113783	Itgb1bp3	0.316801607	0.0029
41378	Olfir1509	-0.18984245	0.00312148
104345	LOC6802 <sup>Ⓢ</sup>	0.420756428	0.00325828
114519	Cd209g	0.224085149	0.00341367
27072	A330049M	0.215087101	0.00348459
12281	RGD13080	-0.21493136	0.00397285
77326	Zfp52	0.33674368	0.0039854
99855	Agmat	-0.15017764	0.0047176
110478	Olfir672	0.482514016	0.00499443
35234	Pddc1	0.160100112	0.0054081
75198	Ankrd36	0.35318104	0.00592135
11488	Smtnl1	0.207571119	0.00597194
18544	Rnf222	0.531926369	0.00728218
110771	Svs3	-0.21042565	0.00775244
10957	Cd200r1	0.33606348	0.00820976
84597	Tusc1	-0.21056139	0.00826404
103867	49334151 <sup>Ⓢ</sup>	0.174474914	0.00840595
77918	170006511	-0.25231707	0.00870332
122178	Cyp2j5	0.168201503	0.00870845
23416	Slco1a6	-0.18459302	0.00938508
104304	Psbpc1	-0.24382829	0.00950761
32697	Nphp3	0.178084932	0.00952455

<sup>Ⓢ</sup> indicates text missing or illegible when filed

APPENDIX E

[0187]

TABLE S5

Network cluster membership		Serum cytokines	Chemokines
Th1		INF-A2	Eotaxin
Th2		INF-G	IL-12p40
		II-4	IP-10
		IL-5	
		IL-7	

Gene Expression	Probe ID	Entrez ID	Gene Symbol	Gene Description
GC1	A_23_P107735	973	CD79A	CD79a molecule, immunoglobulin-associated alpha
	A_23_P116387	3619	INCENP	inner centromere protein antigens 135/155 kDa
	A_23_P116765	3906	LALBA	lactalbumin, alpha-
	A_23_P125990	1870	E2F2	E2F transcription factor 2
	A_23_P127385	4607	MYBPC3	myosin binding protein C, cardiac
	A_23_P130836	3004	GZMM	granzyme M (lymphocyte metase 1)

TABLE S5-continued

A__23__P132115	150094	SIK1	salt-inducible kinase 1
A__23__P133665	2444	FRK	fyn-related kinase
A__23__P140057	55504	TNFRSF19	tumor necrosis factor receptor superfamily, member 19
A__23__P145264	3134	HLA-F	major histocompatibility complex, class I, F
A__23__P15369	124599	CD300LB	CD300 molecule-like family member b
A__23__P156550	340205	TREML1	triggering receptor expressed on myeloid cells-like 1
A__23__P158775	7369	UMOD	uromodulin
A__23__P160849	2207	FCER1G	Fc fragment of IgE, high affinity I, receptor for; gamma polypeptide
A__23__P164307	50488	MINK1	misshapen-like kinase 1 (zebrafish)
A__23__P167537	10814	CPLX2	complexin 2
A__23__P17224	130026	ICA1L	islet cell autoantigen 1, 69 kDa-like
A__23__P201156	57863	CADM3	cell adhesion molecule 3
A__23__P202667	156	ADRBK1	adrenergic, beta, receptor kinase 1
A__23__P203215	643	CXCR5	chemokine (C—X—C motif) receptor 5
A__23__P207842	5914	RARA	retinoic acid receptor, alpha
A__23__P208132	596	BCL2	B-cell CLL/lymphoma 2
A__23__P209389	841	CASP8	caspase 8, apoptosis-related cysteine peptidase
A__23__P215491	6369	CCL24	chemokine (C-C motif) ligand 24
A__23__P218269	9344	TAOK2	TAO kinase 2
A__23__P258377	23085	ERC1	ELKS/RAB6-interacting/CAST family member 1
A__23__P29800	5010	CLDN11	claudin 11
A__23__P306730	5465	PPARA	peroxisome proliferator-activated receptor alpha
A__23__P30755	171558	PTCRA	pre T-cell antigen receptor alpha
A__23__P324813	255877	BCL6B	B-cell CLL/lymphoma 6, member B (zinc finger protein)
A__23__P325991	4771	NF2	neurofibromin 2 (merlin)
A__23__P334271	4086	SMAD1	SMAD family member 1
A__23__P364592	57502	NLGN4X	neuroligin 4, X-linked
A__23__P371794	784	CACNB3	calcium channel, voltage-dependent, beta 3 subunit
A__23__P390518	8792	TNFRSF11A	tumor necrosis factor receptor superfamily, member 11a, NFkB activator
A__23__P398574	4059	BCAM	basal cell adhesion molecule (Lutheran blood group)
A__23__P402899	162394	SLFN5	schlafen family member 5
A__23__P408095	11034	DSTN	destinin (actin depolymerizing factor)
A__23__P411277	6524	SLC5A2	solute carrier family 5 (sodium/glucose cotransporter), member 2
A__23__P41166	8706	B3GALNT1	beta-1,3-N-acetylgalactosaminyltransferase 1 (globoside blood group)
A__23__P430764	56990	CDC42SE2	CDC42 small effector 2
A__23__P48109	4815	NINJ2	ninjurin 2
A__23__P6321	7122	CLDN5	claudin 5
A__23__P68910	6753	SSTR3	somatostatin receptor 3
A__23__P70520	1041	CDSN	corneodesmosin
A__23__P7535	3274	HRH2	histamine receptor H2

TABLE S5-continued

A__23_P78526	56971	CEACAM19	carcinoembryonic antigen-related cell adhesion molecule 19
A__23_P82959	8928	FOXH1	forkhead box H1
A__23_P86390	8829	NRP1	neuropilin 1
A__23_P95672	10644	IGF2BP2	insulin-like growth factor 2 mRNA binding protein 2
A__24_P134195	91663	MYADM	myeloid-associated differentiation marker
A__24_P139901	2995	GYPC	glycophorin C (Gerbich blood group)
A__24_P151295	4298	MLLT1	myeloid/lymphoid or mixed-lineage leukemia (trithorax homolog, <i>Drosophila</i> ); translocated to, 1
A__24_P17048	2692	GHRHR	growth hormone releasing hormone receptor
A__24_P194068	79156	PLEKHF1	pleckstrin homology domain containing, family F (with FYVE domain) member 1
A__24_P207003	8660	IRS2	insulin receptor substrate 2
A__24_P209389	51085	MLXIPL	MLX interacting protein-like
A__24_P22174	84334	C14orf153	chromosome 14 open reading frame 153
A__24_P239183	4585	MUC4	mucin 4, cell surface associated
A__24_P240487	5340	PLG	plasminogen
A__24_P252934	337	APOA4	apolipoprotein A-IV
A__24_P282416	25	ABL1	c-abl oncogene 1, receptor tyrosine kinase
A__24_P288298	3805	KIR2DL4	killer cell immunoglobulin-like receptor, two domains, long cytoplasmic tail, 4
A__24_P291278	54900	LAX1	lymphocyte transmembrane adaptor 1
A__24_P292470	7352	UCP3	uncoupling protein 3 (mitochondrial, proton carrier)
A__24_P295999	920	CD4	CD4 molecule
A__24_P308096	3718	JAK3	Janus kinase 3
A__24_P341897	91	ACVR1B	activin A receptor, type IB
A__24_P354800	3111	HLA-DOA	major histocompatibility complex, class II, DO alpha
A__24_P363896	85301	COL27A1	collagen, type XXVII, alpha 1
A__24_P366967	54874	FNBP1L	formin binding protein 1-like
A__24_P385326	375033	PEAR1	platelet endothelial aggregation receptor 1
A__24_P38702	159296	NKX2-3	NK2 transcription factor related, locus 3 ( <i>Drosophila</i> )
A__24_P401990	2068	ERCC2	excision repair cross-complementing rodent repair deficiency, complementation group 2
A__24_P50767	5871	MAP4K2	mitogen-activated protein kinase kinase kinase 2
A__24_P881527	1500	CTNND1	catenin (cadherin-associated protein), delta
A__24_P917783	861	RUNX1	runt-related transcription factor 1
A__32_P150735	55973	BCAP29	B-cell receptor-associated protein 29
A__32_P183609	51665	ASB1	ankyrin repeat and SOCS box-containing 1
A__32_P187875	1499	CTNNB1	catenin (cadherin-associated protein), beta 1, 88 kDa

TABLE S5-continued

	A__32__P197942	22256	FLJ23834	hypothetical protein FLJ23834
	A__32__P215404	5159	PDGFRB	platelet-derived growth factor receptor, beta polypeptide
	A__32__P460973	3133	HLA-E	major histocompatibility complex, class I, E
	A__32__P6062	5592	PRKG1	protein kinase, cGMP- dependent, type I
GC2	A__32__P72622	1291	COL6A1	collagen, type VI, alpha 1
	A__23__P100704	5598	MAPK7	mitogen-activated protein kinase 7
	A__23__P102192	9448	MAP4K4	mitogen-activated protein kinase kinase kinase kinase 4
	A__23__P112554	1306	COL15A1	collagen, type XV, alpha 1
	A__23__P119562	1675	CFD	complement factor D (adipsin)
	A__23__P127627	8525	DGKZ	diacylglycerol kinase, zeta 104 kDa
	A__23__P134517	5814	PURB	purine-rich element binding protein B
	A__23__P144054	5580	PRKCD	protein kinase C, delta
	A__23__P164691	3385	ICAM3	intercellular adhesion molecule 3
	A__23__P166633	3693	ITGB5	integrin, beta 5
	A__23__P168419	58508	MLL3	myeloid/lymphoid or mixed-lineage leukemia 3
	A__23__P168556	6804	STX1A	syntaxin 1A (brain)
	A__23__P169117	10670	RRAGA	Ras-related GTP binding A
	A__23__P170058	5690	PSMB2	proteasome (prosome, macropain) subunit, beta type, 2
	A__23__P18372	84002	B3GNT5	UDP-GlcNAc:betaGal beta- 1,3-N- acetylglucosaminyltransferase 5
	A__23__P19134	84059	GPR98	G protein-coupled receptor 98
	A__23__P201636	3918	LAMC2	laminin, gamma 2
	A__23__P205499	26020	LRP10	low density lipoprotein receptor-related protein 10
	A__23__P206359	999	CDH1	cadherin 1, type 1, E- cadherin (epithelial)
	A__23__P212360	10803	CCR9	chemokine (C-C motif) receptor 9
	A__23__P218770	5880	RAC2	ras-related C3 botulinum toxin substrate 2 (rho family, small GTP binding protein Rac2)
	A__23__P250701	65125	WNK1	WNK lysine deficient protein kinase 1
	A__23__P251051	4771	NF2	neurofibromin 2 (merlin)
	A__23__P252362	10884	MRPS30	mitochondrial ribosomal protein S30
	A__23__P35912	837	CASP4	caspase 4, apoptosis- related cysteine peptidase
	A__23__P40174	4318	MMP9	matrix metalloproteinase 9 (gelatinase B, 92 kDa gelatinase, 92 kDa type IV collagenase)
	A__23__P428260	261729	STEAP2	six transmembrane epithelial antigen of the prostate 2
	A__23__P47867	8496	PPFIBP1	PTPRF interacting protein, binding protein 1 (liprin beta 1)
	A__23__P52647	10938	EHD1	EH-domain containing 1
	A__23__P53557	4055	LTBR	lymphotoxin beta receptor (TNFR superfamily, member 3)
	A__23__P56898	8942	KYNU	kynureninase (L- kynurenine hydrolase)
	A__23__P56933	57142	RTN4	reticulon 4

TABLE S5-continued

A_23_P6878	6405	SEMA3F	sema domain, immunoglobulin domain (Ig), short basic domain, secreted, (semaphorin) 3F
A_23_P75283	5950	RBP4	retinol binding protein 4, plasma
A_23_P82420	6804	STX1A	syntaxin 1A (brain)
A_23_P84344	59307	SIGIRR	single immunoglobulin and toll-interleukin 1 receptor (TIR) domain
A_23_P84399	26047	CNTNAP2	contactin associated protein-like 2
A_23_P87049	6653	SORL1	sortilin-related receptor, L(DLR class) A repeats-containing
A_23_P91802	1890	TYMP	thymidine phosphorylase
A_24_P102636	5925	RB1	retinoblastoma 1
A_24_P106681	7532	YWHAG	tyrosine 3-monooxygenase/tryptophan 5-monooxygenase activation protein, gamma polypeptide
A_24_P137897	3475	IFRD1	interferon-related developmental regulator 1
A_24_P174550	387	RHOA	ras homolog gene family, member A
A_24_P187218	5101	PCDH9	protocadherin 9
A_24_P243373	56129	PCDHB7	protocadherin beta 7
A_24_P254949	5239	PGM5	phosphoglucomutase 5
A_24_P287043	10581	IFITM2	interferon induced transmembrane protein 2 (1-8D)
A_24_P376483	3105	HLA-A	major histocompatibility complex, class I, A
A_24_P402438	7042	TGFB2	transforming growth factor, beta 2
A_24_P407717	2885	GRB2	growth factor receptor-bound protein 2
A_24_P48898	23780	APOL2	apolipoprotein L, 2
A_24_P62505	23127	GLT25D2	glycosyltransferase 25 domain containing 2
A_24_P769359	65125	WNK1	WNK lysine deficient protein kinase 1
A_24_P90637	122809	SOCS4	suppressor of cytokine signaling 4
A_24_P926770	26020	LRP10	low density lipoprotein receptor-related protein 10
A_24_P944054	6387	CXCL12	chemokine (C-X-C motif) ligand 12 (stromal cell-derived factor 1)
A_24_P97104	1803	DPP4	dipeptidyl-peptidase 4
A_32_P109002	4087	SMAD2	SMAD family member 2
A_32_P132748	731884	LOC731884	similar to programmed cell death 6 interacting protein
A_32_P162187	717	C2	complement component 2
A_32_P206123	5340	PLG	plasminogen
A_32_P43664	3512	IGJ	immunoglobulin J polypeptide, linker protein for immunoglobulin alpha and mu polypeptides
A_32_P61684	55824	PAG1	phosphoprotein associated with glycosphingolipid microdomains 1
A_32_P78528	203068	TUBB	tubulin, beta
A_32_P85999	1012	CDH13	cadherin 13, H-cadherin (heart)
A_32_P98683	4302	MLLT6	myeloid/lymphoid or mixed-lineage leukemia (trithorax homolog, <i>Drosophila</i> ); translocated to, 6

TABLE S5-continued

GC3	A_23_P100556	23265	EXOC7	exocyst complex component 7
	A_23_P116435	51214	IGF2AS	insulin-like growth factor 2 antisense
	A_23_P121851	56121	PCDHB15	protocadherin beta 15
	A_23_P130040	5245	PHB	prohibitin
	A_23_P137196	3597	IL13RA1	interleukin 13 receptor, alpha 1
	A_23_P143994	2177	FANCD2	Fanconi anemia, complementation group D2
	A_23_P144274	152789	JAKMIP1	Janus kinase and microtubule interacting protein 1
	A_23_P151710	5732	PTGER2	prostaglandin E receptor 2 (subtype EP2), 53 kDa
	A_23_P153741	566	AZU1	azurocidin 1
	A_23_P15727	60681	FKBP10	FK506 binding protein 10, 65 kDa
	A_23_P171255	3476	IGBP1	immunoglobulin (CD79A) binding protein 1
	A_23_P210048	9759	HDAC4	histone deacetylase 4
	A_23_P212715	868	CBLB	Cas-Br-M (murine) ecotropic retroviral transforming sequence b
	A_23_P215406	5879	RAC1	ras-related C3 botulinum toxin substrate 1 (rho family, small GTP binding protein Rac1)
	A_23_P30693	5340	PLG	plasminogen
	A_23_P313632	2530	FUT8	fucosyltransferase 8 (alpha (1,6) fucosyltransferase)
	A_23_P32217	10210	TOPORS	topoisomerase I binding, arginine/serine-rich
	A_23_P345692	53342	IL17D	interleukin 17D
	A_23_P40880	152189	CMTM8	CKLF-like MARVEL transmembrane domain containing 8
	A_23_P43946	84324	SARNP	SAP domain containing ribonucleoprotein
	A_23_P46924	9184	BUB3	budding uninhibited by benzimidazoles 3 homolog (yeast)
	A_23_P48713	145482	PTGR2	prostaglandin reductase 2
	A_23_P56922	3336	HSPE1	heat shock 10 kDa protein 1 (chaperonin 10)
	A_23_P62021	7058	THBS2	thrombospondin 2
	A_23_P69109	5359	PLSCR1	phospholipid scramblase 1
	A_23_P70688	9450	LY86	lymphocyte antigen 86
	A_23_P85004	1730	DIAPH2	diaphanous homolog 2 ( <i>Drosophila</i> )
	A_24_P111342	842	CASP9	caspase 9, apoptosis-related cysteine peptidase
	A_24_P124992	5685	PSMA4	proteasome (prosome, macropain) subunit, alpha type, 4
	A_24_P142118	7057	THBS1	thrombospondin 1
	A_24_P161933	3106	HLA-B	major histocompatibility complex, class I, B
	A_24_P228130	414062	CCL3L3	chemokine (C-C motif) ligand 3-like 3
	A_24_P286465	5814	PURB	purine-rich element binding protein B
	A_24_P291973	989	7-Sep	septin 7
	A_24_P29665	54205	CYCS	cytochrome c, somatic
	A_24_P319647	79368	FCRL2	Fc receptor-like 2
	A_24_P353638	57823	SLAMF7	SLAM family member 7
	A_24_P355944	1948	EFNB2	ephrin-B2
	A_24_P40055	114823	LENG8	leukocyte receptor cluster (LRC) member 8
	A_24_P876734	59269	HIVEP3	human immunodeficiency virus type I enhancer binding protein 3

TABLE S5-continued

	A__24__P923251	7052	TGM2	transglutaminase 2 (C polypeptide, protein-glutamine-gamma-glutamyltransferase)
	A__24__P942786	8445	DYRK2	dual-specificity tyrosine-(Y)-phosphorylation regulated kinase 2
	A__32__P141664	5089	PBX2	pre-B-cell leukemia homeobox 2
	A__32__P222335	3921	RPSA	ribosomal protein SA
	A__32__P230838	2547	XRCC6	X-ray repair complementing defective repair in Chinese hamster cells 6
	A__32__P29759	3550	IK	IK cytokine, down-regulator of HLA II
	A__32__P36217	6651	SON	SON DNA binding protein
	A__32__P58280	54536	EXOC6	exocyst complex component 6
G4C	A__23__P100754	64750	SMURF2	SMAD specific E3 ubiquitin protein ligase 2
	A__23__P113716	3107	HLA-C	major histocompatibility complex, class I, C
	A__23__P122068	114899	C1QTNF3	C1q and tumor necrosis factor related protein 3
	A__23__P125107	3106	HLA-B	major histocompatibility complex, class I, B
	A__23__P132611	7428	VHL	von Hippel-Lindau tumor suppressor
	A__23__P148473	3561	IL2RG	interleukin 2 receptor, gamma (severe combined immunodeficiency)
	A__23__P151614	5720	PSME1	proteasome (prosome, macropain) activator subunit 1 (PA28 alpha)
	A__23__P151649	328	APEX1	APEX nuclease (multifunctional DNA repair enzyme) 1
	A__23__P157795	8727	CTNNAL1	catenin (cadherin-associated protein), alpha-like 1
	A__23__P157809	22949	PTGR1	prostaglandin reductase 1
	A__23__P162171	4162	MCAM	melanoma cell adhesion molecule
	A__23__P163087	22795	NID2	nidogen 2 (osteonidogen)
	A__23__P16438	10683	DLL3	delta-like 3 ( <i>Drosophila</i> )
	A__23__P19673	6446	SGK1	serum/glucocorticoid regulated kinase 1
	A__23__P200928	4811	NID1	nidogen 1
	A__23__P201338	51150	SDF4	stromal cell derived factor 4
	A__23__P251118	4026	LPP	LIM domain containing preferred translocation partner in lipoma
	A__23__P258769	3115	HLA-DPB1	major histocompatibility complex, class II, DP beta 1
	A__23__P26094	79811	SLTM	SAFB-like, transcription modulator
	A__23__P308673	9344	TAOK2	TAO kinase 2
	A__23__P314070	392	ARHGAP1	Rho GTPase activating protein 1
	A__23__P320883	56882	CDC42SE1	CDC42 small effector 1
	A__23__P321501	10202	DHRS2	dehydrogenase/reductase (SDR family) member 2
	A__23__P330209	117584	RFFL	ring finger and FYVE-like domain containing 1
	A__23__P33216	506	ATP5B	ATP synthase, H+ transporting, mitochondrial F1 complex, beta polypeptide
	A__23__P3532	9516	LITAF	lipopolysaccharide-induced TNF factor
	A__23__P408708	665	BNIP3L	BCL2/adenovirus E1B 19 kDa interacting protein 3-like
	A__23__P42498	8724	SNX3	sorting nexin 3

TABLE S5-continued

	A_23_P71067	7291	TWIST1	twist homolog 1 ( <i>Drosophila</i> )
	A_23_P9756	22827	PUF60	poly-U binding splicing factor 60 KDa
	A_23_P99582	5411	PNN	pinin, desmosome associated protein
	A_24_P113674	3106	HLA-B	major histocompatibility complex, class I, B
	A_24_P114739	817	CAMK2D	calcium/calmodulin- dependent protein kinase II delta
	A_24_P181506	9726	ZNF646	zinc finger protein 646
	A_24_P27412	10073	SNUPN	snurportin 1
	A_24_P284893	5690	PSMB2	proteasome (prosome, macropain) subunit, beta type, 2
	A_24_P336754	4170	MCL1	myeloid cell leukemia sequence 1 (BCL2-related)
	A_24_P410952	8682	PEA15	phosphoprotein enriched in astrocytes 15
	A_24_P418044	3137	HLA-J	major histocompatibility complex, class I, J (pseudogene)
	A_24_P73599	3603	IL16	interleukin 16 (lymphocyte chemoattractant factor)
	A_24_P912799	9037	SEMA5A	sema domain, seven thrombospondin repeats (type 1 and type 1-like), transmembrane domain (TM) and short cytoplasmic domain, (semaphorin) 5A
	A_24_P927404	91419	XRCC6BP1	XRCC6 binding protein 1
	A_32_P170406	83660	TLN2	talin 2
	A_32_P177024	51119	SBDS	Shwachman-Bodian- Diamond syndrome
	A_32_P217655	645166	LOC645166	lymphocyte-specific protein 1 pseudogene
	A_32_P2738	26123	TCTN3	tectonic family member 3
	A_32_P88965	4921	DDR2	discoidin domain receptor tyrosine kinase 2
GC5	A_23_P13382	4046	LSP1	lymphocyte-specific protein 1
	A_23_P138376	22931	RAB18	RAB18, member RAS oncogene family
	A_23_P140725	9742	IFT140	intraflagellar transport 140 homolog ( <i>Chlamydomonas</i> )
	A_23_P157875	2219	FCN1	ficolin (collagen/fibrinogen domain containing) 1
	A_23_P157879	2219	FCN1	ficolin (collagen/fibrinogen domain containing) 1
	A_23_P15995	8778	SIGLEC5	sialic acid binding Ig-like lectin 5
	A_23_P165219	84106	PRAM1	PML-RARA regulated adaptor molecule 1
	A_23_P167256	79960	PHF17	PHD finger protein 17
	A_23_P200728	2214	FCGR3A	Fc fragment of IgG, low affinity IIIa, receptor (CD16a)
	A_23_P22444	5199	CFP	complement factor properdin
	A_23_P259561	3109	HLA-DMB	major histocompatibility complex, class II, DM beta
	A_23_P259621	7462	LAT2	linker for activation of T cells family, member 2
	A_23_P27994	7305	TYROBP	TYRO protein tyrosine kinase binding protein
	A_23_P31006	3127	HLA-DRB5	major histocompatibility complex, class II, DR beta 5
	A_23_P38795	2357	FPR1	formyl peptide receptor 1
	A_23_P41765	3659	IRF1	interferon regulatory factor 1

TABLE S5-continued

	A_23_P48997	9051	PSTPIP1	proline-serine-threonine phosphatase interacting protein 1
	A_23_P51534	6846	XCL2	chemokine (C motif) ligand 2
	A_23_P85716	2212	FCGR2A	Fc fragment of IgG, low affinity IIa, receptor (CD32)
	A_24_P134229	126282	TNFAIP8L1	tumor necrosis factor, alpha-induced protein 8-like 1
	A_24_P192914	120425	AMICA1	adhesion molecule, interacts with CXADR antigen 1
	A_24_P283189	929	CD14	CD14 molecule
	A_24_P343233	3123	HLA-DRB1	major histocompatibility complex, class II, DR beta 1
GC6	A_24_P365807	1947	EFNB1	ephrin-B1
	A_23_P100240	1014	CDH16	cadherin 16, KSP-cadherin
	A_23_P121987	85480	TSLP	thymic stromal lymphopoietin
	A_23_P143331	650	BMP2	bone morphogenetic protein 2
	A_23_P147786	9699	RIMS2	regulating synaptic membrane exocytosis 2
	A_23_P158096	85301	COL27A1	collagen, type XXVII, alpha 1
	A_23_P168259	80328	ULBP2	UL16 binding protein 2
	A_23_P252721	10395	DLC1	deleted in liver cancer 1
	A_23_P66117	83986	ITFG3	integrin alpha FG-GAP repeat containing 3
	A_24_P113295	1175	AP2S1	adaptor-related protein complex 2, sigma 1 subunit
	A_24_P285163	57645	POGK	pogo transposable element with KRAB domain
	A_24_P334130	2335	FN1	fibronectin 1
	A_24_P51909	10815	CPLX1	complexin 1
	A_24_P84898	2237	FEN1	flap structure-specific endonuclease 1
	A_24_P88870	8706	B3GALNT1	beta-1,3-N-acetylgalactosaminyltransferase 1 (globoside blood group)
	A_24_P935252	8087	FXR1	fragile X mental retardation, autosomal homolog 1
	A_32_P106615	9353	SLIT2	slit homolog 2 ( <i>Drosophila</i> )
	A_32_P121651	57534	MIB1	mindbomb homolog 1 ( <i>Drosophila</i> )
	A_32_P157539	79031	PDCL3	phosducin-like 3
	A_32_P200600	5518	PPP2R1A	protein phosphatase 2 (formerly 2A), regulatory subunit A, alpha isoform
	A_32_P29806	8738	CRADD	CASP2 and RIPK1 domain containing adaptor with death domain
	A_32_P43717	9413	C9orf61	chromosome 9 open reading frame 61
	A_32_P72541	9037	SEMA5A	sema domain, seven thrombospondin repeats (type 1 and type 1-like), transmembrane domain (TM) and short cytoplasmic domain, (semaphorin) 5A
	A_32_P84009	146223	CMTM4	CKLF-like MARVEL transmembrane domain containing 4

APPENDIX F

[0188]

TABLE S6

Weights of sparse CCA				
Cytokine responses	B-cells	CD8	CD4	Monocytes
Correlation Factors	0.9	0.88	0.87	0.75
Baseline-B-cells	-0.9	-0.88	-0.95	-0.75
Baseline-CD4	-0.76	-0.68	-0.79	-0.36
CD8 Naive	0.76	0.72	0.6	0.49
CD8 TDEM	-0.67	-0.65	-0.65	-0.49
CD8+CD28-	0.81	0.6	0.7	0.32
CD4 TDEM	-0.35	-0.59	-0.56	-0.63
CD4+CD28-	0.19	0.55	0.39	0.65
GC 6	0.52	0.46	0.4	0.26
GC 1	-0.21	-0.39	-0.38	-0.54
NK T	-0.4	-0.41	-0.42	-0.18
GC 5	-0.21	-0.32	-0.27	-0.49
GC 3	0.24	0.15	0.24	0.24
Baseline-cd8	-0.42	-0.22	-0.23	-0.02

TABLE S6-continued

Weights of sparse CCA				
Cytokine responses	B-cells	CD8	CD4	Monocytes
IL-17	0.38	0	0.16	0
GC 4	0.25	0.18	0.05	0
MPZL2 (A_24_P278552)	0	0.08	0.05	0.18
mono	0	-0.01	0	-0.21
IFI30 (A_23_P153745)	-0.06	-0.01	-0.05	-0.07
GC 2	0	0	-0.02	-0.17
TGF-a	0	0.05	0.1	0
Th1	-0.15	0	0	0
MCP-3	0	0.06	0.06	0
Th2	0	0.07	0	0
TNF-a	0	-0.02	0	-0.01
chemokines	0	0	0	0
CD8 CenMem	0	0	0	0

APPENDIX G

[0189]

TABLE S7

Cytokine stimulation response	Significant differences between CR and CNR						
	CR	Cytokine response		Age: 60-65 yo vs 74+ yo		Gender	
		p-value	q-value	p-value	q-value	p-value	q-value
cd4_IFNa_STAT3	4	0	0	0.947037	0.460211	0.153556	0.376565
cd4_IL6_STAT3	6.28	0	0	0.900331	0.443676	0.299048	0.482754
cd4_IL21_STAT3	4.08	0	0	0.829489	0.428303	0.13378	0.376565
cd4_IL10_STAT3	3.8	0	0.000001	0.802164	0.428303	0.340265	0.482754
mono_IFNg_STAT3	1.54	0.000006	0.000025	0.714285	0.420019	0.70903	0.702136
cd8_IL7_STAT1	1.25	0.000015	0.000047	0.135552	0.420019	0.060505	0.291589
mono_IL6_STAT3	3.59	0.000015	0.000047	0.684827	0.420019	0.776648	0.702136
cd8_IFNg_STAT1	2.45	0.000023	0.000064	0.290331	0.420019	0.014834	0.291589
cd8_IL6_STAT3	4.35	0.000034	0.000083	0.24283	0.420019	0.065875	0.291589
cd4_IL6_STAT1	6.81	0.000039	0.000085	0.345614	0.420019	0.310418	0.482754
cd4_IFNa_STAT1	3.16	0.000057	0.000106	0.493856	0.420019	0.166634	0.380318
mono_IFNa_STAT5	1.62	0.000058	0.000106	0.319297	0.420019	0.977993	0.725487
cd4_IL6_STAT5	2.93	0.00007	0.000119	0.53263	0.420019	0.822851	0.708112
mono_IFNa_STAT3	1.75	0.000095	0.000149	0.37638	0.420019	0.995002	0.725487
cd4_IFNg_STAT1	2.22	0.000121	0.000177	0.198227	0.420019	0.092476	0.373417
cd8_IFNa_STAT3	1.78	0.000156	0.000215	0.381077	0.420019	0.066656	0.291589
cd4_IL7_STAT3	1.31	0.00019	0.000241	0.39983	0.420019	0.405702	0.519438
cd8_IL6_STAT1	7.41	0.000197	0.000241	0.340202	0.420019	0.049192	0.291589
cd4_IL21_STAT1	1.83	0.000217	0.000251	0.555918	0.420019	0.108496	0.376565
cd8_IFNa_STAT1	2.79	0.000262	0.000288	0.218327	0.420019	0.137566	0.376565
mono_IFNg_STAT5	1.65	0.000303	0.000318	0.457462	0.420019	0.664712	0.691429
cd8_IL7_STAT3	1.17	0.000936	0.000936	0.730943	0.420019	0.03782	0.291589
mono_IL7_STAT5	1.17	0.001112	0.001063	0.41378	0.420019	0.505697	0.63205
cd20_IFNa_STAT1	2.42	0.001232	0.00113	0.427269	0.420019	0.784512	0.702136
cd4_IL10_STAT1	1.83	0.001462	0.001287	0.840156	0.428303	0.958775	0.725487
cd20_IFNg_STAT1	2.05	0.001556	0.001317	0.618695	0.420019	0.791049	0.702136
cd4_IFNg_STAT3	1.13	0.001933	0.001575	0.514195	0.420019	0.113051	0.376565
mono_IFNa_STAT1	1.71	0.003477	0.002732	0.37889	0.420019	0.839715	0.710969
cd8_IL10_STAT1	1.57	0.003883	0.002947	0.091318	0.420019	0.97801	0.725487
cd8_IFNa_STAT5	2.02	0.004273	0.003134	0.253498	0.420019	0.042724	0.291589
cd8_IL6_STAT5	1.85	0.005126	0.003525	0.493479	0.420019	0.193612	0.423479
cd8_IL21_STAT1	1.51	0.005003	0.003525	0.58113	0.420019	0.133924	0.376565
mono_IFNg_STAT1	1.55	0.009067	0.006046	0.634593	0.420019	0.802532	0.702136
cd20_IL21_STAT1	1.46	0.010978	0.007106	0.330071	0.420019	0.338943	0.482754
mono_IL10_STAT3	1.16	0.028449	0.017863	0.558034	0.420019	0.995066	0.725487
mono_IL21_STAT3	1.11	0.029221	0.017863	0.744283	0.420019	0.315413	0.482754
cd20_IL21_STAT3	1.15	0.042992	0.02557	0.641946	0.420019	0.117569	0.376565

TABLE S7-continued

	Significant differences between CR and CNR						
	Fold-change CNR vs	Cytokine response		Age: 60-65 yo vs 74+ yo		Gender	
		CR	p-value	q-value	p-value	q-value	p-value
cd8_IL7_STAT5	1.22	0.044731	0.025904	0.069506	0.420019	0.157816	0.376565
cd8_IFNg_STAT5	1.1	0.049497	0.02793	0.682996	0.420019	0.059991	0.291589
cd20_IFNa_STAT3	1.17	0.051587	0.028381	0.337448	0.420019	0.033475	0.291589
cd4_IL7_STAT1	1.19	0.05989	0.032146	0.375581	0.420019	0.629986	0.691429
cd4_IL21_STAT5	1.18	0.080319	0.042084	0.856894	0.428303	0.155441	0.376565
cd4_IFNa_STAT5	1.33	0.092694	0.047439	0.633135	0.420019	0.785958	0.702136
cd8_IL21_STAT5	1.18	0.114836	0.057435	0.718208	0.420019	0.03049	0.291589
cd20_IFNg_STAT3	-1.05	0.14128	0.069091	0.594073	0.420019	0.061708	0.291589
cd4_IFNg_STAT5	1.03	0.154626	0.073974	0.58423	0.420019	0.335123	0.482754
cd20_IL7_STAT1	1.1	0.17748	0.0831	0.471045	0.420019	0.958544	0.725487
cd8_IL10_STAT5	1.13	0.215206	0.098212	0.462871	0.420019	0.684921	0.691429
cd8_IL21_STAT3	1.1	0.21868	0.098212	0.744099	0.420019	0.86352	0.719519
phosphoprotein baseline							
cd20_Unstimulated_STAT1	-2.57	0.000117	0.000644	0.373293	0.777023	0.619702	0.308798
cd4_Unstimulated_STAT3	-4.2	0.000273	0.000753	0.485768	0.777023	0.062525	0.066939
cd20_Unstimulated_STAT5	-1.11	0.076648	0.070499	0.33538	0.777023	0.841783	0.349551
cd20_Unstimulated_STAT3	-1.11	0.007217	0.009957	0.57577	0.777023	0.024649	0.040941
cd4_Unstimulated_STAT1	-2.15	0.006027	0.009957	0.812278	0.777023	0.010133	0.025246
cd4_Unstimulated_STAT5	-1.05	0.090487	0.071338	0.296912	0.777023	0.00931	0.025246
mono_Unstimulated_STAT1	-1.2	0.019564	0.021594	0.433673	0.777023	0.379235	0.20997
Cell subsets							
CD8+CD28-	-4.21	0.000008	0.000032	0.630348	0.607903	0.005759	0.037864
CD8 TERM DIFF EFFECTOR MEMORY	-9.49	0.000032	0.000068	0.389149	0.585539	0.039951	0.058839
CD8 NAIVE	2.14	0.001718	0.002449	0.694365	0.618129	0.032877	0.058839
B CELLS	3.54	0.004612	0.004932	0.817871	0.630998	0.541342	0.237297
CD4 EFFECTOR MEMORY	-5.62	0.012042	0.010302	0.477152	0.585539	0.457482	0.231389
CD4 NAIVE	1.48	0.019374	0.013811	0.519746	0.585539	0.111156	0.117433
CD4 TERM DIFF EFFECTOR MEMORY	-53.39	0.024124	0.014741	0.556562	0.585539	0.378876	0.217652
NK T CELLS	-6.67	0.034716	0.018562	0.163185	0.585539	0.246943	0.202964
CD8 CENTRAL MEMORY	1.92	0.053228	0.023628	0.549683	0.585539	0.291454	0.208139
CD4+CD28- GAMMA DELTA CELLS	-31.87	0.055239	0.023628	0.319976	0.585539	0.523354	0.237297
CD4 CENTRAL MEMORY	-2.58	0.164423	0.063936	0.215857	0.585539	0.044742	0.058839
CD8 EFFECTOR MEMORY	-2.44	0.294813	0.099883	0.3442	0.585539	0.39722	0.217652
Gene expression							
CNTFR	1271 A_23_P5②	1.42	0.000002	0.003052	0.468716	0.999497	0.681992
CD33	945 A_24_P3②	1.55	0.000019	0.014378	0.65498	0.999497	0.569891
CCL5	6352 A_23_P1②	-8.16	0.000025	0.014378	0.852489	0.999497	0.771658
UBE2I	7329 A_23_P1②	1.59	0.001915	0.036104	0.935523	0.999497	0.9852
NAE1	8883 A_23_P7②	-1.72	0.000889	0.036104	0.528884	0.999497	0.609482
F5	2153 A_32_P4②	1.48	0.001425	0.036104	0.401274	0.999497	0.503965
PGM5	5239 A_24_P1②	1.41	0.001015	0.036104	0.327167	0.999497	0.051766
CRYAB	1410 A_24_P2②	1.71	0.001353	0.036104	0.870361	0.999497	0.77123
FOS	2353 A_23_P1②	1.66	0.001921	0.036104	0.630412	0.999497	0.655547
NUPR1	26471 A_24_P1②	1.72	0.001261	0.036104	0.544316	0.999497	0.86663
COL6A2	1292 A_23_P2②	2.12	0.001914	0.036104	0.443149	0.999497	0.685136
ACTN4	81 A_23_P3②	2	0.001969	0.036104	0.477143	0.999497	0.541507
NOG	9241 A_23_P3②	1.9	0.000533	0.036104	0.851653	0.999497	0.264467
CAPN10	11132 A_23_P3②	1.93	0.001745	0.036104	0.113584	0.999497	0.295294
HDAC5	10014 A_23_P2②	1.85	0.001396	0.036104	0.755511	0.999497	0.244218
CUTA	51596 A_23_P2②	1.6	0.000807	0.036104	0.612211	0.999497	0.241352
TGFB1I1	7041 A_23_P1②	1.99	0.000809	0.036104	0.822061	0.999497	0.246581
SOD1	6647 A_23_P1②	1.62	0.001546	0.036104	0.662823	0.999497	0.535483
NRP2	8828 A_24_P5②	1.72	0.001623	0.036104	0.952429	0.999497	0.133472

TABLE S7-continued

Significant differences between CR and CNR								
		Fold-change CNR vs	Cytokine response		Age: 60-65 yo vs 74+ yo		Gender	
			CR	p-value	q-value	p-value	q-value	p-value
FOLR1	2348 A_23_P5	1.93	0.000554	0.036104	0.892212	0.999497	0.193482	0.999623
MKNK2	2872 A_24_P5	1.74	0.001284	0.036104	0.769347	0.999497	0.224105	0.999623
RAMP3	10268 A_23_P1	1.86	0.000877	0.036104	0.846338	0.999497	0.58297	0.999623
IGF1R	3480 A_23_P2	1.67	0.000913	0.036104	0.644569	0.999497	0.996777	0.999623
FXYS5	53827 A_24_P1	1.65	0.000561	0.036104	0.387527	0.999497	0.632614	0.999623
ZNF346	23567 A_23_P4	1.55	0.001565	0.036104	0.956026	0.999497	0.621718	0.999623
CIAPIN1	57019 A_23_P8	1.4	0.000741	0.036104	0.91067	0.999497	0.828879	0.999623
DAB2	1601 A_23_P2	1.65	0.001499	0.036104	0.734123	0.999497	0.216778	0.999623
CEACAM1	634 A_24_P3	-2.09	0.00171	0.036104	0.818157	0.999497	0.367309	0.999623
LSP1	4046 A_32_P1	1.38	0.001183	0.036104	0.858935	0.999497	0.539176	0.999623
CCL3	6348 A_23_P3	1.47	0.00082	0.036104	0.753777	0.999497	0.835003	0.999623
HIC1	3090 A_23_P1	1.39	0.001829	0.036104	0.756911	0.999497	0.266203	0.999623
RICTOR	253260 A_32_P1	-3.17	0.000688	0.036104	0.892103	0.999497	0.896246	0.999623
LOC731884	731884 A_32_P1	-1.52	0.000346	0.036104	0.546338	0.999497	0.970792	0.999623
C11orf82	220042 A_23_P4	-1.83	0.000382	0.036104	0.969107	0.999497	0.454269	0.999623
ADH5	128 A_24_P2	-1.83	0.000181	0.036104	0.991188	0.999497	0.537529	0.999623
LRP12	29967 A_23_P8	-2.5	0.001269	0.036104	0.615746	0.999497	0.632577	0.999623
RIMS4	140730 A_24_P3	-1.89	0.000957	0.036104	0.922956	0.999497	0.49328	0.999623
BMI1	648 A_23_P3	-5.23	0.001737	0.036104	0.47677	0.999497	0.588522	0.999623
FNBP1L	54874 A_23_P4	-2.18	0.000321	0.036104	0.592882	0.999497	0.4161	0.999623
KCNMA1	3778 A_32_P1	1.28	0.001967	0.036104	0.735474	0.999497	0.411288	0.999623
SCRN1	9805 A_23_P3	1.51	0.001041	0.036104	0.413517	0.999497	0.643565	0.999623
NRTN	4902 A_23_P5	2.19	0.001956	0.036104	0.480441	0.999497	0.274495	0.999623
GZMH	2999 A_23_P1	-20.32	0.000372	0.036104	0.48478	0.999497	0.732471	0.999623
MAP4K2	5871 A_24_P2	2.04	0.00125	0.036104	0.95861	0.999497	0.783462	0.999623
PCDHB11	56125 A_23_P1	1.62	0.001861	0.036104	0.644295	0.999497	0.471202	0.999623
HCG18	414777 A_32_P1	1.93	0.001725	0.036104	0.718093	0.999497	0.310781	0.999623
FSCN1	6624 A_23_P1	2.08	0.000886	0.036104	0.959932	0.999497	0.756668	0.999623
MUC5AC	4586 A_24_P7	1.91	0.000211	0.036104	0.565104	0.999497	0.972326	0.999623
NIN1	4814 A_23_P1	1.97	0.001275	0.036104	0.954106	0.999497	0.255055	0.999623
PSMD4	5710 A_23_P1	1.62	0.00196	0.036104	0.662586	0.999497	0.272692	0.999623
CLN3	1201 A_24_P1	1.62	0.001455	0.036104	0.84645	0.999497	0.546117	0.999623
PYCARD	29108 A_23_P2	1.46	0.001903	0.036104	0.995796	0.999497	0.50099	0.999623
UTP14A	10813 A_24_P1	-1.96	0.001041	0.036104	0.973791	0.999497	0.634985	0.999623
RPS3A	6189 A_32_P1	-1.64	0.001684	0.036104	0.741683	0.999497	0.677281	0.999623
TYMP	1890 A_23_P5	1.88	0.000299	0.036104	0.963687	0.999497	0.535271	0.999623
PLD2	5338 A_23_P4	1.43	0.001952	0.036104	0.59288	0.999497	0.9276	0.999623
FGFR1	2260 A_24_P4	1.75	0.001282	0.036104	0.510266	0.999497	0.702185	0.999623
TGM2	7052 A_24_P5	1.44	0.001857	0.036104	0.406185	0.999497	0.678772	0.999623
AP2A1	160 A_23_P4	1.54	0.001371	0.036104	0.657812	0.999497	0.805783	0.999623
C16orf5	29965 A_23_P1	1.45	0.000499	0.036104	0.79947	0.999497	0.456699	0.999623
AREG	374 A_23_P2	1.6	0.00181	0.036104	0.425941	0.999497	0.55855	0.999623
CHST10	9486 A_23_P1	1.56	0.000695	0.036104	0.524686	0.999497	0.752694	0.999623
LOC91316	91316 A_24_P5	1.35	0.000436	0.036104	0.512559	0.999497	0.65309	0.999623
ARHGEF11	9826 A_23_P4	1.58	0.001814	0.036104	0.829165	0.999497	0.794249	0.999623
IL3RA	3563 A_23_P2	1.7	0.000099	0.036104	0.95942	0.999497	0.34963	0.999623
YKT6	10652 A_24_P3	1.72	0.000851	0.036104	0.917946	0.999497	0.584568	0.999623
PEX5	5830 A_24_P3	1.71	0.001585	0.036104	0.832499	0.999497	0.935308	0.999623
RAB5B	5869 A_23_P1	1.44	0.000215	0.036104	0.605261	0.999497	0.777266	0.999623
TCTA	6988 A_24_P1	1.8	0.000417	0.036104	0.272418	0.999497	0.520236	0.999623
TRAP1	10131 A_23_P3	1.44	0.001417	0.036104	0.249931	0.999497	0.377573	0.999623
KYNU	8942 A_23_P5	1.42	0.001445	0.036104	0.582003	0.999497	0.598451	0.999623
FN1	2335 A_32_P5	1.81	0.000524	0.036104	0.77332	0.999497	0.2	0.999623
TRIP10	9322 A_23_P5	1.78	0.00032	0.036104	0.476946	0.999497	0.552793	0.999623
PIN1	5300 A_23_P6	1.67	0.001732	0.036104	0.8874	0.999497	0.272875	0.999623
RIN2	54453 A_23_P8	1.64	0.000727	0.036104	0.689161	0.999497	0.820036	0.999623
BSC12	26580 A_24_P2	1.72	0.00045	0.036104	0.692057	0.999497	0.61986	0.999623
PCDHA1	56147 A_24_P1	1.62	0.000977	0.036104	0.526039	0.999497	0.447015	0.999623
ZNF346	23567 A_23_P4	1.58	0.000724	0.036104	0.490382	0.999497	0.592862	0.999623
CCND1	595 A_24_P1	1.75	0.001864	0.036104	0.703558	0.999497	0.411183	0.999623
EPO	2056 A_23_P1	1.76	0.000322	0.036104	0.959527	0.999497	0.840031	0.999623
FAT1	2195 A_23_P6	1.39	0.000235	0.036104	0.646189	0.999497	0.852769	0.999623
DBNL	28988 A_23_P1	1.87	0.000995	0.036104	0.74013	0.999497	0.345923	0.999623
PDLIM7	9260 A_23_P1	1.58	0.001505	0.036104	0.818648	0.999497	0.993117	0.999623
SNCG	6623 A_23_P2	1.66	0.001516	0.036104	0.519845	0.999497	0.314046	0.999623
PTPRF	5792 A_23_P2	2.14	0.000486	0.036104	0.898652	0.999497	0.867885	0.999623
FOXO1	2308 A_24_P2	1.43	0.001	0.036104	0.289655	0.999497	0.979632	0.999623
SNAPIN	23557 A_23_P1	1.32	0.000764	0.036104	0.738372	0.999497	0.441884	0.999623

TABLE S7-continued

		Significant differences between CR and CNR						
		Fold-change CNR vs	Cytokine response		Age: 60-65 yo vs 74+ yo		Gender	
			CR	p-value	q-value	p-value	q-value	p-value
BAALC	79870_A_23_P1	1.61	0.001112	0.036104	0.338482	0.999497	0.795973	0.999623
GSS	2937_A_23_P2	1.36	0.001469	0.036104	0.798475	0.999497	0.45919	0.999623
ADAL	161823_A_32_P2	1.5	0.001468	0.036104	0.931525	0.999497	0.881205	0.999623
MLF1	4291_A_23_P1	1.46	0.000909	0.036104	0.453641	0.999497	0.677062	0.999623
FOXO4	4303_A_24_P3	1.27	0.000497	0.036104	0.56281	0.999497	0.274221	0.999623
EMILIN1	11117_A_32_P7	1.43	0.000714	0.036104	0.986821	0.999497	0.646397	0.999623
C1QTNF1	114897_A_23_P3	1.54	0.001265	0.036104	0.881114	0.999497	0.746563	0.999623
CD99L2	83692_A_23_P2	1.71	0.004014	0.036799	0.523831	0.999497	0.828093	0.999623
CLSTN3	9746_A_23_P5	1.47	0.003655	0.036799	0.552344	0.999497	0.995555	0.999623
PI4KB	5298_A_23_P3	1.76	0.003335	0.036799	0.678786	0.999497	0.727324	0.999623
LAMA5	3911_A_23_P1	2.03	0.003997	0.036799	0.943309	0.999497	0.531834	0.999623
FEZ2	9637_A_23_P3	1.24	0.002046	0.036799	0.626235	0.999497	0.372874	0.999623
PPP1R15A	23645_A_23_P5	1.72	0.003598	0.036799	0.672479	0.999497	0.386734	0.999623
PPIG	9360_A_23_P1	-1.81	0.00368	0.036799	0.584021	0.999497	0.704251	0.999623
NKG7	4818_A_23_P1	-8.38	0.002739	0.036799	0.96245	0.999497	0.65534	0.999623
RAB3B	5865_A_24_P5	-1.34	0.002854	0.036799	0.977899	0.999497	0.311996	0.999623
MAP4K4	9448_A_23_P5	-1.63	0.003976	0.036799	0.708133	0.999497	0.50406	0.999623
NOS3	4846_A_23_P7	1.66	0.002663	0.036799	0.64946	0.999497	0.911586	0.999623
TCL1A	8115_A_23_P3	3.84	0.003301	0.036799	0.250558	0.999497	0.449763	0.999623
LTBP2	4053_A_23_P2	1.66	0.00387	0.036799	0.502699	0.999497	0.480426	0.999623
MGMT	4255_A_23_P1	1.62	0.002836	0.036799	0.833298	0.999497	0.295631	0.999623
PARVB	29780_A_23_P4	1.57	0.002688	0.036799	0.348734	0.999497	0.503429	0.999623
ERBB2	2064_A_23_P8	2.17	0.002514	0.036799	0.750799	0.999497	0.790942	0.999623
RRAD	6236_A_23_P8	2.06	0.003003	0.036799	0.685343	0.999497	0.202877	0.999623
ACIN1	22985_A_23_P1	1.75	0.002299	0.036799	0.917116	0.999497	0.446935	0.999623
FANCC	2176_A_23_P3	1.5	0.002675	0.036799	0.903823	0.999497	0.727957	0.999623
RSPH3	83861_A_23_P5	1.39	0.002969	0.036799	0.564778	0.999497	0.330631	0.999623
MYC	4609_A_24_P3	1.62	0.003476	0.036799	0.72846	0.999497	0.515281	0.999623
HDAC5	10014_A_24_P1	1.64	0.002221	0.036799	0.787224	0.999497	0.351233	0.999623
PRKRA	8575_A_24_P5	-2.37	0.002484	0.036799	0.819817	0.999497	0.404809	0.999623
CD276	80381_A_23_P5	1.56	0.00329	0.036799	0.407954	0.999497	0.530047	0.999623
ITGB8	3696_A_24_P7	-3.02	0.003897	0.036799	0.766779	0.999497	0.530018	0.999623
DDR1	780_A_24_P3	1.65	0.003704	0.036799	0.831862	0.999497	0.19632	0.999623
DCTN3	11258_A_23_P1	1.39	0.003757	0.036799	0.734811	0.999497	0.13659	0.999623
CSNK1E	1454_A_24_P5	1.49	0.002487	0.036799	0.842292	0.999497	0.311868	0.999623
ADRA1B	147_A_23_P3	1.77	0.002217	0.036799	0.434475	0.999497	0.939526	0.999623
LGALS12	85329_A_23_P1	1.9	0.002282	0.036799	0.50909	0.999497	0.705245	0.999623
HLA-C	3107_A_23_P7	1.88	0.00371	0.036799	0.691174	0.999497	0.597814	0.999623
RALA	5898_A_24_P1	-1.44	0.003584	0.036799	0.711675	0.999497	0.240291	0.999623
C1QTNF4	114900_A_23_P5	1.53	0.00299	0.036799	0.70973	0.999497	0.560858	0.999623
HSPA8	3312_A_32_P1	-2.16	0.003663	0.036799	0.893335	0.999497	0.511234	0.999623
IFNA4	3441_A_24_P4	-2.8	0.003451	0.036799	0.638658	0.999497	0.312166	0.999623
RAB18	22931_A_24_P1	-1.67	0.003088	0.036799	0.567201	0.999497	0.417807	0.999623
LRP12	29967_A_24_P4	-2.71	0.00382	0.036799	0.939237	0.999497	0.323012	0.999623
CD320	51293_A_23_P1	1.66	0.003495	0.036799	0.933906	0.999497	0.526329	0.999623
NEDD4L	23327_A_23_P2	1.29	0.003033	0.036799	0.387082	0.999497	0.016414	0.999623
GHI	2688_A_23_P2	-1.87	0.002357	0.036799	0.478376	0.999497	0.26117	0.999623
PSMG2	56984_A_24_P3	-1.66	0.002488	0.036799	0.448467	0.999497	0.467237	0.999623
NLGN1	22871_A_23_P1	-1.44	0.003168	0.036799	0.926995	0.999497	0.723127	0.999623
LIN7C	55327_A_24_P5	-3.08	0.002742	0.036799	0.310595	0.999497	0.185406	0.999623
CXADR	1525_A_24_P3	-1.93	0.003767	0.036799	0.895248	0.999497	0.420753	0.999623
HLA-C	3107_A_32_P1	-1.95	0.003887	0.036799	0.944433	0.999497	0.981696	0.999623
MUC5AC	4586_A_24_P5	-2.44	0.002238	0.036799	0.456842	0.999497	0.190606	0.999623
COL14A1	7373_A_24_P2	-2.69	0.003725	0.036799	0.873276	0.999497	0.607016	0.999623
5-Sep	5413_A_23_P1	1.73	0.002616	0.036799	0.661674	0.999497	0.262184	0.999623
SKAP2	8935_A_24_P8	1.46	0.002665	0.036799	0.171854	0.999497	0.504189	0.999623
BCL2L12	83596_A_23_P5	1.61	0.003724	0.036799	0.384718	0.999497	0.243259	0.999623
FXYD5	53827_A_23_P1	1.83	0.003836	0.036799	0.379437	0.999497	0.559681	0.999623
TMX1	81542_A_23_P7	1.39	0.002725	0.036799	0.673962	0.999497	0.601861	0.999623
IL3RA	3563_A_32_P2	1.93	0.003195	0.036799	0.619472	0.999497	0.483508	0.999623
PKD1	5310_A_24_P4	1.53	0.003118	0.036799	0.562036	0.999497	0.723101	0.999623
CX3CL1	6376_A_23_P3	2.01	0.003135	0.036799	0.972373	0.999497	0.800236	0.999623
BMF	90427_A_23_P3	1.76	0.00305	0.036799	0.854947	0.999497	0.599953	0.999623
NFATC1	4772_A_23_P3	1.96	0.003188	0.036799	0.744964	0.999497	0.38305	0.999623
KEL	3792_A_23_P2	1.47	0.002375	0.036799	0.521584	0.999497	0.723356	0.999623
CTSD	1509_A_23_P5	2.11	0.00327	0.036799	0.689915	0.999497	0.102454	0.999623
LOC644297	644297_A_23_P1	1.74	0.002326	0.036799	0.966498	0.999497	0.123516	0.999623
EMD1	2010_A_23_P8	2.27	0.003097	0.036799	0.973726	0.999497	0.271842	0.999623

TABLE S7-continued

Significant differences between CR and CNR								
		Fold-change CNR vs	Cytokine response		Age: 60-65 yo vs 74+ yo		Gender	
			CR	p-value	q-value	p-value	q-value	p-value
CD1A	909 A_23_P4	1.49	0.002533	0.036799	0.824906	0.999497	0.720479	0.999623
GZMA	3001 A_23_P1	-2.87	0.003841	0.036799	0.484362	0.999497	0.997193	0.999623
UCP2	7351 A_23_P4	1.96	0.002975	0.036799	0.739123	0.999497	0.455132	0.999623
WFS1	7466 A_23_P1	1.68	0.002796	0.036799	0.803433	0.999497	0.543886	0.999623
RAB22A	57403 A_32_P1	1.49	0.003676	0.036799	0.943042	0.999497	0.874004	0.999623
PCDHB2	56133 A_24_P1	1.35	0.00383	0.036799	0.993183	0.999497	0.174231	0.999623
BECN1	8678 A_23_P4	-1.27	0.002554	0.036799	0.580946	0.999497	0.957391	0.999623
PRDX2	7001 A_24_P1	1.66	0.003664	0.036799	0.452472	0.999497	0.979373	0.999623
TTRAP	51567 A_23_P8	-2.25	0.003941	0.036799	0.751661	0.999497	0.841923	0.999623
MRPS30	10884 A_23_P1	-1.33	0.002741	0.036799	0.57551	0.999497	0.400199	0.999623
IL17RD	54756 A_32_P1	-1.88	0.002724	0.036799	0.927843	0.999497	0.664638	0.999623
AIFI	199 A_23_P1	1.94	0.004012	0.036799	0.461864	0.999497	0.348074	0.999623
RNF216	54476 A_24_P1	-1.6	0.002874	0.036799	0.780076	0.999497	0.8195	0.999623
HMGB1	3146 A_23_P5	-2.4	0.002061	0.036799	0.561096	0.999497	0.275322	0.999623
BSG	682 A_32_P1	1.71	0.003834	0.036799	0.971549	0.999497	0.157925	0.999623
ERBB3	2065 A_23_P1	1.64	0.002964	0.036799	0.997041	0.999497	0.505466	0.999623
TNFRSF10B	8795 A_23_P1	1.47	0.003361	0.036799	0.72306	0.999497	0.811524	0.999623
PLD1	5337 A_23_P3	1.49	0.002554	0.036799	0.264221	0.999497	0.791086	0.999623
MYST4	23522 A_23_P1	1.57	0.002953	0.036799	0.942193	0.999497	0.829364	0.999623
COL16A1	1307 A_23_P1	1.39	0.003366	0.036799	0.120822	0.999497	0.934672	0.999623
BMP1	649 A_23_P1	1.86	0.003944	0.036799	0.63638	0.999497	0.629346	0.999623
RAB3D	9545 A_23_P4	1.39	0.003287	0.036799	0.446421	0.999497	0.2315	0.999623
DCHS1	8642 A_23_P5	1.82	0.002777	0.036799	0.650747	0.999497	0.391191	0.999623
AQP3	360 A_23_P1	1.53	0.002361	0.036799	0.643996	0.999497	0.807047	0.999623
B3GNTL1	146712 A_24_P1	1.71	0.002961	0.036799	0.83054	0.999497	0.598684	0.999623
COL24A1	255631 A_23_P7	1.81	0.003256	0.036799	0.933385	0.999497	0.785361	0.999623
LAMA1	284217 A_23_P1	1.82	0.002498	0.036799	0.546325	0.999497	0.524802	0.999623
HMGB3	3149 A_23_P1	1.42	0.002816	0.036799	0.61878	0.999497	0.89304	0.999623
IGSF8	93185 A_23_P1	1.68	0.00376	0.036799	0.999039	0.999497	0.719943	0.999623
MMP12	4321 A_23_P1	1.29	0.002657	0.036799	0.592962	0.999497	0.921481	0.999623
HSPA8	3312 A_24_P1	-1.98	0.003382	0.036799	0.119957	0.999497	0.901493	0.999623
ARVCF	421 A_23_P1	1.59	0.002613	0.036799	0.759477	0.999497	0.366938	0.999623
PVR	5817 A_23_P1	1.4	0.003357	0.036799	0.491225	0.999497	0.474115	0.999623
HIF1A	3091 A_23_P4	-1.71	0.004371	0.036858	0.92804	0.999497	0.387877	0.999623
TRAF1	7185 A_23_P1	1.99	0.004122	0.036858	0.978755	0.999497	0.699893	0.999623
SECTM1	6398 A_24_P1	2.07	0.004322	0.036858	0.821937	0.999497	0.82145	0.999623
PRKCD	5580 A_23_P1	1.47	0.004481	0.036858	0.914646	0.999497	0.799097	0.999623
RAB5C	5878 A_23_P1	1.49	0.004129	0.036858	0.503106	0.999497	0.673735	0.999623
SERPINB2	5055 A_23_P1	1.88	0.004089	0.036858	0.428911	0.999497	0.152952	0.999623
VPREB3	29802 A_23_P1	1.45	0.004403	0.036858	0.980636	0.999497	0.644839	0.999623
TOLLIP	54472 A_24_P1	-2.02	0.004345	0.036858	0.688941	0.999497	0.146524	0.999623
MIB1	57534 A_24_P1	-1.49	0.00443	0.036858	0.540753	0.999497	0.639846	0.999623
NEIL3	55247 A_23_P1	-4.87	0.004452	0.036858	0.608058	0.999497	0.360265	0.999623
MLXIPL	51085 A_23_P1	1.62	0.004438	0.036858	0.447741	0.999497	0.220519	0.999623
GYPA	2993 A_23_P4	-1.56	0.004533	0.036858	0.923595	0.999497	0.225265	0.999623
PACSIN3	29763 A_24_P1	1.69	0.004502	0.036858	0.847646	0.999497	0.868742	0.999623
BAT2	7916 A_24_P1	2.13	0.004534	0.036858	0.612267	0.999497	0.871152	0.999623
EIF5A	1984 A_24_P1	1.46	0.004298	0.036858	0.272048	0.999497	0.639329	0.999623
RIN1	9610 A_23_P1	2.09	0.004233	0.036858	0.606987	0.999497	0.933581	0.999623
CPXM1	56265 A_23_P1	1.76	0.004096	0.036858	0.420615	0.999497	0.996511	0.999623
OXSR1	9943 A_24_P1	1.77	0.004221	0.036858	0.876339	0.999497	0.879169	0.999623
THBS4	7060 A_24_P1	1.41	0.004154	0.036858	0.881901	0.999497	0.417252	0.999623
DOK1	1796 A_23_P1	1.29	0.004495	0.036858	0.978146	0.999497	0.650775	0.999623
FLNA	2316 A_23_P1	1.41	0.00425	0.036858	0.596631	0.999497	0.761419	0.999623
NDM2	4193 A_23_P1	1.4	0.004394	0.036858	0.764841	0.999497	0.521728	0.999623
NCAM1	4684 A_23_P1	1.47	0.004492	0.036858	0.542844	0.999497	0.155061	0.999623
MAPK13	5603 A_24_P1	1.52	0.004418	0.036858	0.852344	0.999497	0.867762	0.999623
CD8A	925 A_32_P1	-4.02	0.004597	0.036918	0.582391	0.999497	0.425898	0.999623
FIS1	51024 A_24_P1	1.38	0.004627	0.036918	0.625394	0.999497	0.756806	0.999623
RAB13	5872 A_23_P4	-1.89	0.004574	0.036918	0.738182	0.999497	0.778696	0.999623
PDLIM7	9260 A_24_P1	1.38	0.004608	0.036918	0.081496	0.999497	0.470102	0.999623
BGLAP	632 A_24_P1	1.79	0.004673	0.036962	0.879465	0.999497	0.252697	0.999623
DDIT4	54541 A_23_P1	1.48	0.004676	0.036962	0.988634	0.999497	0.783134	0.999623
HRAS	3265 A_23_P1	1.44	0.004932	0.036987	0.329159	0.999497	0.667962	0.999623
NAIP	4671 A_23_P1	-2.54	0.004925	0.036987	0.75741	0.999497	0.648142	0.999623
C7	730 A_23_P1	-2.26	0.004791	0.036987	0.790559	0.999497	0.249087	0.999623
TRGV5	6978 A_24_P1	-2.17	0.004796	0.036987	0.932939	0.999497	0.694945	0.999623
HAPLN3	145864 A_23_P1	1.44	0.004737	0.036987	0.337781	0.999497	0.514733	0.999623

TABLE S7-continued

Significant differences between CR and CNR								
		Fold-change CNR vs	Cytokine response		Age: 60-65 yo vs 74+ yo		Gender	
			CR	p-value	q-value	p-value	q-value	p-value
HDAC4	9759 A_24_P3	1.58	0.00483	0.036987	0.924326	0.999497	0.332864	0.999623
FN1	2335 A_24_P8	1.86	0.004957	0.036987	0.330315	0.999497	0.353643	0.999623
P2RX7	5027 A_24_P3	1.6	0.004958	0.036987	0.491895	0.999497	0.473055	0.999623
DEFB4	1673 A_23_P1	-1.54	0.004745	0.036987	0.642515	0.999497	0.472583	0.999623
LSM14B	149986 A_23_P3	1.52	0.004897	0.036987	0.57233	0.999497	0.670692	0.999623
TCTA	6988 A_23_P2	1.79	0.004727	0.036987	0.92342	0.999497	0.754902	0.999623
NAB2	4665 A_23_P3	1.72	0.004896	0.036987	0.188646	0.999497	0.784659	0.999623
PODXL2	50512 A_23_P1	1.38	0.004862	0.036987	0.458616	0.999497	0.688154	0.999623
GDF6	392255 A_32_P1	-2.06	0.005064	0.037134	0.945682	0.999497	0.567596	0.999623
SCD5	79966 A_24_P4	-1.62	0.005043	0.037134	0.845392	0.999497	0.33532	0.999623
ITGA11	22801 A_23_P2	1.95	0.005028	0.037134	0.972503	0.999497	0.807434	0.999623
CD38	952 A_23_P1	1.55	0.00501	0.037134	0.468403	0.999497	0.769658	0.999623
N-PAC	84656 A_23_P2	1.55	0.00517	0.037756	0.19692	0.999497	0.622897	0.999623
CLDN14	23562 A_23_P6	2.03	0.005196	0.037781	0.831003	0.999497	0.563221	0.999623
SDF2L1	23753 A_23_P6	1.79	0.005308	0.038434	0.840802	0.999497	0.951897	0.999623
HOXB7	3217 A_23_P4	1.62	0.005445	0.038772	0.89319	0.999497	0.47444	0.999623
HSPA5	3309 A_24_P5	1.47	0.005433	0.038772	0.42492	0.999497	0.453205	0.999623
PDGFC	56034 A_23_P2	-1.64	0.005383	0.038772	0.92027	0.999497	0.698472	0.999623
TNFSF13	8741 A_23_P1	1.43	0.005431	0.038772	0.119195	0.999497	0.94806	0.999623
ATP6V1H	51606 A_24_P1	-2.05	0.005562	0.039126	0.885499	0.999497	0.39461	0.999623
BAX	581 A_23_P2	1.42	0.005542	0.039126	0.168214	0.999497	0.648696	0.999623
NEIL2	252969 A_32_P1	1.43	0.005523	0.039126	0.239915	0.999497	0.303618	0.999623
EPN2	22905 A_23_P8	1.6	0.005599	0.039227	0.403423	0.999497	0.729579	0.999623
CXCL14	9547 A_23_P2	1.27	0.005651	0.039425	0.959343	0.999497	0.967797	0.999623
BOC	91653 A_23_P2	1.49	0.005835	0.039662	0.962864	0.999497	0.925063	0.999623
AKAP11	11215 A_23_P2	-1.85	0.00588	0.039662	0.851873	0.999497	0.590879	0.999623
3-Sep	55964 A_23_P2	1.56	0.005927	0.039662	0.768511	0.999497	0.969072	0.999623
N-PAC	84656 A_32_P7	1.84	0.006007	0.039662	0.81878	0.999497	0.609	0.999623
SEMA3C	10512 A_23_P2	-1.79	0.00588	0.039662	0.797983	0.999497	0.995553	0.999623
C3orf38	285237 A_23_P4	-1.99	0.005996	0.039662	0.086769	0.999497	0.901564	0.999623
PRSS2	5645 A_23_P3	1.55	0.005948	0.039662	0.710419	0.999497	0.131909	0.999623
WNK1	65125 A_24_P7	-1.81	0.005813	0.039662	0.265821	0.999497	0.292153	0.999623
DOCK7	85440 A_23_P2	-1.73	0.00582	0.039662	0.580693	0.999497	0.140506	0.999623
IGHV1-69	28461 A_24_P1	1.71	0.005994	0.039662	0.818702	0.999497	0.768258	0.999623
ASB1	51665 A_23_P1	1.68	0.005896	0.039662	0.63158	0.999497	0.474956	0.999623
AP1B1	162 A_23_P6	1.56	0.005872	0.039662	0.593906	0.999497	0.053772	0.999623
PRKCC	5588 A_23_P1	1.25	0.005884	0.039662	0.268524	0.999497	0.118193	0.999623
RAE1	8480 A_23_P3	1.27	0.006	0.039662	0.574388	0.999497	0.441716	0.999623
CFL1	1072 A_23_P3	1.57	0.006039	0.039725	0.834753	0.999497	0.423084	0.999623
CISH	1154 A_24_P5	1.75	0.006192	0.039811	0.957882	0.999497	0.838468	0.999623
NFKBIL1	4795 A_23_P1	2.06	0.006091	0.039811	0.666764	0.999497	0.296183	0.999623
BMP1	649 A_24_P1	1.48	0.00623	0.039811	0.765526	0.999497	0.075354	0.999623
TRIB3	57761 A_24_P2	1.87	0.006237	0.039811	0.566477	0.999497	0.47545	0.999623
PLAGL2	5326 A_23_P6	-1.68	0.006188	0.039811	0.79153	0.999497	0.351673	0.999623
CDH16	1014 A_23_P1	1.58	0.006166	0.039811	0.613212	0.999497	0.481024	0.999623
HTT	3064 A_23_P2	1.72	0.006125	0.039811	0.759241	0.999497	0.135237	0.999623
CROP	51747 A_23_P2	1.32	0.0062	0.039811	0.233464	0.999497	0.201247	0.999623
RP11-138L21.1	389722 A_24_P6	1.28	0.00632	0.039896	0.569351	0.999497	0.38752	0.999623
INHBC	3626 A_24_P1	-2.23	0.006301	0.039896	0.239035	0.999497	0.254386	0.999623
TNXB	7148 A_23_P1	1.8	0.006276	0.039896	0.24883	0.999497	0.190948	0.999623
GLT2SD2	23127 A_24_P6	1.25	0.006343	0.039897	0.665854	0.999497	0.624613	0.999623
CD163L1	283316 A_23_P6	1.79	0.006394	0.040067	0.597613	0.999497	0.974297	0.999623
PEX5	5830 A_23_P4	1.57	0.006757	0.040193	0.55322	0.999497	0.393006	0.999623
TP53	7157 A_23_P2	1.45	0.006593	0.040193	0.329323	0.999497	0.229693	0.999623
EGF	1950 A_23_P1	1.54	0.006706	0.040193	0.380675	0.999497	0.847549	0.999623
WDR59	79726 A_23_P2	1.46	0.006684	0.040193	0.643522	0.999497	0.658962	0.999623
STXB2	6813 A_24_P5	1.53	0.006513	0.040193	0.997036	0.999497	0.248488	0.999623
SLIT2	9353 A_23_P1	1.78	0.006488	0.040193	0.411598	0.999497	0.557526	0.999623
GPR98	84059 A_23_P1	-1.54	0.006643	0.040193	0.388514	0.999497	0.809156	0.999623
HDAC4	9759 A_23_P2	-1.33	0.006618	0.040193	0.060507	0.999497	0.79865	0.999623
ICAM3	3385 A_23_P1	1.73	0.006764	0.040193	0.503806	0.999497	0.315636	0.999623
LMLN	89782 A_23_P6	1.46	0.006627	0.040193	0.514015	0.999497	0.949942	0.999623
TNFRSF6B	8771 A_23_P2	1.65	0.006541	0.040193	0.474909	0.999497	0.401812	0.999623
ARF6	382 A_24_P6	-2.6	0.00665	0.040193	0.295516	0.999497	0.157962	0.999623
JUB	84962 A_23_P6	-1.4	0.006721	0.040193	0.665982	0.999497	0.635921	0.999623
ELMOD3	84173 A_23_P1	1.47	0.006751	0.040193	0.76838	0.999497	0.690694	0.999623
CDS9	966 A_24_P6	1.89	0.006571	0.040193	0.178875	0.999497	0.711986	0.999623
DLG1	1739 A_24_P1	-1.84	0.006882	0.040756	0.858759	0.999497	0.640739	0.999623

TABLE S7-continued

Significant differences between CR and CNR								
		Fold-change CNR vs	Cytokine response		Age: 60-65 yo vs 74+ yo		Gender	
			p-value	q-value	p-value	q-value	p-value	q-value
COL14A1	7373 A_32_P8	1.76	0.007048	0.040877	0.599642	0.999497	0.416598	0.999623
CAV3	859 A_24_P2	-1.31	0.007088	0.040877	0.305798	0.999497	0.317434	0.999623
TGM2	7052 A_32_P8	1.42	0.007119	0.040877	0.831014	0.999497	0.131657	0.999623
TNIP1	10318 A_23_P2	1.53	0.007087	0.040877	0.947415	0.999497	0.046481	0.999623
MEN1	4221 A_23_P7	1.68	0.007056	0.040877	0.911128	0.999497	0.159982	0.999623
ARRB2	409 A_23_P1	1.59	0.007077	0.040877	0.779283	0.999497	0.615331	0.999623
CTNND2	1501 A_23_P1	1.56	0.00707	0.040877	0.759584	0.999497	0.73204	0.999623
THBS2	7058 A_23_P6	-1.48	0.007122	0.040877	0.533028	0.999497	0.934161	0.999623
PBX2	5089 A_32_P1	1.25	0.00714	0.040877	0.428924	0.999497	0.430511	0.999623
CSNK2B	1460 A_24_P8	1.29	0.007037	0.040877	0.538916	0.999497	0.391645	0.999623
CLDN23	137075 A_23_P1	1.56	0.007175	0.040946	0.308815	0.999497	0.041708	0.999623
THBS1	7057 A_23_P2	1.44	0.007267	0.040951	0.561238	0.999497	0.402662	0.999623
DCBLD2	131566 A_24_P1	-1.63	0.007231	0.040951	0.684511	0.999497	0.780267	0.999623
CBX4	8535 A_23_P8	1.65	0.007227	0.040951	0.721296	0.999497	0.873026	0.999623
ISG20L2	81875 A_23_P1	1.39	0.007271	0.040951	0.949767	0.999497	0.722942	0.999623
LY75	4065 A_23_P3	-2.1	0.007393	0.0411	0.280371	0.999497	0.554946	0.999623
ARHGDI1	396 A_24_P2	1.65	0.007441	0.0411	0.381574	0.999497	0.805743	0.999623
CCL16	6360 A_23_P2	1.44	0.007347	0.0411	0.660933	0.999497	0.812475	0.999623
EMILIN2	84034 A_23_P2	1.43	0.007433	0.0411	0.873004	0.999497	0.924728	0.999623
MAF	4094 A_23_P3	1.62	0.007349	0.0411	0.280531	0.999497	0.933361	0.999623
MYBPH	4608 A_23_P1	2.2	0.00741	0.0411	0.381457	0.999497	0.449587	0.999623
ULBP2	80328 A_23_P1	1.82	0.007477	0.041165	0.673118	0.999497	0.267142	0.999623
FBF1	85302 A_24_P7	1.81	0.007547	0.041205	0.530159	0.999497	0.324689	0.999623
TCIRG1	10312 A_23_P7	1.75	0.007515	0.041205	0.807324	0.999497	0.336722	0.999623
CUL2	8453 A_24_P2	-2.44	0.007571	0.041205	0.833332	0.999497	0.548846	0.999623
FOXO3	2309 A_32_P1	1.22	0.00758	0.041205	0.993458	0.999497	0.821457	0.999623
FKBP8	23770 A_23_P2	1.49	0.007665	0.041315	0.359148	0.999497	0.380361	0.999623
IFT172	26160 A_23_P4	1.53	0.00772	0.041315	0.703408	0.999497	0.597845	0.999623
RFX2	5990 A_23_P2	1.5	0.007694	0.041315	0.645075	0.999497	0.75437	0.999623
STX1A	6804 A_23_P8	1.46	0.007702	0.041315	0.364024	0.999497	0.258177	0.999623
BNIP1	662 A_23_P7	1.57	0.007629	0.041315	0.947384	0.999497	0.241845	0.999623
DAPK2	23604 A_24_P1	1.45	0.007805	0.041645	0.836353	0.999497	0.040823	0.999623
DYRK2	8445 A_23_P2	1.27	0.007862	0.04169	0.993595	0.999497	0.593907	0.999623
BBC3	27113 A_23_P2	1.49	0.007854	0.04169	0.652506	0.999497	0.695162	0.999623
FUT4	2526 A_24_P2	1.5	0.007921	0.041874	0.756507	0.999497	0.805845	0.999623
TH1L	51497 A_24_P2	1.38	0.008004	0.04218	0.570652	0.999497	0.640054	0.999623
CYTH2	9266 A_23_P1	1.51	0.008084	0.042473	0.265899	0.999497	0.921536	0.999623
MFAP4	4239 A_23_P1	1.62	0.008144	0.042661	0.820137	0.999497	0.810928	0.999623
IGFALS	3483 A_23_P1	1.76	0.008414	0.042748	0.869832	0.999497	0.649025	0.999623
CLDN4	1364 A_24_P1	2.13	0.008418	0.042748	0.578741	0.999497	0.743621	0.999623
RPS3A	6189 A_32_P1	-6.71	0.008272	0.042748	0.339463	0.999497	0.302119	0.999623
BIN3	55909 A_24_P1	1.69	0.008205	0.042748	0.221195	0.999497	0.308429	0.999623
BSG	682 A_24_P2	1.83	0.008386	0.042748	0.358983	0.999497	0.36206	0.999623
PCSK9	255738 A_32_P1	-2.31	0.008448	0.042748	0.87887	0.999497	0.858256	0.999623
YWHAG	7532 A_24_P1	-1.57	0.008284	0.042748	0.692892	0.999497	0.900717	0.999623
BCL2A1	597 A_23_P1	-2.14	0.008483	0.042748	0.894468	0.999497	0.539085	0.999623
CFB	629 A_23_P1	1.47	0.00835	0.042748	0.467483	0.999497	0.918707	0.999623
CROP	51747 A_24_P2	-2.88	0.008461	0.042748	0.799301	0.999497	0.839386	0.999623
MSLN	10232 A_23_P7	1.42	0.008228	0.042748	0.306015	0.999497	0.280281	0.999623
WWP2	11060 A_23_P2	1.46	0.008446	0.042748	0.560331	0.999497	0.465721	0.999623
CD200	4345 A_23_P1	1.63	0.008448	0.042748	0.25547	0.999497	0.901291	0.999623
PSMD12	5718 A_23_P7	-2.08	0.008603	0.043102	0.958158	0.999497	0.63048	0.999623
CCND3	896 A_23_P2	1.45	0.008629	0.043102	0.930372	0.999497	0.318564	0.999623
COL15A1	1306 A_24_P3	1.59	0.00862	0.043102	0.62631	0.999497	0.777929	0.999623
RAB3B	5865 A_32_P1	1.3	0.008685	0.043133	0.63651	0.999497	0.247465	0.999623
AIFM2	84883 A_32_P7	1.58	0.008675	0.043133	0.448982	0.999497	0.746676	0.999623
RPS6KA1	6195 A_24_P3	1.8	0.008792	0.043542	0.844551	0.999497	0.859124	0.999623
HIP1	3092 A_23_P7	1.42	0.00884	0.043652	0.984356	0.999497	0.706868	0.999623
ICAM2	3384 A_23_P1	1.38	0.008886	0.043754	0.574412	0.999497	0.773073	0.999623
ISLR2	57611 A_32_P2	-1.56	0.008919	0.043789	0.293109	0.999497	0.275047	0.999623
AGGF1	55109 A_24_P2	1.34	0.009025	0.043934	0.9808	0.999497	0.920873	0.999623
LIF	3976 A_24_P1	1.7	0.00901	0.043934	0.684537	0.999497	0.304884	0.999623
CDH7	1005 A_23_P1	1.3	0.009022	0.043934	0.744671	0.999497	0.93517	0.999623
GMD5	2762 A_23_P7	1.45	0.009147	0.04414	0.190757	0.999497	0.953153	0.999623
HSPA1A	3303 A_24_P1	1.75	0.009119	0.04414	0.770009	0.999497	0.281256	0.999623
ACSF3	197322 A_23_P2	1.47	0.009182	0.04414	0.7574	0.999497	0.979474	0.999623
SFRS17A	8227 A_24_P1	1.3	0.009348	0.04414	0.899318	0.999497	0.841563	0.999623
RBM4	5936 A_23_P1	1.64	0.009269	0.04414	0.686055	0.999497	0.901274	0.999623

TABLE S7-continued

Significant differences between CR and CNR								
		Fold-change CNR vs	Cytokine response		Age: 60-65 yo vs 74+ yo		Gender	
			CR	p-value	q-value	p-value	q-value	p-value
XAF1	54739_A_23_P4	1.29	0.009205	0.04414	0.571241	0.999497	0.278729	0.999623
CD2BP2	10421_A_23_P6	2.43	0.009285	0.04414	0.864105	0.999497	0.924686	0.999623
TUBB	203068_A_23_P3	-1.27	0.009241	0.04414	0.701621	0.999497	0.433631	0.999623
WFIKKN1	117166_A_23_P1	1.79	0.009333	0.04414	0.882626	0.999497	0.983759	0.999623
MARK4	57787_A_23_P1	1.72	0.009295	0.04414	0.610972	0.999497	0.849994	0.999623
DOCK3	1795_A_24_P2	-2.09	0.009349	0.04414	0.99466	0.999497	0.096042	0.999623
TRAF7	84231_A_23_P2	1.68	0.009411	0.044311	0.612181	0.999497	0.292044	0.999623
HGF	3082_A_23_P5	1.52	0.009569	0.044882	0.198441	0.999497	0.50498	0.999623
EEF1A2	1917_A_23_P2	2.02	0.009584	0.044882	0.534017	0.999497	0.417562	0.999623
RAD9A	5883_A_23_P1	1.36	0.009796	0.044899	0.420983	0.999497	0.774342	0.999623
NDUFS1	4719_A_23_P1	-3.13	0.009784	0.044899	0.562165	0.999497	0.668457	0.999623
TAGAP	117289_A_23_P2	-3.04	0.009658	0.044899	0.280321	0.999497	0.521664	0.999623
TAX1BP1	8887_A_24_P5	-1.23	0.009719	0.044899	0.469163	0.999497	0.420653	0.999623
CD109	135228_A_23_P3	-2.13	0.009739	0.044899	0.814845	0.999497	0.336296	0.999623
TOLLIP	54472_A_23_P7	1.69	0.009629	0.044899	0.652502	0.999497	0.944066	0.999623
BCL11B	64919_A_23_P2	1.36	0.009749	0.044899	0.353575	0.999497	0.943937	0.999623
RTN3	10313_A_24_P3	1.38	0.009788	0.044899	0.58224	0.999497	0.571566	0.999623
PVRL3	25945_A_23_P8	-1.62	0.009854	0.045045	0.330796	0.999497	0.450665	0.999623
ERBB3	2065_A_24_P5	1.37	0.009892	0.045098	0.444707	0.999497	0.606208	0.999623
TTYH1	57348_A_23_P5	1.81	0.01008	0.04524	0.513414	0.999497	0.981078	0.999623
TCF3	6929_A_24_P3	1.64	0.009991	0.04524	0.628151	0.999497	0.54057	0.999623
PCMT1	5110_A_24_P1	-1.81	0.010046	0.04524	0.841975	0.999497	0.613309	0.999623
NLGN3	54413_A_23_P6	1.44	0.010021	0.04524	0.535075	0.999497	0.603253	0.999623
NRXN2	9379_A_24_P2	1.44	0.01008	0.04524	0.623422	0.999497	0.420966	0.999623
GTF2H2	2966_A_24_P2	-1.57	0.009963	0.04524	0.661375	0.999497	0.218962	0.999623
GNA12	2768_A_23_P2	1.45	0.010123	0.045312	0.603611	0.999497	0.392406	0.999623
TNFRSF1A	7132_A_24_P3	1.71	0.010194	0.045513	0.669489	0.999497	0.685361	0.999623
PTGIS	5740_A_24_P4	-2.43	0.010325	0.045576	0.652291	0.999497	0.282921	0.999623
AXIN1	8312_A_24_P2	1.58	0.010341	0.045576	0.652531	0.999497	0.43497	0.999623
C9orf61	9413_A_24_P2	1.31	0.010306	0.045576	0.14166	0.999497	0.930086	0.999623
CCL17	6361_A_23_P2	1.39	0.010272	0.045576	0.764709	0.999497	0.247562	0.999623
TSTA3	7264_A_23_P5	1.47	0.010236	0.045576	0.571615	0.999497	0.867314	0.999623
BOK	666_A_23_P2	1.79	0.010547	0.045815	0.590899	0.999497	0.212588	0.999623
MLLT1	4298_A_24_P4	1.52	0.010509	0.045815	0.785998	0.999497	0.587068	0.999623
CMKLR1	1240_A_24_P7	1.55	0.010444	0.045815	0.723016	0.999497	0.43937	0.999623
MST1R	4486_A_23_P2	1.81	0.010581	0.045815	0.49545	0.999497	0.541623	0.999623
FGFR3	2261_A_23_P5	1.33	0.010471	0.045815	0.591985	0.999497	0.728747	0.999623
C1QTNF6	114904_A_24_P2	1.86	0.010542	0.045815	0.797733	0.999497	0.521666	0.999623
ITFG2	55846_A_24_P1	1.52	0.010559	0.045815	0.872446	0.999497	0.184621	0.999623
KCNH3	23416_A_23_P8	1.49	0.010616	0.045853	0.716099	0.999497	0.361986	0.999623
AGPAT2	10555_A_32_P1	2.16	0.011394	0.046008	0.883506	0.999497	0.932464	0.999623
MACF1	23499_A_24_P4	1.24	0.011639	0.046008	0.413313	0.999497	0.755876	0.999623
MAMDC4	158056_A_23_P7	1.69	0.01093	0.046008	0.885796	0.999497	0.33709	0.999623
ITGB2	3689_A_23_P2	-2.6	0.011337	0.046008	0.577022	0.999497	0.1366	0.999623
DGKZ	8525_A_24_P1	1.75	0.011766	0.046008	0.683759	0.999497	0.658028	0.999623
SLC26A6	65010_A_23_P1	1.44	0.010777	0.046008	0.990628	0.999497	0.929937	0.999623
AP2A2	161_A_24_P3	1.3	0.011777	0.046008	0.758622	0.999497	0.071888	0.999623
LAIR1	3903_A_23_P2	1.3	0.011816	0.046008	0.798188	0.999497	0.445371	0.999623
SIX4	51804_A_23_P3	1.31	0.011577	0.046008	0.662808	0.999497	0.967053	0.999623
7-Sep	989_A_32_P7	-2.54	0.011163	0.046008	0.707334	0.999497	0.548829	0.999623
IL23A	51561_A_23_P7	2.19	0.011657	0.046008	0.795485	0.999497	0.601849	0.999623
CLDN12	9069_A_23_P1	-1.75	0.011527	0.046008	0.952433	0.999497	0.187921	0.999623
NFE2L3	9603_A_23_P4	-2.04	0.011594	0.046008	0.30672	0.999497	0.699681	0.999623
AR	367_A_23_P1	1.41	0.011739	0.046008	0.722581	0.999497	0.845551	0.999623
FGFR1	2260_A_23_P3	-4.3	0.011933	0.046008	0.416966	0.999497	0.640217	0.999623
FASTKD2	22868_A_23_P3	-2.68	0.011045	0.046008	0.644005	0.999497	0.302389	0.999623
MYH9	4627_A_23_P5	1.76	0.011765	0.046008	0.422758	0.999497	0.886066	0.999623
SLPI	6590_A_23_P5	1.43	0.011265	0.046008	0.209007	0.999497	0.089489	0.999623
LATS2	26524_A_24_P7	1.39	0.011702	0.046008	0.492726	0.999497	0.538383	0.999623
RPS6KA2	6196_A_23_P3	1.52	0.011932	0.046008	0.780008	0.999497	0.445324	0.999623
CD19	930_A_23_P1	2.19	0.010793	0.046008	0.213669	0.999497	0.834861	0.999623
CD3EAP	10849_A_23_P1	1.73	0.011621	0.046008	0.718564	0.999497	0.703033	0.999623
ADAR	103_A_23_P2	1.71	0.011759	0.046008	0.872095	0.999497	0.997358	0.999623
PRKACA	5566_A_24_P3	1.82	0.011515	0.046008	0.936106	0.999497	0.030038	0.999623
C1QTNF2	114898_A_23_P5	1.56	0.011866	0.046008	0.975072	0.999497	0.524615	0.999623
FIS1	51024_A_23_P2	2.08	0.010736	0.046008	0.956333	0.999497	0.517864	0.999623
MST1	4485_A_24_P1	1.48	0.011737	0.046008	0.520318	0.999497	0.219025	0.999623
MYD88	4615_A_23_P5	1.66	0.011705	0.046008	0.627416	0.999497	0.473691	0.999623

TABLE S7-continued

Significant differences between CR and CNR								
		Fold-change CNR vs	Cytokine response		Age: 60-65 yo vs 74+ yo		Gender	
			CR	p-value	q-value	p-value	q-value	p-value
CLDN3	1365 A_23_P7	1.73	0.011827	0.046008	0.959934	0.999497	0.150042	0.999623
FCGR1	2217 A_23_P5	1.49	0.010887	0.046008	0.871968	0.999497	0.733417	0.999623
PLAUR	5329 A_23_P1	1.72	0.011721	0.046008	0.913173	0.999497	0.959682	0.999623
NFAT5	10725 A_23_P2	-1.59	0.01097	0.046008	0.927355	0.999497	0.231058	0.999623
RNF130	55819 A_23_P4	-1.54	0.011328	0.046008	0.624961	0.999497	0.199011	0.999623
JMY	133746 A_32_P1	-1.6	0.010749	0.046008	0.993441	0.999497	0.897651	0.999623
PHLDA1	22822 A_24_P2	-1.65	0.011663	0.046008	0.623252	0.999497	0.22338	0.999623
UBE2Z	65264 A_24_P2	-1.4	0.011561	0.046008	0.35366	0.999497	0.76336	0.999623
EHD1	10938 A_23_P2	1.19	0.011932	0.046008	0.556726	0.999497	0.933536	0.999623
RFX5	5993 A_24_P2	-1.43	0.011832	0.046008	0.714182	0.999497	0.443883	0.999623
LTBR	4055 A_23_P2	1.35	0.010873	0.046008	0.74031	0.999497	0.870839	0.999623
SNX17	9784 A_23_P2	1.37	0.011097	0.046008	0.678232	0.999497	0.817956	0.999623
GDF15	9518 A_23_P1	1.62	0.011923	0.046008	0.701642	0.999497	0.446223	0.999623
NME3	4832 A_23_P1	1.57	0.011402	0.046008	0.626596	0.999497	0.245007	0.999623
TBX21	30009 A_23_P1	-1.38	0.011205	0.046008	0.593257	0.999497	0.823812	0.999623
SOCS3	9021 A_23_P2	1.28	0.011613	0.046008	0.839539	0.999497	0.088534	0.999623
WISP1	8840 A_23_P2	1.49	0.010885	0.046008	0.685025	0.999497	0.867964	0.999623
CDC2L2	728642 A_24_P5	1.32	0.010948	0.046008	0.942452	0.999497	0.499853	0.999623
YWHAZ	7534 A_32_P5	-1.79	0.010923	0.046008	0.39737	0.999497	0.535257	0.999623
MAPK7	5598 A_23_P1	1.5	0.01148	0.046008	0.334768	0.999497	0.64556	0.999623
CDC2L1	984 A_23_P2	1.72	0.011987	0.046113	0.709495	0.999497	0.893553	0.999623
PIWIL4	143689 A_23_P4	1.51	0.012061	0.046291	0.854777	0.999497	0.737882	0.999623
ADRB3	155 A_23_P1	-1.31	0.012105	0.046359	0.665715	0.999497	0.527794	0.999623
DDIT4	54541 A_32_P2	1.48	0.01217	0.0464	0.785068	0.999497	0.665712	0.999623
CALR	811 A_24_P2	1.28	0.012168	0.0464	0.048403	0.999497	0.792997	0.999623
SOC7	30837 A_32_P4	1.72	0.012371	0.046958	0.968504	0.999497	0.879769	0.999623
METTL11A	28989 A_23_P1	1.48	0.012369	0.046958	0.474362	0.999497	0.648279	0.999623
TNFAIP3	7128 A_24_P1	-1.59	0.012484	0.047179	0.670444	0.999497	0.430055	0.999623
EP300	2033 A_23_P4	-2.34	0.012471	0.047179	0.102764	0.999497	0.444003	0.999623
LYST	1130 A_23_P2	-2.23	0.012682	0.047422	0.643012	0.999497	0.597959	0.999623
PACSIN1	29993 A_24_P1	1.44	0.012592	0.047422	0.810806	0.999497	0.319026	0.999623
IGHMBP2	3508 A_23_P2	1.86	0.012685	0.047422	0.536694	0.999497	0.559356	0.999623
POLM	27434 A_24_P2	1.73	0.012615	0.047422	0.74306	0.999497	0.630574	0.999623
LRP4	4038 A_24_P4	-1.89	0.01267	0.047422	0.385702	0.999497	0.259541	0.999623
NLK	51701 A_23_P1	1.57	0.012716	0.047431	0.959462	0.999497	0.362725	0.999623
RAG1AP1	55974 A_24_P2	1.63	0.012996	0.047513	0.825239	0.999497	0.72817	0.999623
RAF1	5894 A_23_P4	1.4	0.013268	0.047513	0.604929	0.999497	0.864017	0.999623
LEFTY2	7044 A_23_P1	1.35	0.013316	0.047513	0.835132	0.999497	0.79175	0.999623
KLRF1	51348 A_32_P1	-2.47	0.013194	0.047513	0.094166	0.999497	0.497135	0.999623
BAT3	7917 A_23_P1	1.44	0.013123	0.047513	0.830021	0.999497	0.605435	0.999623
GADD45B	4616 A_23_P1	1.67	0.013118	0.047513	0.418033	0.999497	0.561697	0.999623
ITGB4	3691 A_23_P2	1.88	0.012977	0.047513	0.884416	0.999497	0.850481	0.999623
NDRG1	10397 A_24_P2	1.39	0.013316	0.047513	0.431376	0.999497	0.338149	0.999623
FOXL2	668 A_23_P1	1.4	0.01325	0.047513	0.623953	0.999497	0.756941	0.999623
CRKL	1399 A_24_P2	-3.21	0.013096	0.047513	0.989163	0.999497	0.618805	0.999623
FKBP5	2289 A_23_P1	1.48	0.013028	0.047513	0.805064	0.999497	0.180509	0.999623
L1CAM	3897 A_24_P2	1.48	0.012946	0.047513	0.948151	0.999497	0.973372	0.999623
BAG3	9531 A_23_P2	-1.99	0.013304	0.047513	0.889016	0.999497	0.9404	0.999623
RHOA	387 A_23_P2	1.53	0.01318	0.047513	0.672895	0.999497	0.646367	0.999623
SMAD6	4091 A_23_P2	1.71	0.012827	0.047513	0.844195	0.999497	0.658975	0.999623
GPR98	84059 A_24_P1	-1.41	0.012977	0.047513	0.684207	0.999497	0.179322	0.999623
IRS2	8660 A_23_P2	1.5	0.012997	0.047513	0.942002	0.999497	0.602622	0.999623
PML	5371 A_24_P1	1.3	0.013099	0.047513	0.879066	0.999497	0.92679	0.999623
PACS2	23241 A_24_P2	1.75	0.013226	0.047513	0.433797	0.999497	0.355999	0.999623
PSMD9	5715 A_23_P2	1.31	0.013234	0.047513	0.457114	0.999497	0.757866	0.999623
SOCS1	8651 A_23_P4	1.25	0.012857	0.047513	0.596738	0.999497	0.43267	0.999623
EP300	2033 A_24_P7	1.29	0.013457	0.047522	0.518843	0.999497	0.836977	0.999623
MLL5	55904 A_24_P1	-2.12	0.013431	0.047522	0.853142	0.999497	0.367771	0.999623
SH2D1A	4068 A_24_P2	-1.53	0.013432	0.047522	0.354116	0.999497	0.768015	0.999623
UBP1	7342 A_23_P2	-1.91	0.013397	0.047522	0.864577	0.999497	0.584273	0.999623
CLN8	2055 A_23_P2	1.35	0.013435	0.047522	0.97432	0.999497	0.823165	0.999623
NOL3	8996 A_23_P2	1.28	0.01352	0.047649	0.885717	0.999497	0.216732	0.999623
MKL1	57591 A_23_P2	1.28	0.013636	0.047959	0.213954	0.999497	0.218478	0.999623
PSMB2	5690 A_23_P1	1.66	0.013703	0.048095	0.172869	0.999497	0.889876	0.999623
IBTK	25998 A_23_P2	-1.49	0.013747	0.048101	0.847817	0.999497	0.427783	0.999623
CAT	847 A_23_P1	1.32	0.01376	0.048101	0.349021	0.999497	0.498228	0.999623
NTN1	9423 A_32_P2	1.57	0.013797	0.04813	0.625534	0.999497	0.525615	0.999623
TNF	7124 A_24_P2	1.42	0.013975	0.048193	0.496325	0.999497	0.252806	0.999623

TABLE S7-continued

Significant differences between CR and CNR								
		Fold-change CNR vs	Cytokine response		Age: 60-65 yo vs 74+ yo		Gender	
			CR	p-value	q-value	p-value	q-value	p-value
DBNL	28988 A_24_P4	1.87	0.013971	0.048193	0.962298	0.999497	0.497226	0.999623
RABEP1	9135 A_23_P7	-2.29	0.014175	0.048193	0.230644	0.999497	0.897774	0.999623
HFE	3077 A_23_P1	-2.54	0.014178	0.048193	0.90836	0.999497	0.616177	0.999623
POLD1	5424 A_23_P5	1.54	0.01398	0.048193	0.577717	0.999497	0.748243	0.999623
DDR1	780 A_23_P5	1.81	0.014078	0.048193	0.549439	0.999497	0.982262	0.999623
ZFYVE9	9372 A_23_P3	1.31	0.014041	0.048193	0.24404	0.999497	0.234146	0.999623
SNAP29	9342 A_23_P2	-2.08	0.013989	0.048193	0.833414	0.999497	0.455003	0.999623
AQP3	360 A_23_P1	1.54	0.014039	0.048193	0.469185	0.999497	0.622415	0.999623
PSMF1	9491 A_24_P1	1.26	0.014135	0.048193	0.850782	0.999497	0.82084	0.999623
PBX4	80714 A_23_P5	1.33	0.013989	0.048193	0.228749	0.999497	0.538604	0.999623
BDNF	627 A_23_P1	1.41	0.014073	0.048193	0.323296	0.999497	0.764656	0.999623
COL7A1	1294 A_23_P1	1.66	0.014106	0.048193	0.54834	0.999497	0.460984	0.999623
ATP2A2	488 A_24_P1	1.32	0.014283	0.048454	0.164309	0.999497	0.215689	0.999623
SRPK1	6732 A_23_P1	-1.64	0.014417	0.048811	0.938567	0.999497	0.575052	0.999623
NISCH	11188 A_24_P5	1.46	0.014487	0.048916	0.914042	0.999497	0.524538	0.999623
AMOTL1	154810 A_23_P1	1.7	0.014504	0.048916	0.441658	0.999497	0.566352	0.999623
PKN2	5586 A_24_P3	-1.51	0.014633	0.049157	0.651112	0.999497	0.540453	0.999623
ICAM5	7087 A_24_P2	1.64	0.014627	0.049157	0.709284	0.999497	0.406186	0.999623
LTBP2	4053 A_23_P4	1.55	0.014726	0.049278	0.78761	0.999497	0.050492	0.999623
PDCD10	11235 A_23_P1	-2.23	0.014706	0.049278	0.219256	0.999497	0.625871	0.999623
EMR1	2015 A_23_P2	1.39	0.014778	0.049356	0.461514	0.999497	0.088336	0.999623
HSPB1	3315 A_24_P8	1.64	0.014813	0.049377	0.895272	0.999497	0.507419	0.999623
RAB4A	5867 A_24_P1	-1.9	0.014942	0.049477	0.68528	0.999497	0.805571	0.999623
PSMG3	84262 A_24_P1	1.33	0.014935	0.049477	0.509811	0.999497	0.910752	0.999623
CD86	942 A_23_P1	-2.1	0.015025	0.049477	0.47095	0.999497	0.349895	0.999623
COTL1	23406 A_23_P8	1.63	0.015133	0.049477	0.104524	0.999497	0.467965	0.999623
TUBB	203068 A_23_P8	1.34	0.015187	0.049477	0.24464	0.999497	0.530503	0.999623
COL6A1	1291 A_32_P3	1.43	0.015105	0.049477	0.427278	0.999497	0.481937	0.999623
CEACAM19	56971 A_23_P7	1.84	0.01516	0.049477	0.546633	0.999497	0.168758	0.999623
UBE2Z	65264 A_24_P3	1.77	0.015088	0.049477	0.981491	0.999497	0.894359	0.999623
ENG	2022 A_23_P8	1.56	0.01488	0.049477	0.853209	0.999497	0.622503	0.999623
NAIF1	203245 A_24_P8	1.59	0.014961	0.049477	0.447055	0.999497	0.609572	0.999623
FAM3C	10447 A_23_P1	-1.83	0.015015	0.049477	0.979811	0.999497	0.749666	0.999623
SCFD2	152579 A_23_P9	1.67	0.015134	0.049477	0.884615	0.999497	0.762606	0.999623
FOXC1	2296 A_23_P3	1.56	0.015239	0.049551	0.742861	0.999497	0.263313	0.999623
RPS3	6188 A_23_P1	1.39	0.01535	0.049784	0.6263	0.999497	0.27172	0.999623
PNN	5411 A_32_P2	1.9	0.015455	0.049784	0.701619	0.999497	0.099695	0.999623
LPP	4026 A_24_P1	-1.89	0.0154	0.049784	0.3246	0.999497	0.596791	0.999623
YWHAZ	7534 A_32_P1	-1.55	0.015381	0.049784	0.564362	0.999497	0.865171	0.999623
TAPBP1	55080 A_23_P3	1.47	0.015437	0.049784	0.46879	0.999497	0.870077	0.999623
PYDC1	260434 A_23_P4	1.55	0.015517	0.049856	0.859028	0.999497	0.294833	0.999623
MAP2K3	5606 A_24_P2	1.96	0.015535	0.049856	0.576898	0.999497	0.357913	0.999623
DOCK11	139818 A_23_P1	-1.9	0.015696	0.049953	0.636569	0.999497	0.855811	0.999623
HTATIP2	10553 A_23_P1	-1.58	0.015739	0.049953	0.869306	0.999497	0.459502	0.999623
SRF	6722 A_24_P3	-2.44	0.015601	0.049953	0.792965	0.999497	0.702688	0.999623
HDAC4	9759 A_24_P8	-2.51	0.015763	0.049953	0.362259	0.999497	0.877712	0.999623
SP3	6670 A_23_P3	-1.77	0.015825	0.049953	0.80038	0.999497	0.197154	0.999623
MAP1S	55201 A_23_P1	1.81	0.01571	0.049953	0.549605	0.999497	0.360408	0.999623
FEN1	2237 A_24_P7	1.5	0.015928	0.049953	0.634676	0.999497	0.246327	0.999623
NISCH	11188 A_24_P4	1.68	0.015908	0.049953	0.53073	0.999497	0.589713	0.999623
HAX1	10456 A_23_P1	1.51	0.015846	0.049953	0.520141	0.999497	0.27338	0.999623
RASSF5	83593 A_24_P1	-1.42	0.015661	0.049953	0.617751	0.999497	0.722341	0.999623
GNLY	10578 A_23_P2	-3.67	0.015862	0.049953	0.540932	0.999497	0.6485	0.999623
STK17A	9263 A_23_P8	1.19	0.015943	0.049953	0.186936	0.999497	0.471213	0.999623
THAP3	90326 A_23_P3	1.84	0.015971	0.049953	0.340718	0.999497	0.544535	0.999623
TREML2	79865 A_23_P7	2.03	0.015817	0.049953	0.440179	0.999497	0.775578	0.999623
HMGBl	3146 A_24_P8	-1.38	0.016067	0.050069	0.52182	0.999497	0.148462	0.999623
MYO18A	399687 A_23_P7	1.29	0.016065	0.050069	0.998903	0.999497	0.324238	0.999623
DUB3	377630 A_24_P2	-1.85	0.016161	0.050192	0.196264	0.999497	0.491006	0.999623
XRCC5	7520 A_24_P3	-1.63	0.016194	0.050192	0.659552	0.999497	0.398873	0.999623
PDCD6IP	10015 A_24_P5	-2.76	0.01618	0.050192	0.720101	0.999497	0.279458	0.999623
PANX1	24145 A_23_P4	1.41	0.016242	0.050251	0.417255	0.999497	0.488458	0.999623
CD40	958 A_23_P5	1.54	0.016274	0.050262	0.589716	0.999497	0.824097	0.999623
PAFAH1B1	5048 A_24_P3	-1.47	0.016423	0.050509	0.567136	0.999497	0.712043	0.999623
EFS	10278 A_23_P4	1.45	0.016397	0.050509	0.59346	0.999497	0.817169	0.999623
LMNA	4000 A_24_P1	1.41	0.016472	0.050509	0.591051	0.999497	0.698601	0.999623
GDF3	9573 A_23_P7	1.76	0.016448	0.050509	0.454274	0.999497	0.873001	0.999623
MLL4	9757 A_23_P1	1.81	0.01651	0.050536	0.663526	0.999497	0.484866	0.999623

TABLE S7-continued

Significant differences between CR and CNR								
		Fold-change CNR vs	Cytokine response		Age: 60-65 yo vs 74+ yo		Gender	
			CR	p-value	q-value	p-value	q-value	p-value
RABEP2	79874_A_23_P1	1.62	0.016647	0.050686	0.72717	0.999497	0.505663	0.999623
IRAK1BP1	134728_A_32_P2	-1.63	0.016622	0.050686	0.873052	0.999497	0.271013	0.999623
EPS15L1	58513_A_23_P1	1.37	0.016609	0.050686	0.558181	0.999497	0.997655	0.999623
SERPINF2	5345_A_23_P1	1.78	0.016727	0.050841	0.751593	0.999497	0.417585	0.999623
RACGAP1	29127_A_32_P1	-2.21	0.016765	0.050865	0.333038	0.999497	0.999402	0.999623
AP3B2	8120_A_23_P1	1.52	0.01684	0.051003	0.851386	0.999497	0.57374	0.999623
GYG2	8908_A_32_P1	1.45	0.016875	0.05102	0.530844	0.999497	0.142388	0.999623
CBL	867_A_23_P1	1.56	0.016983	0.051041	0.806197	0.999497	0.899872	0.999623
SYNJ2BP	55333_A_24_P1	1.51	0.016967	0.051041	0.798666	0.999497	0.981506	0.999623
DLC1	10395_A_24_P1	-1.95	0.017	0.051041	0.843286	0.999497	0.450104	0.999623
CREBBP	1387_A_24_P1	-2.25	0.016942	0.051041	0.817713	0.999497	0.419253	0.999623
DST	667_A_23_P1	1.41	0.017075	0.051142	0.296653	0.999497	0.711256	0.999623
CELSR3	1951_A_23_P1	1.4	0.017093	0.051142	0.982517	0.999497	0.820933	0.999623
LRDD	55367_A_32_P1	1.67	0.017205	0.051298	0.928012	0.999497	0.404034	0.999623
HIVEP3	59269_A_24_P1	1.4	0.017179	0.051298	0.892249	0.999497	0.356162	0.999623
ITIH1	3697_A_23_P1	1.37	0.01738	0.051376	0.611713	0.999497	0.22151	0.999623
SPG7	6687_A_24_P1	1.49	0.01738	0.051376	0.689204	0.999497	0.774355	0.999623
BMP4	652_A_23_P1	1.46	0.017375	0.051376	0.348872	0.999497	0.686438	0.999623
HLA-DMA	3108_A_23_P1	1.72	0.017325	0.051376	0.270348	0.999497	0.921517	0.999623
CUL4A	8451_A_24_P1	-1.51	0.017319	0.051376	0.427646	0.999497	0.363818	0.999623
S100B	6285_A_23_P1	-2.33	0.017479	0.051579	0.383508	0.999497	0.47419	0.999623
HIPK2	28996_A_24_P1	-2.02	0.017655	0.051664	0.880894	0.999497	0.189806	0.999623
TRIP6	7205_A_24_P1	1.32	0.017616	0.051664	0.224741	0.999497	0.413981	0.999623
RPSA	3921_A_24_P1	-2.29	0.017658	0.051664	0.689339	0.999497	0.494854	0.999623
TNFRSF8	943_A_23_P1	1.47	0.01763	0.051664	0.713048	0.999497	0.355213	0.999623
DHCR24	1718_A_23_P1	-1.44	0.017589	0.051664	0.997665	0.999497	0.603534	0.999623
GCNT2	2651_A_24_P1	-2.02	0.017693	0.051681	0.851155	0.999497	0.51601	0.999623
ACSF3	197322_A_32_P1	1.4	0.017812	0.05185	0.800768	0.999497	0.64634	0.999623
LRIG1	26018_A_23_P1	1.46	0.01779	0.05185	0.625735	0.999497	0.191008	0.999623
UBL7	84993_A_23_P1	1.61	0.017843	0.051854	0.592493	0.999497	0.553974	0.999623
NEDD4L	23327_A_24_P1	-1.48	0.017927	0.051924	0.54472	0.999497	0.482055	0.999623
TRAF2	7186_A_23_P1	1.64	0.017906	0.051924	0.661343	0.999497	0.861379	0.999623
CXCL12	6387_A_23_P1	1.34	0.018001	0.05205	0.543554	0.999497	0.423963	0.999623
DPT	1805_A_23_P1	-1.63	0.018103	0.05217	0.605565	0.999497	0.072208	0.999623
MFGE8	4240_A_23_P1	1.43	0.018092	0.05217	0.64808	0.999497	0.524613	0.999623
C1RL	51279_A_23_P1	-1.83	0.01829	0.052194	0.975317	0.999497	0.171012	0.999623
JAK1	3716_A_23_P1	1.29	0.018292	0.052194	0.796622	0.999497	0.631485	0.999623
HDAC3	8841_A_23_P1	1.46	0.018293	0.052194	0.745046	0.999497	0.560529	0.999623
NF2	4771_A_23_P1	-1.31	0.018246	0.052194	0.953115	0.999497	0.791877	0.999623
PPIH	10465_A_23_P1	1.37	0.018156	0.052194	0.800519	0.999497	0.687063	0.999623
DAP	1611_A_24_P1	1.68	0.018176	0.052194	0.254917	0.999497	0.998228	0.999623
RASSF5	83593_A_24_P1	1.42	0.018386	0.052374	0.217375	0.999497	0.6456	0.999623
FGF	2244_A_23_P1	-1.76	0.018452	0.052473	0.941636	0.999497	0.641752	0.999623
COL9A1	1297_A_24_P1	1.73	0.018791	0.052571	0.535609	0.999497	0.292217	0.999623
MIA3	375056_A_24_P1	-1.52	0.018669	0.052571	0.963688	0.999497	0.563596	0.999623
AGGF1	55109_A_23_P1	-1.57	0.018757	0.052571	0.525892	0.999497	0.321101	0.999623
ANLN	54443_A_23_P1	-1.83	0.018522	0.052571	0.911901	0.999497	0.453283	0.999623
PKN3	29941_A_23_P1	1.55	0.018662	0.052571	0.967297	0.999497	0.534119	0.999623
CES1	1066_A_23_P1	1.28	0.018566	0.052571	0.989327	0.999497	0.31366	0.999623
PSMD2	5708_A_24_P1	1.3	0.018693	0.052571	0.734936	0.999497	0.85722	0.999623
CDK5	1020_A_23_P1	1.36	0.018722	0.052571	0.948372	0.999497	0.902436	0.999623
RAB7A	7879_A_24_P1	1.38	0.018778	0.052571	0.685641	0.999497	0.748355	0.999623
SH3GL2	6456_A_23_P1	1.26	0.018774	0.052571	0.99059	0.999497	0.3713	0.999623
LENG9	94059_A_32_P1	-1.43	0.018823	0.052573	0.995231	0.999497	0.049609	0.999623
MNDA	4332_A_23_P1	-3.26	0.019013	0.052678	0.201131	0.999497	0.820534	0.999623
GZMB	3002_A_23_P1	-4.13	0.01891	0.052678	0.95404	0.999497	0.727099	0.999623
TMBIM6	7009_A_23_P1	1.65	0.018934	0.052678	0.912088	0.999497	0.730606	0.999623
EXOC4	60412_A_24_P1	-1.32	0.018975	0.052678	0.297355	0.999497	0.26402	0.999623
BAG4	9530_A_24_P1	-2.5	0.018999	0.052678	0.909919	0.999497	0.568578	0.999623
LTBP4	8425_A_23_P1	1.75	0.019121	0.052893	0.663471	0.999497	0.710995	0.999623
DHCR24	1718_A_23_P1	1.81	0.019155	0.052901	0.890871	0.999497	0.400115	0.999623
COL8A1	1295_A_23_P1	1.36	0.019206	0.052957	0.791072	0.999497	0.614035	0.999623
INHBB	3625_A_23_P1	1.23	0.019281	0.053079	0.403749	0.999497	0.971628	0.999623
RPS3A	6189_A_24_P1	-1.67	0.019398	0.053231	0.794357	0.999497	0.502794	0.999623
CLCF1	23529_A_23_P1	1.52	0.019385	0.053231	0.826001	0.999497	0.909078	0.999623
DGKE	8526_A_32_P1	1.56	0.019464	0.053328	0.972552	0.999497	0.771683	0.999623
AKT1	207_A_23_P1	1.7	0.019564	0.053495	0.786708	0.999497	0.686243	0.999623
SMAD4	4089_A_23_P1	-1.7	0.019649	0.053495	0.502666	0.999497	0.175732	0.999623

TABLE S7-continued

Significant differences between CR and CNR								
	CR	Cytokine response		Age: 60-65 yo vs 74+ yo		Gender		
		Fold-change CNR vs	p-value	q-value	p-value	q-value	p-value	q-value
GPR77	27202 A_23_P1	1.57	0.019626	0.053495	0.491916	0.999497	0.410461	0.999623
RABEP1	9135 A_24_P5	-1.66	0.01964	0.053495	0.612789	0.999497	0.396126	0.999623
CDC42	998 A_23_P2	-1.77	0.019749	0.053533	0.22318	0.999497	0.780298	0.999623
RTN3	10313 A_32_P2	1.39	0.019788	0.053533	0.690649	0.999497	0.264794	0.999623
LOC728613	728613 A_24_P5	1.34	0.019784	0.053533	0.217679	0.999497	0.20341	0.999623
SHB	6461 A_23_P2	1.48	0.019711	0.053533	0.841275	0.999497	0.778223	0.999623
ELMO2	63916 A_24_P1	1.56	0.019866	0.053541	0.768714	0.999497	0.638768	0.999623
DGCR6	8214 A_24_P2	1.55	0.019884	0.053541	0.942565	0.999497	0.58851	0.999623
CCR6	1235 A_24_P2	-2.17	0.019826	0.053541	0.156564	0.999497	0.297857	0.999623
LAMA5	3911 A_32_P1	1.79	0.01993	0.053582	0.84655	0.999497	0.81709	0.999623
PRKAR1B	5575 A_32_P7	1.71	0.020007	0.053624	0.626371	0.999497	0.149768	0.999623
AMIGO1	57463 A_24_P2	1.27	0.020008	0.053624	0.7741	0.999497	0.90952	0.999623
KRAS	3845 A_23_P4	-1.85	0.020192	0.054035	0.391977	0.999497	0.399416	0.999623
KNG1	3827 A_23_P2	1.29	0.020374	0.054369	0.984157	0.999497	0.945638	0.999623
LDLRAP1	26119 A_32_P2	1.59	0.020381	0.054369	0.413619	0.999497	0.848391	0.999623
PSME3	10197 A_24_P2	1.47	0.020416	0.054381	0.134221	0.999497	0.588152	0.999623
RAB35	11021 A_23_P2	1.41	0.020663	0.054867	0.925716	0.999497	0.900051	0.999623
CCL27	10850 A_23_P1	1.32	0.020634	0.054867	0.555063	0.999497	0.607125	0.999623
FNBP1	23048 A_24_P2	-1.59	0.020837	0.054915	0.943748	0.999497	0.374231	0.999623
HIF1A	3091 A_24_P2	-2.63	0.020904	0.054915	0.506111	0.999497	0.425761	0.999623
MIF	4282 A_23_P5	2.35	0.020884	0.054915	0.9379	0.999497	0.170699	0.999623
IFRD1	3475 A_24_P1	-2.06	0.020772	0.054915	0.481302	0.999497	0.634188	0.999623
MARK3	4140 A_23_P1	1.19	0.020904	0.054915	0.495457	0.999497	0.35198	0.999623
CASP8AP2	9994 A_23_P5	-1.67	0.020872	0.054915	0.960732	0.999497	0.48113	0.999623
BCL6B	255877 A_23_P3	1.32	0.02081	0.054915	0.396926	0.999497	0.719695	0.999623
BCL9L	283149 A_24_P1	1.51	0.021124	0.055409	0.748984	0.999497	0.274008	0.999623
BTBD9	114781 A_32_P5	1.64	0.021164	0.055417	0.738167	0.999497	0.28085	0.999623
RAB26	25837 A_23_P2	1.63	0.021191	0.055417	0.93245	0.999497	0.670129	0.999623
HIP1	3092 A_24_P5	-1.85	0.02134	0.055721	0.575538	0.999497	0.250488	0.999623
TERF1	7013 A_24_P1	-2.32	0.021372	0.055721	0.515626	0.999497	0.892773	0.999623
GATA2	2624 A_24_P1	1.63	0.021461	0.055826	0.764621	0.999497	0.351429	0.999623
COL6A2	1292 A_23_P3	1.99	0.021477	0.055826	0.796434	0.999497	0.64886	0.999623
MAP4K4	9448 A_23_P1	-1.87	0.021568	0.055977	0.877988	0.999497	0.58069	0.999623
PXN	5829 A_32_P4	2	0.021875	0.056142	0.938061	0.999497	0.319663	0.999623
IGKC	3514 A_32_P1	1.69	0.022022	0.056142	0.701558	0.999497	0.329592	0.999623
TLX2	3196 A_23_P3	1.7	0.021845	0.056142	0.775794	0.999497	0.77374	0.999623
NTSR1	4923 A_23_P3	1.39	0.021794	0.056142	0.614617	0.999497	0.235568	0.999623
NFATC3	4775 A_23_P7	1.87	0.021799	0.056142	0.819628	0.999497	0.865093	0.999623
JAK3	3718 A_24_P5	1.59	0.021816	0.056142	0.490451	0.999497	0.687042	0.999623
PTPRS	5802 A_23_P5	1.33	0.021992	0.056142	0.073697	0.999497	0.028188	0.999623
SEMA4C	54910 A_23_P5	1.45	0.02197	0.056142	0.748578	0.999497	0.521656	0.999623
IFT81	28981 A_23_P7	-1.72	0.021961	0.056142	0.815794	0.999497	0.46504	0.999623
WWTR1	25937 A_23_P2	1.19	0.021808	0.056142	0.267907	0.999497	0.815463	0.999623
MSN	4478 A_24_P1	1.55	0.021903	0.056142	0.463843	0.999497	0.300839	0.999623
IL4I1	259307 A_23_P5	1.43	0.021876	0.056142	0.798508	0.999497	0.4201	0.999623
NFKBIB	4793 A_24_P1	1.65	0.022342	0.056377	0.878305	0.999497	0.860706	0.999623
MAG	4099 A_24_P2	1.39	0.022377	0.056377	0.568829	0.999497	0.090688	0.999623
ARHGAP27	201176 A_23_P1	1.5	0.022406	0.056377	0.316917	0.999497	0.27609	0.999623
PTPRU	10076 A_23_P1	1.51	0.022407	0.056377	0.669712	0.999497	0.772528	0.999623
HSPB1	3315 A_23_P2	1.66	0.022296	0.056377	0.800525	0.999497	0.236396	0.999623
MAL	4118 A_23_P1	1.38	0.022409	0.056377	0.240071	0.999497	0.979282	0.999623
SPIN2B	474343 A_23_P1	1.29	0.022305	0.056377	0.56812	0.999497	0.280096	0.999623
MED1	5469 A_23_P4	1.93	0.022333	0.056377	0.70843	0.999497	0.564714	0.999623
RHOT2	89941 A_23_P1	1.5	0.022339	0.056377	0.901844	0.999497	0.343098	0.999623
PAG1	55824 A_32_P1	-1.44	0.022711	0.056646	0.96324	0.999497	0.93506	0.999623
STEAP2	261729 A_23_P4	-1.5	0.022586	0.056646	0.482959	0.999497	0.664367	0.999623
NFTN	72020 A_24_P5	1.48	0.022781	0.056646	0.703564	0.999497	0.976427	0.999623
ORM2	5005 A_23_P5	1.48	0.023091	0.056646	0.593209	0.999497	0.171531	0.999623
MATN3	4148 A_23_P1	-3.17	0.023056	0.056646	0.897744	0.999497	0.944137	0.999623
RNF216	54476 A_24_P2	2.64	0.022954	0.056646	0.399745	0.999497	0.961986	0.999623
CP110	9738 A_24_P3	-1.8	0.023131	0.056646	0.422223	0.999497	0.281232	0.999623
ATP2A2	488 A_24_P7	-2.67	0.023137	0.056646	0.914603	0.999497	0.625231	0.999623
ICK	22858 A_23_P3	-1.33	0.022649	0.056646	0.40055	0.999497	0.663226	0.999623
ELMO1	9844 A_23_P1	1.22	0.02263	0.056646	0.408629	0.999497	0.935388	0.999623
CLPTM1L	81037 A_32_P1	1.84	0.023171	0.056646	0.856714	0.999497	0.241929	0.999623
GLRX2	51022 A_23_P1	-1.33	0.023121	0.056646	0.904378	0.999497	0.293382	0.999623
RUNX3	864 A_23_P5	-1.2	0.022822	0.056646	0.742994	0.999497	0.58824	0.999623
VCP	7415 A_23_P8	1.46	0.022818	0.056646	0.736891	0.999497	0.715977	0.999623

TABLE S7-continued

Significant differences between CR and CNR								
		Fold-change CNR vs	Cytokine response		Age: 60-65 yo vs 74+ yo		Gender	
			CR	p-value	q-value	p-value	q-value	p-value
LOC645166	645166 A_32_P2	1.25	0.022817	0.056646	0.15421	0.999497	0.685198	0.999623
PRKCDDBP	112464 A_23_P2	2.92	0.022754	0.056646	0.405562	0.999497	0.190765	0.999623
RAC2	5880 A_23_P2	1.39	0.023173	0.056646	0.440046	0.999497	0.937421	0.999623
ILF2	3608 A_23_P2	1.8	0.022875	0.056646	0.556435	0.999497	0.867959	0.999623
DBN1	1627 A_24_P5	1.81	0.022907	0.056646	0.889694	0.999497	0.669193	0.999623
NFKBIL2	4796 A_23_P2	1.58	0.022988	0.056646	0.858402	0.999497	0.269339	0.999623
NFE2L1	4779 A_23_P7	1.54	0.023301	0.056759	0.855912	0.999497	0.650591	0.999623
PCDH1	5097 A_23_P2	1.53	0.023351	0.056759	0.751946	0.999497	0.205484	0.999623
CEACAM7	1087 A_24_P2	1.35	0.023344	0.056759	0.21966	0.999497	0.269926	0.999623
TAF8	129685 A_23_P1	1.31	0.023253	0.056759	0.835292	0.999497	0.422309	0.999623
FASTK	10922 A_23_P2	1.73	0.023404	0.056806	0.863451	0.999497	0.740462	0.999623
STAT5A	6776 A_24_P1	1.83	0.023464	0.056872	0.602291	0.999497	0.704537	0.999623
PPM1D	8493 A_32_P1	1.13	0.023563	0.056876	0.662459	0.999497	0.92021	0.999623
TLN2	83660 A_24_P3	1.29	0.023582	0.056876	0.134377	0.999497	0.241966	0.999623
APOA4	337 A_23_P8	1.47	0.023597	0.056876	0.826018	0.999497	0.23829	0.999623
IGF2	3481 A_23_P4	1.9	0.023596	0.056876	0.367862	0.999497	0.560618	0.999623
EDA	1896 A_23_P3	1.39	0.023641	0.056901	0.810786	0.999497	0.664527	0.999623
TNFRSF25	8718 A_23_P1	1.41	0.023674	0.056902	0.440383	0.999497	0.327934	0.999623
TPT1	7178 A_24_P3	-2.01	0.024225	0.057014	0.989532	0.999497	0.763209	0.999623
EXOC6	54536 A_23_P1	1.27	0.02423	0.057014	0.090174	0.999497	0.834501	0.999623
TAX1BP3	30851 A_23_P3	1.74	0.023911	0.057014	0.632985	0.999497	0.689932	0.999623
SHISA5	51246 A_23_P2	-1.36	0.023864	0.057014	0.666164	0.999497	0.623782	0.999623
NME2	4831 A_23_P1	-1.65	0.02417	0.057014	0.575399	0.999497	0.259454	0.999623
PPIL2	23759 A_24_P3	-2.02	0.024157	0.057014	0.666113	0.999497	0.369511	0.999623
IGJ	3512 A_23_P1	-1.38	0.023992	0.057014	0.537089	0.999497	0.514473	0.999623
FCHO2	115548 A_23_P3	-1.6	0.023998	0.057014	0.696781	0.999497	0.197378	0.999623
CAPN10	11132 A_23_P3	-5.87	0.023902	0.057014	0.397217	0.999497	0.886854	0.999623
NHEJ1	79840 A_24_P3	-1.68	0.023847	0.057014	0.69479	0.999497	0.90056	0.999623
GREM2	64388 A_23_P5	-1.48	0.023944	0.057014	0.858879	0.999497	0.551297	0.999623
PML	5371 A_23_P3	1.74	0.024224	0.057014	0.994814	0.999497	0.683126	0.999623
CTSK	1513 A_23_P3	1.42	0.024268	0.057014	0.731985	0.999497	0.504504	0.999623
PPIL2	23759 A_24_P2	1.85	0.024349	0.057014	0.814733	0.999497	0.900514	0.999623
IFT122	55764 A_23_P2	1.45	0.024348	0.057014	0.738776	0.999497	0.848825	0.999623
MAEA	10296 A_23_P1	-1.52	0.024173	0.057014	0.791352	0.999497	0.275621	0.999623
DLL3	10683 A_24_P3	1.48	0.023761	0.057014	0.317412	0.999497	0.865777	0.999623
CTNNA1	1495 A_24_P8	1.68	0.024278	0.057014	0.961889	0.999497	0.590684	0.999623
XRCC1	7515 A_23_P1	1.72	0.024315	0.057014	0.415487	0.999497	0.941061	0.999623
BAT5	7920 A_23_P1	1.79	0.024507	0.057306	0.406512	0.999497	0.268181	0.999623
GSR	2936 A_23_P1	1.43	0.024587	0.057414	0.447782	0.999497	0.402011	0.999623
CSNK2B	1460 A_24_P5	1.41	0.024627	0.05743	0.872929	0.999497	0.423811	0.999623
ILIRN	3557 A_23_P2	1.26	0.024757	0.057565	0.325441	0.999497	0.662672	0.999623
ELMO2	63916 A_24_P3	2.07	0.024782	0.057565	0.608839	0.999497	0.153068	0.999623
XRCC6	2547 A_32_P2	1.2	0.024785	0.057565	0.653775	0.999497	0.046736	0.999623
TP63	8626 A_23_P3	1.31	0.024828	0.057588	0.359601	0.999497	0.427082	0.999623
UACA	55075 A_23_P3	-2.36	0.024868	0.057601	0.96785	0.999497	0.599824	0.999623
CD1B	910 A_23_P3	1.25	0.024905	0.05761	0.838072	0.999497	0.64236	0.999623
TIRAP	114609 A_23_P2	1.45	0.024995	0.057741	0.623572	0.999497	0.353426	0.999623
C8A	731 A_23_P4	1.39	0.025118	0.057856	0.338603	0.999497	0.088464	0.999623
IFI27L1	122509 A_23_P5	1.55	0.025112	0.057856	0.915004	0.999497	0.643707	0.999623
CDKN1B	1027 A_23_P2	1.57	0.025145	0.057856	0.311175	0.999497	0.756093	0.999623
APOA4	337 A_24_P2	-1.41	0.025181	0.057862	0.53623	0.999497	0.197791	0.999623
FKBP1	63943 A_23_P7	1.53	0.025326	0.057892	0.560314	0.999497	0.128645	0.999623
SERPINB9	5272 A_24_P2	-1.65	0.025329	0.057892	0.568829	0.999497	0.58219	0.999623
COL6A2	1292 A_32_P2	1.46	0.025261	0.057892	0.872014	0.999497	0.418784	0.999623
TSLP	85480 A_23_P1	1.23	0.02532	0.057892	0.147663	0.999497	0.78859	0.999623
KRAS	3845 A_23_P3	-1.81	0.025434	0.057925	0.350719	0.999497	0.395689	0.999623
APAF1	317 A_23_P3	-1.98	0.025489	0.057925	0.284157	0.999497	0.889888	0.999623
VSIG2	23584 A_23_P3	-1.31	0.025512	0.057925	0.857542	0.999497	0.311081	0.999623
COL13A1	1305 A_24_P5	-1.33	0.0255	0.057925	0.451096	0.999497	0.824942	0.999623
TPD52	7163 A_23_P2	-1.85	0.025495	0.057925	0.84194	0.999497	0.600095	0.999623
GHSR	2693 A_23_P1	-1.83	0.025652	0.058091	0.655901	0.999497	0.755184	0.999623
COL15A1	1306 A_23_P1	-1.52	0.02565	0.058091	0.381867	0.999497	0.461919	0.999623
GNA13	10672 A_24_P3	-2.38	0.025698	0.058119	0.708494	0.999497	0.176524	0.999623
PRKCB	5579 A_23_P4	-1.39	0.02578	0.058161	0.19234	0.999497	0.531901	0.999623
DCTN3	11258 A_24_P3	1.59	0.025784	0.058161	0.526632	0.999497	0.357129	0.999623
CKAP2	26586 A_23_P1	-1.36	0.025879	0.058196	0.603597	0.999497	0.885128	0.999623
ULBP2	80328 A_23_P1	1.47	0.025877	0.058196	0.716694	0.999497	0.949984	0.999623
PAFAH1B3	5050 A_23_P1	1.33	0.025901	0.058196	0.765951	0.999497	0.813546	0.999623

TABLE S7-continued

Significant differences between CR and CNR								
		Fold-change CNR vs	Cytokine response		Age: 60-65 yo vs 74+ yo		Gender	
			CR	p-value	q-value	p-value	q-value	p-value
CD248	57124_A_23_P5	1.52	0.025939	0.058205	0.740171	0.999497	0.263471	0.999623
ATP2A2	488_A_23_P5	1.45	0.025984	0.058231	0.855788	0.999497	0.825546	0.999623
CFLAR	8837_A_23_P2	-1.4	0.026045	0.058288	0.395349	0.999497	0.96893	0.999623
PSMF1	9491_A_23_P7	-1.34	0.026111	0.058288	0.349748	0.999497	0.867932	0.999623
FBLIM1	54751_A_23_P2	1.37	0.026085	0.058288	0.122642	0.999497	0.2457	0.999623
TUSC4	10641_A_23_P1	1.48	0.026168	0.058339	0.40297	0.999497	0.075194	0.999623
SART3	9733_A_23_P8	1.57	0.026244	0.058434	0.933546	0.999497	0.69472	0.999623
ITFG2	55846_A_23_P2	1.99	0.026393	0.058689	0.727136	0.999497	0.651347	0.999623
CSF2RB	1439_A_23_P1	1.47	0.026635	0.059	0.786508	0.999497	0.977127	0.999623
ADAM22	53616_A_24_P2	1.25	0.026632	0.059	0.431297	0.999497	0.690916	0.999623
RACGAP1	29127_A_23_P6	-1.86	0.026629	0.059	0.398668	0.999497	0.839477	0.999623
RRAGC	64121_A_23_P5	-1.71	0.026678	0.059018	0.188304	0.999497	0.043924	0.999623
ZFR2	23217_A_23_P2	1.38	0.026762	0.059052	0.222351	0.999497	0.435681	0.999623
BCL7A	605_A_32_P7	1.51	0.026748	0.059052	0.75426	0.999497	0.516311	0.999623
SNPH	9751_A_23_P1	1.43	0.027005	0.059512	0.744087	0.999497	0.358138	0.999623
EXOC2	55770_A_23_P2	1.16	0.027117	0.059532	0.182019	0.999497	0.422793	0.999623
FANCG	2189_A_23_P7	1.63	0.027117	0.059532	0.67724	0.999497	0.863808	0.999623
LTPB2	4053_A_24_P1	1.62	0.027107	0.059532	0.918361	0.999497	0.34478	0.999623
VEZF1	7716_A_24_P5	-3.39	0.027161	0.059551	0.2347	0.999497	0.459209	0.999623
BCAP31	10134_A_32_P6	1.3	0.0272	0.059561	0.828339	0.999497	0.814044	0.999623
TYK2	7297_A_23_P1	1.61	0.02731	0.059651	0.718789	0.999497	0.305446	0.999623
DNAJB6	10049_A_24_P6	-2.94	0.027306	0.059651	0.768725	0.999497	0.601868	0.999623
PRSS2	5645_A_32_P5	1.48	0.027445	0.059718	0.254523	0.999497	0.123377	0.999623
ATP2A1	487_A_23_P7	1.33	0.027434	0.059718	0.390992	0.999497	0.439009	0.999623
BBS7	55212_A_23_P2	1.26	0.027395	0.059718	0.679015	0.999497	0.781101	0.999623
KLRC2	3822_A_23_P2	-1.96	0.027513	0.05979	0.523282	0.999497	0.263981	0.999623
VPS45	11311_A_23_P2	1.57	0.027561	0.059821	0.486518	0.999497	0.948904	0.999623
PLDN	26258_A_23_P2	-2.14	0.027632	0.059822	0.271162	0.999497	0.807566	0.999623
MLL2	8085_A_24_P2	-1.5	0.027605	0.059822	0.925297	0.999497	0.438707	0.999623
UTP11L	51118_A_23_P1	-1.65	0.027951	0.060438	0.712349	0.999497	0.341129	0.999623
WDR92	116143_A_32_P1	1.35	0.028014	0.060499	0.959143	0.999497	0.631753	0.999623
LY6E	4061_A_24_P3	1.67	0.028104	0.06054	0.639579	0.999497	0.801153	0.999623
SPG7	6687_A_24_P2	1.32	0.028103	0.06054	0.815515	0.999497	0.187053	0.999623
SBDS	51119_A_23_P1	-1.81	0.028224	0.060572	0.637322	0.999497	0.855503	0.999623
PTX3	5806_A_23_P1	-1.54	0.028185	0.060572	0.545358	0.999497	0.666942	0.999623
ACVRL1	94_A_24_P5	1.28	0.028223	0.060572	0.399627	0.999497	0.675879	0.999623
MLL3	58508_A_32_P2	1.26	0.028549	0.060651	0.55675	0.999497	0.778025	0.999623
CCR10	2826_A_23_P1	1.65	0.028465	0.060651	0.753723	0.999497	0.189758	0.999623
PTPN12	5782_A_23_P8	-1.71	0.028409	0.060651	0.672264	0.999497	0.445015	0.999623
POSTN	10631_A_24_P2	-1.6	0.028613	0.060651	0.648284	0.999497	0.020574	0.999623
GPR126	57211_A_23_P2	1.13	0.028563	0.060651	0.132732	0.999497	0.306654	0.999623
SEMA3B	7869_A_24_P2	1.65	0.028588	0.060651	0.551926	0.999497	0.365382	0.999623
BIRC3	330_A_23_P5	-1.39	0.028389	0.060651	0.273709	0.999497	0.675393	0.999623
CUL5	8065_A_23_P2	-1.59	0.028487	0.060651	0.69055	0.999497	0.612001	0.999623
TOPORS	10210_A_23_P2	-1.36	0.02849	0.060651	0.561509	0.999497	0.941162	0.999623
FAF1	11124_A_23_P5	1.17	0.028357	0.060651	0.814361	0.999497	0.964896	0.999623
MLF2	8079_A_23_P1	1.35	0.028813	0.060753	0.542433	0.999497	0.705194	0.999623
IGSF1	3547_A_23_P1	1.47	0.028819	0.060753	0.842061	0.999497	0.602729	0.999623
SCARB1	949_A_23_P2	1.36	0.028837	0.060753	0.945806	0.999497	0.666927	0.999623
KLF10	7071_A_23_P1	-2.07	0.02879	0.060753	0.957562	0.999497	0.434456	0.999623
CBR1	873_A_23_P2	-1.65	0.028769	0.060753	0.302828	0.999497	0.13344	0.999623
RAB5C	5878_A_23_P1	1.36	0.028886	0.060781	0.398687	0.999497	0.499714	0.999623
TNFRSF13B	23495_A_23_P8	1.5	0.028959	0.060839	0.468352	0.999497	0.202085	0.999623
PTGS1	5742_A_23_P2	1.59	0.028984	0.060839	0.850501	0.999497	0.911628	0.999623
RHCE	6006_A_23_P6	-1.28	0.029031	0.060864	0.372412	0.999497	0.659916	0.999623
BBC3	27113_A_24_P2	1.42	0.02926	0.061195	0.922857	0.999497	0.755122	0.999623
TXLNA	200081_A_32_P8	1.48	0.029249	0.061195	0.719249	0.999497	0.62894	0.999623
FEZ1	9638_A_23_P2	1.3	0.029481	0.061583	0.302527	0.999497	0.741929	0.999623
IL27RA	9466_A_23_P2	1.47	0.029555	0.061663	0.096732	0.999497	0.219257	0.999623
PCDHB5	26167_A_23_P6	-1.28	0.029601	0.061683	0.519939	0.999497	0.243401	0.999623
MLLT4	4301_A_23_P2	1.36	0.029685	0.061784	0.292715	0.999497	0.339077	0.999623
HSPD1	3329_A_32_P7	-3.09	0.029737	0.061817	0.515284	0.999497	0.494684	0.999623
MRC2	9902_A_23_P4	1.82	0.029815	0.061906	0.428232	0.999497	0.834295	0.999623
PPP2R1A	5518_A_23_P1	1.52	0.029953	0.062117	0.912085	0.999497	0.216815	0.999623
TCF3	6929_A_23_P6	1.55	0.030032	0.062206	0.51389	0.999497	0.401865	0.999623
MAPK8	5599_A_23_P3	1.45	0.030224	0.062529	0.869519	0.999497	0.374373	0.999623
SYTL1	84958_A_32_P2	1.58	0.030264	0.062537	0.999751	0.999957	0.236159	0.999623
TNFRSF1A	7132_A_23_P1	-2.64	0.030305	0.062546	0.650778	0.999497	0.384675	0.999623

TABLE S7-continued

Significant differences between CR and CNR								
		Fold-change CNR vs	Cytokine response		Age: 60-65 yo vs 74+ yo		Gender	
			CR	p-value	q-value	p-value	q-value	p-value
TLR9	54106_A_23_P1	1.57	0.030412	0.06261	0.804853	0.999497	0.838006	0.999623
LAMC2	3918_A_23_P2	1.28	0.030445	0.06261	0.947975	0.999497	0.332588	0.999623
ERC1	23085_A_24_P2	1.23	0.030398	0.06261	0.486291	0.999497	0.561453	0.999623
PRKCA	5578_A_23_P2	1.41	0.030626	0.062682	0.763036	0.999497	0.313272	0.999623
MSH3	4437_A_23_P1	-1.28	0.030547	0.062682	0.245368	0.999497	0.945702	0.999623
5-Sep	5413_A_24_P2	1.55	0.030596	0.062682	0.715949	0.999497	0.459014	0.999623
NDUFA13	51079_A_23_P1	1.6	0.030558	0.062682	0.782875	0.999497	0.274226	0.999623
CYFIP2	26999_A_23_P1	1.66	0.030695	0.06275	0.368667	0.999497	0.634073	0.999623
BID	637_A_23_P1	1.85	0.030794	0.062877	0.661313	0.999497	0.84687	0.999623
PARVA	55742_A_23_P2	1.25	0.030877	0.062897	0.959506	0.999497	0.920002	0.999623
MAGED1	9500_A_24_P2	1.29	0.030857	0.062897	0.369865	0.999497	0.287833	0.999623
RAB18	22931_A_23_P1	1.19	0.031017	0.063095	0.577327	0.999497	0.285604	0.999623
CDKN1A	1026_A_24_P2	1.49	0.031197	0.063095	0.788278	0.999497	0.200461	0.999623
CEBPA	1050_A_24_P2	1.5	0.031126	0.063095	0.306921	0.999497	0.188434	0.999623
ADAM33	80332_A_23_P2	1.55	0.031097	0.063095	0.485134	0.999497	0.592091	0.999623
MYBPC3	4607_A_23_P1	-2.51	0.03123	0.063095	0.456002	0.999497	0.385035	0.999623
CCL4	6351_A_23_P2	-2.79	0.031197	0.063095	0.360911	0.999497	0.22704	0.999623
IL21R	50615_A_24_P2	1.39	0.031176	0.063095	0.765221	0.999497	0.826481	0.999623
CYBA	1535_A_23_P1	1.48	0.031498	0.063104	0.820061	0.999497	0.40144	0.999623
CHRN2	1141_A_23_P2	1.49	0.031385	0.063104	0.585591	0.999497	0.645168	0.999623
TNNC2	7125_A_23_P1	1.45	0.031527	0.063104	0.945366	0.999497	0.610019	0.999623
TFPT	29844_A_23_P2	1.53	0.03146	0.063104	0.883172	0.999497	0.350379	0.999623
EHD2	30846_A_24_P1	1.5	0.031355	0.063104	0.993684	0.999497	0.734683	0.999623
CDH18	1016_A_23_P2	1.29	0.031368	0.063104	0.828265	0.999497	0.679675	0.999623
LTBP3	4054_A_24_P2	1.53	0.031475	0.063104	0.902998	0.999497	0.95695	0.999623
CD63	967_A_23_P1	1.5	0.031524	0.063104	0.441376	0.999497	0.107585	0.999623
EIF5A	1984_A_24_P2	1.55	0.031679	0.063261	0.263799	0.999497	0.594688	0.999623
AEBP1	165_A_23_P1	1.46	0.031645	0.063261	0.442664	0.999497	0.395607	0.999623
LENG1	79165_A_23_P2	1.47	0.031818	0.063414	0.646664	0.999497	0.933681	0.999623
SIRT6	51548_A_23_P2	1.34	0.031903	0.063414	0.522245	0.999497	0.421646	0.999623
API51	1174_A_24_P2	1.3	0.031872	0.063414	0.711261	0.999497	0.504707	0.999623
TIMP2	7077_A_23_P1	1.54	0.031872	0.063414	0.882487	0.999497	0.207987	0.999623
GULP1	51454_A_23_P2	-1.93	0.031986	0.063433	0.689299	0.999497	0.543041	0.999623
DAPK1	1612_A_23_P2	1.29	0.031953	0.063433	0.505182	0.999497	0.564311	0.999623
SFRS17A	8227_A_23_P2	1.25	0.032068	0.063445	0.082378	0.999497	0.492234	0.999623
PRKAR2B	5577_A_23_P4	-2.2	0.032103	0.063445	0.7629	0.999497	0.300333	0.999623
PSMA1	5682_A_23_P1	-1.37	0.032058	0.063445	0.299438	0.999497	0.527897	0.999623
LEPR	3953_A_24_P2	-1.96	0.032218	0.063527	0.785813	0.999497	0.410247	0.999623
MYBPC2	4606_A_23_P1	1.43	0.032212	0.063527	0.949079	0.999497	0.137534	0.999623
NPM1	4869_A_32_P4	-1.94	0.032263	0.063534	0.902419	0.999497	0.467736	0.999623
CCND3	896_A_23_P1	1.52	0.032295	0.063534	0.878017	0.999497	0.72382	0.999623
THOC5	8563_A_23_P1	1.29	0.032341	0.063551	0.962271	0.999497	0.941392	0.999623
ALDH1A3	220_A_23_P1	-1.32	0.032482	0.063565	0.750488	0.999497	0.270208	0.999623
PKD1	5310_A_23_P7	1.83	0.032532	0.063565	0.408551	0.999497	0.973099	0.999623
MAF	4094_A_32_P2	1.62	0.032459	0.063565	0.794258	0.999497	0.936076	0.999623
VCP	7415_A_24_P2	1.22	0.032519	0.063565	0.346933	0.999497	0.608681	0.999623
FCRLB	127943_A_23_P3	1.73	0.032444	0.063565	0.429888	0.999497	0.416771	0.999623
CTSB	1508_A_23_P2	-1.47	0.032578	0.063581	0.488009	0.999497	0.977433	0.999623
FGB	2244_A_24_P2	1.4	0.03266	0.06367	0.497199	0.999497	0.559463	0.999623
CTSC	1075_A_24_P1	-1.61	0.033185	0.063796	0.995805	0.999497	0.615207	0.999623
BBS9	27241_A_23_P2	1.19	0.033317	0.063796	0.31653	0.999497	0.913647	0.999623
ARHGDI1	396_A_24_P1	1.51	0.033156	0.063796	0.840647	0.999497	0.773433	0.999623
FGFR3	2261_A_23_P2	1.59	0.033108	0.063796	0.881589	0.999497	0.496839	0.999623
TNFRSF21	27242_A_23_P2	1.46	0.032849	0.063796	0.278269	0.999497	0.846903	0.999623
HCFC1R1	54985_A_23_P1	1.54	0.033024	0.063796	0.748762	0.999497	0.205968	0.999623
VEGFA	7422_A_24_P1	1.71	0.032983	0.063796	0.944173	0.999497	0.703621	0.999623
HBP1	26959_A_24_P2	-1.59	0.033215	0.063796	0.798522	0.999497	0.245275	0.999623
BBS2	583_A_23_P1	1.23	0.033285	0.063796	0.1723	0.999497	0.261281	0.999623
PTGFR	5737_A_24_P3	1.25	0.033071	0.063796	0.619445	0.999497	0.938937	0.999623
NGFR	4804_A_23_P3	1.44	0.033202	0.063796	0.810191	0.999497	0.472641	0.999623
FBLIM1	54751_A_24_P2	1.48	0.032872	0.063796	0.768085	0.999497	0.76898	0.999623
ADAMTS1	11173_A_23_P1	1.33	0.033246	0.063796	0.514772	0.999497	0.250831	0.999623
SIVA1	10572_A_24_P1	1.43	0.033253	0.063796	0.825935	0.999497	0.482239	0.999623
FCGR3B	2215_A_23_P1	-3.65	0.032777	0.063796	0.504655	0.999497	0.63578	0.999623
XPA	7507_A_23_P2	1.31	0.033168	0.063796	0.973303	0.999497	0.318812	0.999623
TAPBP	6892_A_23_P3	1.35	0.033357	0.063801	0.617357	0.999497	0.52104	0.999623
COL18A1	80781_A_24_P2	2.23	0.033707	0.064009	0.369159	0.999497	0.785081	0.999623
COL20A1	57642_A_32_P1	1.32	0.03358	0.064009	0.483373	0.999497	0.239762	0.999623

TABLE S7-continued

Significant differences between CR and CNR								
		Fold-change CNR vs	Cytokine response		Age: 60-65 yo vs 74+ yo		Gender	
			CR	p-value	q-value	p-value	q-value	p-value
RNF34	80196_A_32_P7	-1.41	0.033591	0.064009	0.916876	0.999497	0.090264	0.999623
C9orf127	51754_A_23_P2	-1.35	0.033696	0.064009	0.301834	0.999497	0.387275	0.999623
TXLNA	200081_A_23_P5	1.51	0.033687	0.064009	0.919058	0.999497	0.794959	0.999623
MALL	7851_A_24_P8	1.45	0.033716	0.064009	0.838832	0.999497	0.614491	0.999623
TBXAS1	6916_A_32_P2	1.29	0.033725	0.064009	0.476815	0.999497	0.497037	0.999623
NFATC1	4772_A_24_P2	2.31	0.033788	0.064058	0.484876	0.999497	0.188787	0.999623
TERT	7015_A_23_P1	2.15	0.033887	0.064123	0.904127	0.999497	0.891923	0.999623
ZFYVE16	9765_A_24_P2	-2.49	0.033909	0.064123	0.562591	0.999497	0.318679	0.999623
FUT3	2525_A_23_P3	1.53	0.033934	0.064123	0.875302	0.999497	0.621745	0.999623
HAPLN4	404037_A_23_P4	1.37	0.033975	0.06413	0.492467	0.999497	0.118386	0.999623
VAV1	7409_A_23_P3	1.61	0.034064	0.064213	0.380843	0.999497	0.861607	0.999623
HRK	8739_A_23_P2	1.36	0.034093	0.064213	0.54629	0.999497	0.493787	0.999623
IFI27L2	83982_A_23_P1	1.53	0.034226	0.064345	0.542263	0.999497	0.208311	0.999623
TOM1	10043_A_23_P1	1.49	0.034294	0.064345	0.422176	0.999497	0.643378	0.999623
SLPI	6590_A_24_P1	1.44	0.034284	0.064345	0.255446	0.999497	0.596129	0.999623
FKBP1A	2280_A_23_P1	1.65	0.034313	0.064345	0.355904	0.999497	0.748701	0.999623
TERF1	7013_A_32_P2	-1.78	0.034374	0.064348	0.606755	0.999497	0.565852	0.999623
IRF7	3665_A_24_P3	1.33	0.034412	0.064348	0.398343	0.999497	0.717063	0.999623
C2	717_A_32_P1	1.31	0.034427	0.064348	0.742981	0.999497	0.353564	0.999623
RRAD	6236_A_24_P2	1.41	0.03452	0.064453	0.301818	0.999497	0.626374	0.999623
ICOSLG	23308_A_23_P1	-1.56	0.034668	0.064659	0.789295	0.999497	0.107452	0.999623
EEF2	1938_A_24_P8	1.45	0.034707	0.064661	0.296008	0.999497	0.285848	0.999623
CHRNA7	1139_A_23_P1	1.55	0.034872	0.064724	0.58819	0.999497	0.408751	0.999623
SCD5	79966_A_23_P2	1.45	0.034902	0.064724	0.6819	0.999497	0.314801	0.999623
ATHL1	80162_A_23_P5	1.47	0.034966	0.064724	0.318446	0.999497	0.427014	0.999623
GCLM	2730_A_23_P1	-1.49	0.034959	0.064724	0.924876	0.999497	0.331781	0.999623
MLLT6	4302_A_32_P5	1.29	0.034953	0.064724	0.825453	0.999497	0.568063	0.999623
WWTR1	25937_A_32_P1	1.36	0.034797	0.064724	0.323648	0.999497	0.863363	0.999623
PRDX1	5052_A_23_P1	1.34	0.035081	0.064868	0.231794	0.999497	0.6463	0.999623
PXN	5829_A_23_P4	1.56	0.035123	0.064876	0.842538	0.999497	0.30583	0.999623
PRKCSH	5589_A_24_P3	1.79	0.035235	0.065012	0.531771	0.999497	0.921556	0.999623
BCLAF1	9774_A_24_P8	-1.8	0.035453	0.065255	0.846611	0.999497	0.829268	0.999623
TNFAIP8L1	126282_A_23_P4	1.56	0.035448	0.065255	0.483639	0.999497	0.701125	0.999623
BAT2L	84726_A_24_P5	1.5	0.03548	0.065255	0.301971	0.999497	0.432894	0.999623
RTKN	6242_A_23_P1	1.46	0.035523	0.065265	0.457554	0.999497	0.302307	0.999623
CTNND1	1500_A_23_P2	-1.41	0.03565	0.065286	0.7144	0.999497	0.245176	0.999623
MYST3	7994_A_23_P4	1.22	0.035735	0.065286	0.59063	0.999497	0.520196	0.999623
MLL	4297_A_24_P5	1.74	0.035679	0.065286	0.678586	0.999497	0.972241	0.999623
CSRNP1	64651_A_23_P1	1.27	0.035762	0.065286	0.224143	0.999497	0.960358	0.999623
LY6K	54742_A_32_P2	1.24	0.035583	0.065286	0.750624	0.999497	0.45165	0.999623
PLDN	26258_A_23_P2	1.21	0.035698	0.065286	0.259189	0.999497	0.033897	0.999623
IGBP1	3476_A_23_P1	-1.68	0.035812	0.065308	0.628936	0.999497	0.43381	0.999623
CLDN1	9076_A_24_P1	1.28	0.035893	0.065323	0.672177	0.999497	0.017062	0.999623
LY86	9450_A_23_P7	1.27	0.035896	0.065323	0.634683	0.999497	0.73318	0.999623
SEMA3B	7869_A_23_P1	1.19	0.035945	0.065344	0.237064	0.999497	0.408716	0.999623
IGF2BP1	10642_A_23_P8	1.4	0.036054	0.065472	0.208519	0.999497	0.335448	0.999623
FANCI	55215_A_23_P3	-2.62	0.036106	0.065499	0.475677	0.999497	0.588487	0.999623
GRN	2896_A_23_P4	1.49	0.036236	0.065559	0.410007	0.999497	0.210933	0.999623
SMOC1	64093_A_24_P1	1.54	0.036368	0.065559	0.751552	0.999497	0.588362	0.999623
CBARA1	10367_A_23_P4	-1.24	0.036358	0.065559	0.275835	0.999497	0.97784	0.999623
BGLAP	632_A_23_P1	1.54	0.036338	0.065559	0.658997	0.999497	0.331015	0.999623
AP1S2	8905_A_24_P1	-1.44	0.036294	0.065559	0.09235	0.999497	0.358259	0.999623
UACA	55075_A_24_P2	1.47	0.03622	0.065559	0.31198	0.999497	0.39171	0.999623
AATK	9625_A_23_P1	1.31	0.036427	0.065597	0.473991	0.999497	0.956776	0.999623
MAP3K5	4217_A_23_P1	-2.36	0.036467	0.065601	0.494233	0.999497	0.366173	0.999623
CD5	921_A_24_P3	1.3	0.036675	0.065905	0.814369	0.999497	0.292644	0.999623
PTK2B	2185_A_23_P1	2.03	0.037067	0.06621	0.339483	0.999497	0.265766	0.999623
SRC	6714_A_23_P3	1.35	0.037344	0.06621	0.627243	0.999497	0.955467	0.999623
IMPDH1	3614_A_24_P8	1.59	0.037174	0.06621	0.659222	0.999497	0.612172	0.999623
LIMS1	3987_A_23_P2	-1.55	0.037261	0.06621	0.629349	0.999497	0.549508	0.999623
CD4	920_A_24_P2	-2.75	0.037125	0.06621	0.966905	0.999497	0.286739	0.999623
FRAP1	2475_A_23_P3	1.46	0.037277	0.06621	0.809112	0.999497	0.566189	0.999623
HSPA1A	3303_A_24_P1	1.59	0.036909	0.06621	0.887857	0.999497	0.415038	0.999623
PRDX2	7001_A_32_P2	1.84	0.03694	0.06621	0.555601	0.999497	0.861216	0.999623
VAMP3	9341_A_23_P5	1.36	0.037161	0.06621	0.864031	0.999497	0.65595	0.999623
TOP2B	7155_A_23_P1	-1.33	0.037062	0.06621	0.941946	0.999497	0.51165	0.999623
ERCC1	2067_A_23_P1	1.35	0.037233	0.06621	0.873782	0.999497	0.66258	0.999623
PHB	5245_A_24_P2	1.17	0.037113	0.06621	0.633978	0.999497	0.067449	0.999623

TABLE S7-continued

Significant differences between CR and CNR								
		Fold-change CNR vs	Cytokine response		Age: 60-65 yo vs 74+ yo		Gender	
			p-value	q-value	p-value	q-value	p-value	q-value
YWHAZ	7534 A_32_P2	-1.43	0.037331	0.06621	0.607754	0.999497	0.720726	0.999623
UBE2N	7334 A_32_P1	-1.28	0.03743	0.066295	0.543764	0.999497	0.42914	0.999623
C8orf4	56892 A_23_P2	-1.86	0.037619	0.066561	0.725317	0.999497	0.615774	0.999623
CD97	976 A_23_P5	1.5	0.037696	0.066629	0.966568	0.999497	0.409637	0.999623
CBLB	868 A_23_P2	1.23	0.037782	0.066677	0.200474	0.999497	0.518392	0.999623
GP1BB	2812 A_23_P2	2.12	0.037967	0.066677	0.49344	0.999497	0.479874	0.999623
WWTR1	25937 A_24_P5	-1.68	0.037822	0.066677	0.866945	0.999497	0.547464	0.999623
DNASE1L3	1776 A_23_P2	1.14	0.038125	0.066677	0.317968	0.999497	0.493312	0.999623
PPP1R13B	23368 A_23_P2	1.44	0.038021	0.066677	0.546261	0.999497	0.8945	0.999623
EBI3	10148 A_23_P1	1.14	0.037841	0.066677	0.730837	0.999497	0.16421	0.999623
CEBPB	1051 A_23_P1	1.43	0.038082	0.066677	0.414807	0.999497	0.430171	0.999623
OSCAR	126014 A_23_P5	1.3	0.038096	0.066677	0.501881	0.999497	0.970502	0.999623
SGPL1	8879 A_23_P2	1.32	0.038128	0.066677	0.569951	0.999497	0.507742	0.999623
ADAM12	8038 A_23_P2	1.34	0.037935	0.066677	0.050751	0.999497	0.627833	0.999623
PDZD2	23037 A_23_P7	1.44	0.038149	0.066677	0.26995	0.999497	0.301539	0.999623
TEK	7010 A_23_P2	1.48	0.038188	0.066678	0.218137	0.999497	0.415731	0.999623
FLVCR1	28982 A_23_P1	1.33	0.038289	0.066786	0.676007	0.999497	0.815572	0.999623
PSMA3	5684 A_23_P1	-1.33	0.038396	0.066838	0.429774	0.999497	0.404923	0.999623
CSF1	1435 A_23_P4	1.19	0.038392	0.066838	0.262292	0.999497	0.194732	0.999623
CD68	968 A_23_P1	1.64	0.038438	0.066843	0.186404	0.999497	0.619938	0.999623
PCDHB7	56129 A_24_P2	1.19	0.038495	0.066853	0.903951	0.999497	0.426421	0.999623
JAG1	182 A_23_P2	-1.4	0.038521	0.066853	0.379778	0.999497	0.349641	0.999623
ELF1	1997 A_24_P7	-2.17	0.038608	0.066868	0.648052	0.999497	0.404488	0.999623
COL18A1	80781 A_23_P2	1.37	0.038572	0.066868	0.316143	0.999497	0.97801	0.999623
MSRA	4482 A_23_P2	1.27	0.038699	0.066894	0.889898	0.999497	0.940286	0.999623
FGFR1	2260 A_23_P3	1.46	0.0387	0.066894	0.912491	0.999497	0.213834	0.999623
IGF2BP2	10644 A_23_P2	1.25	0.039017	0.067051	0.205824	0.999497	0.856667	0.999623
FERMT2	10979 A_23_P2	-1.47	0.039058	0.067051	0.449805	0.999497	0.327004	0.999623
METTL1	4234 A_23_P4	1.45	0.038859	0.067051	0.816033	0.999497	0.583595	0.999623
PECR	55825 A_23_P5	1.51	0.038948	0.067051	0.884259	0.999497	0.820681	0.999623
CCRL2	9034 A_23_P2	1.28	0.039102	0.067051	0.734989	0.999497	0.392005	0.999623
ISG20	3669 A_23_P3	1.46	0.03902	0.067051	0.330731	0.999497	0.806808	0.999623
VEGFB	7423 A_24_P5	1.68	0.039039	0.067051	0.796219	0.999497	0.472839	0.999623
SMOC2	64094 A_23_P2	1.22	0.039102	0.067051	0.58029	0.999497	0.428484	0.999623
PRF1	5551 A_23_P1	-2.85	0.039259	0.067197	0.250656	0.999497	0.651678	0.999623
CALR	811 A_23_P2	1.6	0.039265	0.067197	0.331002	0.999497	0.554073	0.999623
SFN	2810 A_23_P2	1.4	0.039388	0.06734	0.756443	0.999497	0.927541	0.999623
RPH3AL	9501 A_23_P5	1.48	0.039521	0.067366	0.35573	0.999497	0.808914	0.999623
AIRE	326 A_23_P2	-1.41	0.039517	0.067366	0.619415	0.999497	0.551874	0.999623
ADORA2A	135 A_24_P2	1.68	0.03951	0.067366	0.570034	0.999497	0.813103	0.999623
MTC1	23787 A_24_P2	1.34	0.039611	0.067394	0.45622	0.999497	0.917992	0.999623
GSG2	83903 A_23_P2	1.35	0.039615	0.067394	0.10052	0.999497	0.844113	0.999623
TM2D1	83941 A_23_P1	-2.07	0.039693	0.06746	0.872628	0.999497	0.986858	0.999623
NFATC2IP	84901 A_23_P1	1.21	0.039962	0.06785	0.31469	0.999497	0.910653	0.999623
IRF3	3661 A_23_P2	1.66	0.040046	0.067925	0.741216	0.999497	0.098662	0.999623
TGFB1	7040 A_24_P7	1.7	0.040109	0.067965	0.797209	0.999497	0.292058	0.999623
EEF1A1	1915 A_32_P4	-1.87	0.040328	0.068109	0.900192	0.999497	0.92053	0.999623
FOXP1	27086 A_24_P2	-1.58	0.040352	0.068109	0.3515	0.999497	0.899575	0.999623
CBLB	868 A_23_P2	-1.33	0.040295	0.068109	0.534774	0.999497	0.943076	0.999623
HLA-DOB	3112 A_23_P3	1.49	0.040279	0.068109	0.300797	0.999497	0.332659	0.999623
BAT4	7918 A_23_P1	1.25	0.040486	0.068269	0.351473	0.999497	0.412532	0.999623
NOSTRIN	115677 A_23_P7	1.48	0.040846	0.068541	0.163568	0.999497	0.198707	0.999623
NPM1	4869 A_24_P8	1.33	0.04083	0.068541	0.441115	0.999497	0.290941	0.999623
PCDHGA8	9708 A_23_P3	1.39	0.040769	0.068541	0.358886	0.999497	0.639883	0.999623
WISP2	8839 A_23_P1	2.1	0.040729	0.068541	0.752003	0.999497	0.762391	0.999623
SIPA1	6494 A_23_P1	1.44	0.040756	0.068541	0.753914	0.999497	0.69068	0.999623
HIVEP2	3097 A_23_P2	1.58	0.040923	0.068604	0.735097	0.999497	0.43867	0.999623
FKBP9	11328 A_23_P2	1.16	0.04097	0.068615	0.739192	0.999497	0.737438	0.999623
BTG1	694 A_32_P2	1.35	0.041055	0.068625	0.89781	0.999497	0.103594	0.999623
MAST1	22983 A_23_P1	1.34	0.041027	0.068625	0.689448	0.999497	0.320766	0.999623
SERPING1	710 A_23_P1	1.48	0.041165	0.068629	0.537946	0.999497	0.585445	0.999623
IRAK1	3654 A_23_P7	1.82	0.041217	0.068629	0.346895	0.999497	0.397119	0.999623
PTGES3	10728 A_24_P2	-1.7	0.041217	0.068629	0.400474	0.999497	0.899976	0.999623
ARHGDLA	396 A_23_P2	1.42	0.041146	0.068629	0.937183	0.999497	0.797306	0.999623
PTCD2	79810 A_24_P1	-2.25	0.041264	0.068641	0.804729	0.999497	0.312599	0.999623
CYTIP	9595 A_23_P5	-1.43	0.041387	0.068658	0.402373	0.999497	0.26584	0.999623
BIRC7	79444 A_23_P7	1.39	0.041362	0.068658	0.826231	0.999497	0.932431	0.999623
CDH4	1002 A_23_P2	1.27	0.041394	0.068658	0.984845	0.999497	0.506975	0.999623

TABLE S7-continued

		Significant differences between CR and CNR						
		Fold-change CNR vs	Cytokine response		Age: 60-65 yo vs 74+ yo		Gender	
			CR	p-value	q-value	p-value	q-value	p-value
RYBP	23429 A_23_P3	1.25	0.041476	0.068729	0.973564	0.999497	0.950795	0.999623
ABCA1	19 A_24_P2	-1.44	0.041522	0.068737	0.994963	0.999497	0.233991	0.999623
TRAF7	84231 A_24_P3	-2.6	0.041571	0.068754	0.998076	0.999497	0.560697	0.999623
DCBLD1	285761 A_23_P4	1.23	0.041836	0.068772	0.305884	0.999497	0.724295	0.999623
PSMC1	5700 A_24_P3	-1.31	0.042055	0.068772	0.799563	0.999497	0.530682	0.999623
NFASC	23114 A_24_P3	1.27	0.041644	0.068772	0.087798	0.999497	0.296733	0.999623
RAD9A	5883 A_24_P2	1.33	0.041975	0.068772	0.962305	0.999497	0.558778	0.999623
TAL2	6887 A_23_P4	1.31	0.042007	0.068772	0.264624	0.999497	0.304782	0.999623
UCP3	7352 A_23_P2	1.51	0.042132	0.068772	0.694175	0.999497	0.234801	0.999623
MAMDC2	256691 A_32_P4	1.38	0.041863	0.068772	0.79643	0.999497	0.633976	0.999623
SDF2	6388 A_23_P1	1.41	0.042031	0.068772	0.399052	0.999497	0.635088	0.999623
CD81	975 A_23_P1	1.56	0.04191	0.068772	0.419469	0.999497	0.762805	0.999623
STK17A	9263 A_24_P3	-1.64	0.042013	0.068772	0.847399	0.999497	0.358757	0.999623
AURKC	6795 A_23_P3	1.4	0.042006	0.068772	0.480049	0.999497	0.54651	0.999623
ITGA7	3679 A_23_P1	1.47	0.041848	0.068772	0.710712	0.999497	0.283288	0.999623
PSMD14	10213 A_23_P1	-1.36	0.042141	0.068772	0.458016	0.999497	0.274646	0.999623
FSCN1	6624 A_23_P1	1.5	0.042083	0.068772	0.689746	0.999497	0.849582	0.999623
MAPK9	5601 A_23_P1	-1.71	0.042221	0.068773	0.745508	0.999497	0.424412	0.999623
HSP90AA1	3320 A_32_P1	-2.34	0.042189	0.068773	0.970412	0.999497	0.777715	0.999623
ICAM4	3386 A_23_P1	1.54	0.042372	0.068887	0.865075	0.999497	0.326853	0.999623
CXCR3	2833 A_23_P1	-2.58	0.042355	0.068887	0.823285	0.999497	0.314022	0.999623
RIN2	54453 A_23_P1	1.39	0.04255	0.069112	0.172327	0.999497	0.654862	0.999623
PSEN1	5663 A_23_P2	1.37	0.042646	0.069203	0.374946	0.999497	0.988842	0.999623
SECTM1	6398 A_24_P4	-1.59	0.042703	0.06923	0.402995	0.999497	0.507383	0.999623
LYAR	55646 A_23_P4	-1.53	0.042853	0.069343	0.318999	0.999497	0.799633	0.999623
GRK5	2869 A_23_P1	1.21	0.042815	0.069343	0.325056	0.999497	0.974853	0.999623
ROM1	6094 A_23_P1	1.52	0.042908	0.069366	0.721971	0.999497	0.489213	0.999623
SH2D1A	4068 A_23_P4	-1.65	0.042988	0.069431	0.23822	0.999497	0.86803	0.999623
CLN3	1201 A24P2	1.36	0.043199	0.069433	0.609698	0.999497	0.494394	0.999623
ANGPTL4	51129 A_23_P1	1.8	0.043231	0.069433	0.562689	0.999497	0.654075	0.999623
FUT4	2526 A_23_P1	1.33	0.04319	0.069433	0.189847	0.999497	0.331627	0.999623
ENPP2	5168 A_23_P3	1.24	0.043185	0.069433	0.397435	0.999497	0.822373	0.999623
BMPRI1A	657 A_24_P3	1.28	0.043121	0.069433	0.941555	0.999497	0.637727	0.999623
EI24	9538 A_24_P4	1.39	0.043099	0.069433	0.592521	0.999497	0.708771	0.999623
CROP	51747 A_24_P3	-1.85	0.043511	0.069568	0.878013	0.999497	0.49499	0.999623
SERPINA3	12 A_23_P1	1.2	0.043506	0.069568	0.194155	0.999497	0.539888	0.999623
EXOC4	60412 A_23_P1	1.14	0.043431	0.069568	0.460005	0.999497	0.739296	0.999623
PDCL3	79031 A_32_P1	-1.31	0.043597	0.069568	0.82953	0.999497	0.882722	0.999623
CDC42SE2	56990 A_23_P4	1.65	0.043592	0.069568	0.941825	0.999497	0.973747	0.999623
TGFBR2	7048 A_23_P3	1.32	0.043564	0.069568	0.445034	0.999497	0.962719	0.999623
CRYAA	1409 A_23_P3	1.3	0.043526	0.069568	0.977503	0.999497	0.456865	0.999623
ATL1	51062 A_23_P3	1.33	0.043673	0.069624	0.350602	0.999497	0.46682	0.999623
MZF1	7593 A_23_P1	1.51	0.0439	0.06992	0.688516	0.999497	0.935398	0.999623
FNDCSA	22862 A_23_P3	-2.64	0.044282	0.070403	0.592107	0.999497	0.609437	0.999623
CDC2L2	728642 A_24_P3	1.55	0.044284	0.070403	0.861503	0.999497	0.991662	0.999623
3-Mar	115123 A_23_P3	1.32	0.044347	0.070438	0.293459	0.999497	0.650932	0.999623
SIRPA	140885 A_24_P2	1.44	0.044492	0.07055	0.560109	0.999497	0.249875	0.999623
PTPRF	5792 A_24_P3	-1.32	0.0445	0.07055	0.454858	0.999497	0.764493	0.999623
GSTP1	2950 A_23_P2	1.39	0.044573	0.070602	0.828026	0.999497	0.13349	0.999623
FKBP1A	2280 A_32_P3	-1.53	0.044868	0.070777	0.65713	0.999497	0.745111	0.999623
PCNA	5111 A_23_P2	-1.51	0.045095	0.070777	0.728671	0.999497	0.361769	0.999623
ATF2	1386 A_24_P2	1.32	0.045028	0.070777	0.69581	0.999497	0.63401	0.999623
MNT	4335 A_24_P3	-1.72	0.045044	0.070777	0.382325	0.999497	0.327378	0.999623
ATP5O	539 A_23_P1	1.31	0.044989	0.070777	0.171139	0.999497	0.592729	0.999623
APIP	51074 A_23_P1	-1.43	0.045078	0.070777	0.129824	0.999497	0.3636	0.999623
CD36	948 A_23_P1	1.41	0.044796	0.070777	0.969281	0.999497	0.152155	0.999623
NME5	8382 A_23_P1	1.3	0.045049	0.070777	0.500561	0.999497	0.34537	0.999623
HCG18	414777 A_24_P3	1.43	0.044934	0.070777	0.879112	0.999497	0.293233	0.999623
MUC4	4585 A_24_P2	1.63	0.044783	0.070777	0.742799	0.999497	0.495826	0.999623
PDGFRL	5157 A_23_P3	-1.44	0.045146	0.070794	0.615637	0.999497	0.330274	0.999623
TOLLIP	54472 A_24_P2	-1.71	0.045435	0.071067	0.933862	0.999497	0.453475	0.999623
GNL1	2794 A_23_P1	1.5	0.045377	0.071067	0.949038	0.999497	0.420492	0.999623
DGCR8	54487 A_23_P2	1.48	0.045444	0.071067	0.466895	0.999497	0.44656	0.999623
PPFBP1	8496 A_23_P3	-3.99	0.045722	0.071192	0.813694	0.999497	0.676853	0.999623
TXN	7295 A_24_P1	-1.35	0.045731	0.071192	0.527585	0.999497	0.140613	0.999623
OPA1	4976 A_23_P2	1.3	0.045702	0.071192	0.968662	0.999497	0.768005	0.999623
SOCS1	8651 A_24_P4	1.31	0.045645	0.071192	0.619718	0.999497	0.206638	0.999623
ALG9	79796 A_32_P4	1.62	0.045727	0.071192	0.255926	0.999497	0.353473	0.999623

TABLE S7-continued

Significant differences between CR and CNR								
		Fold-change CNR vs	Cytokine response		Age: 60-65 yo vs 74+ yo		Gender	
			CR	p-value	q-value	p-value	q-value	p-value
CUL5	8065 A_32_P1	1.2	0.045806	0.071244	0.386454	0.999497	0.95481	0.999623
IKBKAP	8518 A_23_P1	-1.91	0.045952	0.071388	0.954821	0.999497	0.806443	0.999623
DDX41	51428 A_23_P1	1.31	0.045981	0.071388	0.843995	0.999497	0.810098	0.999623
PIWIL2	55124 A_23_P2	1.33	0.046063	0.071429	0.826224	0.999497	0.283979	0.999623
COL6A1	1291 A_24_P5	1.41	0.04609	0.071429	0.903557	0.999497	0.13481	0.999623
PRKRIR	5612 A_23_P2	1.21	0.04619	0.07152	0.215995	0.999497	0.415878	0.999623
ASGR1	432 A_23_P1	1.4	0.046274	0.071585	0.328991	0.999497	0.511678	0.999623
SIRPA	140885 A_23_P2	1.53	0.046507	0.071762	0.666027	0.999497	0.589137	0.999623
SHFM1	7979 A_23_P4	-1.37	0.046459	0.071762	0.515968	0.999497	0.69132	0.999623
PCDHGA3	56112 A_24_P3	1.25	0.046513	0.071762	0.258594	0.999497	0.137665	0.999623
SCYE1	9255 A_23_P1	-1.56	0.04672	0.071766	0.812198	0.999497	0.315334	0.999623
MYC	4609 A_24_P1	-1.59	0.046802	0.071766	0.977739	0.999497	0.296596	0.999623
IL17RA	23765 A_23_P1	1.32	0.046815	0.071766	0.371759	0.999497	0.118861	0.999623
PAGE1	8712 A_24_P3	1.16	0.046785	0.071766	0.935663	0.999497	0.550923	0.999623
ZAK	51776 A_23_P3	-1.44	0.046667	0.071766	0.777675	0.999497	0.567119	0.999623
CALM3	808 A_24_P2	1.5	0.04675	0.071766	0.811511	0.999497	0.194461	0.999623
CD55	1604 A_24_P1	-1.26	0.046892	0.071766	0.259449	0.999497	0.884425	0.999623
H2AFX	3014 A_24_P3	1.36	0.046959	0.071766	0.095474	0.999497	0.293479	0.999623
CP110	9738 A_23_P2	-1.72	0.04697	0.071766	0.549938	0.999497	0.930941	0.999623
ITGA9	3680 A_24_P1	1.31	0.046745	0.071766	0.221123	0.999497	0.285706	0.999623
DNM2	1785 A_23_P4	1.61	0.046974	0.071766	0.952938	0.999497	0.614731	0.999623
CD96	10225 A_23_P4	1.25	0.047027	0.071784	0.20498	0.999497	0.086648	0.999623
TNIP2	79155 A_23_P2	1.45	0.047183	0.071939	0.655112	0.999497	0.999335	0.999623
ALG1	56052 A_32_P1	1.3	0.047213	0.071939	0.572971	0.999497	0.61471	0.999623
SCYE1	9255 A_24_P3	-1.68	0.047277	0.071973	0.766268	0.999497	0.57458	0.999623
MCL1	4170 A_24_P3	-2.16	0.047418	0.072053	0.889888	0.999497	0.381535	0.999623
PRKAR1A	5573 A_24_P3	-1.64	0.047401	0.072053	0.511529	0.999497	0.177114	0.999623
IGF2BP3	10643 A_23_P1	1.26	0.047454	0.072053	0.591045	0.999497	0.864679	0.999623
MLH1	4292 A_23_P1	-1.63	0.047976	0.072653	0.630992	0.999497	0.122333	0.999623
FLRT3	23767 A_23_P1	1.37	0.047953	0.072653	0.838091	0.999497	0.790526	0.999623
PBX1	5087 A_23_P1	1.33	0.047962	0.072653	0.359381	0.999497	0.59874	0.999623
RELA	5970 A_23_P1	1.49	0.048214	0.072949	0.73911	0.999497	0.263018	0.999623
FOXC1	2296 A_23_P2	-1.56	0.048476	0.073281	0.387431	0.999497	0.900154	0.999623
MLLT1	4298 A_23_P1	1.52	0.048922	0.073693	0.648386	0.999497	0.211593	0.999623
PDIA3	2923 A_32_P1	-1.79	0.049133	0.073693	0.20452	0.999497	0.609904	0.999623
CYCS	54205 A_32_P1	1.48	0.049129	0.073693	0.639667	0.999497	0.26236	0.999623
NFE2L2	4780 A_24_P5	1.32	0.049107	0.073693	0.266244	0.999497	0.239128	0.999623
HTATSF1	27336 A_23_P4	-1.49	0.048971	0.073693	0.359184	0.999497	0.214235	0.999623
TRIB3	57761 A_23_P2	1.48	0.048901	0.073693	0.970463	0.999497	0.565315	0.999623
FOXP1	27086 A_23_P1	-1.19	0.048856	0.073693	0.732264	0.999497	0.857483	0.999623
ADAM11	4185 A_23_P2	-1.3	0.049132	0.073693	0.710373	0.999497	0.858642	0.999623
CCL28	56477 A_23_P3	-1.49	0.04885	0.073693	0.585233	0.999497	0.981947	0.999623
PPM1F	9647 A_24_P1	1.54	0.049182	0.073702	0.605032	0.999497	0.477826	0.999623
TIMP3	7078 A_23_P3	1.64	0.049266	0.073763	0.465532	0.999497	0.707186	0.999623
F7	2155 A_23_P1	1.39	0.049347	0.073821	0.59254	0.999497	0.236397	0.999623
COPG	22820 A_23_P4	1.24	0.049474	0.073946	0.858751	0.999497	0.54968	0.999623
PDIA3	2923 A_24_P1	-1.31	0.049589	0.074054	0.522978	0.999497	0.684458	0.999623
PTPN11	5781 A_23_P5	1.46	0.049759	0.074116	0.711278	0.999497	0.902129	0.999623
CX3CL1	6376 A_24_P3	1.58	0.049724	0.074116	0.934763	0.999497	0.728325	0.999623
IL6ST	3572 A_23_P5	1.36	0.049726	0.074116	0.821297	0.999497	0.75394	0.999623
MPZL3	196264 A_24_P2	-1.49	0.049947	0.074236	0.804556	0.999497	0.184604	0.999623
PCDH8	56128 A_23_P4	1.33	0.049969	0.074236	0.987622	0.999497	0.506273	0.999623
DLG5	9231 A_24_P1	-1.79	0.0499	0.074236	0.744695	0.999497	0.188498	0.999623
CDH23	64072 A_24_P5	1.53	0.05054	0.074955	0.938805	0.999497	0.522084	0.999623
BCL2	596 A_23_P5	-1.75	0.050506	0.074955	0.490873	0.999497	0.477736	0.999623
ICA1	3382 A_24_P3	1.45	0.050587	0.07496	0.828191	0.999497	0.836975	0.999623
ITGB3BP	23421 A_23_P2	1.35	0.050776	0.075175	0.500913	0.999497	0.901291	0.999623
MAPK11	5600 A_23_P5	1.6	0.050917	0.075319	0.626765	0.999497	0.385447	0.999623
CDKN2C	1031 A_23_P8	1.33	0.051088	0.075378	0.50526	0.999497	0.343098	0.999623
DOCK4	9732 A_23_P5	-1.98	0.051014	0.075378	0.929724	0.999497	0.373991	0.999623
KIAA0368	23392 A_23_P1	-1.4	0.051049	0.075378	0.47502	0.999497	0.675111	0.999623
CLN3	1201 A_32_P5	-1.47	0.051216	0.075502	0.916349	0.999497	0.984168	0.999623
ADAM15	8751 A_23_P1	1.45	0.051276	0.075526	0.519439	0.999497	0.246545	0.999623
EDN1	1906 A_23_P2	1.37	0.051411	0.075661	0.803693	0.999497	0.664785	0.999623
FCGBP	8857 A_32_P2	-1.73	0.051757	0.075976	0.704005	0.999497	0.552795	0.999623
BICD2	23299 A_24_P4	1.17	0.05175	0.075976	0.510926	0.999497	0.715863	0.999623
IRF7	3665 A_24_P1	1.39	0.051675	0.075976	0.818667	0.999497	0.179341	0.999623
NOXA1	10811 A_23_P2	1.56	0.051885	0.076078	0.936563	0.999497	0.606702	0.999623

TABLE S7-continued

Significant differences between CR and CNR								
		Fold-change CNR vs	Cytokine response		Age: 60-65 yo vs 74+ yo		Gender	
			CR	p-value	q-value	p-value	q-value	p-value
GALNTL1	57452 A_23_P7	1.58	0.05192	0.076078	0.480342	0.999497	0.736755	0.999623
BBS4	585 A_24_P1	1.31	0.051959	0.076078	0.993054	0.999497	0.954196	0.999623
FOXO1	2308 A_23_P1	-1.21	0.052208	0.076378	0.227461	0.999497	0.914728	0.999623
PPP1CA	5499 A_23_P4	1.44	0.052271	0.076404	0.988265	0.999497	0.198388	0.999623
LIN7C	55327 A_24_P1	1.28	0.052533	0.076625	0.498493	0.999497	0.671202	0.999623
ADRM1	11047 A_24_P3	1.6	0.052555	0.076625	0.945303	0.999497	0.776911	0.999623
SRF	6722 A_24_P3	1.3	0.05255	0.076625	0.527336	0.999497	0.744148	0.999623
SSX2IP	117178 A_23_P2	-1.6	0.052655	0.076657	0.974178	0.999497	0.789061	0.999623
LAX1	54900 A_24_P1	-1.95	0.052666	0.076657	0.487883	0.999497	0.422744	0.999623
ZNF503	84858 A_23_P1	1.44	0.052814	0.076807	0.728954	0.999497	0.466738	0.999623
PTK7	5754 A_24_P3	1.35	0.052966	0.076963	0.910405	0.999497	0.232492	0.999623
RAB5A	5868 A_24_P2	-1.23	0.053024	0.076982	0.566482	0.999497	0.295912	0.999623
CYBB	1536 A_24_P3	-1.79	0.053283	0.077294	0.688119	0.999497	0.312165	0.999623
YARS	8565 A_23_P3	1.74	0.054031	0.077326	0.821487	0.999497	0.494963	0.999623
MUC5AC	4586 A_24_P5	1.94	0.05393	0.077326	0.232507	0.999497	0.2196	0.999623
CNTR0B	116840 A_23_P5	1.66	0.05389	0.077326	0.91235	0.999497	0.439556	0.999623
PHF17	79960 A_23_P1	1.34	0.053962	0.077326	0.494722	0.999497	0.250703	0.999623
ADRM1	11047 A_23_P1	1.59	0.053526	0.077326	0.70912	0.999497	0.521504	0.999623
C2CD2L	9854 A_23_P3	1.43	0.053976	0.077326	0.427937	0.999497	0.522298	0.999623
LAMP2	3920 A_23_P4	-1.41	0.054068	0.077326	0.759732	0.999497	0.672658	0.999623
SPON2	10417 A_23_P1	1.35	0.053374	0.077326	0.893937	0.999497	0.790237	0.999623
ING4	51147 A_23_P4	1.56	0.054062	0.077326	0.602712	0.999497	0.635273	0.999623
CXCL16	58191 A_23_P3	-1.2	0.053583	0.077326	0.945917	0.999497	0.989261	0.999623
AMICA1	120425 A_23_P1	-2.06	0.053736	0.077326	0.090903	0.999497	0.60496	0.999623
NPHP1	4867 A_24_P8	1.27	0.053724	0.077326	0.545708	0.999497	0.132466	0.999623
BUB1B	701 A_23_P1	1.48	0.053759	0.077326	0.811355	0.999497	0.876344	0.999623
SCARB1	949 A_23_P3	1.26	0.053636	0.077326	0.781537	0.999497	0.630622	0.999623
SMAD2	4087 A_24_P2	1.13	0.054062	0.077326	0.947205	0.999497	0.917569	0.999623
RAD52	5893 A_23_P1	1.28	0.053548	0.077326	0.876668	0.999497	0.263014	0.999623
CD151	977 A_23_P5	1.48	0.053984	0.077326	0.942078	0.999497	0.176278	0.999623
DERL1	79139 A_24_P1	-1.59	0.054229	0.077428	0.925115	0.999497	0.380825	0.999623
AEN	64782 A_32_P8	1.39	0.054207	0.077428	0.185031	0.999497	0.447625	0.999623
ZNF675	171392 A_23_P3	-3.09	0.054631	0.077937	0.755138	0.999497	0.526513	0.999623
EZR	7430 A_32_P1	-1.96	0.054723	0.078004	0.542415	0.999497	0.088239	0.999623
EDN2	1907 A_23_P3	1.38	0.054794	0.07804	0.31998	0.999497	0.750237	0.999623
TRAF5	7188 A_23_P2	1.2	0.054863	0.078075	0.198244	0.999497	0.688574	0.999623
CYCS	54205 A_24_P3	-1.96	0.054981	0.078125	0.303888	0.999497	0.309641	0.999623
SIGIRR	59307 A_23_P8	1.36	0.054989	0.078125	0.905737	0.999497	0.71141	0.999623
PICALM	8301 A_23_P1	-1.64	0.055061	0.078162	0.981661	0.999497	0.451614	0.999623
C8G	733 A_23_P2	1.72	0.055299	0.078435	0.800602	0.999497	0.265125	0.999623
CDH3	1001 A_23_P4	1.26	0.055548	0.078724	0.612362	0.999497	0.787921	0.999623
DNAJB6	10049 A_23_P2	-2.4	0.055707	0.078884	0.803694	0.999497	0.195436	0.999623
MAPT	4137 A_23_P2	1.28	0.05579	0.078937	0.668231	0.999497	0.577542	0.999623
NBN	4683 A_24_P2	-1.86	0.055899	0.079026	0.690918	0.999497	0.308075	0.999623
CLDN10	9071 A_23_P4	1.24	0.05598	0.079044	0.763734	0.999497	0.247918	0.999623
PSMC6	5706 A_23_P1	-1.59	0.056003	0.079044	0.58957	0.999497	0.683695	0.999623
C1D	10438 A_23_P1	-1.7	0.05632	0.079426	0.541511	0.999497	0.552801	0.999623
PKP4	8502 A_23_P1	-1.81	0.056369	0.07943	0.953047	0.999497	0.552642	0.999623
CREB1	1385 A_23_P7	-1.47	0.056448	0.079477	0.64991	0.999497	0.370657	0.999623
SAP30BP	29115 A_24_P3	1.43	0.056551	0.079556	0.611487	0.999497	0.593313	0.999623
KCNIP3	30818 A_23_P3	-1.38	0.056702	0.079703	0.982035	0.999497	0.844064	0.999623
FCGBP	8857 A_23_P2	1.64	0.056862	0.079864	0.636412	0.999497	0.219441	0.999623
RNF144B	255488 A_24_P4	-1.78	0.056909	0.079864	0.865156	0.999497	0.541439	0.999623
SIX4	51804 A_32_P2	-1.99	0.057173	0.080039	0.561118	0.999497	0.36626	0.999623
PACSL1	29993 A_23_P1	1.39	0.057154	0.080039	0.242498	0.999497	0.709506	0.999623
MYEF2	50804 A_23_P7	-1.26	0.057136	0.080039	0.978938	0.999497	0.870922	0.999623
RAB4A	5867 A_23_P3	-1.43	0.057222	0.080043	0.989662	0.999497	0.391131	0.999623
FKBP15	23307 A_32_P1	1.33	0.057299	0.080086	0.687	0.999497	0.103788	0.999623
MUC4	4585 A_24_P2	-2.6	0.057632	0.080486	0.383032	0.999497	0.243007	0.999623
PAK2	5062 A_32_P1	1.59	0.057814	0.080675	0.584236	0.999497	0.717854	0.999623
NXT2	55916 A_24_P5	-1.64	0.058072	0.080969	0.881595	0.999497	0.390267	0.999623
STON2	85439 A_23_P3	1.7	0.058194	0.081008	0.436436	0.999497	0.02588	0.999623
LENG8	114823 A_24_P4	-1.3	0.05815	0.081008	0.933947	0.999497	0.932755	0.999623
PHLDA2	7262 A_23_P4	-1.69	0.058265	0.081042	0.397296	0.999497	0.248374	0.999623
NR3C1	2908 A_23_P2	1.3	0.058418	0.081189	0.093748	0.999497	0.896398	0.999623
RYR2	6262 A_23_P1	1.16	0.058594	0.08136	0.398575	0.999497	0.137126	0.999623
LOC442421	442421 A_23_P4	1.34	0.058636	0.08136	0.716192	0.999497	0.103469	0.999623
CASP2	835 A_24_P2	1.3	0.058887	0.081643	0.97231	0.999497	0.839865	0.999623

TABLE S7-continued

Significant differences between CR and CNR								
		Fold-change CNR vs	Cytokine response		Age: 60-65 yo vs 74+ yo		Gender	
			p-value	q-value	p-value	q-value	p-value	q-value
GAPVD1	26130_A_23_P3	-2.47	0.059076	0.08184	0.592779	0.999497	0.281485	0.999623
NP	4860_A_23_P1	1.38	0.059154	0.081881	0.590482	0.999497	0.952225	0.999623
TPT1	7178_A_24_P1	-1.49	0.059233	0.081905	0.643797	0.999497	0.754788	0.999623
PSMD1	5707_A_23_P2	-1.2	0.059266	0.081905	0.064632	0.999497	0.952043	0.999623
IGF1	3479_A_24_P3	1.5	0.059535	0.082145	0.508421	0.999497	0.954962	0.999623
GPR56	9289_A_23_P2	1.55	0.059494	0.082145	0.734577	0.999497	0.65396	0.999623
TLR6	10333_A_23_P3	1.41	0.059765	0.082396	0.723133	0.999497	0.717354	0.999623
BUB3	9184_A_23_P3	-2.01	0.059886	0.082497	0.385659	0.999497	0.55939	0.999623
UBB	7314_A_23_P2	1.68	0.060013	0.0825	0.293768	0.999497	0.480511	0.999623
NID1	4811_A_23_P2	-1.34	0.060032	0.0825	0.181672	0.999497	0.654073	0.999623
SEMA6A	57556_A_23_P7	1.38	0.059936	0.0825	0.558867	0.999497	0.473839	0.999623
HIPK2	28996_A_23_P1	2.3	0.060245	0.08259	0.794381	0.999497	0.739402	0.999623
PPIL3	53938_A_23_P1	1.27	0.060286	0.08259	0.262102	0.999497	0.165681	0.999623
ROCK1	6093_A_24_P5	-1.71	0.060289	0.08259	0.782182	0.999497	0.481754	0.999623
VNN1	8876_A_23_P2	1.39	0.060223	0.08259	0.364005	0.999497	0.722212	0.999623
BMP7	655_A_24_P5	1.62	0.060355	0.082615	0.597849	0.999497	0.77366	0.999623
UNC13B	10497_A_23_P1	1.45	0.060475	0.082714	0.152818	0.999497	0.241637	0.999623
PATL1	219988_A_23_P3	1.32	0.060673	0.082878	0.476153	0.999497	0.53564	0.999623
NME6	10201_A_23_P3	1.5	0.060756	0.082878	0.927312	0.999497	0.468945	0.999623
HSP90B1	7184_A_24_P1	-1.94	0.060787	0.082878	0.81706	0.999497	0.188363	0.999623
B3GNT5	84002_A_23_P1	-1.28	0.060787	0.082878	0.996076	0.999497	0.565651	0.999623
PVRL1	5818_A_23_P7	1.28	0.060875	0.082932	0.832488	0.999497	0.755851	0.999623
SFRP1	6422_A_23_P1	1.45	0.060928	0.082938	0.3416	0.999497	0.678176	0.999623
IGDCC3	9543_A_23_P3	1.36	0.061027	0.082952	0.477997	0.999497	0.145097	0.999623
CTSZ	1522_A_23_P4	-1.29	0.061034	0.082952	0.319291	0.999497	0.295555	0.999623
THBS3	7059_A_23_P2	1.32	0.061087	0.082958	0.976554	0.999497	0.443927	0.999623
MYL10	93408_A_23_P3	1.35	0.061208	0.082992	0.534713	0.999497	0.329238	0.999623
ITGB8	3696_A_23_P1	1.23	0.061199	0.082992	0.478355	0.999497	0.376422	0.999623
PVR	5817_A_32_P7	-1.43	0.061456	0.083215	0.957821	0.999497	0.265836	0.999623
METTL1	4234_A_23_P4	1.47	0.06147	0.083215	0.3862	0.999497	0.508648	0.999623
HES1	3280_A_24_P5	-1.36	0.061548	0.083255	0.295761	0.999497	0.529289	0.999623
TBRG4	9238_A_23_P2	1.25	0.061633	0.083262	0.36624	0.999497	0.981103	0.999623
FLJ23834	222256_A_32_P1	1.3	0.061649	0.083262	0.313687	0.999497	0.887795	0.999623
DGCR6L	85359_A_23_P1	1.39	0.061797	0.083397	0.412568	0.999497	0.314466	0.999623
ICAM1	3383_A_23_P1	1.31	0.062045	0.083404	0.680372	0.999497	0.634968	0.999623
STAT2	6773_A_23_P7	1.28	0.062019	0.083404	0.976264	0.999497	0.907148	0.999623
SLC1A6	6511_A_24_P1	1.47	0.061969	0.083404	0.598053	0.999497	0.712889	0.999623
APOC3	345_A_23_P1	1.44	0.061899	0.083404	0.929606	0.999497	0.205063	0.999623
ERCC3	2071_A_23_P5	1.16	0.061899	0.083404	0.959732	0.999497	0.917013	0.999623
UNC13D	201294_A_24_P5	1.55	0.062123	0.083445	0.778546	0.999497	0.769676	0.999623
POMP	51371_A_23_P1	-1.39	0.062428	0.083789	0.441242	0.999497	0.372817	0.999623
COL14A1	7373_A_24_P2	-2.11	0.062566	0.083863	0.33844	0.999497	0.744663	0.999623
PSME3	10197_A_24_P3	-2.48	0.06258	0.083863	0.322004	0.999497	0.898924	0.999623
LAMC1	3915_A_23_P2	-1.23	0.063032	0.084271	0.409845	0.999497	0.326379	0.999623
IFI27	3429_A_24_P2	-2.16	0.062994	0.084271	0.774557	0.999497	0.043282	0.999623
VCP	7415_A_32_P1	1.27	0.063002	0.084271	0.63139	0.999497	0.160201	0.999623
HLA-E	3133_A_23_P3	1.61	0.063098	0.084294	0.998624	0.999497	0.63157	0.999623
PTPRH	5794_A_23_P1	1.69	0.06328	0.084386	0.984408	0.999497	0.956971	0.999623
ID2	3398_A_32_P1	-1.69	0.06346	0.084386	0.430629	0.999497	0.797506	0.999623
THBS1	7057_A_32_P1	-1.28	0.063461	0.084386	0.485432	0.999497	0.565239	0.999623
HFE	3077_A_23_P3	1.58	0.063337	0.084386	0.236346	0.999497	0.053636	0.999623
ALCAM	214_A_32_P1	1.48	0.063406	0.084386	0.964084	0.999497	0.207685	0.999623
RALA	5898_A_23_P1	-1.86	0.063278	0.084386	0.10191	0.999497	0.298542	0.999623
PPP1R13L	10848_A_23_P1	1.55	0.063529	0.084412	0.731581	0.999497	0.521979	0.999623
CIQTNF3	114899_A_23_P1	-1.4	0.063721	0.084601	0.451521	0.999497	0.858492	0.999623
ITGA1	3672_A_23_P2	-1.17	0.063888	0.084698	0.876454	0.999497	0.578364	0.999623
SEMA3A	10371_A_24_P1	-1.96	0.063916	0.084698	0.979359	0.999497	0.515413	0.999623
HMGBl	3146_A_23_P5	-1.55	0.063941	0.084698	0.658136	0.999497	0.792064	0.999623
TRIM35	23087_A_23_P3	1.3	0.064022	0.084703	0.303103	0.999497	0.421854	0.999623
MAPK13	5603_A_23_P1	1.47	0.064043	0.084703	0.420345	0.999497	0.464172	0.999623
CDKN1B	1027_A_24_P8	-1.86	0.064135	0.084759	0.907395	0.999497	0.135679	0.999623
CTSS	1520_A_24_P2	-3.58	0.064236	0.084829	0.803693	0.999497	0.585641	0.999623
BIN1	274_A_24_P1	1.66	0.0643	0.084847	0.573023	0.999497	0.6276	0.999623
TNFRSF18	8784_A_24_P4	1.96	0.064504	0.084921	0.420216	0.999497	0.762135	0.999623
RAPGEF3	10411_A_32_P3	-1.46	0.064454	0.084921	0.423967	0.999497	0.871848	0.999623
GPR135	64582_A_23_P1	1.14	0.064458	0.084921	0.336918	0.999497	0.45434	0.999623
RAD51	5888_A_23_P8	2.16	0.064646	0.085043	0.74582	0.999497	0.723942	0.999623
CLN3	1201_A_23_P8	1.65	0.064885	0.085293	0.377334	0.999497	0.726209	0.999623

TABLE S7-continued

Significant differences between CR and CNR								
		Fold-change CNR vs	Cytokine response		Age: 60-65 yo vs 74+ yo		Gender	
			CR	p-value	q-value	p-value	q-value	p-value
CASP10	843 A_23_P1	1.27	0.06517	0.085602	0.274417	0.999497	0.294492	0.999623
VCL	7414 A_24_P4	-1.74	0.065316	0.085729	0.173592	0.999497	0.637623	0.999623
HLA-DMA	3108 A_24_P5	1.37	0.065525	0.085741	0.769045	0.999497	0.176254	0.999623
CDH9	1007 A_23_P5	1.22	0.065399	0.085741	0.401308	0.999497	0.74778	0.999623
ABCA7	10347 A_23_P3	1.5	0.065482	0.085741	0.349054	0.999497	0.300378	0.999623
CUL3	8452 A_24_P1	1.21	0.06552	0.085741	0.194174	0.999497	0.186183	0.999623
IRF2BP1	26145 A_23_P3	1.56	0.065592	0.085764	0.530011	0.999497	0.171747	0.999623
PVRL4	81607 A_23_P4	1.31	0.065907	0.085791	0.898216	0.999497	0.289891	0.999623
SEMA5A	9037 A_24_P5	-1.43	0.065961	0.085791	0.086627	0.999497	0.657199	0.999623
NFKBIZ	64332 A_23_P1	1.18	0.065715	0.085791	0.732808	0.999497	0.450879	0.999623
PML	5371 A_23_P3	1.49	0.065847	0.085791	0.232513	0.999497	0.950817	0.999623
LGALS1	3956 A_23_P1	1.2	0.065827	0.085791	0.452585	0.999497	0.43499	0.999623
XRCC3	7517 A_23_P4	1.42	0.065881	0.085791	0.812737	0.999497	0.280094	0.999623
VPS45	11311 A_24_P3	1.26	0.065935	0.085791	0.760386	0.999497	0.366523	0.999623
CD99	4267 A_23_P2	1.37	0.066036	0.085824	0.415802	0.999497	0.877285	0.999623
NFATC4	4776 A_23_P1	1.56	0.066216	0.085933	0.278112	0.999497	0.880446	0.999623
HIP1	3092 A_24_P5	-1.32	0.066219	0.085933	0.973124	0.999497	0.968862	0.999623
LAT	27040 A_23_P1	1.45	0.066315	0.085992	0.739856	0.999497	0.527527	0.999623
TDGF1	6997 A_23_P3	2.44	0.066785	0.086537	0.286719	0.999497	0.420839	0.999623
GDF11	10220 A_23_P1	1.63	0.067033	0.086792	0.614453	0.999497	0.67061	0.999623
IGFN1	91156 A_32_P4	1.4	0.067271	0.08697	0.467572	0.999497	0.627504	0.999623
COPG2	26958 A_23_P1	-1.54	0.067235	0.08697	0.842821	0.999497	0.770027	0.999623
CD74	972 A_23_P1	1.44	0.067389	0.087057	0.836028	0.999497	0.142043	0.999623
TLR3	7098 A_23_P2	-1.44	0.067634	0.087309	0.005284	0.999497	0.41004	0.999623
NFE2L2	4780 A_23_P5	-1.49	0.067864	0.087539	0.557611	0.999497	0.55885	0.999623
ERCC6	2074 A_23_P1	-1.16	0.068412	0.088181	0.167979	0.999497	0.103066	0.999623
XRCC6	2547 A_23_P1	1.55	0.068528	0.088196	0.876559	0.999497	0.595161	0.999623
FBNP1	23048 A_23_P3	1.22	0.068502	0.088196	0.210089	0.999497	0.109915	0.999623
RAB34	83871 A_23_P1	1.36	0.068578	0.088196	0.164692	0.999497	0.609719	0.999623
FCRLA	84824 A_23_P4	1.44	0.068685	0.088268	0.413456	0.999497	0.767929	0.999623
SELPLG	6404 A_23_P1	1.7	0.068895	0.088472	0.978322	0.999497	0.293404	0.999623
PCMT1	5110 A_24_P2	-1.66	0.069042	0.088595	0.982318	0.999497	0.32771	0.999623
IL1R1	3554 A_24_P2	1.34	0.06911	0.088616	0.32048	0.999497	0.293248	0.999623
ALG1	56052 A_24_P5	1.67	0.069308	0.088803	0.375108	0.999497	0.758572	0.999623
ROCK2	9475 A_23_P2	-1.68	0.069371	0.088819	0.807761	0.999497	0.569649	0.999623
MUC5B	727897 A_24_P3	-1.42	0.069701	0.088911	0.844397	0.999497	0.58056	0.999623
PTPN1	5770 A_23_P3	-1.46	0.069674	0.088911	0.697717	0.999497	0.372209	0.999623
PSMD3	5709 A_24_P2	1.85	0.069639	0.088911	0.721566	0.999497	0.556409	0.999623
CDH6	1004 A_23_P2	1.29	0.069576	0.088911	0.849494	0.999497	0.484046	0.999623
COL20A1	57642 A_32_P1	-1.58	0.069579	0.088911	0.318531	0.999497	0.288065	0.999623
HESX1	8820 A_23_P1	1.2	0.069763	0.088924	0.119815	0.999497	0.60995	0.999623
UBE4B	10277 A_23_P1	-1.38	0.070071	0.089251	0.911792	0.999497	0.876165	0.999623
PLAU	5328 A_23_P2	1.15	0.070349	0.089314	0.92319	0.999497	0.628993	0.999623
IFI16	3428 A_23_P2	1.43	0.070218	0.089314	0.50821	0.999497	0.640024	0.999623
MAEA	10296 A_23_P1	1.21	0.07038	0.089314	0.25731	0.999497	0.481224	0.999623
UBB	7314 A_24_P1	2.48	0.070303	0.089314	0.123697	0.999497	0.49861	0.999623
HEPACAM	220296 A_24_P2	1.21	0.070325	0.089314	0.234704	0.999497	0.189901	0.999623
CASP2	835 A_23_P1	-1.85	0.070579	0.089501	0.924106	0.999497	0.363611	0.999623
TTYH1	57348 A_23_P3	1.46	0.070699	0.089543	0.932101	0.999497	0.844342	0.999623
MAPK3	5595 A_23_P3	1.36	0.070716	0.089543	0.518378	0.999497	0.496882	0.999623
CYBB	1536 A_23_P2	1.25	0.070904	0.089706	0.557522	0.999497	0.935803	0.999623
AZGP1	563 A_23_P1	1.23	0.070949	0.089706	0.341404	0.999497	0.942304	0.999623
LRP1	4035 A_23_P1	1.42	0.071153	0.089898	0.32079	0.999497	0.58229	0.999623
NFE2	4778 A_23_P1	1.23	0.071239	0.089941	0.467874	0.999497	0.800485	0.999623
MAP3K10	4294 A_24_P2	1.73	0.071317	0.089973	0.797461	0.999497	0.915787	0.999623
TUBB	203068 A_32_P7	1.15	0.071646	0.090323	0.774126	0.999497	0.148739	0.999623
ITGA5	3678 A_23_P3	1.47	0.071722	0.090351	0.890551	0.999497	0.297712	0.999623
CTSE	1510 A_23_P1	-1.26	0.071836	0.09043	0.799191	0.999497	0.612963	0.999623
ELN	2006 A_24_P1	-1.8	0.071983	0.090482	0.959394	0.999497	0.495364	0.999623
CLU	1191 A_23_P2	1.21	0.071959	0.090482	0.6467	0.999497	0.281353	0.999623
MSX2	4488 A_24_P1	-2.12	0.072309	0.09076	0.356266	0.999497	0.638407	0.999623
FBLN5	10516 A_23_P1	1.26	0.072289	0.09076	0.421469	0.999497	0.434594	0.999623
PPT1	5538 A_24_P2	1.33	0.072512	0.090948	0.876872	0.999497	0.343297	0.999623
DOCK7	85440 A_24_P2	1.34	0.072634	0.091035	0.223385	0.999497	0.851233	0.999623
PARVG	64098 A_23_P1	1.35	0.072897	0.091298	0.769423	0.999497	0.641898	0.999623
DAXX	1616 A_23_P1	1.36	0.073115	0.091373	0.904887	0.999497	0.844909	0.999623
CD300A	11314 A_24_P1	-3.19	0.073035	0.091373	0.853224	0.999497	0.635397	0.999623
CD300C	10871 A_23_P1	1.25	0.073077	0.091373	0.29654	0.999497	0.432398	0.999623

TABLE S7-continued

Significant differences between CR and CNR								
		Fold-change CNR vs	Cytokine response		Age: 60-65 yo vs 74+ yo		Gender	
			CR	p-value	q-value	p-value	q-value	p-value
HLA-DPB1	3115 A_24_P1	1.66	0.073373	0.091561	0.829101	0.999497	0.406965	0.999623
TERF1	7013 A_23_P2	-1.68	0.073368	0.091561	0.713932	0.999497	0.338605	0.999623
SPP1	6696 A_23_P7	-1.53	0.073483	0.091632	0.656317	0.999497	0.215219	0.999623
PCDH16	57717 A_23_P3	-1.3	0.073663	0.091791	0.84965	0.999497	0.198622	0.999623
CD244	51744 A_24_P1	-1.58	0.073895	0.091947	0.755374	0.999497	0.621937	0.999623
SRPK2	6733 A_23_P4	-1.68	0.073858	0.091947	0.582662	0.999497	0.317296	0.999623
HLA-DRB4	3126 A_24_P3	1.89	0.074152	0.0922	0.792213	0.999497	0.240951	0.999623
CD37	951 A_24_P6	1.71	0.074286	0.092233	0.303824	0.999497	0.979279	0.999623
RHOA	387 A_24_P1	1.28	0.074234	0.092233	0.067586	0.999497	0.830572	0.999623
RB1	5925 A_24_P1	-1.28	0.07469	0.092602	0.616952	0.999497	0.739005	0.999623
SOCSS5	9655 A_24_P3	-1.62	0.074675	0.092602	0.292014	0.999497	0.228861	0.999623
NEK6	10783 A_23_P2	1.6	0.07497	0.092679	0.694387	0.999497	0.565284	0.999623
PCDH15	56121 A_23_P1	-1.26	0.074951	0.092679	0.759314	0.999497	0.36976	0.999623
TGFBR1	7046 A_32_P1	1.38	0.074864	0.092679	0.292577	0.999497	0.259074	0.999623
DAPL1	92196 A_23_P1	1.28	0.074982	0.092679	0.051096	0.999497	0.958694	0.999623
NR2E1	7101 A_23_P3	1.22	0.075021	0.092679	0.601793	0.999497	0.556365	0.999623
HSPA9	3313 A_24_P7	-1.83	0.075085	0.092691	0.63554	0.999497	0.555625	0.999623
PSMG1	8624 A_23_P6	1.35	0.075234	0.092809	0.130119	0.999497	0.099576	0.999623
CREBBP	1387 A_23_P1	1.63	0.076077	0.093586	0.75556	0.999497	0.596916	0.999623
RECQL4	9401 A_23_P7	1.31	0.076082	0.093586	0.751386	0.999497	0.876279	0.999623
IFIT5	24138 A_24_P3	-1.52	0.075929	0.093586	0.410888	0.999497	0.220902	0.999623
BUB3	9184 A_23_P2	-1.27	0.076012	0.093586	0.225825	0.999497	0.138415	0.999623
AP2A2	161 A_23_P2	1.11	0.07617	0.093629	0.524319	0.999497	0.916485	0.999623
SCARF1	8578 A_23_P1	1.32	0.076793	0.094193	0.751116	0.999497	0.821842	0.999623
SNAP25	6616 A_23_P2	1.25	0.076778	0.094193	0.840024	0.999497	0.388759	0.999623
NLRC3	197358 A_23_P3	-1.31	0.076715	0.094193	0.781645	0.999497	0.681294	0.999623
DSC2	1824 A_23_P4	-2.67	0.077134	0.094544	0.023971	0.999497	0.756781	0.999623
ALDH1A2	8854 A_24_P7	-2.72	0.077249	0.094617	0.102973	0.999497	0.417413	0.999623
BAD	572 A_23_P1	1.39	0.077703	0.095105	0.927524	0.999497	0.277576	0.999623
HSPG2	3339 A_23_P2	1.29	0.077788	0.095142	0.631973	0.999497	0.991037	0.999623
VEGFA	7422 A_24_P1	-2.86	0.077975	0.095168	0.693386	0.999497	0.176198	0.999623
NPC1	4864 A_23_P1	-1.17	0.077911	0.095168	0.376908	0.999497	0.620903	0.999623
GPR183	1880 A_23_P2	-1.22	0.077926	0.095168	0.510821	0.999497	0.71278	0.999623
SEMA3F	6405 A_24_P3	1.36	0.078435	0.095595	0.765867	0.999497	0.93079	0.999623
PDPN	10630 A_24_P2	1.39	0.078386	0.095595	0.704501	0.999497	0.153662	0.999623
TRPC4AP	26133 A_23_P1	1.49	0.078556	0.095642	0.722258	0.999497	0.544348	0.999623
BLNK	29760 A_24_P6	-1.53	0.078585	0.095642	0.340908	0.999497	0.521439	0.999623
ZAP70	7535 A_24_P1	1.4	0.078715	0.095732	0.987112	0.999497	0.741617	0.999623
HINT1	3094 A_23_P3	-1.52	0.078936	0.095866	0.823136	0.999497	0.201455	0.999623
HRH1	3269 A_24_P2	-1.39	0.078892	0.095866	0.870706	0.999497	0.123979	0.999623
NFKBID	84807 A_23_P3	2.26	0.079123	0.095958	0.503013	0.999497	0.563525	0.999623
VTN	7448 A_23_P7	1.44	0.079123	0.095958	0.620538	0.999497	0.513387	0.999623
PRKRIR	5612 A_24_P3	-1.71	0.079207	0.095992	0.689103	0.999497	0.204232	0.999623
CNTNAP3	79937 A_24_P4	1.29	0.079318	0.096058	0.686473	0.999497	0.535152	0.999623
ITGAE	3682 A_23_P2	-1.5	0.079398	0.096088	0.659209	0.999497	0.580435	0.999623
PTPRS	5802 A_24_P2	1.46	0.079634	0.096104	0.843672	0.999497	0.190119	0.999623
CCL23	6368 A_24_P3	1.3	0.079621	0.096104	0.459304	0.999497	0.68307	0.999623
NCF1	653361 A_32_P1	1.72	0.079532	0.096104	0.885633	0.999497	0.311725	0.999623
SRGN	5552 A_23_P6	-1.79	0.07953	0.096104	0.996046	0.999497	0.627648	0.999623
THYN1	29087 A_23_P2	-1.21	0.079778	0.09621	0.336967	0.999497	0.528377	0.999623
MBD4	8930 A_23_P5	-1.84	0.079838	0.096216	0.600026	0.999497	0.298133	0.999623
NAMPT	10135 A_23_P3	-1.66	0.080101	0.096465	0.339861	0.999497	0.921301	0.999623
IL10RA	3587 A_24_P1	-1.26	0.080304	0.096642	0.717485	0.999497	0.961952	0.999623
NFATC3	4775 A_24_P3	1.25	0.08054	0.096725	0.657845	0.999497	0.894317	0.999623
AIFM2	84883 A_23_P1	2.09	0.080542	0.096725	0.658303	0.999497	0.615127	0.999623
PARD3	56288 A_24_P3	1.33	0.080538	0.096725	0.37714	0.999497	0.802016	0.999623
RB1CC1	9821 A_23_P5	-1.4	0.080638	0.096774	0.329588	0.999497	0.782272	0.999623
SART1	9092 A_23_P6	1.42	0.08084	0.096917	0.850047	0.999497	0.844076	0.999623
SIK1	150094 A_23_P1	-1.54	0.08087	0.096917	0.757172	0.999497	0.29682	0.999623
SYNJ2BP	55333 A_23_P6	-1.51	0.081024	0.097034	0.952809	0.999497	0.552324	0.999623
ITGB3	3690 A_24_P3	1.52	0.081293	0.097289	0.672961	0.999497	0.574028	0.999623
NFKB2	4791 A_23_P2	1.48	0.081789	0.097353	0.713252	0.999497	0.415635	0.999623
ITGAM	3684 A_23_P1	-1.52	0.081799	0.097353	0.507717	0.999497	0.167789	0.999623
ACTN1	87 A_24_P1	1.34	0.081746	0.097353	0.585676	0.999497	0.911428	0.999623
MLL	4297 A_24_P2	1.21	0.081631	0.097353	0.031315	0.999497	0.930933	0.999623
ZYX	7791 A_23_P2	1.47	0.081758	0.097353	0.247784	0.999497	0.323588	0.999623
MAP4K3	8491 A_23_P1	1.38	0.081682	0.097353	0.840367	0.999497	0.770612	0.999623
CADPS2	93664 A_24_P2	1.34	0.081597	0.097353	0.271639	0.999497	0.373297	0.999623



TABLE S7-continued

Significant differences between CR and CNR							
Fold-change CNR vs	Cytokine response		Age: 60-65 yo vs 74+ yo		Gender		
	CR	p-value	q-value	p-value	q-value	p-value	q-value
0							
1							
0							
0							
0							
0							
0							
0							
1							
0							
0							
0							
0							
0							
0							
0							
0							
1							
0							
0							
0							
0							
0							
0							
0							
0							
0							
0							
0							
0							
0							
0							
0							
0							
2							
0							
0							
0							
1							
0							
0							
0							
0							
0							
0							
0							
0							
0							
0							
0							
0							
0							
0							
1							
0							
0							
0							
0							
0							
0							
0							
0							
0							
0							
0							
0							
1							
0							
1							
0							
0							
0							
0							
0							
0							
0							
0							
0							
0							
1							
0							
1							
0							
0							
1							











































TABLE S8-continued

Medication category listing for CR and CNR					
Medical Code	Category Name	Medication/Medication combination taken	Number of CR taking medication	Number of CNR taking medication	
6	Anti-cholesterol/Anti-hyperlipidemic	Mevacor, Zocor		1	
6	Anti-cholesterol/Anti-hyperlipidemic	Liptor		1	
7	Anti-coagulants	Coumadin	1		
7	Anti-coagulants	Aggrenox	1		
7	Anti-coagulants	Warfarin	1		
7	Anti-coagulants	Aspirin		3	
8	Antibiotics/anti-infectives/anti-parasitics/anti-microbials	Augmentin		1	
9	Antidepressants/mood-altering drugs	Prozac	1		
10	Antihistamines/Decongestants	Loratadine		1	
10	Antihistamines/Decongestants	NyQuil		1	
11, 12	Antihypertensives and Cardiovascular, other than hyperlipidemic/HTN	Maxzide		1	
11, 12	Antihypertensives and Cardiovascular, other than hyperlipidemic/HTN	Lisinopril, Hydrochlorothiazide		1	
11, 12	Antihypertensives and Cardiovascular, other than hyperlipidemic/HTN	Lisinopril, Metoprolol		1	
11, 12	Antihypertensives and Cardiovascular, other than hyperlipidemic/HTN	Lisinopril; Lasix; Atenol		1	
11, 12	Antihypertensives and Cardiovascular, other than hyperlipidemic/HTN	Atenol; Captopril; Furosemide	1		
11, 12	Antihypertensives and Cardiovascular, other than hyperlipidemic/HTN	Diltiazem	1		
15	Endocrine/Metabolic agents	Fosamax	1		
15	Endocrine/Metabolic agents	Levothroid	1	1	
18	Hormones/steroids	Estradiol	1		
18	Hormones/steroids	Premarin		1	
21	Vitamins, minerals, food supplements	Vitamin D; Aplpha-Lipoic Acid; Multi-vitamin, Tumeric Acid		1	
21	Vitamins, minerals, food supplements	Calcium with Vitamin D	1		
21	Vitamins, minerals, food supplements	Ferrous Sulphate	1		
21	Vitamins, minerals, food supplements	Multi-vitamin	2		
99	Other	Allopurinol		1	
99	Other	Doxazosin		1	
99	Other	Terazosin		1	
99	Other	Potassium Cholride	1		

APPENDIX I  
[0191]

TABLE S9

Age associated differences common to both CR and CNR					
	Name	FC CR vs Yng	FC CNR vs Yng	QV CR vs Yng	QC CNR vs Yng
phenoD	GAMMA DELTA CELLS	-3.5	-1.4	0.12	0.2
phenoD	MONOCYTES	1.3	1.1	0.16	0.17
CytM	EOTAXIN	2	1.4	0.02	0.17
cytM	IP10	1.8	1.8	0.05	0.15
pfD	cd8_IFNa_STAT1	-1.4	-4	0.11	0
pfD	cd8_IL21_STAT1	-1.4	-2.1	0.11	0

TABLE S9-continued

Age associated differences common to both CR and CNR					
Name		FC CR vs Yng	FC CNR vs Yng	QV CR vs Yng	QC CNR vs Yng
pfBaselineD	cd8_Unstimulated_STAT5	1.1	1.1	0.09	0.02
pfBaselineD	cd8_Unstimulated_STAT3	1.2	1.2	0.09	0
pfBaselineD	cd8_Unstimulated_STAT1	1.6	1.7	0.05	0
geD	NUDCD2	-2.1	-1.9	0.02	0.07
geD	CTNND2	-2	-1.9	0.02	0.13
geD	TNFRSF11A	-1.3	-1.8	0.05	0.07
geD	HIVEP3	-1.2	-1.7	0.12	0.07
geD	NF2	-1.7	-1.7	0.02	0.17
geD	BAG5	-1.4	-1.6	0.03	0.07
geD	IGF2BP2	-1.4	-1.6	0.04	0.07
geD	CDH1	-1.8	-1.6	0.02	0.1
geD	CEACAM6	-1.3	-1.6	0.06	0.11
geD	PSME1	-1.6	-1.6	0.05	0.12
geD	TNFAIP8L1	-1.5	-1.6	0.04	0.13
geD	CARD14	-1.3	-1.6	0.06	0.13
geD	SMAD3	-1.3	-1.6	0.11	0.17
geD	FRK	-1.5	-1.5	0.02	0.07
geD	NLGN4X	-1.4	-1.5	0.02	0.07
geD	NF2	-1.3	-1.5	0.05	0.07
geD	SARNP	-1.3	-1.5	0.05	0.07
geD	XRCC6	-1.2	-1.5	0.03	0.07
geD	FLJ23834	-1.1	-1.5	0.12	0.07
geD	CTNNAL1	-2	-1.5	0.04	0.1
geD	ERC1	-1.3	-1.5	0.06	0.1
geD	ICA1L	-1.2	-1.5	0.12	0.1
geD	PCDH7	-1.2	-1.5	0.15	0.1
geD	PEA15	-1.4	-1.5	0.12	0.11
geD	RIMS2	-1.3	-1.5	0.06	0.11
geD	ROBO1	-1.3	-1.5	0.06	0.11
geD	CDH13	-1.7	-1.5	0.02	0.12
geD	RABEP1	-3.3	-1.5	0.02	0.14
geD	REL	-1.4	-1.5	0.04	0.14
geD	C14orf153	-1.4	-1.5	0.11	0.14
geD	FGA	-1.2	-1.5	0.09	0.14
geD	IFT52	-1.5	-1.5	0.06	0.15
geD	LEAP2	-1.4	-1.5	0.06	0.15
geD	FCRLA	-1.3	-1.5	0.09	0.15
geD	HM13	-1.2	-1.5	0.18	0.15
geD	MAG1	-1.3	-1.5	0.04	0.17
geD	NDUFS1	-1.2	-1.5	0.12	0.17
geD	SOCS4	-1.6	-1.5	0.05	0.18
geD	RAC1	-1.8	-1.5	0.02	0.19
geD	SIK2	-1.3	-1.5	0.09	0.19
geD	AP1G1	-2	-1.4	0.02	0.07
geD	ATP5B	-1.9	-1.4	0.03	0.07
geD	STXBP5	-1.6	-1.4	0.03	0.07
geD	APEX1	-1.6	-1.4	0.07	0.07
geD	DLL3	-1.5	-1.4	0.09	0.07
geD	PUF60	-1.4	-1.4	0.08	0.07
geD	SEMA5A	-1.3	-1.4	0.03	0.07
geD	BCAP29	-1.3	-1.4	0.04	0.07
geD	INCENP	-1.3	-1.4	0.05	0.07
geD	EXOC6	-1.3	-1.4	0.05	0.07
geD	IL17D	-1.3	-1.4	0.07	0.07
geD	PTPN11	-1.2	-1.4	0.06	0.07
geD	PPARA	-1.2	-1.4	0.07	0.07
geD	DLC1	-1.2	-1.4	0.12	0.07
geD	MIB1	-1.1	-1.4	0.15	0.07
geD	ITGB8	-1.1	-1.4	0.16	0.07
geD	MAP4K4	-2.5	-1.4	0.02	0.08
geD	THRA	-1.8	-1.4	0.03	0.08
geD	CD1E	-1.6	-1.4	0.18	0.09
geD	RFFL	-1.3	-1.4	0.12	0.09
geD	CLN8	-1.2	-1.4	0.12	0.09
geD	SOCS5	-1.2	-1.4	0.15	0.09
geD	CDH4	-1.1	-1.4	0.18	0.09
geD	EBF1	-1.3	-1.4	0.03	0.1
geD	XCL2	-1.3	-1.4	0.04	0.1
geD	DNM3	-1.3	-1.4	0.04	0.1
geD	FXR1	-1.3	-1.4	0.06	0.1
geD	PTGER2	-1.5	-1.4	0.02	0.11
geD	SMAD1	-1.3	-1.4	0.03	0.11

TABLE S9-continued

Age associated differences common to both CR and CNR					
Name	FC CR vs Yng	FC CNR vs Yng	QV CR vs Yng	QC CNR vs Yng	
geD	SLTM	-1.8	-1.4	0.04	0.12
geD	SNAP29	-1.5	-1.4	0.03	0.12
geD	TLN2	-1.5	-1.4	0.07	0.12
geD	PPFIBP1	-1.4	-1.4	0.02	0.12
geD	IL28RA	-1.3	-1.4	0.04	0.12
geD	EFNB1	-1.1	-1.4	0.18	0.12
geD	STEAP2	-2	-1.4	0.02	0.13
geD	USP33	-1.5	-1.4	0.02	0.13
geD	IRAK4	-1.5	-1.4	0.05	0.13
geD	TGFB2	-1.4	-1.4	0.03	0.13
geD	PRUNE2	-1.4	-1.4	0.06	0.13
geD	CASP9	-1.3	-1.4	0.06	0.13
geD	PSMB1	-1.2	-1.4	0.12	0.13
geD	PHB	-1.2	-1.4	0.14	0.13
geD	TIA1	-1.3	-1.4	0.07	0.14
geD	SP3	-1.2	-1.4	0.18	0.14
geD	ASB1	-1.1	-1.4	0.17	0.14
geD	MIA3	-1.6	-1.4	0.02	0.15
geD	PCDH9	-1.3	-1.4	0.07	0.15
geD	NOD2	-1.3	-1.4	0.09	0.15
geD	NEK11	-1.3	-1.4	0.1	0.15
geD	ERMAP	-1.2	-1.4	0.08	0.15
geD	DYRK2	-1.6	-1.4	0.02	0.16
geD	HMGB2	-1.5	-1.4	0.03	0.16
geD	RSPH1	-1.4	-1.4	0.05	0.16
geD	RALBP1	-1.4	-1.4	0.11	0.16
geD	FKBP1B	-1.3	-1.4	0.1	0.16
geD	ZFYVE9	-1.2	-1.4	0.13	0.16
geD	IL13RA1	-1.2	-1.4	0.13	0.16
geD	SOD2	-1.6	-1.4	0.02	0.17
geD	ERAP1	-1.2	-1.4	0.17	0.17
geD	APAF1	-2.8	-1.4	0.02	0.18
geD	ELMOD2	-1.4	-1.4	0.05	0.18
geD	COL3A1	-1.5	-1.4	0.09	0.19
geD	MCAM	-1.4	-1.4	0.12	0.19
geD	PSMB1	-1.3	-1.4	0.07	0.19
geD	TCTN3	-1.9	-1.3	0.07	0.07
geD	PTGR1	-1.8	-1.3	0.02	0.07
geD	IL7	-1.4	-1.3	0.04	0.07
geD	TPBG	-1.4	-1.3	0.05	0.07
geD	DDR2	-1.3	-1.3	0.12	0.07
geD	C7orf16	-1.2	-1.3	0.05	0.07
geD	MYST4	-1.1	-1.3	0.18	0.07
geD	TSLP	-1.1	-1.3	0.2	0.07
geD	L3MBTL4	-1.5	-1.3	0.03	0.09
geD	CMTM8	-1.4	-1.3	0.02	0.09
geD	PTGR2	-1.2	-1.3	0.02	0.09
geD	CDC42	-1.5	-1.3	0.03	0.1
geD	MASP1	-1.4	-1.3	0.02	0.1
geD	DMBT1	-1.2	-1.3	0.02	0.1
geD	TAOK2	-1.6	-1.3	0.04	0.11
geD	DNM1L	-1.4	-1.3	0.03	0.11
geD	FXR1	-1.2	-1.3	0.11	0.11
geD	B3GALNT1	-1.1	-1.3	0.2	0.11
geD	PSMA4	-1.6	-1.3	0.02	0.12
geD	RRAGA	-1.5	-1.3	0.03	0.12
geD	IGBP1	-1.4	-1.3	0.02	0.12
geD	ABL1	-1.2	-1.3	0.05	0.12
geD	CRADD	-1.2	-1.3	0.09	0.12
geD	C9orf61	-1.1	-1.3	0.1	0.12
geD	PURB	-1.5	-1.3	0.02	0.13
geD	DSTN	-1.4	-1.3	0.03	0.13
geD	CXCL12	-1.3	-1.3	0.04	0.13
geD	PLDN	-1.6	-1.3	0.03	0.14
geD	SULF1	-1.5	-1.3	0.03	0.14
geD	FKBP10	-1.4	-1.3	0.04	0.14
geD	BUB3	-1.3	-1.3	0.06	0.14
geD	BMP2	-1.3	-1.3	0.07	0.14
geD	MIG7	-1.2	-1.3	0.09	0.14
geD	CMTM4	-1.2	-1.3	0.19	0.14
geD	SEMA5A	-1.9	-1.3	0.02	0.15
geD	DCBLD1	-1.5	-1.3	0.03	0.15

TABLE S9-continued

Age associated differences common to both CR and CNR					
Name	FC CR vs Yng	FC CNR vs Yng	QV CR vs Yng	QC CNR vs Yng	
geD	DRAM	-1.4	-1.3	0.04	0.15
geD	SIK1	-1.3	-1.3	0.1	0.15
geD	PLG	-1.5	-1.3	0.02	0.16
geD	HNMT	-1.4	-1.3	0.03	0.16
geD	TNFRSF19	-1.3	-1.3	0.05	0.16
geD	IFT140	-1.1	-1.3	0.09	0.16
geD	CUL1	-1.1	-1.3	0.16	0.16
geD	IL1RAP	-1.6	-1.3	0.03	0.17
geD	CYCS	-1.5	-1.3	0.02	0.17
geD	PPM1F	-1.3	-1.3	0.06	0.17
geD	RNMTL1	-1.1	-1.3	0.17	0.17
geD	RYR2	-1.1	-1.3	0.19	0.17
geD	SMURF2	-1.8	-1.3	0.04	0.18
geD	NF2	-1.7	-1.3	0.02	0.18
geD	ZNF346	-1.5	-1.3	0.18	0.18
geD	KRT18	-1.4	-1.3	0.02	0.18
geD	CDC42SE2	-1.4	-1.3	0.04	0.18
geD	RND1	-1.4	-1.3	0.08	0.18
geD	NOTCH2	-1.4	-1.3	0.09	0.18
geD	STK38	-1.4	-1.3	0.16	0.18
geD	SMAD2	-1.3	-1.3	0.04	0.18
geD	FBNP1L	-1.3	-1.3	0.07	0.18
geD	SNIP	-1.3	-1.3	0.1	0.18
geD	TRIB1	-1.2	-1.3	0.14	0.18
geD	PPIC	-1.5	-1.3	0.04	0.19
geD	TGFBI	-1.4	-1.3	0.06	0.19
geD	TXLNA	-1.3	-1.3	0.05	0.19
geD	SLFN5	-1.3	-1.3	0.08	0.19
geD	SMAD5	-1.2	-1.3	0.14	0.19
geD	SON	-1.6	-1.3	0.02	0.2
geD	SWAP70	-1.5	-1.3	0.04	0.2
geD	ALK	-1.4	-1.3	0.06	0.2
geD	AGGF1	-1.3	-1.3	0.11	0.2
geD	CASP10	-1.5	-1.2	0.09	0.07
geD	DIAPH2	-1.1	-1.2	0.19	0.1
geD	GREM2	-1.3	-1.2	0.04	0.11
geD	SPN	-1.3	-1.2	0.1	0.12
geD	HBXIP	-1.2	-1.2	0.18	0.15
geD	C14orf153	-1.7	-1.2	0.1	0.16
geD	JAKMIP1	-1.3	-1.2	0.05	0.16
geD	COL27A1	-1.3	-1.2	0.06	0.16
geD	TIAM2	-1.1	-1.2	0.14	0.16
geD	IK	-1.2	-1.2	0.07	0.17
geD	CD9	-1.1	-1.2	0.18	0.17
geD	VNN1	-1.5	-1.2	0.03	0.18
geD	IFT88	-1.5	-1.2	0.04	0.18
geD	PTK2	-1.4	-1.2	0.06	0.18
geD	SRA1	-1.2	-1.2	0.11	0.18
geD	SNX1	-1.2	-1.2	0.12	0.18
geD	PRKDC	-1.3	-1.2	0.06	0.19
geD	POLA1	-1.1	-1.2	0.19	0.19
geD	FGG	-2.6	-1.2	0.04	0.2
geD	SNX4	-1.4	-1.2	0.1	0.2
geD	FAT3	-1.2	-1.2	0.06	0.2
geD	LOC645166	1.4	1.1	0.02	0.18
geD	TUBB	1.4	1.2	0.02	0.1
geD	FAF1	1.4	1.2	0.02	0.12
geD	PSMB2	1.2	1.2	0.05	0.13
geD	TH1L	1.3	1.2	0.02	0.14
geD	MAEA	1.1	1.2	0.16	0.15
geD	PVRL2	1.2	1.2	0.11	0.16
geD	MPZL2	1.3	1.2	0.03	0.17
geD	FKBP4	1.3	1.2	0.04	0.17
geD	RBP4	1.3	1.2	0.02	0.18
geD	LAMC2	1.6	1.2	0.02	0.2
geD	CTSC	1.3	1.3	0.03	0.07
geD	CASP4	1.3	1.3	0.04	0.07
geD	BECN1	1.3	1.3	0.06	0.07
geD	C2	1.7	1.3	0.02	0.1
geD	EXOC7	1.4	1.3	0.03	0.12
geD	CEACAM1	1.2	1.3	0.07	0.13
geD	CCM2	1.4	1.3	0.13	0.14

TABLE S9-continued

Age associated differences common to both CR and CNR					
Name	FC CR vs Yng	FC CNR vs Yng	QV CR vs Yng	QC CNR vs Yng	
geD	PURB	1.3	1.3	0.05	0.15
geD	CTSS	1.3	1.3	0.07	0.15
geD	LGALS3BP	1.5	1.3	0.02	0.15
geD	GPR135	1.2	1.3	0.12	0.16
geD	MYLPF	1.3	1.3	0.09	0.16
geD	MUC5AC	1.3	1.3	0.17	0.16
geD	RHOA	1.7	1.3	0.02	0.17
geD	GP6	1.5	1.3	0.03	0.19
geD	IFB30	1.5	1.3	0.03	0.19
geD	TNFAIP8	1.7	1.3	0.03	0.2
geD	LITAF	1.2	1.4	0.1	0.07
geD	EHD1	1.7	1.4	0.02	0.07
geD	CNTNAP2	1.2	1.4	0.06	0.08
geD	NRP1	1.3	1.4	0.04	0.11
geD	WNK1	1.4	1.4	0.04	0.11
geD	TNFAIP2	1.5	1.4	0.04	0.12
geD	IFITM2	1.7	1.4	0.02	0.12
geD	MLLT6	1.8	1.4	0.02	0.12
geD	FCGR2A	1.3	1.4	0.03	0.14
geD	SORL1	1.7	1.4	0.03	0.15
geD	B3GALNT1	1.6	1.4	0.02	0.16
geD	IGF2AS	1.6	1.4	0.03	0.16
geD	CEBPB	2	1.4	0.02	0.16
geD	CNTN2	1.3	1.4	0.03	0.17
geD	LRRN2	1.8	1.4	0.02	0.17
geD	THBS1	1.7	1.4	0.03	0.18
geD	SLC13A2	1.2	1.4	0.17	0.19
geD	ADRB3	1.2	1.5	0.15	0.07
geD	CTF1	1.3	1.5	0.07	0.07
geD	IRS2	1.4	1.5	0.02	0.07
geD	SP3	1.2	1.5	0.13	0.08
geD	LTBP2	1.4	1.5	0.04	0.1
geD	ITFG3	1.2	1.5	0.14	0.12
geD	STX1A	1.5	1.5	0.03	0.12
geD	PRKCD	2.1	1.5	0.02	0.14
geD	THRA	1.1	1.5	0.19	0.16
geD	TAL1	1.4	1.5	0.07	0.16
geD	PLEKHF1	2	1.5	0.02	0.16
geD	CR2	1.3	1.5	0.12	0.18
geD	ACTC1	1.4	1.5	0.09	0.18
geD	NINJ2	1.7	1.5	0.03	0.18
geD	LIMS2	2.1	1.5	0.03	0.18
geD	LAMA4	1.2	1.5	0.17	0.19
geD	GYLTL1B	1.8	1.5	0.04	0.19
geD	RABEP1	2	1.5	0.04	0.19
geD	G6PD	1.2	1.6	0.12	0.09
geD	TNR	1.6	1.6	0.14	0.1
geD	MASP2	1.4	1.6	0.06	0.11
geD	PGM5	1.5	1.6	0.05	0.11
geD	RAC2	2.2	1.6	0.02	0.12
geD	ZFR2	1.7	1.6	0.04	0.13
geD	UMOD	1.8	1.6	0.02	0.13
geD	TNXB	1.4	1.6	0.09	0.14
geD	EBI3	1.4	1.6	0.09	0.15
geD	COL27A1	2	1.6	0.02	0.16
geD	CEBPE	1.7	1.6	0.04	0.17
geD	MMP9	1.9	1.6	0.03	0.19
geD	CFD	2.2	1.6	0.03	0.19
geD	DGKZ	2.1	1.6	0.03	0.2
geD	APOA4	1.2	1.7	0.07	0.07
geD	HLA-DPB1	1.4	1.7	0.08	0.07
geD	IL28A	1.3	1.7	0.05	0.13
geD	LILRA5	2	1.7	0.03	0.13
geD	APOL2	1.9	1.7	0.03	0.14
geD	GZMM	1.9	1.7	0.04	0.16
geD	MYADM	1.7	1.7	0.05	0.17
geD	SEMA4A	1.8	1.7	0.05	0.19
geD	LY86	2.1	1.7	0.03	0.19
geD	TNFSF13B	1.7	1.8	0.02	0.08
geD	MAP4K2	1.3	1.8	0.09	0.1
geD	IL12RB1	1.2	1.8	0.18	0.13
geD	SSTR3	1.6	1.8	0.06	0.14

TABLE S9-continued

Age associated differences common to both CR and CNR					
Name	FC CR vs Yng	FC CNR vs Yng	QV CR vs Yng	QC CNR vs Yng	
geD	FOXH1	1.8	1.8	0.03	0.16
geD	ZBP1	2.2	1.8	0.03	0.17
geD	DEFB4	1.2	1.9	0.1	0.07
geD	CASP5	1.6	1.9	0.07	0.08
geD	RAPGEF3	1.3	1.9	0.18	0.1
geD	PTGIR	1.6	1.9	0.07	0.1
geD	HRH2	1.4	1.9	0.07	0.14
geD	LSP1	2.3	1.9	0.03	0.14
geD	ADAM33	2	1.9	0.06	0.15
geD	WAS	2.1	1.9	0.03	0.16
geD	CD244	1.3	2	0.09	0.07
geD	CLDN11	1.6	2	0.04	0.07
geD	MYADM	1.7	2	0.02	0.07
geD	COL20A1	1.2	2	0.15	0.1
geD	PEAR1	1.4	2	0.07	0.1
geD	MUC2	1.3	2	0.11	0.12
geD	LAT2	2.1	2	0.03	0.12
geD	PSTPIP1	2.8	2.1	0.02	0.11
geD	MARCO	2.1	2.1	0.07	0.16
geD	UNC5A	1.1	2.1	0.2	0.19
geD	FCN2	2	2.1	0.1	0.19
geD	HLA-DPB1	3.6	2.1	0.02	0.19
geD	CD300LB	1.9	2.2	0.02	0.07
geD	HLA-F	2.2	2.2	0.02	0.07
geD	LILRA5	3.2	2.2	0.02	0.07
geD	CASP8	1.7	2.2	0.09	0.1
geD	GHRHR	1.9	2.2	0.05	0.1
geD	PIK3CD	2.5	2.2	0.02	0.13
geD	ITGB2	1.8	2.2	0.05	0.16
geD	IRF1	2.8	2.2	0.04	0.2
geD	FCGBP	1.3	2.3	0.2	0.1
geD	TREML1	1.7	2.3	0.06	0.1
geD	PDGFRB	1.7	2.3	0.1	0.17
geD	ERCC2	2.2	2.4	0.02	0.07
geD	SLC5A2	2.2	2.4	0.04	0.14
geD	IL10RA	1.9	2.4	0.1	0.16
geD	MUC4	1.8	2.4	0.12	0.18
geD	NKX2-3	1.6	2.5	0.08	0.07
geD	HRH3	2.4	2.5	0.08	0.1
geD	CDSN	1.6	2.6	0.06	0.07
geD	MINK1	2	2.6	0.04	0.1
geD	ACVR1B	2	2.7	0.03	0.07
geD	UCP3	2.8	2.7	0.02	0.07
geD	MUC4	1.9	2.7	0.06	0.1
geD	PTCRA	1.6	2.7	0.14	0.12
geD	PROP1	1.7	2.7	0.12	0.12
geD	HLA-J	3.9	2.7	0.02	0.16
geD	POLM	2.1	2.7	0.1	0.18
geD	KIR2DL4	1.7	2.8	0.06	0.07
geD	GYPC	2.1	2.8	0.03	0.07
geD	CACNB3	2.4	2.8	0.07	0.15
geD	LILRA3	2.8	2.8	0.06	0.16
geD	LAX1	1.5	2.9	0.13	0.07
geD	GHSR	1.6	2.9	0.1	0.07
geD	RARA	1.7	2.9	0.12	0.1
geD	RUNX1	2.2	3	0.04	0.07
geD	HLA-B	3.4	3	0.04	0.1
geD	HLA-DOA	3.5	3	0.03	0.14
geD	JAK3	2.2	3.1	0.02	0.07
geD	CEACAM19	2.8	3.1	0.04	0.15
geD	CPLX2	2.6	3.3	0.06	0.12
geD	TCL6	1.8	3.5	0.19	0.15
geD	E2F2	2.1	3.6	0.03	0.14
geD	PTAFR	5.6	3.7	0.03	0.18
geD	HLA-DRB1	2.5	3.8	0.11	0.15
geD	CD14	4.2	4	0.03	0.11
geD	MUC4	1.6	4.1	0.06	0.07
geD	LALBA	2.1	4.2	0.03	0.13
geD	FCER1G	2.4	4.3	0.14	0.16
geD	TAOK2	2.7	4.4	0.04	0.07
geD	BCAM	2.9	4.4	0.07	0.13
geD	MLXIPL	3.1	4.5	0.07	0.13

TABLE S9-continued

Age associated differences common to both CR and CNR					
Name	FC CR vs Yng	FC CNR vs Yng	QV CR vs Yng	QC CNR vs Yng	
geD	CCL24	2.6	4.6	0.1	0.14
geD	HLA-DRB3	2.6	4.8	0.14	0.14
geD	LILRA6	8.8	4.8	0.03	0.18
geD	IL8RA	4.3	5	0.1	0.2
geD	CD79A	4	5.7	0.08	0.15
geD	HLA-DRB5	4.2	5.7	0.09	0.16
geD	FCN1	4.6	5.7	0.09	0.18
geD	BCL2	3.5	6	0.06	0.1
geD	ADAMTS7	3.8	6.9	0.1	0.16
geD	CD4	3.1	8.5	0.07	0.07
geD	RTN3	5.4	19.7	0.1	0.18
geD	FCGR3B	6.5	23.6	0.12	0.12

## APPENDIX J

[0192]

TABLE S10

CR-specific measurements			
DataType	Name	Fold-change	Q-value
phenoD	CD8 CENTRAL MEMORY	2.1	0.06
phenoD	B CELLS	1.5	0.12
phenoD	CD4 EFFECTOR MEMORY	-2.7	0.12
phenoD	NK T CELLS	-2.6	0.12
phenoD	CD4	-6.5	0.15
geD	CD99L2	2.2	0
geD	HSPD1	-1.4	0.01
geD	SRF	1.7	0.02
geD	BOK	2.5	0.02
geD	LRP10	2.8	0.02
geD	UBE2I	1.7	0.02
geD	PANX1	1.7	0.02
geD	NFKB1B	1.4	0.02
geD	BLK	1.6	0.02
geD	RAB5C	1.8	0.02
geD	MKL1	1.7	0.02
geD	NFKB2	1.5	0.02
geD	SMAD7	1.6	0.02
geD	IGF1	1.5	0.02
geD	NR3C1	1.5	0.02
geD	ITGA2B	1.4	0.02
geD	C1R	2.2	0.02
geD	BOC	1.4	0.02
geD	CLSTN3	2	0.02
geD	NISCH	2.6	0.02
geD	SP1	1.6	0.02
geD	PI4KB	2.2	0.02
geD	PML	1.6	0.02
geD	LAMA5	1.8	0.02
geD	TNFSF10	2.4	0.02
geD	MUC5AC	1.6	0.02
geD	RAG1AP1	2.2	0.02
geD	LILRA4	1.4	0.02
geD	CLN3	1.7	0.02
geD	CD40	2.1	0.02
geD	AGPAT2	1.6	0.02
geD	RAF1	1.8	0.02
geD	EDN1	1.5	0.02
geD	FEZ2	1.9	0.02
geD	SART3	1.8	0.02
geD	POGK	1.8	0.02
geD	PXN	1.4	0.02
geD	HIVEP2	2.3	0.02
geD	NEK6	1.9	0.02
geD	IGKC	1.6	0.02
geD	SECTM1	1.7	0.02

TABLE S10-continued

CR-specific measurements			
DataType	Name	Fold-change	Q-value
geD	FCN1	1.5	0.02
geD	GRB2	1.4	0.02
geD	PPP1R15A	2	0.02
geD	GPX4	1.3	0.02
geD	MAMDC4	1.6	0.02
geD	SOCS7	2.3	0.02
geD	COL9A1	1.7	0.02
geD	TLR9	1.5	0.02
geD	PTK2B	1.8	0.02
geD	CLDN7	1.8	0.02
geD	RHOA	1.6	0.02
geD	NOXA1	1.5	0.02
geD	PLAU	2.5	0.02
geD	MLL3	1.6	0.02
geD	TNNI2	1.8	0.02
geD	FKBP14	1.6	0.02
geD	AKT1	1.4	0.02
geD	THBS3	1.7	0.02
geD	PCDHA5	2.1	0.02
geD	F8	1.5	0.02
geD	CDKN2A	1.4	0.02
geD	LIN7C	1.5	0.02
geD	APOA1	1.6	0.02
geD	DYRK2	1.3	0.02
geD	KIF13B	1.7	0.02
geD	CCR5	1.5	0.02
geD	DAXX	1.7	0.02
geD	WNK2	1.6	0.02
geD	CD52	1.5	0.02
geD	ALCAM	1.8	0.02
geD	CISH	1.4	0.02
geD	TLX2	1.8	0.02
geD	AHSG	1.7	0.02
geD	AGGF1	3.3	0.02
geD	CREBBP	1.8	0.02
geD	CDKN2C	1.7	0.02
geD	GAPVD1	1.5	0.02
geD	FGB	1.5	0.02
geD	TNIP2	1.3	0.02
geD	TMEM8	1.4	0.02
geD	F5	1.9	0.02
geD	SART1	1.8	0.02
geD	NOS3	1.5	0.02
geD	PSMG3	1.3	0.02
geD	MCL1	2.1	0.02
geD	PPARG	2.1	0.02
geD	NEO1	1.9	0.02
geD	TRPC4AP	1.6	0.02
geD	CRYAB	1.5	0.02

TABLE S10-continued

CR-specific measurements			
DataType	Name	Fold-change	Q-value
geD	CX3CL1	1.7	0.02
geD	FOS	1.5	0.02
geD	FOXC1	1.4	0.02
geD	ICAM1	1.8	0.02
geD	SRC	3.6	0.02
geD	VAMP7	1.7	0.02
geD	BYSL	1.3	0.02
geD	CNTR0B	1.4	0.02
geD	BAK1	1.4	0.02
geD	BBS9	1.4	0.02
geD	PRKRIR	1.6	0.02
geD	POLL	2.1	0.02
geD	CLOCK	-2.3	0.02
geD	HCFC1	-2.8	0.02
geD	CAV1	-1.6	0.02
geD	MALT1	-2.2	0.02
geD	TOX	-1.9	0.02
geD	ITGAE	-2.2	0.02
geD	CD1E	-2	0.02
geD	CDKN1B	-1.3	0.02
geD	SPP1	-2	0.02
geD	IL18	-5.8	0.02
geD	BRCA1	-3.3	0.02
geD	NAE1	-3.1	0.02
geD	PDCD6IP	-2.5	0.02
geD	RAB4A	-1.5	0.02
geD	GLO1	-2.2	0.02
geD	PDCD5	-1.8	0.02
geD	CD8A	-2.1	0.02
geD	HIF1A	-1.6	0.02
geD	ATP6V1H	-1.4	0.02
geD	EDNRB	-1.8	0.02
geD	IGFBP3	-2.9	0.02
geD	FER	-1.9	0.02
geD	PTK2	-2.4	0.02
geD	MIA3	-2.4	0.02
geD	FNBP1	-1.4	0.02
geD	SBDS	-1.9	0.02
geD	SLFN12	-2.8	0.02
geD	RAB3B	-3	0.02
geD	PTPRC	-2.4	0.02
geD	PTGIS	-1.8	0.02
geD	STXBP5	-1.4	0.02
geD	HIF1A	-2.1	0.02
geD	TOP1	-2	0.02
geD	TBP	-2.3	0.02
geD	SMAD4	-2.8	0.02
geD	SEMA6A	-2	0.02
geD	PPFIBP1	-1.6	0.02
geD	MSH3	-1.7	0.02
geD	PCNA	-1.5	0.02
geD	KLRC2	-2.1	0.02
geD	SELS	-2.4	0.02
geD	LAMA4	-2.3	0.02
geD	ADAT1	-2.2	0.02
geD	MCTS1	-2.1	0.02
geD	CD69	-2.4	0.02
geD	ADAM10	-2.6	0.02
geD	CLEC4A	-2	0.02
geD	ERCC4	-4.5	0.02
geD	CARD16	-4.3	0.02
geD	CLDN1	-2	0.02
geD	SYNJ1	-1.9	0.02
geD	UACA	-1.7	0.02
geD	EGR1	-2.1	0.02
geD	FN1	-3.9	0.02
geD	PRKAR2A	-1.6	0.02
geD	ESR1	-1.8	0.02
geD	PSME3	-1.9	0.02
geD	CEACAM6	-1.6	0.02
geD	DOCK11	-1.7	0.02
geD	PSMD1	-2.6	0.02

TABLE S10-continued

CR-specific measurements			
DataType	Name	Fold-change	Q-value
geD	CD247	-1.3	0.02
geD	CASK	-1.7	0.02
geD	LIG4	-2.1	0.02
geD	GCNT2	-2.5	0.02
geD	ADARB1	-1.7	0.02
geD	SNX3	-1.9	0.02
geD	DGCR2	-1.6	0.02
geD	FKBP3	-1.8	0.02
geD	CD59	-1.7	0.02
geD	XRCC2	-1.9	0.02
geD	RND3	-1.5	0.02
geD	RAB5A	-1.9	0.02
geD	PSMD12	-2	0.02
geD	LAMC1	-2.3	0.02
geD	ZEB2	-2.2	0.02
geD	ID2	-1.4	0.02
geD	SLC23A2	-2	0.02
geD	PTPN22	-1.5	0.02
geD	HINT1	-2.2	0.02
geD	STAT3	-1.9	0.02
geD	MCL1	-1.8	0.02
geD	FERMT2	-1.9	0.02
geD	PVRL3	-2	0.02
geD	PTGS2	-2.5	0.02
geD	GAPVD1	-6.3	0.02
geD	BFAR	-2.6	0.02
geD	PDIA3	-1.6	0.02
geD	PACSN2	-2.5	0.02
geD	ITCH	-1.6	0.02
geD	SPOCK1	-1.3	0.02
geD	TNFRSF1A	-1.5	0.02
geD	PTPN1	-2.1	0.02
geD	BUB3	-1.9	0.02
geD	MYC	-1.8	0.02
geD	PRKRA	-1.5	0.02
geD	PDCD2L	-1.9	0.02
geD	EFEMP1	-1.6	0.02
geD	IRS1	-1.4	0.02
geD	IFT81	-1.8	0.02
geD	PKP3	1.8	0.03
geD	IL1RN	1.7	0.03
geD	SUMO1	1.3	0.03
geD	CASP10	1.6	0.03
geD	C3AR1	1.6	0.03
geD	ZFP36	1.5	0.03
geD	CD5	1.7	0.03
geD	PEX5	1.4	0.03
geD	DGKZ	2.3	0.03
geD	BCL2L1	1.3	0.03
geD	NUPR1	1.9	0.03
geD	COL6A2	1.7	0.03
geD	ACTN4	2	0.03
geD	AMOTL1	1.5	0.03
geD	GPR77	1.5	0.03
geD	TCL1A	1.3	0.03
geD	PSEN1	1.4	0.03
geD	ELMO2	1.8	0.03
geD	LTBP2	1.6	0.03
geD	SDK1	1.7	0.03
geD	CYBA	1.5	0.03
geD	NTSR1	1.6	0.03
geD	ITGB3BP	1.6	0.03
geD	TAPBP	1.8	0.03
geD	HOXB7	1.8	0.03
geD	GDF5	1.6	0.03
geD	NOG	1.5	0.03
geD	NF1	1.6	0.03
geD	CD163L1	1.9	0.03
geD	HLA-A	1.3	0.03
geD	PHF17	1.3	0.03
geD	MGMT	1.6	0.03
geD	ROBO3	1.3	0.03

TABLE S10-continued

CR-specific measurements			
DataType	Name	Fold-change	Q-value
geD	HLA-C	1.7	0.03
geD	BAX	1.5	0.03
geD	FOXJ1	1.5	0.03
geD	IFI27	3	0.03
geD	MAPK14	1.6	0.03
clN3	CLN3	1.5	0.03
geD	EGF	1.6	0.03
geD	PARVB	1.6	0.03
geD	CAPN10	2	0.03
geD	TERT	1.6	0.03
geD	PLAGL1	1.4	0.03
geD	IGFALS	1.6	0.03
geD	CFLAR	1.6	0.03
geD	HDACS	1.2	0.03
geD	ERBB2	2.3	0.03
geD	RRAD	1.8	0.03
geD	RPS3	1.8	0.03
geD	ULBP2	1.8	0.03
geD	CSF2RB	1.3	0.03
geD	GHRL	1.7	0.03
geD	CUTA	2	0.03
geD	SIRPA	1.7	0.03
geD	TP53AIP1	2	0.03
geD	GMD5	1.8	0.03
geD	HMOX1	2.4	0.03
geD	TNFRSF10B	1.6	0.03
geD	CLDN19	1.8	0.03
geD	GP9	1.6	0.03
geD	TRAF1	7.7	0.03
geD	TGFB11	1.7	0.03
geD	CHRN2	2.4	0.03
geD	CFHR1	1.3	0.03
geD	ACIN1	1.4	0.03
geD	AQP1	1.7	0.03
geD	ADRM1	1.8	0.03
geD	FANCC	2.1	0.03
geD	IL18BP	1.5	0.03
geD	INHBA	1.5	0.03
geD	LIF	1.5	0.03
geD	ARHGAP1	1.3	0.03
geD	SOD1	1.5	0.03
geD	TGFB1	1.4	0.03
geD	NRP2	2	0.03
geD	GATA2	1.9	0.03
geD	NLRP1	1.5	0.03
geD	FOLR1	1.6	0.03
geD	WDR59	2.6	0.03
geD	CD33	1.5	0.03
geD	HRAS	1.8	0.03
geD	DAD1	1.6	0.03
geD	WDR92	2.2	0.03
geD	PRKAR1B	1.9	0.03
geD	MYC	1.6	0.03
geD	MKNK2	1.4	0.03
geD	IGF2BP2	1.8	0.03
geD	CCR10	1.7	0.03
geD	SECTM1	1.3	0.03
geD	SDF4	1.4	0.03
geD	RAMP3	1.4	0.03
geD	TIAM1	1.3	0.03
geD	SMAD2	-2.4	0.03
geD	DERL1	-2.2	0.03
geD	FASTKD1	-1.8	0.03
geD	UTP11L	-1.8	0.03
geD	PTX3	-2.3	0.03
geD	ITGB8	-1.5	0.03
geD	ACVR1	-2	0.03
geD	MDM4	-2	0.03
geD	GSR	-1.6	0.03
geD	TERF1	-1.5	0.03
geD	SCYE1	-2.2	0.03
geD	C5	-2.1	0.03

TABLE S10-continued

CR-specific measurements			
DataType	Name	Fold-change	Q-value
geD	MAP3K5	-1.7	0.03
geD	EXOC5	-1.6	0.03
geD	LRIG3	-2.1	0.03
geD	FLRT2	-2.6	0.03
geD	HIPK2	-1.6	0.03
geD	C2CD2	-1.8	0.03
geD	NFE2L3	-2.6	0.03
geD	HIVEP1	-2.4	0.03
geD	SCYE1	-1.6	0.03
geD	DCTN3	-3.4	0.03
geD	TDGF1	-1.4	0.03
geD	C1QTNF3	-3.2	0.03
geD	PDCD4	-2.2	0.03
geD	HRH1	-2.4	0.03
geD	ILK	-3.1	0.03
geD	CXCL3	-3.3	0.03
geD	FLI1	-1.6	0.03
geD	M6PR	-1.7	0.03
geD	JAK1	-1.3	0.03
geD	SLC1A2	-2.1	0.03
geD	BCL2	-1.8	0.03
geD	ADH5	-2.7	0.03
geD	CD46	-2.3	0.03
geD	AKAP11	-1.4	0.03
geD	APOH	-1.5	0.03
geD	PAFAH1B1	-1.7	0.03
geD	ROCK2	-1.4	0.03
geD	SEMA3A	-1.7	0.03
geD	CEACAM1	-1.7	0.03
geD	NPHP4	-2.2	0.03
geD	MDM2	-1.4	0.03
geD	SP1	-1.5	0.03
geD	LIMS1	-3.1	0.03
geD	DCBLD2	-1.5	0.03
geD	CSE1L	-1.2	0.03
geD	PKP2	-1.9	0.03
geD	E2F2	-1.3	0.03
geD	SEMA3A	-1.8	0.03
geD	PAFAH1B2	-1.8	0.03
geD	PLDN	-2.2	0.03
geD	HIP1	-1.6	0.03
geD	GDF6	-1.9	0.03
geD	SH3KBP1	-1.7	0.03
geD	THAP2	-2.7	0.03
geD	RPS3A	-2	0.03
geD	ADAL	-1.5	0.03
geD	MTMR3	-2.4	0.03
geD	MBD4	-1.5	0.03
geD	SLC26A6	-1.5	0.03
geD	PRKAR1A	-1.5	0.03
geD	PDLIM5	-1.9	0.03
geD	PDLIM5	-1.7	0.03
geD	STAT3	-1.5	0.03
geD	DYRK2	-1.4	0.03
geD	PSMC6	-2.1	0.03
geD	MLLT11	-1.7	0.03
geD	MPZL3	-1.6	0.03
geD	MAGED1	-1.3	0.03
geD	SERPINB9	-1.6	0.03
geD	SERPINB2	-2.1	0.03
geD	MLLT3	-1.5	0.03
geD	AQP1	-1.4	0.03
geD	RPS6KA3	-1.6	0.03
geD	MYO6	-2.5	0.03
geD	C2	-1.8	0.03
geD	EEF1A1	-1.4	0.03
geD	ROCK2	-1.6	0.03
geD	CCR9	-2	0.03
geD	PSMG2	-4.4	0.03
geD	FBG	-1.6	0.03
geD	PML	-2	0.03
geD	SMNDC1	-1.4	0.03

TABLE S10-continued

CR-specific measurements			
DataType	Name	Fold-change	Q-value
geD	HIVEP3	5.2	0.04
geD	PARVG	1.5	0.04
geD	MAPK8	1.8	0.04
geD	CD3D	1.6	0.04
geD	HDAC5	1.7	0.04
geD	FXYD5	1.9	0.04
geD	CDH23	1.7	0.04
geD	PPT1	3.9	0.04
geD	ZNF346	1.4	0.04
geD	CLAPIN1	1.5	0.04
geD	TRIM69	1.7	0.04
geD	COL18A1	1.6	0.04
geD	MLLT1	1.6	0.04
geD	METTL11A	1.4	0.04
geD	SIRPA	1.5	0.04
geD	CXCL12	1.3	0.04
geD	TMBIM6	2	0.04
geD	MLLT1	1.2	0.04
geD	IF16	1.5	0.04
geD	HSPA5	1.7	0.04
geD	KCNH3	1.5	0.04
geD	COL14A1	1.5	0.04
geD	IMPDH1	1.6	0.04
geD	TNFRSF18	2.1	0.04
geD	SFRS17A	1.4	0.04
geD	MPL	1.9	0.04
geD	RRAGC	1.7	0.04
geD	HPS4	1.8	0.04
geD	MUC2	1.3	0.04
geD	CD276	2.1	0.04
geD	IRAK1	4.5	0.04
geD	PRKD2	1.5	0.04
geD	CDH10	2.2	0.04
geD	DAB2	1.8	0.04
geD	CYBB	1.4	0.04
geD	B2M	1.2	0.04
geD	ACTN1	1.5	0.04
geD	PPM1D	1.9	0.04
geD	C1orf38	1.5	0.04
geD	ABL1	1.5	0.04
geD	NOL3	1.5	0.04
geD	C8A	1.6	0.04
geD	HDAC1	2	0.04
geD	LEFTY2	1.4	0.04
geD	NCF1	2.2	0.04
geD	TTYH1	2.1	0.04
geD	AMICA1	2.5	0.04
geD	SLC26A6	1.8	0.04
geD	FSTL1	1.9	0.04
geD	AP2A2	1.6	0.04
geD	BGLAP	1.9	0.04
geD	CD6	2.9	0.04
geD	FKBP15	1.8	0.04
geD	FASTK	1.4	0.04
geD	PTPN6	1.5	0.04
geD	CMTM5	1.3	0.04
geD	ELN	1.4	0.04
geD	NLRP12	1.6	0.04
geD	CLDN10	1.5	0.04
geD	DAP	1.4	0.04
geD	ADRM1	1.6	0.04
geD	IFITM1	1.3	0.04
geD	LAIR1	1.2	0.04
geD	RP11-138L21.1	1.7	0.04
geD	DDR1	1.8	0.04
geD	RASSF5	1.7	0.04
geD	DCTN3	2.6	0.04
geD	FOXC1	1.6	0.04
geD	LSP1	1.3	0.04
geD	CSNK1E	1.5	0.04
geD	CEBPB	1.7	0.04
geD	RAB5C	2.2	0.04

TABLE S10-continued

CR-specific measurements			
DataType	Name	Fold-change	Q-value
geD	EXOC6	1.9	0.04
geD	CD68	1.4	0.04
geD	TREML2	6.3	0.04
geD	VAV1	1.7	0.04
geD	SERPINB2	1.7	0.04
geD	NME6	1.4	0.04
geD	NFATC4	1.4	0.04
geD	PSME3	1.3	0.04
geD	HLA-DMA	1.4	0.04
geD	ATP2A2	1.7	0.04
geD	ADRA1B	1.9	0.04
geD	CEBPA	2.1	0.04
geD	LYL1	2.9	0.04
geD	ACTN1	1.8	0.04
geD	FCGBP	1.6	0.04
geD	STXBP2	2.2	0.04
geD	NLRP3	1.6	0.04
geD	CFHR3	-2.3	0.04
geD	SLK	-2.6	0.04
geD	AMIGO2	-2.9	0.04
geD	UBE2N	-1.6	0.04
geD	ZFYVE16	-2.6	0.04
geD	GLMN	-2.5	0.04
geD	PTCD2	-2.3	0.04
geD	ID2	-1.9	0.04
geD	ALG9	-1.7	0.04
geD	NBN	-1.5	0.04
geD	AVEN	-2.2	0.04
geD	TIAL1	-1.6	0.04
geD	ZEB2	-2.5	0.04
geD	CTNNA1	-1.7	0.04
geD	BBS7	-1.7	0.04
geD	PIK3R1	-1.5	0.04
geD	MYST4	-1.3	0.04
geD	LEF1	-1.3	0.04
geD	ARF6	-3.3	0.04
geD	PANX1	-1.4	0.04
geD	PTPN12	-2.2	0.04
geD	CLSTN1	-2.8	0.04
geD	IGF2	-2.1	0.04
geD	HMCN1	-1.6	0.04
geD	SLC1A1	-1.3	0.04
geD	TRAT1	-4.3	0.04
geD	HTATIP2	-1.5	0.04
geD	IGBP1	-1.5	0.04
geD	STK38L	-1.6	0.04
geD	RGMB	-2.6	0.04
geD	EXOC1	-1.6	0.04
geD	FCHSD2	-1.5	0.04
geD	7-Sep	-1.4	0.04
geD	RALA	-1.7	0.04
geD	RHOT1	-1.5	0.04
geD	ITGB1	-1.5	0.04
geD	TOLLIP	-2	0.04
geD	ARNTL	-1.4	0.04
geD	BCAP29	-1.7	0.04
geD	AHSG	-1.5	0.04
geD	EXOC8	-2.2	0.04
geD	ADH5	-1.3	0.04
geD	FAF2	-1.9	0.04
geD	NOD1	-2.1	0.04
geD	HPS4	-1.5	0.04
geD	RICTOR	-1.9	0.04
geD	SGK1	-1.6	0.04
geD	FOXC1	-1.5	0.04
geD	PDCL3	-2.4	0.04
geD	CD28	-1.9	0.04
geD	FKBP5	-2.3	0.04
geD	PTPRF	-1.8	0.04
geD	MSX2	-1.6	0.04
geD	SEMA5A	-2.1	0.04
geD	PAG1	-2.1	0.04

TABLE S10-continued

CR-specific measurements			
DataType	Name	Fold-change	Q-value
geD	BLNK	-2.1	0.04
geD	CCL3L3	-2.2	0.04
geD	SMAD3	-2.6	0.04
geD	IFT74	-2.7	0.04
geD	LRP8	-1.4	0.04
geD	MLLT3	-1.4	0.04
geD	WWTR1	-1.7	0.04
geD	DPP4	-2.3	0.04
geD	SHISA5	-2.4	0.04
geD	PRKAR2A	-1.7	0.04
geD	EREG	-2.1	0.04
geD	BLM	-5.3	0.04
geD	ANXA4	-2.5	0.04
geD	GAPVD1	-1.7	0.04
geD	NAIP	-1.6	0.04
geD	CORO1C	-1.2	0.04
geD	LOC731884	-1.8	0.04
geD	CD2BP2	-1.8	0.04
geD	SEMA3C	-1.3	0.04
geD	C11orf82	-2.4	0.04
geD	EIF2AK3	-2.1	0.04
geD	PRKCA	-1.6	0.04
geD	ROBO2	-1.4	0.04
geD	TTYH1	1.9	0.05
geD	CEBPA	1.2	0.05
geD	IGJ	1.6	0.05
geD	ACHE	1.3	0.05
geD	MKNK2	1.2	0.05
geD	NLRC3	1.5	0.05
geD	BTBD9	1.7	0.05
geD	COL6A2	1.6	0.05
geD	FBF1	1.2	0.05
geD	CLDN11	1.6	0.05
geD	HIPK2	1.5	0.05
geD	PPAP2A	1.5	0.05
geD	CTNNB1	1.4	0.05
geD	CECR2	1.5	0.05
geD	BST1	1.6	0.05
geD	PNN	1.9	0.05
geD	PCDH24	1.4	0.05
geD	NFE2L1	1.5	0.05
geD	CCL23	1.6	0.05
geD	GP1BB	1.7	0.05
geD	N-PAC	2.2	0.05
geD	CORO1A	1.4	0.05
geD	LGALS12	1.6	0.05
geD	CASP2	1.6	0.05
geD	HLA-C	1.5	0.05
geD	CCR3	1.4	0.05
geD	IL23A	1.6	0.05
geD	ANGPTL4	1.3	0.05
geD	GATA2	2.9	0.05
geD	PCDH1	1.7	0.05
geD	DDIT4	1.4	0.05
geD	RPH3AL	1.5	0.05
geD	HSPA1A	1.3	0.05
geD	RPS6KA1	1.4	0.05
geD	TFPT	1.5	0.05
geD	SIRT6	1.5	0.05
geD	CHRNA7	1.7	0.05
geD	TROAP	1.6	0.05
geD	TAX1BP3	1.4	0.05
geD	ADAM8	1.4	0.05
geD	TNFRSF1B	1.6	0.05
geD	CSNK2B	1.5	0.05
geD	CD99	4.1	0.05
geD	SERPINA1	1.7	0.05
geD	RAC2	1.2	0.05
geD	MAPK3	1.4	0.05
geD	COL20A1	1.4	0.05
geD	ASGR2	1.8	0.05
geD	NFKBIL1	2.1	0.05

TABLE S10-continued

CR-specific measurements			
DataType	Name	Fold-change	Q-value
geD	MXD1	1.4	0.05
geD	NP	1.3	0.05
geD	C1QTNF4	1.5	0.05
geD	NPTN	1.4	0.05
geD	IFI16	1.4	0.05
geD	DBNL	1.6	0.05
geD	MAMDC2	2.3	0.05
geD	RHOB	1.5	0.05
geD	PCDHB13	1.6	0.05
geD	ADAM33	1.8	0.05
geD	IKBKB	1.5	0.05
geD	ORM2	1.5	0.05
geD	MLXIPL	1.4	0.05
geD	PRSS2	2.6	0.05
geD	DEDD2	1.4	0.05
geD	GNL1	1.2	0.05
geD	TGFBR1	1.6	0.05
geD	VPREB1	1.4	0.05
geD	CD320	1.5	0.05
geD	HLA-C	1.5	0.05
geD	ITIH1	1.8	0.05
geD	NEDD4L	1.3	0.05
geD	PCDHGA7	1.7	0.05
geD	LY6E	1.8	0.05
geD	TNFSF14	1.8	0.05
geD	ACSF3	1.2	0.05
geD	HLA-DQB1	1.6	0.05
geD	IL17RA	1.5	0.05
geD	FCN1	1.3	0.05
geD	MLLT10	1.7	0.05
geD	MFS10	1.5	0.05
geD	BAT3	1.6	0.05
geD	IGHD	1.5	0.05
geD	RABEP2	1.5	0.05
geD	NLRC3	1.2	0.05
geD	DGKA	1.6	0.05
geD	ICAM2	1.4	0.05
geD	VTN	1.4	0.05
geD	RELB	1.6	0.05
geD	PAC3IN3	1.7	0.05
geD	RAB3B	1.3	0.05
geD	SMAD9	1.3	0.05
geD	SIGLEC7	1.5	0.05
geD	LTB	1.4	0.05
geD	CD248	1.5	0.05
geD	GSTA4	1.6	0.05
geD	ACSF3	1.8	0.05
geD	ITGA5	1.8	0.05
geD	FOXO3	1.4	0.05
geD	TSC22D3	1.3	0.05
geD	CYTH2	1.9	0.05
geD	MYST3	1.7	0.05
geD	SDF2	1.5	0.05
geD	F8	-1.8	0.05
geD	SPARCL1	-1.6	0.05
geD	DOCK3	-1.6	0.05
geD	DST	-1.5	0.05
geD	NPM1	-1.8	0.05
geD	AP1GBP1	-1.4	0.05
geD	TNFAIP3	-1.6	0.05
geD	ADH5	-1.8	0.05
geD	GPR98	-1.3	0.05
geD	CDH11	-2.3	0.05
geD	BBS4	-1.7	0.05
geD	SDCBP	-2.3	0.05
geD	C1QTNF3	-1.4	0.05
geD	LRP12	-1.2	0.05
geD	ICAIL	-1.8	0.05
geD	HTATIP2	-1.6	0.05
geD	TRAF1	-1.6	0.05
geD	CDH19	-1.6	0.05
geD	RB1	-2.8	0.05

TABLE S10-continued

CR-specific measurements			
DataType	Name	Fold-change	Q-value
geD	BIRC6	-1.5	0.05
geD	BCL9	-1.3	0.05
geD	THAP3	-1.7	0.05
geD	CDC42	-1.7	0.05
geD	SOD2	-1.6	0.05
geD	LSM14A	-1.4	0.05
geD	CD302	-1.4	0.05
geD	IL2RG	-1.5	0.05
geD	VCL	-2.1	0.05
geD	RIMS4	-2.2	0.05
geD	FOXP1	-1.6	0.05
geD	SNUPN	-1.7	0.05
geD	NME2	-2.6	0.05
geD	SCARB2	-1.4	0.05
geD	MAPK1	-1.2	0.05
geD	PVR	-1.8	0.05
geD	6-Sep	-1.9	0.05
geD	PRC1	-2	0.05
geD	IKBKB	-1.3	0.05
geD	CLDN12	-1.8	0.05
geD	NAMPT	-1.9	0.05
geD	ANGPTL1	-2.3	0.05
geD	IFRD1	-2.8	0.05
geD	RNF34	-1.8	0.05
geD	MAP4K4	-1.5	0.05
geD	TM2D1	-2.1	0.05
geD	CASP8	-1.3	0.05
geD	SRF	-1.4	0.05
geD	TERF1	-1.3	0.05
geD	IF116	-1.5	0.05
geD	NDUFS1	-1.5	0.05
geD	MIB1	-2	0.05
geD	SDCBP	-2	0.05
geD	EP300	-2	0.05
geD	NID1	-2	0.05
geD	EYA1	-1.7	0.05
geD	GPR126	-1.8	0.05
geD	HDAC4	-1.4	0.05
geD	SH2D1A	-2.5	0.05
geD	TLR3	-2.4	0.05
geD	HSPA8	-1.6	0.05
geD	CXADR	-1.3	0.05
geD	FFDN6	-1.4	0.05
geD	SEMA4F	-1.6	0.05
geD	FAM3C	-1.5	0.05
geD	BMI1	-1.4	0.05
geD	CD86	-2	0.05
geD	GRAMD4	-1.7	0.05
geD	HSP90AA1	-1.7	0.05
geD	ANXA5	-1.5	0.05
geD	PTGES3	-2.7	0.05
geD	CAMK2D	-2	0.05
geD	IGSF5	-1.6	0.05
geD	NCK2	1.4	0.06
geD	KCNMA1	1.7	0.06
geD	LOC442421	1.4	0.06
geD	VPS45	1.3	0.06
geD	CD81	1.3	0.06
geD	CAMK1D	1.3	0.06
geD	CALM3	1.8	0.06
geD	BAX	1.3	0.06
geD	HFE	1.6	0.06
geD	CD96	1.7	0.06
geD	NFATC2IP	1.4	0.06
geD	MYH9	1.3	0.06
geD	EEF1A2	1.6	0.06
geD	MLF2	1.3	0.06
geD	NAB2	1.4	0.06
geD	BAT2	1.5	0.06
geD	TNFSF12	1.7	0.06
geD	PAK2	1.5	0.06
geD	CES1	1.5	0.06

TABLE S10-continued

CR-specific measurements			
DataType	Name	Fold-change	Q-value
geD	PAK1	1.5	0.06
geD	KLF6	2.1	0.06
geD	5-Sep	1.5	0.06
geD	GNA12	1.4	0.06
geD	BIN3	1.5	0.06
geD	C4BPB	1.9	0.06
geD	ICAM3	1.3	0.06
geD	SKAP2	1.6	0.06
geD	HMCN2	1.5	0.06
geD	PTPRU	1.3	0.06
geD	COTL1	1.4	0.06
geD	HLA-DPA1	1.3	0.06
geD	TYROBP	1.3	0.06
geD	PGP	1.7	0.06
geD	LATS2	1.5	0.06
geD	FKBP8	1.6	0.06
geD	BSG	1.5	0.06
geD	RPS6KA2	1.4	0.06
geD	SCRN1	1.6	0.06
geD	MLL	1.4	0.06
geD	BID	1.6	0.06
geD	TRBV5-4	1.4	0.06
geD	FGFR1	1.5	0.06
geD	PML	1.7	0.06
geD	TRAF7	1.6	0.06
geD	TLX2	1.4	0.06
geD	DOCK5	2.4	0.06
geD	HIST1H2AL	1.3	0.06
geD	PKD1	1.3	0.06
geD	NCF1	1.3	0.06
geD	EIF5A	1.4	0.06
geD	SPN	1.5	0.06
geD	PECAM1	1.6	0.06
geD	CSNK1E	1.3	0.06
geD	CD19	1.8	0.06
geD	FXYD5	1.3	0.06
geD	3-Mar	1.5	0.06
geD	TIMP3	1.2	0.06
geD	ADAM22	1.3	0.06
geD	PYDC1	1.6	0.06
geD	JAK1	1.4	0.06
geD	RIN1	1.4	0.06
geD	ADORA2A	1.5	0.06
geD	CYFIP2	1.6	0.06
geD	PURB	1.5	0.06
geD	IFT172	1.3	0.06
geD	FEZF2	1.3	0.06
geD	PXN	1.7	0.06
geD	CLDN5	1.6	0.06
geD	HLA-B	1.6	0.06
geD	MAP3K1	1.4	0.06
geD	STAT5B	1.5	0.06
geD	MR1	1.5	0.06
geD	BIN1	1.3	0.06
geD	PCDHGA2	1.2	0.06
geD	STAT5A	1.3	0.06
geD	ITFG2	1.5	0.06
geD	LAMA5	1.3	0.06
geD	RALBP1	1.6	0.06
geD	IGHV1-69	1.6	0.06
geD	GRN	1.4	0.06
geD	PPM1F	1.7	0.06
geD	NKD2	1.6	0.06
geD	SFN	1.2	0.06
geD	CLDN14	2.8	0.06
geD	MARK3	1.6	0.06
geD	GALNTL1	1.3	0.06
geD	GADD45B	1.4	0.06
geD	TNFRSF21	1.5	0.06
geD	NLRP1	1.2	0.06
geD	DDR1	1.5	0.06
geD	NEIL2	1.2	0.06

TABLE S10-continued

CR-specific measurements			
DataType	Name	Fold-change	Q-value
geD	CEACAM19	1.4	0.06
geD	FLRT2	1.4	0.06
geD	F2	1.3	0.06
geD	IRF7	1.6	0.06
geD	CD3EAP	1.3	0.06
geD	FANCG	1.5	0.06
geD	ADAR	1.5	0.06
geD	RBM4	1.6	0.06
geD	TCIRG1	1.4	0.06
geD	NFATC3	1.3	0.06
geD	CMKLR1	1.3	0.06
geD	ITGB4	1.6	0.06
geD	CPXM1	1.4	0.06
geD	TMX1	1.6	0.06
geD	ZFYVE9	1.3	0.06
geD	PRKACA	1.6	0.06
geD	UBE2Z	1.4	0.06
geD	SPG7	1.6	0.06
geD	RNF216	1.4	0.06
geD	RIN3	1.4	0.06
geD	SELPLG	1.9	0.06
geD	NEIL3	-1.6	0.06
geD	INHA	-1.5	0.06
geD	C3orf38	-1.4	0.06
geD	IFNA4	-1.3	0.06
geD	MLL3	-2	0.06
geD	FAM3B	-1.9	0.06
geD	NFE2L3	-1.4	0.06
geD	RALBP1	-2.2	0.06
geD	FNBP1L	-1.5	0.06
geD	KLRF1	-1.6	0.06
geD	COL14A1	-1.8	0.06
geD	CKAP2	-1.6	0.06
geD	ZNF443	-1.9	0.06
geD	IGJ	-1.5	0.06
geD	CTNND1	-1.2	0.06
geD	RAB18	-2	0.06
geD	TXN	-1.5	0.06
geD	IRF4	-1.4	0.06
geD	RPS3A	-1.4	0.06
geD	NFATC2	-2.4	0.06
geD	RYBP	-1.1	0.06
geD	WNK1	-1.4	0.06
geD	DOCK8	-1.6	0.06
geD	DOCK5	-2	0.06
geD	LRP12	-1.8	0.06
geD	VEGFB	-1.6	0.06
geD	RPS3A	-1.8	0.06
geD	RAB27A	-1.7	0.06
geD	IL2RB	-1.3	0.06
geD	S100B	-1.7	0.06
geD	SLFN11	-1.3	0.06
geD	FANCI	-1.6	0.06
geD	LCP1	-1.8	0.06
geD	TRBV27	-1.6	0.06
geD	DOCK7	-1.6	0.06
geD	BNIP3L	-1.8	0.06
geD	BCL10	-1.3	0.06
geD	VEZF1	-1.3	0.06
geD	PDIA3	-1.5	0.06
geD	FEZ1	-2.5	0.06
geD	NGFRAP1	-1.4	0.06
geD	TNFRSF17	-1.5	0.06
geD	AGGF1	-2.2	0.06
geD	PTPN22	-1.9	0.06
geD	PCDHB15	-1.5	0.06
geD	THR3	-1.3	0.06
geD	CARD6	-1.3	0.06
geD	FAM82A2	-2	0.06
geD	YWHAZ	-1.3	0.06
geD	GCLC	-1.3	0.06
geD	HFE	-1.9	0.06

TABLE S10-continued

CR-specific measurements			
DataType	Name	Fold-change	Q-value
geD	DNM1L	-1.2	0.06
geD	FCHO2	-1.8	0.06
geD	IL20RB	-1.7	0.06
geD	KIR3DL3	-1.5	0.06
geD	DLX1	-1.6	0.06
geD	PAWR	-1.8	0.06
geD	FNDC3A	-1.3	0.06
geD	GYPA	-1.3	0.06
geD	IGLL1	-1.4	0.06
geD	MYST3	-1.3	0.06
geD	ITGA6	-1.8	0.06
geD	IL1R1	-1.5	0.06
geD	SCD5	-2.2	0.06
geD	SGK3	-1.9	0.06
geD	VEZF1	-1.9	0.06
geD	SIX4	-1.2	0.06
geD	FGFR1	-1.7	0.06
geD	CMAS	-1.4	0.06
geD	FANCM	-1.6	0.06
geD	NDN	-2.2	0.06
geD	ABCC4	-1.6	0.06
geD	PSMD3	5.5	0.07
geD	BBC3	1.4	0.07
geD	PARVA	1.5	0.07
geD	ITGAL	1.3	0.07
geD	XRCC6	2.2	0.07
geD	BAI1	1.5	0.07
geD	CBL	1.3	0.07
geD	ITGAX	1.6	0.07
geD	NPM1	1.4	0.07
geD	MAP4K2	1.6	0.07
geD	UNC5B	1.6	0.07
geD	OSM	1.4	0.07
geD	TNFRSF6B	1.6	0.07
geD	TNIP1	1.4	0.07
geD	IL6ST	1.6	0.07
geD	XAF1	1.2	0.07
geD	IL3RA	1.3	0.07
geD	PKD1	1.4	0.07
geD	MEN1	1.5	0.07
geD	C1QTNF2	1.7	0.07
geD	HDAC4	1.5	0.07
geD	CX3CL1	1.8	0.07
geD	FIS1	1.4	0.07
geD	BMF	1.5	0.07
geD	CDH18	1.6	0.07
geD	PRDX2	1.2	0.07
geD	FASTKD3	1.3	0.07
geD	NFATC1	1.4	0.07
geD	PCDHB11	1.3	0.07
geD	CADM3	1.3	0.07
geD	HCG18	1.4	0.07
geD	TMBIM6	1.7	0.07
geD	SDF2L1	1.2	0.07
geD	ARRB2	1.4	0.07
geD	OXSRI	1.3	0.07
geD	AATK	1.6	0.07
geD	MUC5AC	1.6	0.07
geD	TNFRSF1A	1.6	0.07
geD	CTSD	1.2	0.07
geD	EXOC5	1.5	0.07
geD	LOC644297	2.5	0.07
geD	EMD	1.3	0.07
geD	DNASE1L3	1.3	0.07
geD	SIAH2	1.5	0.07
geD	MYD88	1.5	0.07
geD	PTGDS	1.2	0.07
geD	NINJ1	1.6	0.07
geD	TRIB3	1.4	0.07
geD	MLL3	1.5	0.07
geD	PCDH21	1.2	0.07
geD	CLDN3	1.6	0.07

TABLE S10-continued

CR-specific measurements			
DataType	Name	Fold-change	Q-value
geD	CD1A	1.3	0.07
geD	FGF3	1.5	0.07
geD	PECR	1.2	0.07
geD	MSRA	2.6	0.07
geD	CTSK	1.4	0.07
geD	TAPBP	1.4	0.07
geD	PCLO	1.4	0.07
geD	LGALS1	1.1	0.07
geD	GPR56	2.5	0.07
geD	TRIP6	1.5	0.07
geD	ASB1	1.4	0.07
geD	TYK2	1.6	0.07
geD	ELMO2	1.5	0.07
geD	ENG	1.3	0.07
geD	NFKB1B	1.6	0.07
geD	NISCH	1.6	0.07
geD	CMTM3	1.3	0.07
geD	FN1	1.2	0.07
geD	CDC2L2	1.6	0.07
geD	FCGRT	1.3	0.07
geD	COQ7	1.5	0.07
geD	SMOC1	5.2	0.07
geD	CAMP	1.5	0.07
geD	DOCK6	2.4	0.07
geD	SYTL1	1.5	0.07
geD	EMR1	1.3	0.07
geD	THY1	2.2	0.07
geD	IFIT1	1.2	0.07
geD	JAK3	1.5	0.07
geD	UBL7	1.2	0.07
geD	FOXL2	2.8	0.07
geD	PLAUR	1.3	0.07
geD	ROBO3	1.3	0.07
geD	NLRP12	1.2	0.07
geD	TBRG4	1.5	0.07
geD	VEGFA	1.3	0.07
geD	CDH3	2.1	0.07
geD	CTNND2	1.4	0.07
geD	CALM3	1.2	0.07
geD	ISG20	1.2	0.07
geD	MAP2K3	1.5	0.07
geD	CSRNP2	1.6	0.07
geD	HAX1	1.3	0.07
geD	SMO	1.3	0.07
geD	DAPK2	1.4	0.07
geD	ALG1	1.5	0.07
geD	IL11RA	1.1	0.07
geD	MAF	1.6	0.07
geD	ARHGDI1A	1.3	0.07
geD	THOC5	1.6	0.07
geD	NPM1	2.6	0.07
geD	PSMG2	-1.3	0.07
geD	C1RL	-2.6	0.07
geD	C3orf38	-1.3	0.07
geD	FANCD2	-1.4	0.07
geD	MAP3K7	-1.5	0.07
geD	RIMS3	-1.2	0.07
geD	NLGN1	-1.5	0.07
geD	ERBB4	-1.6	0.07
geD	LIN7C	-1.2	0.07
geD	PHLDA2	-1.9	0.07
geD	DIAPH2	-2.3	0.07
geD	FANCD2	-2.1	0.07
geD	FASTKD2	-1.9	0.07
geD	NLGN4Y	-1.5	0.07
geD	PAG1	-1.9	0.07
geD	SLC1A3	-2.2	0.07
geD	BIRC2	-1.6	0.07
geD	PSMD3	-1.5	0.07
geD	CAPN10	-1.4	0.07
geD	CXADR	-1.8	0.07
geD	POSTN	-1.5	0.07

TABLE S10-continued

CR-specific measurements			
DataType	Name	Fold-change	Q-value
geD	RNF34	-1.3	0.07
geD	RABEP1	-1.3	0.07
geD	GBP1	-1.5	0.07
geD	ALG9	-2.5	0.07
geD	PSMCS	-1.5	0.07
geD	GULP1	-1.2	0.07
geD	C9orf61	-1.2	0.07
geD	CASP8	-1.6	0.07
geD	NHEJ1	-1.4	0.07
geD	MLH1	-1.4	0.07
geD	ITPR1	-1.2	0.07
geD	C7	-1.6	0.07
geD	CROP	-1.6	0.07
geD	SMURF2	-1.9	0.07
geD	LPP	-1.3	0.07
geD	HMGB1	-1.2	0.07
geD	RABEP1	-1.5	0.07
geD	PCDHA11	-1.3	0.07
geD	CDC42SE2	-1.4	0.07
geD	HLA-C	-1.4	0.07
geD	RAG1	-1.2	0.07
geD	RHOT1	-1.3	0.07
geD	HDAC4	-1.4	0.07
geD	EXOC5	-1.8	0.07
geD	ART4	-2.2	0.07
geD	FANCI	-1.4	0.07
geD	WWTR1	-1.4	0.07
geD	MAPK9	-1.6	0.07
geD	PTK2	-1.4	0.07
geD	COL14A1	-1.2	0.07
geD	HNMT	-1.3	0.07
geD	LY75	-1.4	0.07
geD	LYST	-1.3	0.07
geD	DOCK1	-1.3	0.07
geD	MAF	-2.2	0.07
geD	PRKCB	-1.5	0.07
geD	TNFRSF11B	-1.2	0.07
geD	PSMD9	-1.5	0.07
geD	PTGES3	-1.4	0.07
geD	ALDH1A3	-1.7	0.07
geD	TBRG1	-1.2	0.07
geD	BAG3	-1.2	0.07
geD	CCR6	-1.4	0.07
geD	PSMD10	-1.3	0.07
geD	ANLN	-1.6	0.07
geD	ALDH1A2	-1.8	0.07
geD	PRKCSH	1.5	0.08
geD	MZF1	1.3	0.08
geD	AP3B2	1.7	0.08
geD	SEMA6A	1.5	0.08
geD	IL16	1.6	0.08
geD	ITGAX	1.5	0.08
geD	HLA-DPA1	8.8	0.08
geD	CCND3	1.4	0.08
geD	TGFB3	1.6	0.08
geD	UCP2	1.4	0.08
geD	LTBP3	1.4	0.08
geD	WISP2	2.3	0.08
geD	HLA-E	1.6	0.08
geD	AOAH	1.4	0.08
geD	F7	1.4	0.08
geD	WFS1	1.3	0.08
geD	ADAT3	1.3	0.08
geD	SPON2	1.6	0.08
geD	CLN3	1.2	0.08
geD	PYCARD	1.3	0.08
geD	HLA-DMA	1.3	0.08
geD	LTBP4	1.2	0.08
geD	DGCR8	1.3	0.08
geD	ING4	1.4	0.08
geD	IFI27L2	2.2	0.08
geD	CFP	1.3	0.08

TABLE S10-continued

CR-specific measurements			
DataType	Name	Fold-change	Q-value
geD	HDAC3	1.7	0.08
geD	IRF2	2.3	0.08
geD	MLLT1	1.3	0.08
geD	APOL2	1.4	0.08
geD	PTPRS	1.3	0.08
geD	LST1	1.5	0.08
geD	PCDHB2	1.3	0.08
geD	BTNL2	1.5	0.08
geD	TAPBP1	1.4	0.08
geD	VPS33B	1.3	0.08
geD	CDK5	1.5	0.08
geD	HLA-DRB4	1.4	0.08
geD	CDH7	1.4	0.08
geD	AP1B1	1.3	0.08
geD	PSMB9	1.7	0.08
geD	HEPACAM	1.8	0.08
geD	CD97	1.6	0.08
geD	NFX1	1.2	0.08
geD	EXOC4	1.4	0.08
geD	PRDX2	1.4	0.08
geD	AIFM2	1.6	0.08
geD	ITGB6	1.5	0.08
geD	FKBP9	1.6	0.08
geD	TOM1	1.2	0.08
geD	CLPTM1L	1.4	0.08
geD	BIRC7	1.4	0.08
geD	EPN2	1.9	0.08
geD	PPIL2	1.6	0.08
geD	TIMP2	6.7	0.08
geD	RTN3	1.3	0.08
geD	FKBP5	1.2	0.08
geD	POU4F1	1.2	0.08
geD	CMTM1	1.3	0.08
geD	EBI3	1.4	0.08
geD	LSM14A	1.3	0.08
geD	IL8RB	1.2	0.08
geD	MTCH1	1.3	0.08
geD	BBS2	1.4	0.08
geD	IFT122	1.4	0.08
geD	LY6G6C	1.4	0.08
geD	LTBP4	1.1	0.08
geD	DOCK2	1.3	0.08
geD	MX1	1.3	0.08
geD	INHBB	1.2	0.08
geD	EMILIN1	1.4	0.08
geD	MLL4	1.1	0.08
geD	TYMP	1.3	0.08
geD	ZYX	1.3	0.08
geD	CLDN3	1.4	0.08
geD	PRKG1	1.7	0.08
geD	SPACA3	1.3	0.08
geD	ADAMTS1	-1.3	0.08
geD	DCBLD1	-1.7	0.08
geD	PAFAH1B1	-1.5	0.08
geD	CD164	-1.7	0.08
geD	HBP1	-1.3	0.08
geD	PHLPP	-1.8	0.08
geD	XRCC6BP1	-1.3	0.08
geD	SNX6	-1.5	0.08
geD	ELMOD1	-1.6	0.08
geD	AP1G1	-1.2	0.08
geD	DNAJB6	-1.3	0.08
geD	SYVN1	-1.8	0.08
geD	IKBKAP	-1.5	0.08
geD	RPS6KA3	-1.3	0.08
geD	CD63	-1.3	0.08
geD	USP33	-1.5	0.08
geD	BCLAF1	-1.5	0.08
geD	TNFAIP8L1	-1.3	0.08
geD	PVRL3	-1.6	0.08
geD	UBE2N	-1.5	0.08
geD	DST	-1.4	0.08

TABLE S10-continued

CR-specific measurements			
DataType	Name	Fold-change	Q-value
geD	SLK	-1.4	0.08
geD	4-Sep	-1.4	0.08
geD	BMI1	-1.9	0.08
geD	PTGR2	-1.4	0.08
geD	PTEN	-1.7	0.08
geD	KCNMA1	-1.5	0.08
geD	PROX1	-1.6	0.08
geD	GALNAC4S-6ST	-1.4	0.08
geD	TOP2A	-1.6	0.08
geD	RAB22A	-1.4	0.08
geD	LAMP2	-1.2	0.08
geD	RNF144B	-1.2	0.08
geD	STX1A	-1.6	0.08
geD	PLDN	-1.2	0.08
geD	PSME3	-1.6	0.08
geD	GNAI3	-1.3	0.08
geD	NXT2	-1.7	0.08
geD	COL8A1	-1.3	0.08
geD	DOCK4	-1.2	0.08
geD	SYNJ2BP	-1.4	0.08
geD	RPS3A	-2	0.08
geD	NBN	-1.6	0.08
geD	PIMI1	-1.3	0.08
geD	FLT1	-1.4	0.08
geD	UCHL1	-1.4	0.08
geD	KLRG1	-1.6	0.08
geD	API5	-1.8	0.08
geD	RRAGC	-1.3	0.08
geD	MBL2	-1.3	0.08
geD	MATN3	-1.8	0.08
geD	COL14A1	-1.2	0.08
geD	CADM1	-1.7	0.08
geD	ADAM12	-1.7	0.08
geD	B2M	-1.5	0.08
geD	RBPJ	-1.3	0.08
geD	SHISA5	1.3	0.09
geD	FRAT2	1.2	0.09
geD	PCDHB8	1.5	0.09
geD	ADRBK1	1.2	0.09
geD	ZNF646	1.4	0.09
geD	PARD3	1.3	0.09
geD	DCTN3	1.4	0.09
geD	EBF4	1.3	0.09
geD	CERK	1.4	0.09
geD	POLM	1.3	0.09
geD	PTPN11	1.3	0.09
geD	PTGIR	1.4	0.09
geD	FLVCR1	1.2	0.09
geD	CD2BP2	1.3	0.09
geD	PDCD1	1.6	0.09
geD	BGLAP	1.6	0.09
geD	ATHL1	1.5	0.09
geD	SAP30BP	1.6	0.09
geD	CLU	1.5	0.09
geD	THBS4	1.4	0.09
geD	MST1R	1.8	0.09
geD	NFKBIL2	1.4	0.09
geD	RECQL4	1.8	0.09
geD	FUT4	1.3	0.09
geD	AIF1	1.2	0.09
geD	PTK7	1.3	0.09
geD	CEACAM4	2.5	0.09
geD	C1orf38	1.5	0.09
geD	JUP	1.4	0.09
geD	OSCAR	1.7	0.09
geD	BCAP31	1.5	0.09
geD	COL8A1	1.2	0.09
geD	CAMK1G	2.6	0.09
geD	FGFR3	1.4	0.09
geD	CSF2RA	1.5	0.09
geD	GAS1	1.4	0.09
geD	TH1L	1.8	0.09

TABLE S10-continued

CR-specific measurements			
DataType	Name	Fold-change	Q-value
geD	ICAM5	1.6	0.09
geD	SHISA5	1.9	0.09
geD	FIS1	1.3	0.09
geD	LAG3	1.4	0.09
geD	FGFR1	1.2	0.09
geD	SPHK2	1.3	0.09
geD	NRXN2	1.5	0.09
geD	NPHP1	1.4	0.09
geD	IL1R1	1.4	0.09
geD	ABL1	1.2	0.09
geD	RHOA	1.6	0.09
geD	MLLT6	1.6	0.09
geD	PLD1	1.4	0.09
geD	WNK1	1.6	0.09
geD	ZNF3	1.5	0.09
geD	LST1	1.5	0.09
geD	IL21R	3.9	0.09
geD	TGM2	3.4	0.09
geD	DNASE2	1.7	0.09
geD	FCRL2	1.3	0.09
geD	LILRA1	1.6	0.09
geD	RAB35	1.4	0.09
geD	MYH10	1.1	0.09
geD	MAPK11	1.3	0.09
geD	APOE	1.4	0.09
geD	DOK1	1.5	0.09
geD	CELSR3	1.3	0.09
geD	BUB1B	1.5	0.09
geD	GLT25D2	1.4	0.09
geD	PRAM1	1.6	0.09
geD	SLC4A1	1.4	0.09
geD	SMAD6	1.3	0.09
geD	ERBB3	1.4	0.09
geD	OLFML3	1.4	0.09
geD	HLA-E	1.3	0.09
geD	LSM14B	1.2	0.09
geD	KNG1	1.5	0.09
geD	FBLIM1	1.2	0.09
geD	CSF3R	1.2	0.09
geD	AP2A1	1.6	0.09
geD	SEMA3F	1.4	0.09
geD	ANP32D	1.3	0.09
geD	PBX2	1.4	0.09
geD	CD74	1.5	0.09
geD	CSNK2B	1.3	0.09
geD	SYNJ1	1.3	0.09
geD	VHL	1.3	0.09
geD	HLA-G	1.7	0.09
geD	WFIKKN1	1.3	0.09
geD	MED1	-1.8	0.09
geD	GNA13	-1.3	0.09
geD	PDCD2	-1.4	0.09
geD	STK17A	-1.3	0.09
geD	NPM1	-1.4	0.09
geD	ROCK1	-1.4	0.09
geD	PCDH8	-1.7	0.09
geD	RABGEF1	-1.4	0.09
geD	SP3	-1.7	0.09
geD	AP1S3	-1.6	0.09
geD	PIK3CB	-1.2	0.09
geD	C8orf4	-1.6	0.09
geD	UBR1	-1.5	0.09
geD	HES1	-1.3	0.09
geD	CARD8	-1.3	0.09
geD	RTN4	-1.4	0.09
geD	ALB	-1.7	0.09
geD	TERF1	-1.7	0.09
geD	RHD	-1.4	0.09
geD	MLLT10	-1.6	0.09
geD	ROCK1	-1.5	0.09
geD	CDC42	-1.3	0.09
geD	MAP4K5	-1.8	0.09

TABLE S10-continued

CR-specific measurements			
DataType	Name	Fold-change	Q-value
geD	HSP90B1	-1.2	0.09
geD	CFLAR	-1.7	0.09
geD	PPI4	-1.8	0.09
geD	MICB	-1.4	0.09
geD	CD109	-1.8	0.09
geD	LYAR	-1.7	0.09
geD	PSMC6	-1.4	0.09
geD	MSN	-2.2	0.09
geD	NRAS	-1.3	0.09
geD	CFI	-1.2	0.09
geD	TERF1	-1.7	0.09
geD	DYRK2	-1.7	0.09
geD	RAD21	-2	0.09
geD	BMI1	-1.3	0.09
geD	LAMP2	-1.4	0.09
geD	CFDP1	-1.3	0.09
geD	PTEN	-2.2	0.09
geD	PCDH7	-1.5	0.09
geD	PTGS1	-1.8	0.09
geD	PPARGC1A	-1.7	0.09
geD	MARCKS	-2.1	0.09
geD	GPNMB	-1.7	0.09
geD	DNAJB6	-1.6	0.09
geD	LAMP2	-1.5	0.09
geD	RICTOR	-1.1	0.09
geD	CORO1C	-1.5	0.09
geD	DAD1	-1.3	0.09
geD	SDF2	-1.4	0.09
geD	PTGER4	-1.6	0.09
geD	MLLT4	1.1	0.1
geD	ASGR1	1.2	0.1
geD	VTCN1	1.6	0.1
geD	CXCL14	1.3	0.1
geD	SNX3	1.4	0.1
geD	MLLT6	2.1	0.1
geD	TNFSF13	1.2	0.1
geD	ERCC1	1.3	0.1
geD	DLL3	1.5	0.1
geD	IRGC	1.3	0.1
geD	CD36	1.3	0.1
geD	C16orf5	1.2	0.1
geD	PAFAH1B3	1.2	0.1
geD	CDC2L1	1.6	0.1
geD	CALY	1.3	0.1
geD	ZNF646	1.3	0.1
geD	AZGP1	1.3	0.1
geD	CUBN	1.6	0.1
geD	EEF1A1	1.2	0.1
geD	SHB	1.2	0.1
geD	PSMF1	2.8	0.1
geD	DDX41	1.2	0.1
geD	P14KB	1.3	0.1
geD	PCDHB7	1.3	0.1
geD	GPR126	1.3	0.1
geD	MFAP4	1.2	0.1
geD	ELMOD3	1.4	0.1
geD	CYP26A1	1.4	0.1
geD	XRCC3	1.4	0.1
geD	SERPINA3	1.3	0.1
geD	TP53INP1	1.3	0.1
geD	PRKCCQ	1.3	0.1
geD	RFX2	1.4	0.1
geD	NCOA6	1.6	0.1
geD	DSCAM	1.4	0.1
geD	AZU1	1.4	0.1
geD	TRAF5	1.3	0.1
geD	NTN1	1.4	0.1
geD	CCL27	1.2	0.1
geD	CLCF1	1.3	0.1
geD	IRS2	1.3	0.1
geD	IER3	1.3	0.1
geD	PML	1.2	0.1

TABLE S10-continued

CR-specific measurements			
DataType	Name	Fold-change	Q-value
geD	SLPI	1.9	0.1
geD	LMNA	1.3	0.1
geD	ACVRL1	1.2	0.1
geD	PACS2	1.4	0.1
geD	TAPBP	1.3	0.1
geD	LTBP2	1.4	0.1
geD	MICB	1.2	0.1
geD	PVR	1.5	0.1
geD	MADCAM1	1.2	0.1
geD	TRIM35	1.2	0.1
geD	RAB7A	1.2	0.1
geD	HEPACAM	1.3	0.1
geD	TOLLIP	1.2	0.1
geD	MYO18A	1.4	0.1
geD	VCP	1.5	0.1
geD	NGFR	1.4	0.1
geD	BSG	1.2	0.1
geD	COL15A1	1.4	0.1
geD	BAT4	1.7	0.1
geD	MYST1	2.6	0.1
geD	MAST1	1.3	0.1
geD	PBX4	1.6	0.1
geD	FLNA	1.2	0.1
geD	MALL	1.2	0.1
geD	IL8RB	1.3	0.1
geD	HCG18	1.6	0.1
geD	PVRIG	1.2	0.1
geD	CCL15	1.2	0.1
geD	AREG	1.4	0.1
geD	CCL16	1.3	0.1
geD	CEACAM7	1.4	0.1
geD	CHST10	1.2	0.1
geD	VEGFB	1.4	0.1
geD	TNFRSF8	1.2	0.1
geD	ADAT2	1.4	0.1
geD	CHRD	1.4	0.1
geD	ROM1	1.1	0.1
geD	SHFM1	-1.3	0.1
geD	TOR1AIP2	-1.2	0.1
geD	ATP1A2	-1.4	0.1
geD	PCMT1	-1.4	0.1
geD	CP110	-2.1	0.1
geD	RGN	-1.7	0.1
geD	PICALM	-2.3	0.1
geD	FANCB	-1.3	0.1
geD	ZNF675	-1.6	0.1
geD	IBTK	-1.3	0.1
geD	CCAR1	-1.6	0.1
geD	YWHAZ	-1.3	0.1
geD	ATP2A2	-1.5	0.1
geD	HTATSF1	-1.4	0.1
geD	NR4A1	-1.9	0.1
geD	CREB1	-1.3	0.1
geD	KYNU	-1.3	0.1
geD	CRKL	-1.3	0.1
geD	STON1	-1.3	0.1
geD	MSN	-1.3	0.1
geD	MLL3	-1.6	0.1
geD	MIA3	-1.5	0.1
geD	FANCF	-2.2	0.1
geD	CXADR	-1.3	0.1
geD	ADAR	-1.6	0.1
geD	RP6-213H19.1	-1.6	0.1
geD	TOP2B	-1.3	0.1
geD	FASTKD2	-1.2	0.1
geD	PRKAR2B	-1.5	0.1
geD	CXCL1	-1.9	0.1
geD	PSMC1	-1.2	0.1
geD	LOC442421	-1.8	0.1
geD	COL29A1	-1.4	0.1
geD	NFAT5	-1.2	0.1
geD	DLEU2	-1.5	0.1

TABLE S10-continued

CR-specific measurements			
DataType	Name	Fold-change	Q-value
geD	SRFBP1	-1.3	0.1
geD	ITGAV	-1.4	0.1
geD	ELF1	-1.4	0.1
geD	HBP1	-1.6	0.1
geD	KCNIP3	-1.3	0.1
geD	ICK	-1.2	0.1
geD	EXOC6B	-1.8	0.1
geD	PCDHB9	-1.6	0.1
geD	TNFRSF19	-1.2	0.1
geD	ZMYM2	-1.1	0.1
geD	COPG2	-1.3	0.1
geD	DLC1	-1.2	0.1
geD	ACVR1C	-1.2	0.1
geD	ATR	-1.2	0.1
geD	UBE4B	-1.5	0.1
geD	CAMK2D	-1.3	0.1
geD	IL16	-1.7	0.1
geD	BECN1	-1.2	0.1
geD	COL13A1	-1.9	0.1
geD	BIRC3	-1.5	0.1
geD	CD55	-1.3	0.1
geD	UTP14A	-1.5	0.1
geD	PPT1	-1.3	0.1
geD	GNA12	1.3	0.11
geD	LTBR	1.3	0.11
geD	NFKBIE	1.4	0.11
geD	IL15RA	1.3	0.11
geD	SCARB1	1.4	0.11
geD	RAB26	1.3	0.11
geD	C1QTNF6	1.3	0.11
geD	EMILIN2	1.1	0.11
geD	BICD2	1.6	0.11
geD	ITFG2	1.3	0.11
geD	CD97	1.6	0.11
geD	BBC3	1.3	0.11
geD	LOC91316	1.9	0.11
geD	FOXO3	1.2	0.11
geD	GPX1	3.6	0.11
geD	OLFML3	1.4	0.11
geD	CBX4	1.4	0.11
geD	ERBB3	1.4	0.11
geD	GPR17	1.3	0.11
geD	INHBC	2.7	0.11
geD	ARHGEF11	1.2	0.11
geD	PRDX1	1.9	0.11
geD	SNX17	1.3	0.11
geD	RYBP	1.3	0.11
geD	PNN	2.5	0.11
geD	CLDN9	1.4	0.11
geD	IL3RA	1.2	0.11
geD	TNFRSF10B	1.2	0.11
geD	ADORA2A	1.3	0.11
geD	ACOX1	1.3	0.11
geD	IL10RA	1.2	0.11
geD	FKBP1A	1.5	0.11
geD	IFI27L1	2	0.11
geD	PTAFR	2.5	0.11
geD	GDF15	1.1	0.11
geD	CARD17	1.8	0.11
geD	YKT6	1.4	0.11
geD	ADAM12	1.2	0.11
geD	MYST4	1.3	0.11
geD	RPS6KA5	9.5	0.11
geD	BBS7	1.3	0.11
geD	CXCL5	1.3	0.11
geD	COL16A1	1.3	0.11
geD	CYTL1	1.2	0.11
geD	FBLIM1	1.6	0.11
geD	COL6A1	1.1	0.11
geD	TNFRSF4	1.4	0.11
geD	SYVN1	1.4	0.11
geD	CD300C	1.3	0.11

TABLE S10-continued

CR-specific measurements			
DataType	Name	Fold-change	Q-value
geD	TCTA	1.3	0.11
geD	CCL17	1.3	0.11
geD	PSMD9	1.6	0.11
geD	EPOR	1.3	0.11
geD	ERCC3	1.3	0.11
geD	IGF2BP3	1.5	0.11
geD	PEX5	1.4	0.11
geD	RIMS4	1.5	0.11
geD	PIIH	1.2	0.11
geD	NAB2	1.3	0.11
geD	EXOC4	-1.3	0.11
geD	RHCE	-1.3	0.11
geD	SGMS1	-1.4	0.11
geD	PSMD12	-1.2	0.11
geD	SNAP29	-1.5	0.11
geD	DLG1	-1.3	0.11
geD	FEN1	-1.5	0.11
geD	TTRAP	-1.2	0.11
geD	CUL5	-1.3	0.11
geD	TOPORS	-1.5	0.11
geD	CDON	-1.4	0.11
geD	PCMT1	-1.3	0.11
geD	RPS3A	-1.5	0.11
geD	BMPR1A	-1.3	0.11
geD	PSMA1	-1.1	0.11
geD	POGK	-1.5	0.11
geD	SSX2IP	-1.1	0.11
geD	SRPK1	-1.3	0.11
geD	EZR	-1.5	0.11
geD	KLRC4	-1.4	0.11
geD	PCSK9	-1.3	0.11
geD	PDCD10	-1.2	0.11
geD	CTNND1	-1.4	0.11
geD	ARF6	-1.2	0.11
geD	PPIC	-1.2	0.11
geD	SDCBP	-1.2	0.11
geD	PLG	-1.2	0.11
geD	GNA12	-1.2	0.11
geD	ATP2C1	-1.4	0.11
geD	SNRK	-1.2	0.11
geD	PSMF1	-1.4	0.11
geD	EFNB2	-1.6	0.11
geD	THBS2	-1.5	0.11
geD	MRPS30	-1.4	0.11
geD	JUB	-1.3	0.11
geD	PLAGL2	-1.4	0.11
geD	IL17RD	-1.8	0.11
geD	CP110	-1.2	0.11
geD	TRIB1	-1.4	0.11
geD	OXSRI	-1.3	0.11
geD	TGFB2	-1.7	0.11
geD	NEDD4L	-1.7	0.11
geD	TAX1BP1	-1.3	0.11
geD	STK3	-1.3	0.11
geD	APIP	-1.3	0.11
geD	GCH1	-1.3	0.11
geD	F2R	-1.2	0.11
geD	GNE	-1.3	0.11
geD	HSPE1	-1.3	0.11
geD	PLSCR1	-1.4	0.11
geD	BAG3	-1.4	0.11
geD	MYH9	-1.2	0.11
geD	FAM3C	-1.4	0.11
geD	SMOC1	-1.8	0.11
geD	SLAMF7	-1.2	0.11
geD	YWHAG	-1.5	0.11
geD	IRAK1BP1	-1.8	0.11
geD	CBLB	-1.3	0.11
geD	PSMD14	-1.5	0.11
geD	PDCL3	-1.6	0.11
geD	RAB5B	1.3	0.12
geD	MDM2	1.2	0.12

TABLE S10-continued

CR-specific measurements			
DataType	Name	Fold-change	Q-value
geD	WDR92	1.3	0.12
geD	BMP1	1.4	0.12
geD	CHST4	1.2	0.12
geD	BCL11B	1.1	0.12
geD	TBXAS1	1.4	0.12
geD	N-PAC	1.2	0.12
geD	CD59	1.7	0.12
geD	ITGA11	1.4	0.12
geD	IGFBP3	1.6	0.12
geD	CLDN23	1.3	0.12
geD	TCTA	1.2	0.12
geD	POLG	1.5	0.12
geD	RAB3D	1.1	0.12
geD	TRAP1	1.2	0.12
geD	MAF	1.2	0.12
geD	STX1A	1.3	0.12
geD	VCP	1.2	0.12
geD	KYNU	1.2	0.12
geD	CRKL	1.3	0.12
geD	CD63	1.2	0.12
geD	PODXL2	1.4	0.12
geD	BNIP3L	1.3	0.12
geD	VCP	1.5	0.12
geD	BNIP1	1.2	0.12
geD	HSPB1	1.3	0.12
geD	MYH9	1.2	0.12
geD	CD3E	1.2	0.12
geD	PLG	1.2	0.12
geD	HTT	1.6	0.12
geD	DCHS1	1.3	0.12
geD	AQP3	1.1	0.12
geD	PDPK1	1.3	0.12
geD	TAF8	1.3	0.12
geD	B3GNTL1	1.3	0.12
geD	C8G	1.3	0.12
geD	SIGLEC10	1.2	0.12
geD	CNTRF	1.3	0.12
geD	NID2	2.2	0.12
geD	NME3	1.2	0.12
geD	SNX2	1.9	0.12
geD	COL24A1	1.3	0.12
geD	CROP	1.3	0.12
geD	CXCR5	1.5	0.12
geD	TRIP10	1.4	0.12
geD	PIN1	1.5	0.12
geD	AIFM2	1.1	0.12
geD	NFATC1	19.3	0.12
geD	LDLRAP1	1.5	0.12
geD	PSMB2	1.1	0.12
geD	RIN2	1.1	0.12
geD	BMPR1A	1.5	0.12
geD	PKP4	-1.3	0.12
geD	FUT8	-1.5	0.12
geD	MLLT10	-1.2	0.12
geD	CASP8AP2	-1.2	0.12
geD	HES1	-1.7	0.12
geD	CPLX1	-1.4	0.12
geD	RNF216	-1.2	0.12
geD	HDAC9	-1.1	0.12
geD	SGPP1	-1.9	0.12
geD	PSMD1	-1.7	0.12
geD	HINT1	-2.3	0.12
geD	GRAMD4	-1.2	0.12
geD	JMY	-1.6	0.12
geD	PDGFC	-1.2	0.12
geD	LEPR	-1.3	0.12
geD	B3GNT5	-1.4	0.12
geD	LDLR	-1.3	0.12
geD	POMP	-1.3	0.12
geD	BCL2A1	-1.4	0.12
geD	PDCL3	-1.3	0.12
geD	CXCL12	-1.3	0.12

TABLE S10-continued

CR-specific measurements			
DataType	Name	Fold-change	Q-value
geD	MLLT10	-1.2	0.12
geD	CUL2	-1.2	0.12
geD	MLL5	-1.2	0.12
geD	PRLR	-1.3	0.12
geD	IFIT5	-1.3	0.12
geD	CLSTN2	-1.7	0.12
geD	SH2D1A	-1.2	0.12
geD	HSP90AA1	-1.6	0.12
geD	COL15A1	-1.4	0.12
geD	KRAS	-1.6	0.12
geD	THYN1	-1.3	0.12
geD	FASTKD5	-1.3	0.12
geD	BSCL2	1.6	0.13
geD	RAD51	1.2	0.13
geD	PCDHA1	1.2	0.13
geD	FSCN1	1.2	0.13
geD	DBN1	1.4	0.13
geD	GDF3	1.3	0.13
geD	CCL21	1.5	0.13
geD	EDA	1.1	0.13
geD	S100A9	1.4	0.13
geD	ZNF346	1.3	0.13
geD	MYBPH	1.1	0.13
geD	PRKCDBP	1.3	0.13
geD	MUC5B	1.4	0.13
geD	CCND1	1.2	0.13
geD	EPO	1.2	0.13
geD	FAT1	1.4	0.13
geD	DBNL	1.2	0.13
geD	RAE1	1.3	0.13
geD	NRG1	17.7	0.13
geD	PDLIM7	1.3	0.13
geD	ZBP1	1.4	0.13
geD	TSTA3	1.2	0.13
geD	SCFD2	1.3	0.13
geD	SOCS1	6.1	0.13
geD	PTPRF	1.5	0.13
geD	ESR1	1.2	0.13
geD	CAT	1.4	0.13
geD	FOXO1	1.3	0.13
geD	IGF2	1.3	0.13
geD	MARK4	1.1	0.13
geD	SNAPIN	1.3	0.13
geD	ADAMTS7	1.2	0.13
geD	HLA-DMB	1.2	0.13
geD	ALG9	1.2	0.13
geD	EXTL1	1.7	0.13
geD	ATL1	1.5	0.13
geD	RAC2	1.2	0.13
geD	HMGB3	1.2	0.13
geD	SIGIRR	1.3	0.13
geD	IGSF8	2.2	0.13
geD	CCND3	1.3	0.13
geD	ISG20L2	1.2	0.13
geD	RTN3	1.2	0.13
geD	CFB	1.4	0.13
geD	MLF1	1.5	0.13
geD	CLTCL1	1.2	0.13
geD	THAP3	1.3	0.13
geD	PDZD2	1.3	0.13
geD	DNM2	1.2	0.13
geD	GDF11	1.4	0.13
geD	ARFGEF1	1.9	0.13
geD	CTNNA1	1.2	0.13
geD	HLA-E	1.3	0.13
geD	MAPK13	1.3	0.13
geD	EI24	1.4	0.13
geD	FBLN5	1.3	0.13
geD	FEZ1	1.4	0.13
geD	DAP	1.4	0.13
geD	MYEF2	-1.2	0.13
geD	RAB13	-1.5	0.13

TABLE S10-continued

CR-specific measurements			
DataType	Name	Fold-change	Q-value
geD	HIP1	-1.3	0.13
geD	NPC1	-1.4	0.13
geD	PDGFRL	-1.2	0.13
geD	MAP4K3	-1.2	0.13
geD	RALA	-1.1	0.13
geD	SCARB2	-1.5	0.13
geD	PRKAR1A	-1.5	0.13
geD	UBP1	-1.3	0.13
geD	IFT81	-1.5	0.13
geD	ZFYVE16	-1.6	0.13
geD	VPS41	-1.5	0.13
geD	SEMA4D	-1.5	0.13
geD	PDCD6IP	-1.1	0.13
geD	CD109	-1.7	0.13
geD	GTF2H2	-1.2	0.13
geD	GPR98	-2	0.13
geD	TXNDC5	-1.5	0.13
geD	ZC3H12A	-1.7	0.13
geD	PEG10	-1.2	0.13
geD	GDNF	-2.3	0.13
geD	HMGB1	-1.5	0.13
geD	GAB3	-1.3	0.13
geD	CUL4A	-1.3	0.13
geD	CREBBP	-1.2	0.13
geD	RFX5	-1.2	0.13
geD	BAG5	-1.4	0.13
geD	PCDHB5	-1.6	0.13
geD	BAG4	-1.3	0.13
geD	RALB	-1.6	0.13
geD	RARG	1.4	0.14
geD	CTSH	1.3	0.14
geD	RAD52	1.7	0.14
geD	MSLN	1.2	0.14
geD	CD38	1.5	0.14
geD	NFKBIL2	1.3	0.14
geD	RHOT2	1.3	0.14
geD	WWP2	1.2	0.14
geD	DEDD	1.2	0.14
geD	TRAF2	2.1	0.14
geD	TNFRSF25	1.3	0.14
geD	TREML2	1.3	0.14
geD	MAPK13	1.2	0.14
geD	SEMA4G	1.3	0.14
geD	MAP4K4	1.3	0.14
geD	MYBPC2	1.2	0.14
geD	CD151	1.3	0.14
geD	NRGN	1.4	0.14
geD	MADD	1.2	0.14
geD	MGC29506	1.5	0.14
geD	BCL9L	1.2	0.14
geD	HCP5	1.2	0.14
geD	IL4I1	1.4	0.14
geD	LTB4R2	1.3	0.14
geD	LOC441795	1.2	0.14
geD	CD200	1.2	0.14
geD	LRIG1	1.2	0.14
geD	CIAPIN1	1.4	0.14
geD	RAB34	1.3	0.14
geD	RIN2	1.3	0.14
geD	TFDP1	2	0.14
geD	EEF2	1.3	0.14
geD	ALG1	1.3	0.14
geD	COL7A1	1.3	0.14
geD	CD37	1.2	0.14
geD	HTRA2	1.3	0.14
geD	CD8B	1.2	0.14
geD	NPTN	1.1	0.14
geD	KLF10	-1.2	0.14
geD	PCDHB16	-1.3	0.14
geD	TRAF7	-1.9	0.14
geD	CLN3	-1.3	0.14
geD	SON	-1.3	0.14

TABLE S10-continued

CR-specific measurements			
DataType	Name	Fold-change	Q-value
geD	MPZL2	-1.7	0.14
geD	PSMD5	-1.2	0.14
geD	NCKAP1	-1.2	0.14
geD	NLRC3	-1.2	0.14
geD	DLL1	-1.2	0.14
geD	DHCR24	-1.4	0.14
geD	C1D	-1.4	0.14
geD	BAALC	-1.3	0.14
geD	VHL	-1.3	0.14
geD	RAB27A	-1.3	0.14
geD	CBR1	-1.2	0.14
geD	JAG1	-1.2	0.14
geD	ADAM11	-1.3	0.14
geD	PRKRIR	-1.9	0.14
geD	XCL1	-1.5	0.14
geD	FANCI	-1.4	0.14
geD	FYB	-1.2	0.14
geD	CYCS	-1.6	0.14
geD	CETN2	-1.1	0.14
geD	BCL11A	-1.4	0.14
geD	PSMC6	-1.6	0.14
geD	PBX1	-1.2	0.14
geD	SIRT1	-1.1	0.14
geD	TBX21	-1.3	0.14
geD	HOXA3	-1.5	0.14
geD	LSM14A	-1.3	0.14
geD	TXNDC17	-2.1	0.14
geD	CROP	-1.5	0.14
geD	HDAC5	1.2	0.15
geD	MAPK7	1.3	0.15
geD	ZAN	1.7	0.15
geD	XRCC1	1.8	0.15
geD	ITGB5	1.2	0.15
geD	METTL1	1.2	0.15
geD	SIPA1	1.1	0.15
geD	MRC2	1.3	0.15
geD	HLA-DOB	1.6	0.15
geD	LRP10	1.1	0.15
geD	CDKN1B	1.4	0.15
geD	ARVCF	2.1	0.15
geD	ITGA9	1.4	0.15
geD	CD59	1.2	0.15
geD	VPRBP	1.3	0.15
geD	RELT	1.2	0.15
geD	FCRLB	1.6	0.15
geD	HSF1	1.2	0.15
geD	PSMB3	1.2	0.15
geD	HLA-DMB	2.4	0.15
geD	FBLN7	1.2	0.15
geD	KLF1	1.2	0.15
geD	SH3GL3	1.3	0.15
geD	PHLDA1	1.2	0.15
geD	CLDN9	1.3	0.15
geD	TNFRSF13C	1.2	0.15
geD	PRKAR1B	1.3	0.15
geD	SCFD1	-1.3	0.15
geD	PAX3	-1.2	0.15
geD	SWAP70	-1.3	0.15
geD	MAP4K5	-1.6	0.15
geD	MLL2	-1.6	0.15
geD	RFFL	-1.4	0.15
geD	SOCS5	-1.3	0.15
geD	STK4	-1.4	0.15
geD	AMOTL1	-1.1	0.15
geD	MLF1	-1.3	0.15
geD	RACGAP1	-1.6	0.15
geD	PPID	-1.4	0.15
geD	YWHAZ	-1.4	0.15
geD	GPR183	-1.2	0.15
geD	SRPK2	-1.4	0.15
geD	FAM19A2	-1.5	0.15
geD	HSPA8	-1.3	0.15

TABLE S10-continued

CR-specific measurements			
DataType	Name	Fold-change	Q-value
geD	CELSR1	-1.3	0.15
geD	MYST4	-1.3	0.15
geD	HSPA5	-1.4	0.15
geD	RBM24	-1.5	0.15
geD	MYST4	-1.5	0.15
geD	CCL28	-1.3	0.15

APPENDIX K

[0193]

TABLE S11

CNR-specific measurements			
DataType	Name	Fold-change	Q-value
phenoD	CD4 TERM DIFF EFFECTOR MEMORY	3.4	0
phenoD	CD4 EFFECTOR MEMORY	2.9	0
phenoD	CD8 TERM DIFF EFFECTOR MEMORY	10.9	0.01
phenoD	CD8 EFFECTOR MEMORY	4.9	0.03
phenoD	NK T CELLS	2.1	0.03
phenoD	CD4	2.5	0.03
phenoD	CD8	3.3	0.06
phenoD	CD4 NAIVE	-2.3	0
phenoD	CD8 NAIVE	-2.3	0.01
phenoD	B CELLS	-1.4	0.02
pfBaselineD	cd20_Unstimulated_STAT1	2.6	0
pfBaselineD	cd20_Unstimulated_STAT3	4.3	0
pfBaselineD	cd20_Unstimulated_STAT5	2.5	0
pfBaselineD	cd4_Unstimulated_STAT1	1.1	0
pfBaselineD	cd4_Unstimulated_STAT3	1.2	0
pfBaselineD	cd4_Unstimulated_STAT5	1.1	0.01
pfBaselineD	mono_Unstimulated_STAT1	1.1	0.02
pfBaselineD	mono_Unstimulated_STAT3	1.1	0.06
pfD	cd20_IFNg_STAT3	1.1	0.02
pfD	cd20_IL6_STAT5	1	0.02
pfD	cd20_IL7_STAT3	1.1	0.06
pfD	cd20_IL7_STAT5	1.1	0.07
pfD	cd20_IL10_STAT5	1	0.12
pfD	mono_IL10_STAT5	1.1	0.13
pfD	mono_IL21_STAT1	1	0.14
pfD	mono_IL21_STAT5	1	0.15
pfD	cd20_IFNa_STAT1	-4.2	0
pfD	cd20_IFNa_STAT3	-6	0
pfD	cd20_IFNa_STAT5	-3.7	0
pfD	cd20_IFNg_STAT1	-4	0
pfD	cd20_IL21_STAT1	-3.4	0
pfD	cd20_IL21_STAT3	-2	0
pfD	cd20_IL7_STAT1	-6.6	0
pfD	cd4_IFNa_STAT1	-4.4	0
pfD	cd4_IFNa_STAT3	-1.9	0
pfD	cd4_IFNa_STAT5	-1.7	0
pfD	cd4_IFNg_STAT1	-3.4	0
pfD	cd4_IFNg_STAT3	-1.5	0
pfD	cd4_IL10_STAT1	-3.3	0
pfD	cd4_IL10_STAT3	-2.2	0
pfD	cd4_IL21_STAT1	-1.3	0
pfD	cd4_IL21_STAT3	-2	0
pfD	cd4_IL21_STAT5	-2	0
pfD	cd4_IL6_STAT1	-1.1	0
pfD	cd4_IL6_STAT3	-11.2	0
pfD	cd4_IL6_STAT5	-1.6	0
pfD	cd4_IL7_STAT1	-2.3	0
pfD	cd4_IL7_STAT3	-1.3	0
pfD	cd4_IL7_STAT5	-1.4	0
pfD	cd8_IFNa_STAT3	-1.8	0

TABLE S11-continued

CNR-specific measurements			
DataType	Name	Fold-change	Q-value
pfD	cd8_IFNa_STAT5	-1.5	0
pfD	cd8_IFNg_STAT1	-2.8	0
pfD	cd8_IFNg_STAT3	-1.2	0
pfD	cd8_IFNg_STAT5	-1.9	0
pfD	cd8_IL10_STAT1	-1.7	0
pfD	cd8_IL10_STAT3	-1.4	0
pfD	cd8_IL21_STAT3	-1.7	0
pfD	cd8_IL21_STAT5	-1.2	0
pfD	cd8_IL6_STAT1	-2.4	0
pfD	cd8_IL6_STAT3	-1.3	0
pfD	cd8_IL6_STAT5	-1	0
pfD	cd8_IL7_STAT1	-1.2	0
pfD	cd8_IL7_STAT3	-1.2	0.01
pfD	cd8_IL7_STAT5	-1.2	0.01
pfD	mono_IFNa_STAT1	-1.4	0.01
pfD	mono_IFNa_STAT3	-1.4	0.01
pfD	mono_IFNa_STAT5	-1.1	0.01
pfD	mono_IFNg_STAT1	-1.2	0.02
pfD	mono_IFNg_STAT3	-1.1	0.04
pfD	mono_IFNg_STAT5	-1.1	0.05
pfD	mono_IL10_STAT3	-1	0.07
pfD	mono_IL21_STAT3	-1.1	0.07
pfD	mono_IL6_STAT1	-1.1	0.09
pfD	mono_IL6_STAT3	-1	0.11
pfD	mono_IL7_STAT5	-1.1	0.14
cytM	RANTES	-1.3	0.15
geD	FKBP1A	1.8	0.07
geD	TOLLIP	2.1	0.07
geD	RIMS4	1.5	0.07
geD	CAV3	2.1	0.07
geD	HSPA8	2.3	0.07
geD	AIRE	1.4	0.07
geD	NEIL3	1.5	0.07
geD	INHBC	1.9	0.07
geD	GHI	2.2	0.08
geD	DUB3	2.3	0.09
geD	ICOSLG	1.6	0.1
geD	HIP1	1.5	0.1
geD	ISLR2	1.9	0.1
geD	MYBPC3	1.5	0.1
geD	MUC5AC	1.5	0.1
geD	DSC2	3	0.1
geD	GREM2	1.4	0.11
geD	MNT	2	0.11
geD	ELN	2.1	0.11
geD	PXN	1.3	0.11
geD	CTSE	1.3	0.11
geD	BAG3	1.5	0.12
geD	SORT1	1.6	0.12
geD	CTS5	1.8	0.13
geD	ICAM5	2.9	0.14
geD	YWHAZ	1.2	0.14
geD	SBDS	1.5	0.14
geD	CLN3	1.5	0.14
geD	DOCK3	2	0.15
geD	SERPING1	-1.6	0.03
geD	ICA1	-1.6	0.07
geD	DNASE1	-1.5	0.07
geD	CASQ1	-1.4	0.07
geD	F5	-1.5	0.07
geD	LENG1	-1.4	0.07
geD	PGM5	-1.4	0.07
geD	EP300	-1.6	0.07
geD	DGKE	-1.5	0.07
geD	IGFALS	-1.6	0.07
geD	MYL10	-1.6	0.07
geD	CCL26	-1.4	0.07
geD	MYC	-1.5	0.07
geD	MASP1	-1.4	0.07
geD	IGF1R	-1.6	0.07
geD	THBS1	-1.4	0.07
geD	TNNC2	-1.3	0.07

TABLE S11-continued

CNR-specific measurements			
DataType	Name	Fold-change	Q-value
geD	ZNF346	-1.4	0.07
geD	LEFTY1	-1.4	0.07
geD	DCBLD1	-1.6	0.07
geD	MARK2	-1.4	0.07
geD	3-Sep	-1.4	0.07
geD	CBLB	-1.4	0.07
geD	SIX4	-1.5	0.07
geD	PIK3R2	-1.5	0.07
geD	CAMK1G	-1.4	0.08
geD	ARHGDI A	-1.4	0.08
geD	MIF	-1.4	0.08
geD	SLIT2	-1.3	0.08
geD	XRCC6BP1	-1.4	0.08
geD	TEC	-1.3	0.08
geD	BTG1	-1.4	0.08
geD	LPP	-1.5	0.08
geD	MARK1	-1.3	0.08
geD	LAMB2	-1.4	0.09
geD	HIP1	-1.3	0.09
geD	AR	-1.3	0.09
geD	BCL2L2	-1.4	0.09
geD	SCD5	-1.3	0.09
geD	CD1B	-1.4	0.1
geD	TNFRSF13B	-1.3	0.1
geD	EDNRA	-1.4	0.1
geD	SKAP2	-1.4	0.1
geD	MLLN	-1.3	0.1
geD	TRAF7	-1.5	0.1
geD	SFRS17A	-1.5	0.1
geD	COL6A1	-1.3	0.1
geD	HSPB1	-1.7	0.1
geD	NFE2L2	-1.5	0.1
geD	HAPLN3	-1.4	0.1
geD	C1QTNF2	-1.2	0.1
geD	SYNJ2BP	-1.3	0.1
geD	NPNT	-1.4	0.1
geD	ERCC5	-1.4	0.1
geD	CUL4A	-1.4	0.1
geD	KEL	-1.3	0.1
geD	PSMA5	-1.4	0.1
geD	SOD2	-1.3	0.1
geD	ARHGDI A	-1.5	0.1
geD	RAB22A	-1.4	0.11
geD	MAGED1	-1.3	0.11
geD	LTBP2	-1.3	0.11
geD	PPP1R13B	-1.3	0.11
geD	ULBP2	-1.4	0.11
geD	ATP2A1	-1.4	0.12
geD	BAT1	-1.5	0.12
geD	CSNK1E	-1.3	0.12
geD	NLGN3	-1.4	0.12
geD	ITGA9	-1.5	0.12
geD	XKR3	-1.5	0.12
geD	FMOD	-1.4	0.12
geD	CDC42SE2	-1.3	0.12
geD	ALCAM	-1.3	0.12
geD	FN1	-1.4	0.12
geD	RIPK1	-1.4	0.12
geD	CDH16	-1.3	0.12
geD	STK17A	-1.2	0.12
geD	TXLNA	-1.3	0.12
geD	HESX1	-1.3	0.12
geD	COL6A1	-1.3	0.13
geD	SGPL1	-1.7	0.13
geD	PDLIM7	-1.5	0.13
geD	FUT3	-1.2	0.13
geD	MSN	-1.4	0.13
geD	CLN8	-1.3	0.13
geD	PLDN	-1.4	0.13
geD	PLD1	-1.4	0.13
geD	MYST4	-1.4	0.13
geD	BLID	-1.5	0.13

TABLE S11-continued

CNR-specific measurements			
DataType	Name	Fold-change	Q-value
geD	BCL6B	-1.4	0.13
geD	CNTFR	-1.2	0.13
geD	COL24A1	-1.3	0.13
geD	SH3GL2	-1.3	0.14
geD	GSG2	-1.3	0.14
geD	BAALC	-1.2	0.14
geD	ADAL	-1.5	0.14
geD	BDNF	-2	0.14
geD	WISP1	-1.4	0.14
geD	BCL7A	-1.3	0.14
geD	CDC2L2	-1.2	0.14
geD	NCAM1	-1.3	0.14

TABLE S11-continued

CNR-specific measurements			
DataType	Name	Fold-change	Q-value
geD	CEACAM5	-1.3	0.14
geD	CD96	-1.4	0.14
geD	EMILIN1	-1.3	0.14
geD	HAPLN4	-1.4	0.14
geD	TXLNA	-1.4	0.14
geD	VNN1	-1.4	0.15
geD	C1QTNF1	-1.3	0.15
geD	MMP12	-1.5	0.15

APPENDIX L  
[0194]

TABLE S12

Fold-change - response classification results							
condition	maxFold	Unst <sup>Ⓢ</sup>	FC.d <sup>Ⓢ</sup>	fDR <sup>Ⓢ</sup>	FdiffDR <sup>Ⓢ</sup>	hMF <sup>Ⓢ</sup>	classify notes
Classification of aging associated cytokine response assays (q < 0.15)							
cd20_IFNg_STAT1 <sup>Ⓢ</sup>	1.1	1	0	1	0	1	Baseline Defect
cd20_IL7_STAT3	1.2	1	0	0	0	1	Baseline Defect
cd4_IFNa_STAT1	6.3	1	1	0	0	0	Baseline Defect
cd4_IFNa_STAT3	3.8	1	1	0	1	0	Baseline Defect
cd4_IFNg_STAT1	1.6	1	0	0	1	1	Baseline Defect
cd4_IL10_STAT1	2.2	1	0	1	0	1	Baseline Defect
cd4_IL10_STAT3	6.0	1	1	0	1	0	Baseline Defect
cd4_IL21_STAT1	1.6	1	0	1	0	1	Baseline Defect
cd4_IL21_STAT5	1.5	1	0	1	1	0	Baseline Defect
cd4_IL7_STAT5	5.0	1	1	1	0	0	Baseline Defect
cd8_IL10_STAT1	1.9	1	0	1	0	1	Baseline Defect
cd8_IL21_STAT5	1.4	1	0	1	1	0	Baseline Defect
cd8_IL7_STAT1	1.2	1	0	1	0	1	Baseline Defect
cd8_IL7_STAT3	1.4	1	0	0	0	1	Baseline Defect
cd20_IFNa_STAT1 <sup>Ⓢ</sup>	4.2	1	1	0	0	1	Baseline Resistance Defect
cd20_IFNa_STAT <sup>Ⓢ</sup>	2.8	1	1	1	1	1	Baseline Resistance Defect
cd20_IFNa_STAT <sup>Ⓢ</sup>	1.7	1	1	1	0	1	Baseline Resistance Defect
cd4_IFNa_STAT5	3.4	1	1	1	0	1	Baseline Resistance Defect
cd4_IL21_STAT3	5.5	1	1	1	1	0	Baseline Resistance Defect
cd4_IL6_STAT1	6.0	1	1	0	1	1	Baseline Resistance Defect
cd4_IL6_STAT3	5.9	1	1	1	1	1	Baseline Resistance Defect
cd4_IL6_STAT5	2.1	1	1	1	1	1	Baseline Resistance Defect
cd4_IL7_STAT3	1.3	1	1	1	0	1	Baseline Resistance Defect
cd8_IFNa_STAT1	7.2	1	1	0	0	1	Baseline Resistance Defect
cd8_IFNa_STAT3	3.7	1	1	1	1	1	Baseline Resistance Defect
cd8_IFNa_STAT5	2.8	1	1	0	0	1	Baseline Resistance Defect
cd8_IFNg_STAT1	1.5	1	1	0	1	1	Baseline Resistance Defect
cd8_IL21_STAT1	1.7	1	1	1	1	1	Baseline Resistance Defect
cd8_IL6_STAT1	4.7	1	1	0	1	1	Baseline Resistance Defect
cd8_IL6_STAT3	5.8	1	1	0	1	1	Baseline Resistance Defect
cd8_IL6_STAT5	1.5	1	1	1	1	0	Baseline Resistance Defect
mono_IFNa_STA <sup>Ⓢ</sup>	3.1	0	1	0	0	1	Resistance Defect
mono_IFNa_STA <sup>Ⓢ</sup>	2.3	0	1	0	0	1	Resistance Defect
mono_IFNa_STA <sup>Ⓢ</sup>	1.5	0	1	1	0	1	Resistance Defect
mono_IL6_STA1 <sup>Ⓢ</sup>	2.3	0	1	1	1	1	Resistance Defect
mono_IFNg_STA <sup>Ⓢ</sup>	1.5	0	0	1	1	0	Unknown
mono_IFNg_STA <sup>Ⓢ</sup>	1.6	0	0	1	0	0	Unknown
mono_IL6_STA1 <sup>Ⓢ</sup>	1.2	0	0	0	0	1	Unknown
mono_IL7_STA1 <sup>Ⓢ</sup>	1.3	0	0	1	0	0	Unknown
Classification of cytokine response assays not shown to be different in the aging in the general (29 individuals) population							
cd20_IFNg_STAT1 <sup>Ⓢ</sup>	1.4	1	0	1	0	1	Baseline Defect
cd20_IL10_STA1 <sup>Ⓢ</sup>	1.7	1	0	1	0	1	Baseline Defect
cd20_IL10_STA1 <sup>Ⓢ</sup>	1.3	1	0	1	0	1	Baseline Defect
cd20_IL21_STA1 <sup>Ⓢ</sup>	1.4	1	0	1	0	1	Baseline Defect
cd20_IL6_STAT1	1.2	1	0	1	1	1	Baseline Defect
cd20_IL6_STAT5	1.3	1	0	1	0	1	Baseline Defect

TABLE S12-continued

Fold-change - response classification results							
condition	maxFold	Unst <sup>Ⓢ</sup>	FC.d <sup>Ⓢ</sup>	fDR <sup>Ⓢ</sup>	FdiffDR <sup>Ⓢ</sup>	hMF <sup>Ⓢ</sup>	classify notes
cd20_IL7_STAT5	1.3	1	0	1	0	1	Baseline Defect
cd4_IL10_STAT5	1.5	1	0	1	0	1	Baseline Defect
cd4_IL7_STAT1	1.3	1	0	1	0	1	Baseline Defect
cd8_IFNg_STAT3	1.2	1	0	0	0	1	Baseline Defect
cd8_IFNg_STAT5	1.2	1	0	1	0	1	Baseline Defect
cd8_IL10_STAT5	1.3	1	0	1	0	1	Baseline Defect
cd20_IFNg_STAT <sup>Ⓢ</sup>	3.5	1	0	1	0	1	Baseline Defect
cd20_IL10_STAT <sup>Ⓢ</sup>	5.1	1	0	1	0	0	Baseline Defect
cd20_IL21_STAT <sup>Ⓢ</sup>	1.5	1	0	0	0	1	Baseline Defect
cd20_IL7_STAT1	1.2	1	0	1	0	1	Baseline Defect
cd4_IFNg_STAT3	1.1	1	0	0	0	1	Baseline Defect
cd4_IFNg_STAT5	1.2	1	0	1	0	1	Baseline Defect
cd8_IL10_STAT3	6.1	1	0	1	0	0	Baseline Defect
cd8_IL21_STAT3	5.8	1	1	1	0	0	Baseline Defect
cd20_IL6_STAT3	1.3	1	1	1	1	1	Baseline Resistance Defect
cd20_IL21_STAT <sup>Ⓢ</sup>	3.7	1	1	1	0	1	Baseline Resistance Defect
cd8_IL7_STAT5	3.9	1	1	1	0	1	Baseline Resistance Defect
mono_IL21_STA <sup>Ⓢ</sup>	1.7	0	1	1	0	1	Resistance Defect
mono_IL10_STA <sup>Ⓢ</sup>	1.9	0	0	1	0	1	Unknown
mono_IL10_STA <sup>Ⓢ</sup>	1.4	0	0	1	0	1	Unknown
mono_IL21_STA <sup>Ⓢ</sup>	1.4	0	0	0	0	1	Unknown
mono_IL21_STA <sup>Ⓢ</sup>	1.2	0	0	1	0	1	Unknown
mono_IL6_STA <sup>Ⓢ</sup>	1.2	0	0	1	0	1	Unknown
mono_IL7_STA <sup>Ⓢ</sup>	1.2	0	0	0	0	1	Unknown
mono_IL7_STA <sup>Ⓢ</sup>	1.2	0	0	0	0	1	Unknown
mono_IFNg_STA <sup>Ⓢ</sup>	3.8	0	0	1	0	0	Unknown
mono_IL10_STA <sup>Ⓢ</sup>	5.4	0	0	1	1	0	Unknown

<sup>Ⓢ</sup> indicates text missing or illegible when filed

What is claimed is:

1. A method of diagnosing a state of immune function in an individual, said method comprising

(a) obtaining an immune system profile from said individual in comparison to control individuals, said immune profile comprising measurements of immune cell subset frequencies, gene expression, cytokine levels, chemokine levels, baseline phosphorylation levels of proteins and magnitude of change in phosphorylation level of said proteins in response to stimulation with cytokines ('cytokine response');

(b) physical transformation of said immune system profile into information for graphical display or output to a computer-readable medium, computer or computer network.

2. The method of claim 1, wherein said individual is at least 60 years old.

3. The method of claim 1, wherein said cell subset frequencies are characterized by an age-associated change.

4. The method of claim 3, wherein the age-associated change is a decrease in the frequency of CD8<sup>+</sup> naïve cells.

5. The method of claim 3, wherein the age-associated change is an increase in the frequency of monocytes.

6. The method of claim 3, wherein the age-associated change is an increase in the frequency of CD8<sup>+</sup> and CD4<sup>+</sup> D28<sup>-</sup> naïve cells.

7. The method of claim 3, wherein the age-associated change is an increase in the frequency of natural killer T (NKT) cells.

8. The method of claim 3, wherein the age-associated change is an increase in the frequency of CD8<sup>+</sup> and CD4<sup>+</sup> memory T cells.

9. The method of claim 1, wherein said proteins are STAT proteins.

10. The method of claim 9, wherein said STAT proteins are STAT1, STAT3 and STAT5.

11. The method of claim 9, wherein said STAT proteins are STAT1, STAT3 or STAT5.

12. The method of claim 1, wherein said cytokine response is measured upon stimulation with IFN- $\alpha$ , IFN- $\gamma$ , IL6, IL7, IL10 or IL21.

13. The method of claim 1, wherein said measurements of cytokine levels relate to one or more of the following cytokines: eotaxin, IFN- $\gamma$ , IL-7, MCP-1, MCP-3, IL-12-P70, IL-17, IL-4, TGF- $\alpha$ , IP10, TNF- $\alpha$ , IFNA2, IL-5.

14. The method of claim 1, wherein said measurements of chemokine levels relate to one or more of the following chemokines: CXCL1, CXCL5.

15. The method of claim 1, wherein said measurements of gene expression relate to one or more of the genes from Tables S2, S9, S10 and S11.

16. A method of diagnosing impaired immune function in an individual in comparison to control individuals, said method comprising

(a) obtaining an immune system profile from said individual, said immune profile comprising measurements of baseline phosphorylation of STAT proteins before stimulation with cytokines and measurements of fold-change of phosphorylation of STAT proteins following stimulation with cytokines ('cytokine response') in multiple cell-types,

(b) analyzing said measurements, wherein, decreased fold-change following stimulation with cytokines indicate a cytokine non-response in said individual, and a cytokine non-response indicates impaired immune function in said individual; and

wherein non-increased baseline phosphorylation before said stimulation with cytokines and non-decreased fold-change following stimulation with cytokines indicate a

- cytokine response in said individual, and a cytokine response indicates non-impaired immune function in said individual.
- (b) physical transformation of said immune system profile into information for graphical display or output to a computer-readable medium, computer or computer network.
- 17.** The method of claim **16**, wherein said STAT proteins are STAT1, STAT3 and STAT5.
- 18.** The method of claim **16**, wherein said STAT proteins are STAT1, STAT3 or STAT5.
- 19.** The method of claim **16**, wherein said cytokine response is measured upon stimulation with IFN- $\alpha$ , IFN- $\gamma$ , IL6, IL7, IL10 or IL21.
- 20.** The method of claim **16**, wherein said individual is at least 60 years old.
- 21.** A method of classifying individuals in individuals with impaired immune function and individuals with non-impaired immune function in comparison to control individuals, said method comprising
- (a) obtaining an immune system profile from said individuals, said immune profile comprising measurements of baseline phosphorylation of STAT proteins before stimulation with cytokines and measurements of fold-change of phosphorylation of STAT proteins following stimulation with cytokines ('cytokine response') in multiple cell-types,
- (b) analyzing said measurements, wherein increased baseline phosphorylation before said stimulation with cytokines and decreased fold-change following stimulation with cytokines indicate a cytokine non-response in said individuals, and a cytokine non-response indicates impaired immune function in said individuals; and wherein non-increased baseline phosphorylation before said stimulation with cytokines and non-decreased fold-change following stimulation with cytokines indicate a cytokine response in said individuals, and a cytokine response indicates non-impaired immune function in said individuals.
- (c) physical transformation of said immune system profile into information for graphical display or output to a computer-readable medium, computer or computer network.
- 22.** The method of claim **21**, wherein said STAT proteins are STAT1, STAT3 and STAT5.
- 23.** The method of claim **21**, wherein said STAT proteins are STAT1, STAT3 or STAT5.
- 24.** The method of claim **21**, wherein said cytokine response is measured upon stimulation with IFN- $\alpha$ , IFN- $\gamma$ , IL6, IL7, IL10 or IL21.
- 25.** A method of assessing immune function in an individual in comparison to control individuals, said method comprising
- (a) obtaining an immune system profile from said individual, said immune profile comprising measurements of immune cell subset frequencies, gene expression, cytokine levels, chemokine levels and signaling responses to stimulation with cytokines ('cytokine response');
- (b) physical transformation of said immune system profile into information for graphical display or output to a computer-readable medium, computer or computer network.
- 26.** The method of claim **25**, wherein said individual is at least 60 years old.
- 27.** A method of assessing immune function in an individual in comparison to control individuals, said method comprising
- (a) obtaining an immune system profile from said individual, said immune profile comprising measurements of baseline phosphorylation of STAT proteins before stimulation with cytokines and measurements of fold-change of phosphorylation of STAT proteins following stimulation with cytokines ('cytokine response') in multiple cell-types,
- (b) analyzing said measurements, wherein, in comparison to said control individual, decreased fold-change following stimulation with cytokines indicate a cytokine non-response in said individual, and a cytokine non-response indicates impaired immune function in said individual; and wherein, in comparison to said control individual, non-decreased fold-change following stimulation with cytokines indicate a cytokine response in said individual, and a cytokine response indicates non-impaired immune function in said individual.
- (c) physical transformation of said immune system profile into information for graphical display or output to a computer-readable medium, computer or computer network.
- 28.** The method of claim **27**, wherein said STAT proteins are STAT1, STAT3 and STAT5.
- 29.** The method of claim **27**, wherein said STAT proteins are STAT1, STAT3 or STAT5.
- 30.** The method of claim **27**, wherein said cytokine response is measured upon stimulation with IFN- $\alpha$ , IFN- $\gamma$ , IL6, IL7, IL10 or IL21.
- 31.** A method of assessing immune function in an individual in comparison to a control individual, said method comprising
- (a) obtaining an immune system profile from said individual in comparison to a control individual, said immune profile comprising measurements of baseline phosphorylation of STAT proteins in multiple cell-types;
- (b) analyzing said measurements, wherein, in comparison to said control individual, increased baseline phosphorylation indicates a cytokine non-response in said individual, and a cytokine non-response indicates impaired immune function in said individual; and wherein, in comparison to said control individual, non-increased baseline phosphorylation indicates a cytokine response in said individual, and a cytokine response indicates non-impaired immune function in said individual.
- (c) physical transformation of said immune system profile into information for graphical display or output to a computer-readable medium, computer or computer network.
- 32.** The method of claim **31**, wherein said STAT proteins are STAT1, STAT3 and STAT5.
- 33.** The method of claim **31**, wherein said STAT proteins are STAT1, STAT3 or STAT5.
- 34.** The method of claim **31**, wherein said cytokine response is measured upon stimulation with IFN- $\alpha$ , IFN- $\gamma$ , IL6, IL7, IL10 or IL21.

\* \* \* \* \*

专利名称(译)	免疫衰老的诊断标志物及其使用方法		
公开(公告)号	<a href="#">US20120021414A1</a>	公开(公告)日	2012-01-26
申请号	US13/168974	申请日	2011-06-25
[标]申请(专利权)人(译)	斯坦福大学		
申请(专利权)人(译)	霍华德休斯医学研究所 THE利兰·斯坦福，齐齐哈尔大学董事会		
当前申请(专利权)人(译)	THE利兰·斯坦福，齐齐哈尔大学董事会		
[标]发明人	SHEN ORR SHAI S BUTTE ATUL J DAVIS MARK M FURMAN DAVID KIDD BRIAN A		
发明人	SHEN-ORR, SHAI S. BUTTE, ATUL J. DAVIS, MARK M. FURMAN, DAVID KIDD, BRIAN A.		
IPC分类号	C12Q1/68 G01N33/53		
CPC分类号	G01N33/5091 G01N2333/52 G01N2800/60 G01N2333/70517 G01N2333/70521 G01N2333/70514		
优先权	61/358884 2010-06-25 US		
其他公开文献	US10119959		
外部链接	<a href="#">Espacenet</a> <a href="#">USPTO</a>		

摘要(译)

本发明的实施方案提供免疫衰老的诊断标志物和基于从各种分析获得的这些标志物的组合鉴定免疫功能受损的个体的方法，所述标志物主要来自血液，测试免疫功能，包括免疫细胞子集频率的分析，基因表达，细胞因子和趋化因子水平，以及对细胞因子刺激的信号反应 ( &#39;细胞因子反应&#39; )。标记物的特定组合可以高精度地预测个体是否对活性疫苗接种有反应并且防止复发性疾病。

